

AD-A034 941

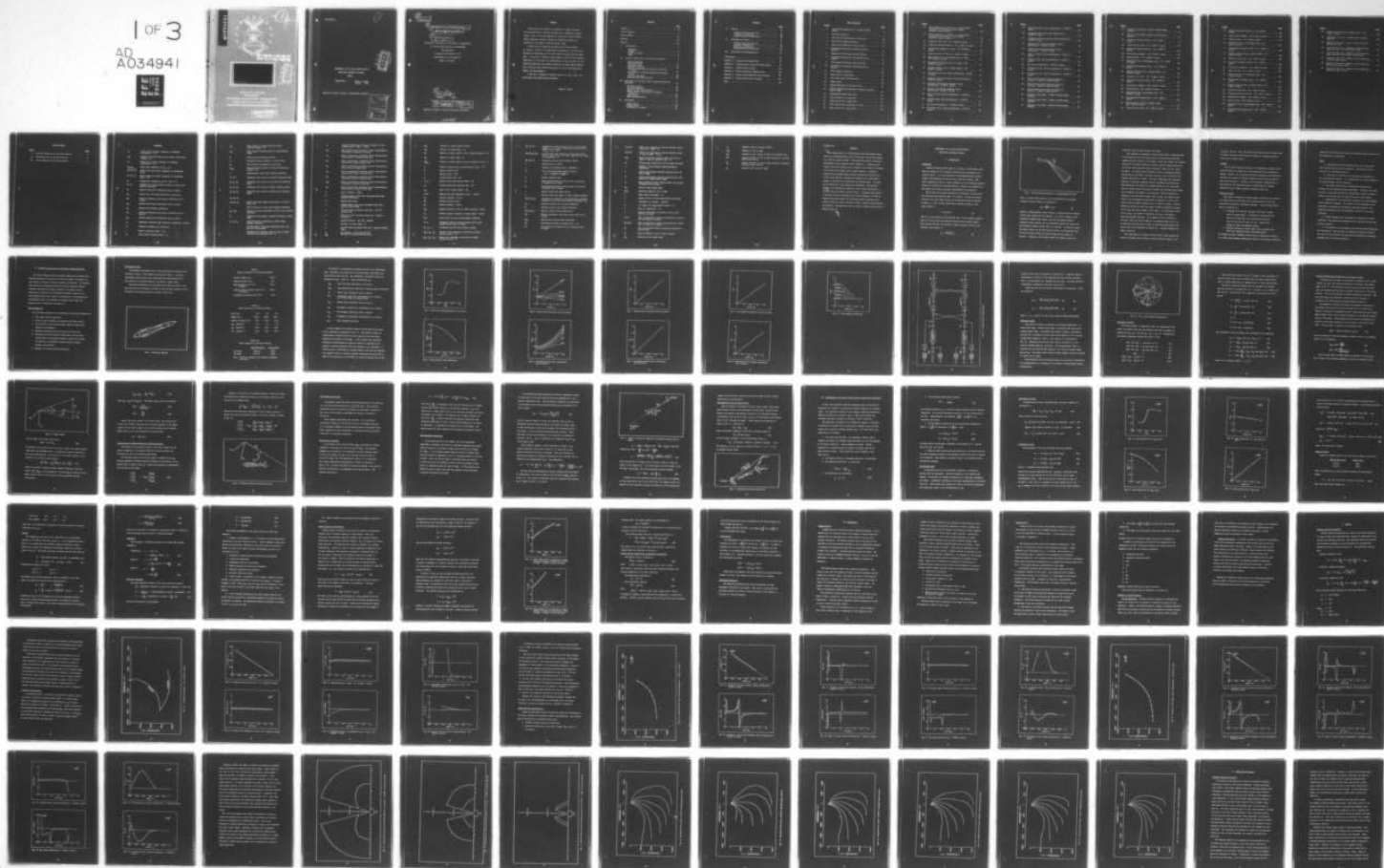
AIR FORCE INST OF TECH WRIGHT-PATTERSON AFB OHIO SCH--ETC F/6 17/9
PERFORMANCE OF AN AIR-TO-GROUND MISSILE EMPLOYING SAR-RETRAN GU--ETC(U)
DEC 76 E H JESSUP
6AE/MC/76D-6

UNCLASSIFIED

NL

1 OF 3

AD
A034941



GAE/MC/76D-6

1

PERFORMANCE OF AN AIR-TO-GROUND MISSILE
EMPLOYING SAR-RETRAN GUIDANCE
THESIS

GAE/MC/76D-6

Edwin H. Jessup
Captain USAF

DDC
JAN 28 1977
RECEIVED

Approved for public release; distribution unlimited.

ACQUISITION FOR	
NTIS	White Section <input checked="" type="checkbox"/>
D G	Buff Section <input type="checkbox"/>
UNANNOUNCED	<input type="checkbox"/>
JUSTIFICATION	
BY	
DISTRIBUTION/AVAILABILITY CODES	
Dist.	AVAIL. NO./OF SPECIAL
A	

14
GAE/MC/76D-6

6
PERFORMANCE OF AN AIR-TO-GROUND MISSILE
EMPLOYING SAR-RETRAN GUIDANCE •

9
Master's THESIS,

Presented to the Faculty of the School of Engineering
of the Air Force Institute of Technology
Air University
in Partial Fulfillment of the
Requirements for the Degree of
Master of Science

10
by
Edwin H. Jessup B.S.
Captain USAF

Graduate Aeronautical Engineering

11 Dec 76

12/229p.

Approved for public release; distribution unlimited.

012225

y/p

Preface

This study is my attempt to determine if a typical tactical air-to-ground missile could be employed with a SAR-Retrans guidance system. Most of the investigation was carried out using a digital flight simulation program, although an optimizing program was developed in an attempt to maximize launch range.

I would like to express my gratitude to my thesis advisor, Dr. Robert A. Calico of the Department of Mechanics of the Air Force Institute of Technology, for his sage advice, patience and encouragement. I also wish to thank Mr. Merrill Habbe of the Air Force Avionics Laboratory, who laid much of the groundwork for this project, for his unfailing enthusiasm and technical guidance; and Major Edward Mirmac, also of the Air Force Avionics Laboratory, for his continuing moral support and encouragement.

I also wish to express my deepest thanks to my wife, Laura, for her patience and understanding throughout.

Edwin H. Jessup

Contents

	<u>Page</u>
Preface	11
List of Figures	v
List of Tables	xi
Notation	xii
Abstract	xix
I. Introduction	1
Background	1
Problem	4
Purpose of Study	4
Scope	5
II. Analytic Formulation of the Missile Simulation	6
Basic Assumptions	6
The Missile Model	7
Reference Frames	16
Equations of Motion	17
Aircraft Maneuvering and Rotation of the Line of Sight	19
Determination of Missile Position and Velocity Errors	21
Guidance Algorithms	23
Retransmitted Frequency Error	27
III. Development of the First Order Gradient Optimization Algorithm	28
The Missile Model	29
The State Equations	35
Payoff Function and Penalties	37
Adjoint Vector, Hamiltonian and Backward Integration	40
Alpha Search	41
Algorithm Termination	41
IV. Programming	42
Program Retran	42
Program Optraj	44
Validation of Programs	45

Contents

	<u>Page</u>
V. Results	47
Guidance Algorithm Selection	47
Trajectory Optimization	48
Launch Envelope Determination	53
VI. Discussion of Results	74
Guidance Algorithm Selection	74
Autopilot Compatibility	76
Trajectory Optimization	77
Launch Envelope Determination	79
VII. Conclusions and Recommendations	80
Bibliography	82
Appendix A: Coordinate Transformations	83
Appendix B: Program Retran Listing and Sample Output . .	87
Appendix C: Program OptraJ Listing	124
Appendix D: Retran Simulation Parameter Plots	146
Appendix E: Guidance Algorithms Which Were Rejected . . .	167
Appendix F: Program OptraJ Output Listings	178
VITA	206

List of Figures .

<u>Figure</u>		<u>Page</u>
1	Velocity Discrimination of a Corange Spatial Extent	2
2	The Retran Missile	7
3	Zero Lift Drag Coefficient at Sea Level	10
4	Skin Friction Drag Coefficient	10
5	Chord Force Coefficient With No Control	11
6	Incremental Chord Force Coefficient Due to Control	11
7	Normal Force Coefficient With No Control	12
8	Incremental Normal Force Coefficient Due to Control	12
9	Pitch Moment Coefficient With No Control	13
10	Incremental Pitch Moment Coefficient Due to Control	13
11	Pitch Damping Coefficient	14
12	Retran Control System Model	15
13	3-2-1 Euler Angle Transformation	17
14	Gimbal Angles	20
15	Missile Position and Velocity Errors	22
16	Lateral Acceleration Required to Maintain Rotating Line of Sight	26
17	Retransmitted Radar Signal Path	27
18	Least Squares Fit to C_{D0} Curve	31
19	Least Squares Fit to ΔC_{Df} Curve	31
20	Least Squares Fit to ΔC_C Curve for $\delta=4^\circ$	32
21	Least Squares Fit to C_{N2} Curve	32

<u>Figure</u>		<u>Page</u>
22	Least Squares Fit to Velocity vs. Range Profile for Missile Established on Line of Sight - 35,000 ft Launch Altitude	39
23	Least Squares Fit to Velocity vs. Range Profile for Missile Established on Line of Sight - 20,000 ft Launch Altitude	39
24	Trajectory Plan View - 45°, 35,000 ft Launch	49
25	Trajectory Vertical Profile - 45°, 35,000 ft Launch . .	50
26	Acceleration Commands vs. Time - 45°, 35,000 ft Launch	50
27	Alpha and Beta vs. Time, 45°, 35,000 ft Launch	51
28	Deceleration Due to Aerodynamic Drag vs. Time - 45°, 35,000 ft Launch	51
29	Retransmitted Frequency Error vs. Time - 45°, 35,000 ft Launch	52
30	Missile Distance Errors, Terminal Phase - 45°, 35,000 ft Launch	52
31	Trajectory Plan View, Optraaj Optimization - 35,000 ft Launch	54
32	Trajectory Vertical Profile, Optraaj Optimization - 35,000 ft Launch	55
33	Horizontal Acceleration Commands, Optraaj Optimization - 35,000 ft Launch	55
34	Vertical Acceleration Commands, Optraaj Optimization - 35,000 ft Launch	56
35	Angle of Attack, Optraaj Optimization - 35,000 ft Launch	56
36	Sideslip Angle, Optraaj Optimization - 35,000 ft Launch	57
37	V_M , Optraaj Optimization - 35,000 ft Launch	57
38	ΔY Distance Error, Optraaj Optimization - 35,000 ft Launch	58

<u>Figure</u>		<u>Page</u>
39	ΔZ Distance Error, Optraaj Optimization - 35,000 ft Launch	58
40	Trajectory Plan View, Optraaj Optimization - 20,000 ft Launch	59
41	Trajectory Vertical Profile, Optraaj Optimization - 20,000 ft Launch	60
42	Horizontal Acceleration Commands, Optraaj Optimization - 20,000 ft Launch	60
43	Vertical Acceleration Commands, Optraaj Optimization - 20,000 ft Launch	61
44	Angle of Attack, Optraaj Optimization - 20,000 ft Launch	61
45	Sideslip Angle, Optraaj Optimization - 20,000 ft Launch	62
46	V_M , Optraaj Optimization - 20,000 ft Launch	62
47	ΔY Distance Error, Optraaj Optimization - 20,000 ft Launch	63
48	ΔZ Distance Error, Optraaj Optimization - 20,000 ft Launch	63
49	Retran Missile Launch Envelope Relative to Aircraft - 35,000 ft Launch Altitude	65
50	Retran Missile Launch Envelope Relative to Aircraft - 20,000 ft Launch Altitude	66
51	Retran Missile Launch Envelope Relative to Aircraft - 5,000 ft Launch Altitude	67
52	Trajectory Plan Views, 35,000 ft Maximum Range Launches	68
53	Trajectory Plan Views, 35,000 ft Minimum Range Launches	69
54	Trajectory Plan Views, 20,000 ft Minimum Range Launches	70

<u>Figure</u>		<u>Page</u>
55	Trajectory Plan Views, 20,000 ft Minimum Range Launches	71
56	Trajectory Plan Views, 5,000 ft Maximum Range Launches	72
57	Trajectory Vertical Profile - 15°, 35,000 ft Launch	73
58	Trajectory Plan View - 15°, 35,000 ft Launch	147
59	Trajectory Vertical Profile - 15°, 35,000 ft Launch	148
60	Acceleration Commands - 15°, 35,000 ft Launch	148
61	Alpha and Beta - 15°, 35,000 ft Launch	149
62	Deceleration Due to Aerodynamic Drag - 15°, 35,000 ft Launch	149
63	Retransmitted Frequency Error - 15°, 35,000 ft Launch	150
64	Missile Distance Errors, Terminal Phase - 15°, 35,000 ft Launch	150
65	Trajectory Plan View - 90°, 35,000 ft Launch	151
66	Trajectory Vertical Profile - 90°, 35,000 ft Launch	152
67	Acceleration Commands - 90°, 35,000 ft Launch	152
68	Alpha and Beta - 90°, 35,000 ft Launch	153
69	Deceleration Due to Aerodynamic Drag - 90°, 35,000 ft Launch	153
70	Retransmitted Frequency Error - 90°, 35,000 ft Launch	154
71	Missile Distance Errors, Terminal Phase - 90°, 35,000 ft Launch	154
72	Trajectory Plan View - 15°, 5,000 ft Launch	155

<u>Figure</u>		<u>Page</u>
73	Trajectory Vertical Profile - 15°, 5,000 ft Launch	156
74	Acceleration Commands - 15°, 5,000 ft Launch	156
75	Alpha and Beta - 15°, 5,000 ft Launch	157
76	Deceleration Due to Aerodynamic Drag - 15°, 5,000 ft Launch	157
77	Retransmitted Frequency Error - 15°, 5,000 ft Launch	158
78	Missile Distance Errors, Terminal Phase - 15°, 5,000 ft Launch	158
79	Trajectory Plan View - 45°, 5,000 ft Launch	159
80	Trajectory Vertical Profile - 45°, 5,000 ft Launch	160
81	Acceleration Commands - 45°, 5,000 ft Launch	160
82	Alpha and Beta - 45°, 5,000 ft Launch	161
83	Deceleration Due to Aerodynamic Drag - 45°, 5,000 ft Launch	161
84	Retransmitted Frequency Error - 45°, 5,000 ft Launch	162
85	Missile Distance Errors, Terminal Phase - 45°, 5,000 ft Launch	162
86	Trajectory Plan View - 90°, 5,000 ft Launch	163
87	Trajectory Vertical Profile - 90°, 5,000 ft Launch	164
88	Acceleration Commands - 90°, 5,000 ft Launch	164
89	Alpha and Beta - 90°, 5,000 ft Launch	165
90	Deceleration Due to Aerodynamic Drag - 90°, 5,000 ft Launch	165
91	Retransmitted Frequency Error - 90°, 5,000 ft Launch	166

<u>Figure</u>		<u>Page</u>
92	Missile Distance Errors, Terminal Phase - 90°, 5,000 ft Launch	166
93	Trajectory Plan View - Straight Ahead Intercept Algorithm	168
94	Trajectory Plan View - Turn to Initial Intercept Heading Algorithm	172
95	Trajectory Plan View - Command to Fixed Intercept Angle Algorithm, Low Squint Angle Launch	173
96	Trajectory Plan View - Command to Fixed Intercept Angle Algorithm, Medium Squint Angle Launch	174
97	Trajectory Plan View - Command to Track Algorithm, Low Squint Angle Launch	175
98	Trajectory Plan View - Command to Track Algorithm, Medium Squint Angle Launch	175
99	Trajectory Plan View - Command to Track Algorithm, High Squint Angle Launch	176

List of Tables

<u>Table</u>		<u>Page</u>
I.	Physical Dimensions of the Retran Missile	8
II.	Mass Properties of the Retran Missile	8
III.	Thrust Schedule of the Retran Missile	8

Notation

a_h	Gimbal axes horizontal component of commanded acceleration - g's
a_{hT}	Command-to-heading algorithm horizontal acceleration command - g's
a_v	Gimbal axes vertical component of commanded acceleration - g's
a_{xg}, a_{yg}	Gimbal axes components of a_{hT} - g's
$\overline{A_x}, \overline{A_y}, \overline{A_z}$	Missile body axes vector components of aerodynamic force
A_x, A_y, A_z	Missile body axes scalar components of aerodynamic force - lbf
C_1	Standard day temperature at sea level - °R
C_1, C_2	Coefficient for missile mass function in first order gradient algorithm
C_C	Missile chord force coefficient with no control
C_{D0}	Missile zero lift drag coefficient at sea level
C_{m1}	Missile incremental pitch moment coefficient due to control
C_{m2}	Missile pitch moment coefficient with no control
C_{mq}	Missile pitch damping coefficient
C_{N1}	Missile incremental normal force coefficient due to control
C_{N2}	Missile normal force coefficient with no control
C_R	Equivalent reference range conversion coefficient - ft/sec
C_T	Command-to-heading turn coefficient
d	Missile reference length - 1 ft
f_d	Radar doppler frequency shift - hz

f_{d1}	Radar doppler frequency shift for direct reflected signal - hz
f_{d2}	Radar doppler frequency shift for retransmitted signal
\bar{g}	Gravitational acceleration vector
g	Acceleration due to gravity - 32.174 ft/sec ²
g_0	Gravitational acceleration at sea level
g_{bias}	Bias acceleration added to vertical acceleration command - g's
H	Hamiltonian in first order gradient algorithm
$\bar{i}, \bar{j}, \bar{k}$	Orthogonal unit vectors in inertial reference frame
$\bar{i}_A, \bar{j}_A, \bar{k}_A$	Orthogonal unit vectors in aircraft body reference frame
$\bar{i}_G, \bar{j}_G, \bar{k}_G$	Orthogonal unit vectors in gimbal reference frame
$\bar{i}_M, \bar{j}_M, \bar{k}_M$	Orthogonal unit vectors in missile body reference frame
I_{xx}, I_{yy}, I_{zz}	
I_{xy}, I_{xz}, I_{yz}	Missile body axes moments and products of inertia - slug - ft ²
J	Payoff function in first order gradient algorithm
k_{01}, k_{02}	Velocity function coefficient in first order gradient algorithm
k_1	Command-to-track guidance algorithm frequency coefficient
k_1, k_2, k_3	Penalty function coefficients in first order gradient algorithm
L	Rolling moment acting about X_M missile body axis - positive rolling right
L	Approximate arc distance normal to line of sight covered during intercept turn - ft

L_o	Lateral acceleration required of missile to track rotating line of sight - ft/sec
L_{AG}	Matrix representing coordinate system transformation from gimbal to aircraft body axes
L_{AI}	Matrix representing coordinate system transformation from inertial to aircraft body axes
L_{GA}	Matrix representing coordinate system transformation from aircraft body to gimbal axes
L_{GI}	Matrix representing coordinate system transformation from inertial to gimbal axes
L_{IA}	Matrix representing coordinate system transformation from aircraft body to inertial axes
L_{IM}	Matrix representing coordinate system transformation from missile body to inertial axes
L_{MG}	Matrix representing coordinate system transformation from gimbal to missile body axes
L_{MI}	Matrix representing coordinate system transformation from inertial to missile body axes
m	Mass of missile - slugs
M	Pitching moment acting about Y_M missile body axis - positive pitching up
M	Missile mach number
N	Yawing moment acting about Z_M missile body axis - positive yawing right
P	roll rate about X_M missile body axis - positive rolling right
Q	Pitch rate about Y_M missile body axis - positive pitching up
q	Dynamic pressure - $\frac{1}{2} \rho V_M^2$ - lbf/ft ²
R	Aircraft to target range - ft
R	Yaw rate about Z_M missile body axis - positive yawing right
$\frac{R}{R_{AM}}$	Air constant - $1716.5 \text{ ft}^2 \text{ sec}^{-2} \text{ R}^{-1}$ Aircraft to missile position vector

\bar{R}_{AT}	Aircraft to target position vector
R_{AT}	Aircraft to target range - ft
R_f	Missile to target range at line of sight intercept - ft
R_{MT}	Missile to target range - ft
$R_{MT_{ST}}$	Missile to target range at start of intercept turn - ft
S	Missile reference area (cross-sectional area) - ft ²
\bar{T}	Missile thrust vector
T	Missile thrust - lbf
t_0	Initial flight time - sec
t_1, t_2	Missile motor stage burnout times - sec
t_R	Guidance algorithm reference time - sec
t_{tg}	Time to go to target impact - sec
U, V, W	Missile body axes components of \bar{V}_M - ft/sec
V_A	Aircraft airspeed - ft/sec
\bar{V}_M	Missile velocity vector
V_M	Missile airspeed - ft/sec
V_{M_f}	Missile airspeed at line of sight intercept - ft/sec
V_T	Missile terminal airspeed at target impact - ft/sec
$\bar{X}(t)$	State vector in first order gradient algorithm
X, Y, Z	Orthogonal inertial reference system with Z-axis pointed toward center of earth
X_A, Y_A, Z_A	Orthogonal aircraft body reference system
X_{AM}, Y_{AM}, Z_{AM}	Inertial axis components of aircraft to missile position vector - ft
X_{AT}, Y_{AT}, Z_{AT}	Gimbal axis components of aircraft to target position vector - ft

X_G, Y_G, Z_G	Orthogonal reference system fixed in radar antenna gimbals. X_G is always aligned with the aircraft to target line of sight
$X_{LOS}, Y_{LOS}, Z_{LOS}$	Inertial body axis components of the point on the line of sight lying at the same range from the target as the missile - ft
X_M, Y_M, Z_M	Orthogonal missile body reference system
α	Missile angle of attack
α	Temperature relaxation rate - deg/1000 ft
α_T	Total effective missile angle of attack - $\tan^{-1} [\sqrt{(\tan\alpha)^2 + (\tan\beta)^2}]$
β	Missile sideslip angle
β_1	Angle between missile velocity vector and missile to target line of sight
β_2	Angle between missile velocity vector and aircraft to missile line of sight
γ	Missile flight path angle $-(\theta - \alpha)$
γ_f	Missile flight path angle at line of sight intercept
$\delta a_h(t), \delta a_v(t)$	Incremental corrections to the acceleration commands obtained in the first order gradient algorithm - g's
δ_B	Effective missile pitch control deflection
δ_C	Effective missile yaw control deflection
$\delta_1, \delta_2, \delta_3, \delta_4$	Missile control surface deflections
ΔC_C	Missile incremental chord force coefficient due to control
ΔC_{D_f}	Missile skin friction drag coefficient
Δf_d	Retransmitted doppler frequency error - hz
Δt_T	Time required to complete turn to intercept line of sight

$\Delta X, \Delta Y, \Delta Z$	Gimbal axis components of missile distance normal from line of sight - ft
$\Delta \dot{X}, \Delta \dot{Y}, \Delta \dot{Z}$	Gimbal axis components of missile velocity normal to line of sight - ft/sec
ΔY_{ST}	Missile horizontal distance normal from line of sight at start of intercept turn - ft
$\Delta \psi$	Turning angle required for line of sight intercept
ζ	Command-to-track guidance algorithm damping coefficient
θ	Squint angle between aircraft velocity vector and line of sight
θ_1	Squint angle between aircraft velocity vector and aircraft to target line of sight
θ_2	Angle between aircraft velocity vector and aircraft to missile line of sight
θ_{GA}	Vertical radar gimbal angle
θ_{LOS}	Depression angle of line of sight
λ	Radar signal wavelength - ft
$\bar{\lambda}$	Adjoint vector in first order gradient algorithm
ρ	Atmospheric air density - slug/ft ³
σ_x	Arc length of corange spatial extent - ft
τ	Free air temperature - °R
ϕ	Angular displacement of missile velocity vector from line of sight
ψ, θ, ϕ	Euler transformation angles representing yaw, pitch, and bank angles of missile
ψ_A, θ_A, ϕ_A	Euler transformation angles representing yaw, pitch, and bank angles of aircraft
ψ_B	Bias angle between missile heading and heading of line of sight
ψ_f	Missile heading at line of sight intercept
ψ_{GA}	Horizontal radar gimbal angle

ψ_I	Computed initial intercept heading
ψ_{LOS}	Heading of line of sight
ψ_{ST}	Heading of line of sight at start of intercept turn
$\bar{\omega}_{GA}$	Angular velocity of line of sight relative to aircraft body frame (vector)
$\bar{\omega}_{GI}$	Angular velocity of line of sight relative to inertial reference frame (vector)
ω_z	Rotation rate of line of sight

Abstract

The compatibility of a representative 500 pound weight boost-glide air-to-ground missile with the trajectory constraints imposed by a Synthetic Aperture Radar - Retransmission guidance system was investigated using a digital flight simulation. A demonstration flight profile was assumed, with a minimum of 20 seconds of tracking on the aircraft-to-target line of sight required. A guidance algorithm was developed which produced satisfactory trajectories. A first order gradient technique was employed in an unsuccessful attempt to optimize the trajectories for maximum range. A useable launch envelope for this missile was determined. The azimuthal extent of the envelope was limited by radar system constraints to ^{deg} 15°-90° from the aircraft velocity vector. A maximum slant range of 21 nautical miles was obtained from a launch altitude of 35,000 ft. Range deteriorated rapidly with decreasing launch altitude, with 5,000 ft being the lowest altitude at which a useable launch envelope was obtained. Maximum slant range at 5,000 ft launch altitude was 5.5 nautical miles.

PERFORMANCE OF AN AIR-TO-GROUND MISSILE
EMPLOYING SAR-RETRAN GUIDANCE

I. Introduction

Background

Synthetic Aperture Radar (SAR) is a coherent, pulse-doppler radar which is capable of finer azimuth resolution than conventional non-coherent radars. It is also capable of distinguishing small surface targets from background clutter and can track such targets. With these capabilities, SAR is a prime candidate for an all-weather guidance system for tactical air-to-ground missiles. However, the operation of SAR imposes some unique trajectory requirements on the missile.

SAR attains fine azimuth resolution by utilizing a relative velocity discrimination approach (Ref 1: 4.d.(2)-3). An array of points located at the same range R from an aircraft-mounted SAR is depicted in Figure 1. Each of these points has a velocity relative to the radar antenna of

$$V = V_A \cos \theta \quad (1)$$

where V_A is the velocity of the aircraft and θ is the angular displacement of the point from the aircraft velocity vector (squint angle). This relative velocity will produce a doppler frequency shift in the reflected radar signal of

$$f_d = \frac{2V_A \cos \theta}{\lambda} \quad (2)$$

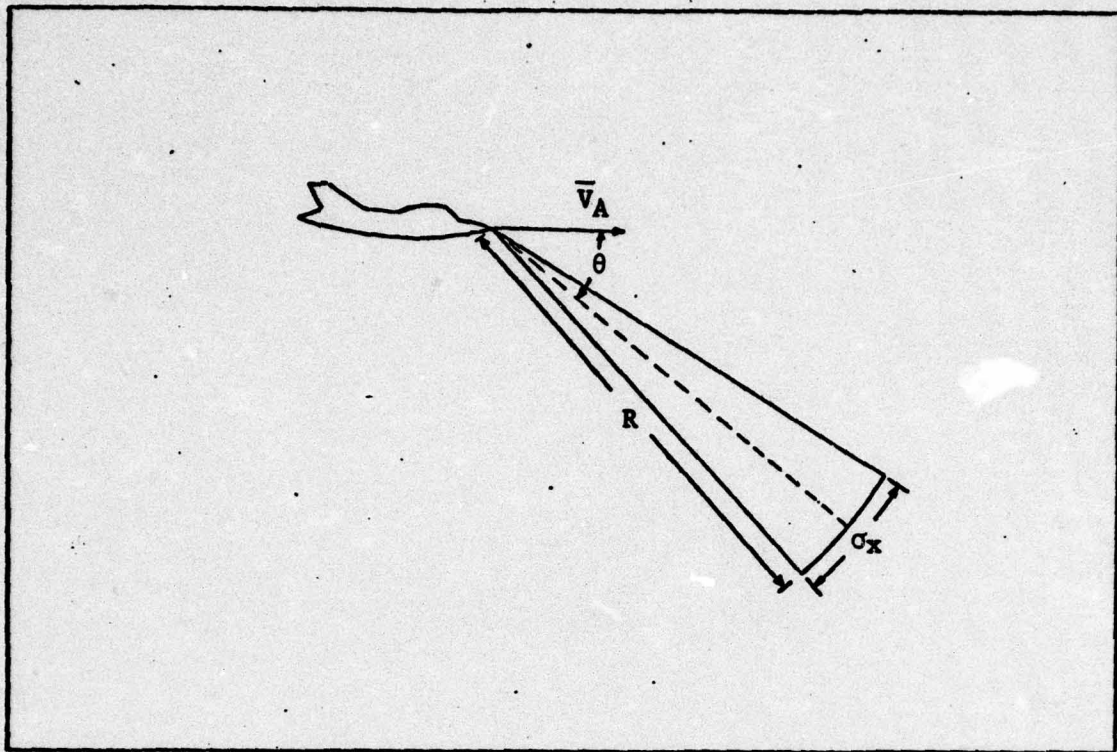


Fig. 1 Velocity Discrimination of a Corange Spatial Extent

Thus, a corange linear extent σ_x can be described by the doppler frequency interval between its endpoints

$$\Delta f_d = \frac{2V_A}{\lambda R} \sigma_x \sin \theta \quad (3)$$

Because a pulsed-coherent radar utilizes a waveform which is systematically time varying and well defined, it is able to measure these incremental doppler phase shifts and thus distinguish between azimuthal extents smaller than its beam width (aperture); hence, the name Synthetic Aperture Radar (Ref 1: 4.d.(2)-4). It should be noted that SAR requires the aircraft velocity vector to be displayed from the line of sight between the radar antenna and the target of interest. Therefore, the aircraft cannot fly directly toward the

target but must fly past or about the target.

One technique for guiding an air-to-ground missile using SAR could be to locate and track the target with an aircraft-mounted SAR and command guide the missile to the target. Under this scheme, the terminal accuracy of the system could be no better than the minimum resolution of the SAR, which decreases as the aircraft's range from the target increases. It would be more desirable to have a convergent guidance system whereby resolution, and hence accuracy, can be refined as the missile approaches the target. One way of obtaining such convergent guidance is through a technique called retransmission (SAR-Retran). With SAR-Retran, the missile is command guided into the radar beam while an antenna aboard the missile receives the reflected radar signal and retransmits this signal to the aircraft. When the missile is squarely on the aircraft-to-target line of sight, the doppler phase shift of the retransmitted signal will be identical to that of the direct reflected signal received by the aircraft's antenna. Now the SAR-Retran system can "see" the target through the missile's antenna as it tracks the line of sight to the target. As the missile closes on the target, the system's resolution increases, concurrently improving terminal accuracy. It is important for the missile to precisely track the line of sight in the terminal phase, for if it is displaced from the line of sight, an additional phase shift will result (more fully discussed in Section II) causing inaccuracy in target resolution.

The requirement for aircraft velocity vector offset causes the aircraft-to-target line of sight to rotate about the target as the

aircraft flies by. Thus, the missile must intercept this rotating line of sight, then must track the line of sight for a minimum period of time in the terminal phase.

Problem

The Air Force Avionics Laboratory is considering available air-to-ground missiles for flight test and demonstration of the SAR-Retrans system. However, the trajectory constraints imposed by the SAR-Retrans technique far exceed the original design criteria of the missiles in the current inventory. Therefore, the aerodynamic compatibility of these missiles with SAR-Retrans must be demonstrated by computer simulation before flight testing is undertaken (Ref 2:1).

Purpose of Study

This study investigates, through computer simulation, the ability of a representative boost-glide air-to-ground missile to fly the trajectories required by SAR-Retrans guidance. The constraints which must be satisfied are:

1. A minimum of 20 seconds tracking of the line of sight prior to target impact. The missile is considered "on" the line of sight when the retransmitted frequency error is less than or equal to 8 Hz. (Constraints imposed by radar and guidance system.)
2. Terminal velocity at target impact must be greater than 700 ft/sec (minimum missile maneuvering speed).

An attempt was made to maximize launch range by applying the results of a first order gradient optimization scheme to the guidance algorithm.

Range-altitude envelopes from which the aforementioned constraints can be satisfied were determined.

Scope

1. A hypothetical missile characteristic of a boost-glide air-to-ground missile will be considered. This missile will be referred to as the Retran Missile.

2. This study is limited to the aerodynamic performance of the representative missile. It is assumed that all other elements of the guidance system operate perfectly.

3. The study concentrates on determining the mid-course trajectories and required guidance algorithms. Tracking of the line of sight in the terminal phase was accomplished; however, terminal guidance and accuracy were not among the goals of this thesis.

4. Optimization of the midcourse trajectory to achieve maximum launch range was attempted. The results of this optimization were considered in formulating the guidance algorithms; however, the resulting trajectories are not necessarily optimal for any launch conditions.

5. Launch envelopes were determined for demonstration flight conditions. The target was stationary and the aircraft did not make tactical maneuvers.

6. The stability of the guidance loop with the missile autopilot was investigated. Modifications in commands and biases provided to the autopilot were made but the circuitry and mechanization remained unchanged from the standard autopilot.

II. Analytic Formulation of the Missile Flight Simulation

The Retran Missile simulation program numerically integrates the missile equations of motion over the time of flight to determine the time history of missile velocity, attitude, and position. The program also updates the launching aircraft's position, computes guidance commands, simulates the missile autopilot to determine control deflections, calculates the retransmitted doppler frequency error and determines when target impact is accomplished. The mathematical relationships used in the program are presented here, while the program itself is discussed in Section IV.

Basic Assumptions

The following assumptions are incorporated in the Retran Simulation:

1. The target remains stationary.
2. Perfect target tracking is achieved by the radar system.
3. The aircraft's radar antenna gimbal angles are physically limited to ± 95 degrees.
4. Missile accelerometers and rate gyros are error-free.
5. Through data link of missile accelerometer and rate gyro outputs back to the guidance computer aboard the aircraft, the computer can determine accurate missile position, velocity, and attitude.
6. Missile roll control operates perfectly.

The Missile Model

The hypothetical missile used in this study will be referred to as the Retran missile. This missile is pictured in Fig. 2. Its size, aerodynamic characteristics and performance are representative of a boost-glide air-to-ground missile in the 500 lb. weight class.

The physical dimensions of the missile are listed in Table I, the mass properties are presented in Table II and the thrust schedule of the two-stage solid propellant motor is given in Table III.

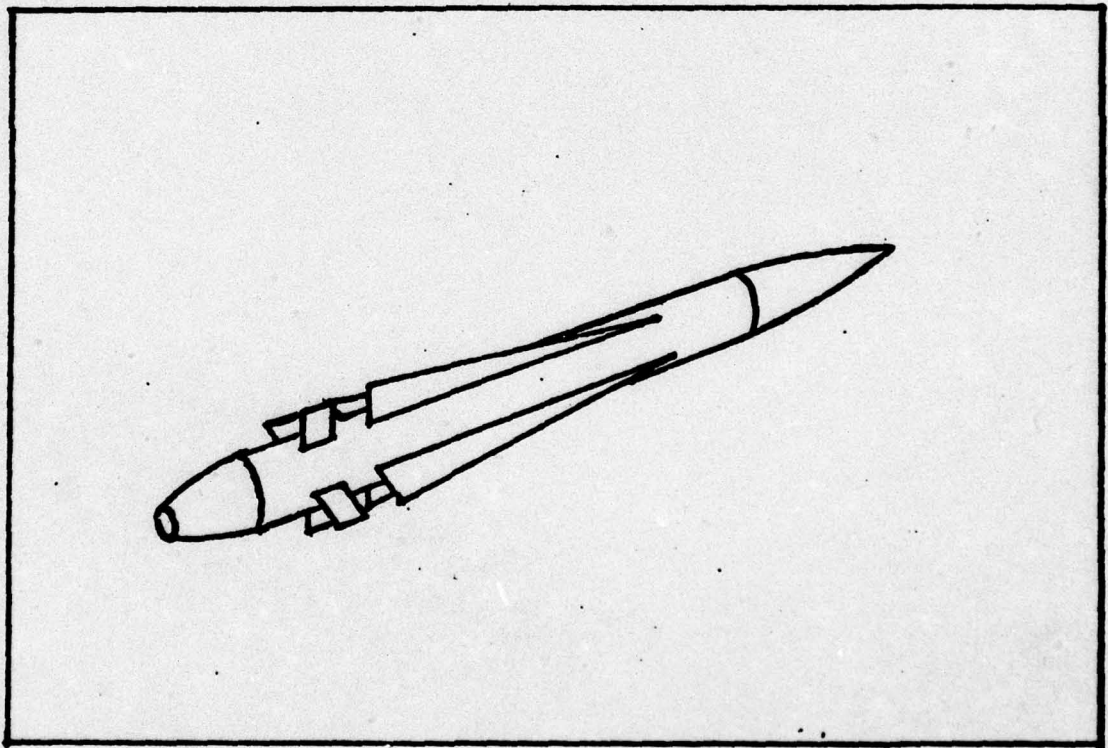


Fig. 2 The Retran Missile

Table I
Physical Dimensions of the Retran Missile

Overall Length (in.)	120.0
Maximum Diameter (in.)	12.3
Wing Planform Area (in. ²) (2 Wings)	475.0
Control Surface Planform Area (in. ²) (2 Surfaces)	105.0
Aerodynamic Reference Area (in. ²)	.825

Table II
Mass Properties of the Retran Missile

Time (sec.)	0.0	0.6	4.5
Weight (lb.)	500.0	460.0	400.0
Center of Gravity (in.)	55.0	54.0	52.0
I _{xx} (slug-ft ²)	2.5	2.5	2.5
I _{yy} (slug-ft ²)	67.0	64.0	58.0
I _{zz} (slug-ft ²)	67.0	64.0	58.0

Table III
Thrust Schedule of the Retran Missile

	<u>Burn Time (sec.)</u>	<u>Thrust (lb.)</u>
1st Stage	0.0-0.6	9500
2nd Stage	0.6-4.5	2000

Note: Thrust is assumed to be constant throughout burn time.

The missile is aerodynamically symmetrical about the longitudinal axis. Therefore, the normal force and pitch moment coefficients are used for both pitch and yaw. The aerodynamic coefficient curves are presented in Figs. 3 thru 11. These coefficients are:

- C_{D_0} - Zero lift drag coefficient at sea level
- ΔC_{D_f} - Skin friction drag coefficient (corrects C_{D_0} for altitude)
- C_C - Chord force coefficient with no control
- ΔC_C - Incremental chord force coefficient due to control
($C_C + \Delta C_C$ account for induced drag)
- C_{N_2} - Normal force coefficient with no control
- C_{N_1} - Incremental normal force coefficient due to control
- C_{m_2} - Pitch moment coefficient with no control
- C_{m_1} - Incremental pitch moment coefficient due to control
- C_{m_q} - Pitch damping coefficient

A block diagram of the missile control system model incorporated in the simulation is presented in Fig. 12. The system includes two accelerometers aligned with the Y_b and Z_b axes and two rate gyros aligned in the planes of the wings. A roll channel which generates differential displacements of opposite surfaces to maintain $P=0$ is assumed to operate perfectly and is not modeled in the simulation. A vertical g-bias acceleration is normally added to the vertical acceleration command in order to maintain missile trajectory above the line of sight in the early part of the flight for terrain clearance (use of the

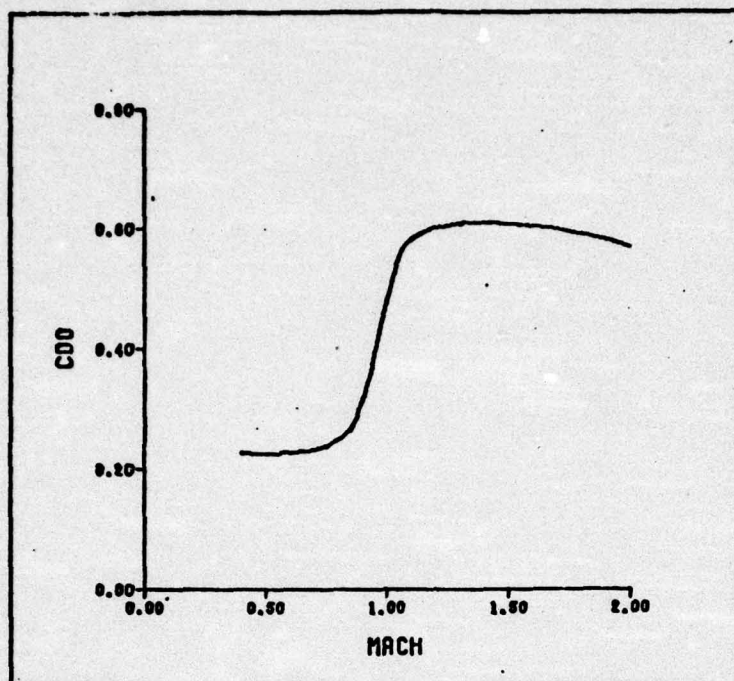


Fig. 3 Zero Lift Drag Coefficient at Sea Level

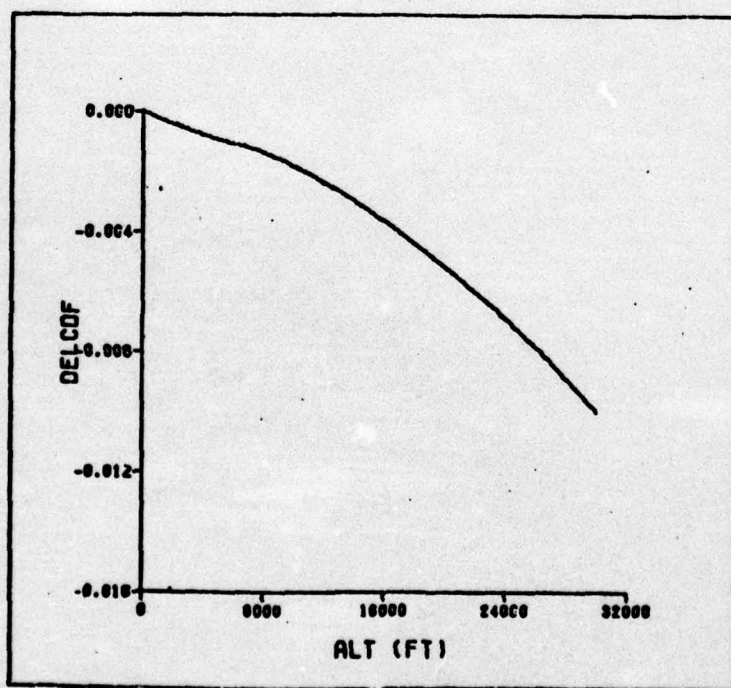


Fig. 4 Skin Friction Drag Coefficient

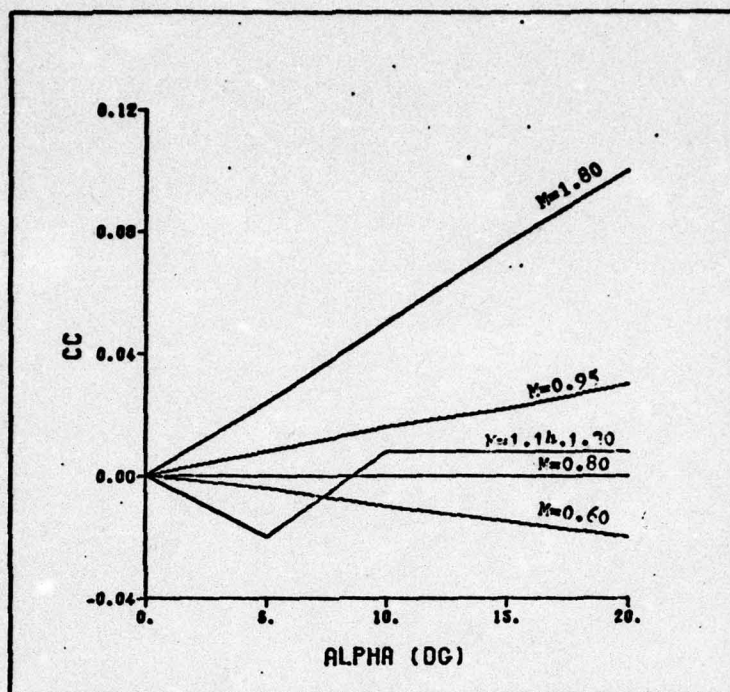


Fig. 5 Chord Force Coefficient With No Control

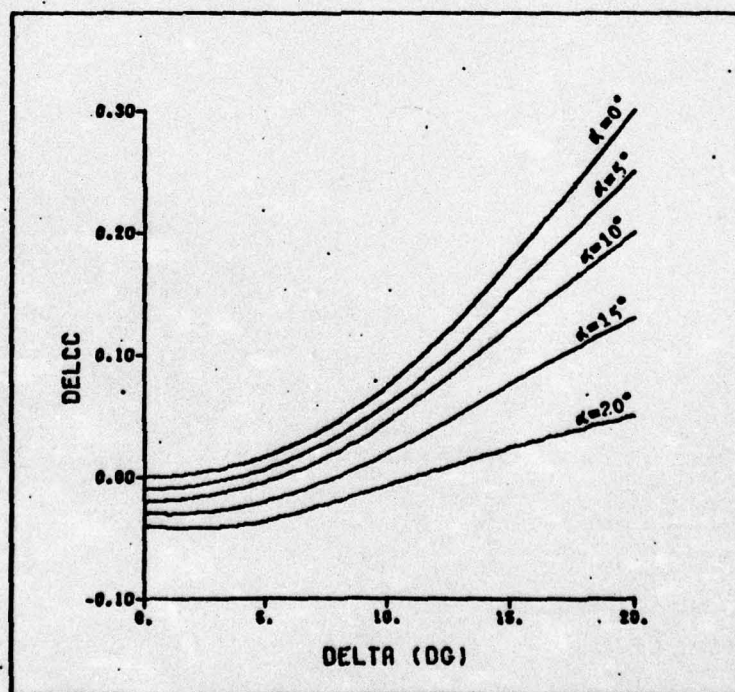


Fig. 6 Incremental Chord Force Coefficient Due to Control

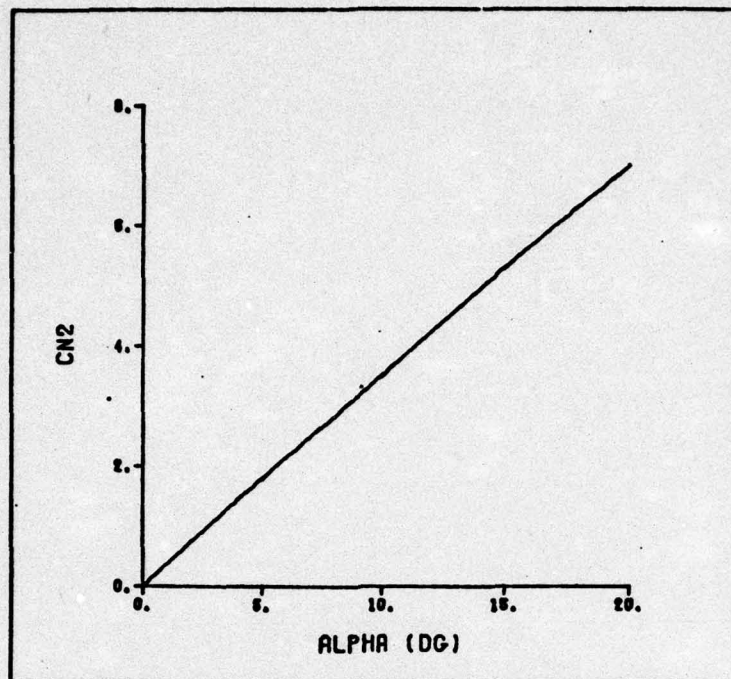


Fig. 7 Normal Force Coefficient With No Control

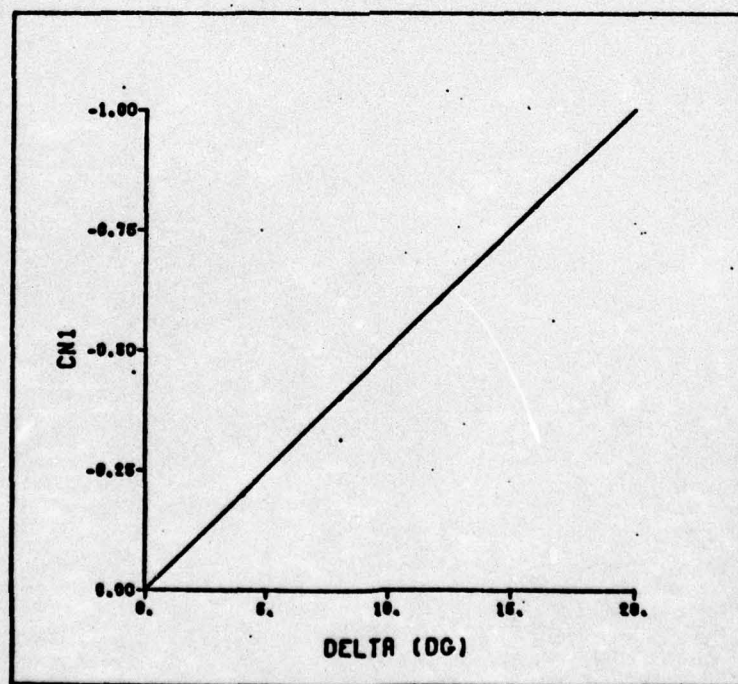


Fig. 8 Incremental Normal Force Coefficient Due to Control

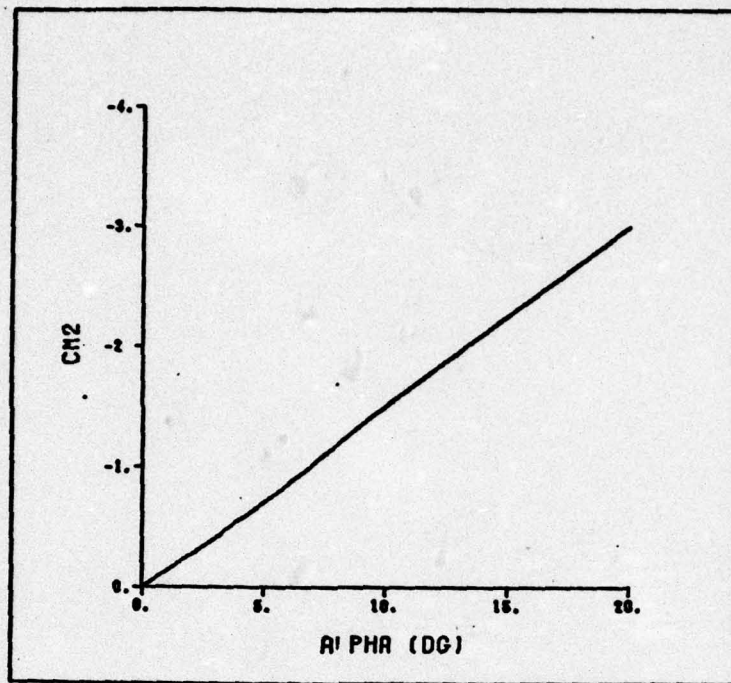


Fig. 9 Pitch Moment Coefficient With No Control

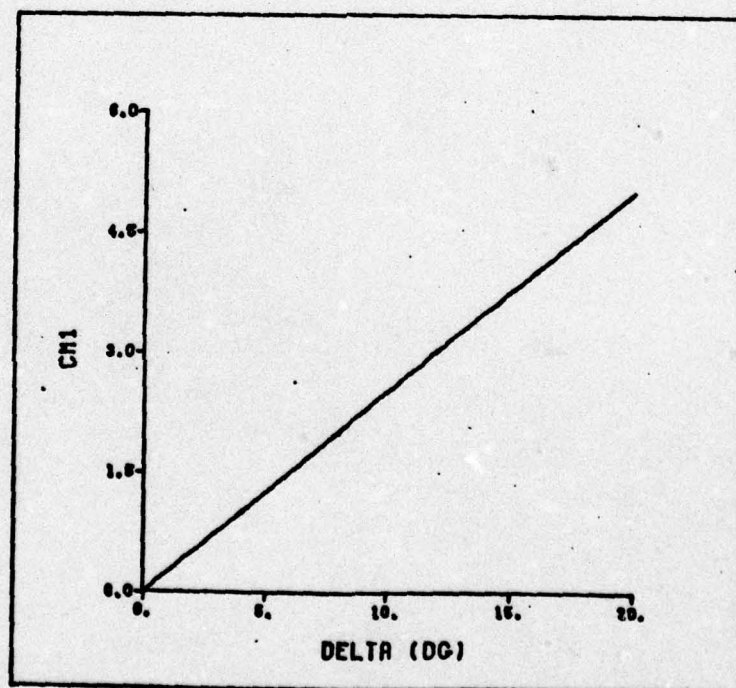


Fig. 10 Incremental Pitch Moment Coefficient Due to Control

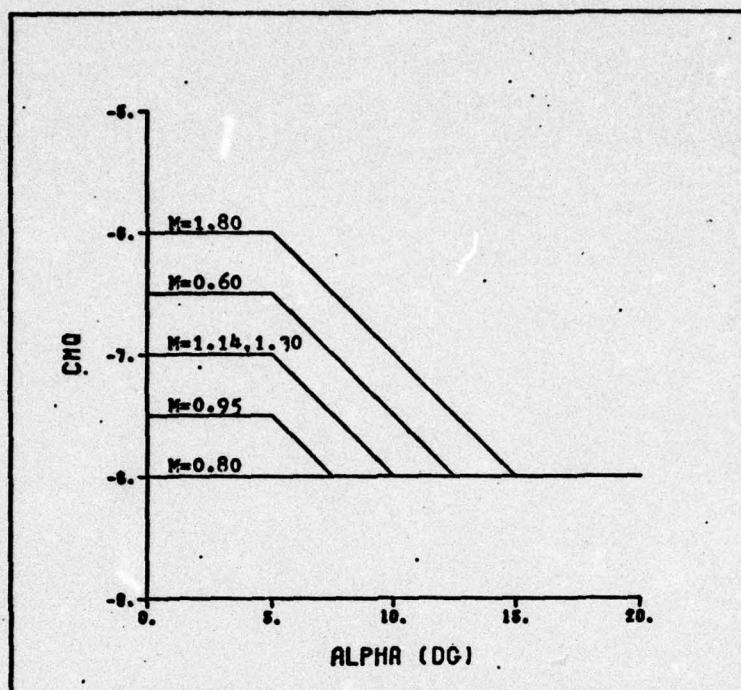


Fig. 11 Pitch Damping Coefficient

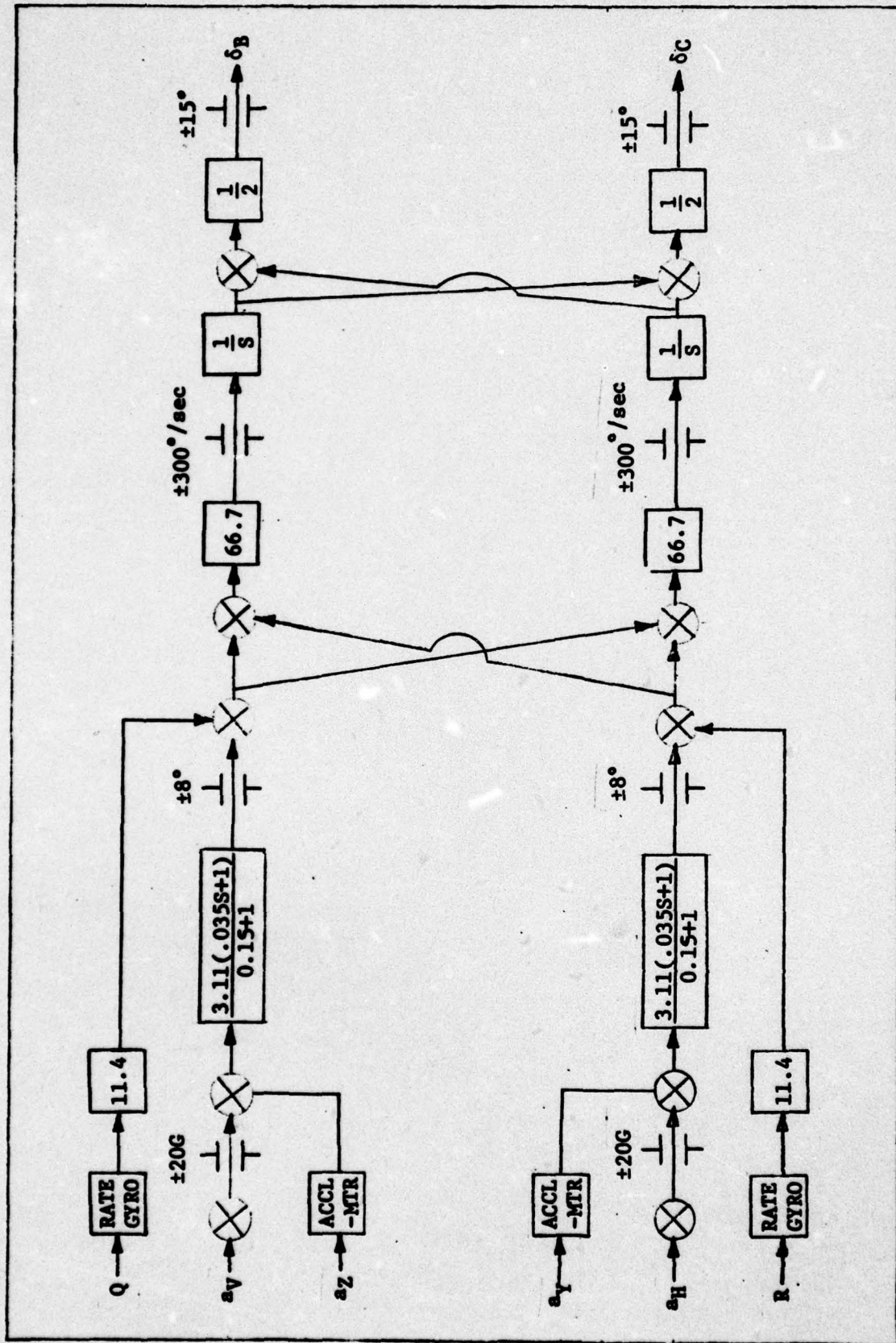


Fig. 12 Retran Control System Model

g-bias in this study is discussed in Section VI). A guidance delay is incorporated to allow for safe separation from the carrier aircraft. Thus, no accelerations are commanded for the first .7 seconds and while longitudinal acceleration is greater than 9.5 g's.

Effective pitch and yaw surface deflections are calculated. These are defined as

$$\delta_B = \frac{-(\delta_1 + \delta_3) + (\delta_2 + \delta_4)}{4} \sqrt{2} \quad (4)$$

$$\delta_C = \frac{(\delta_1 + \delta_3) + (\delta_2 + \delta_4)}{4} \sqrt{2} \quad (5)$$

where δ_1 , δ_2 , δ_3 and δ_4 are the actual control surface deflections.

Reference Frames

Four reference frames are employed in the Retran Simulation: an earth fixed frame, a missile body frame, an aircraft body frame and an antenna gimbal frame. The missile body frame is fixed in the missile airframe and is obtained from the earth fixed frame by a 3-2-1 rotation through Euler angles ψ , θ and ϕ . This rotation is illustrated in Fig. 13. Similarly, the aircraft body frame is obtained by a 3-2-1 rotation through angles ψ_A , θ_A and ϕ_A . The antenna gimbal frame is obtained from the aircraft body frame by a 3-2 rotation through angles ψ_{GA} and θ_{GA} . The gimbal frame X axis is always aligned along the aircraft to target line of sight.

Transformations between reference frames are presented in Appendix A. The transformations are calculated on the basis of instantaneous angular relationships.

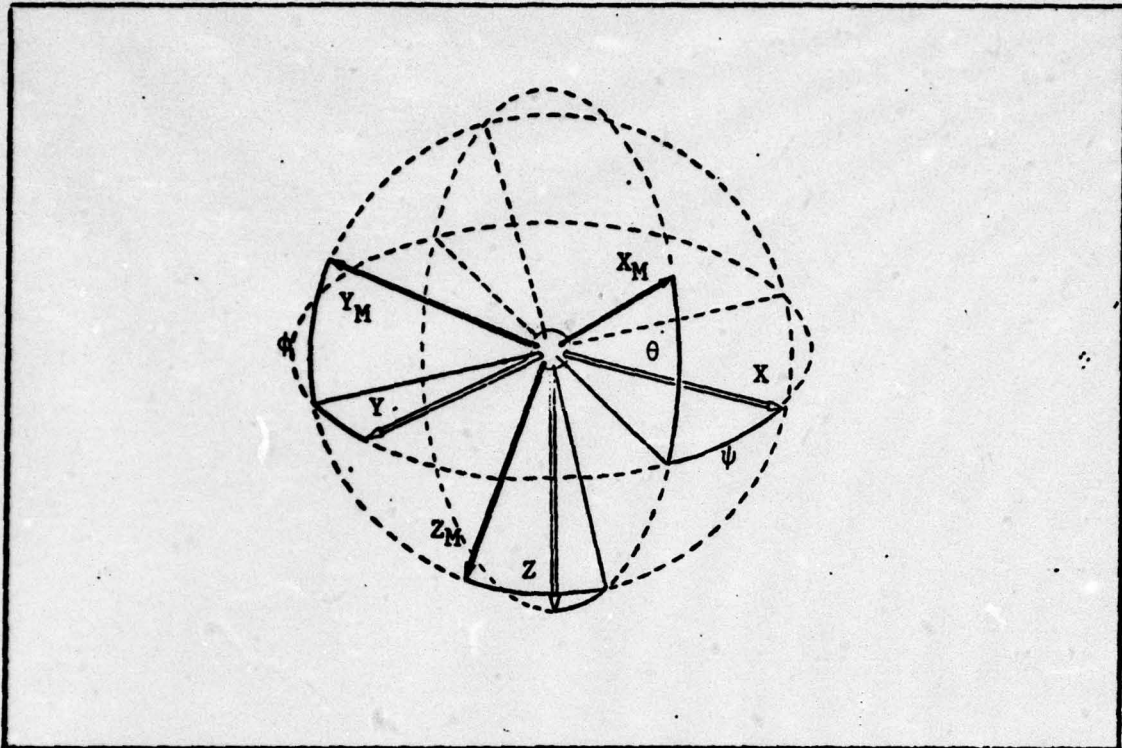


Fig. 13 3-2-1 Euler Angle Transformation

Equations of Motion

The Retran missile is symmetrical about its longitudinal axis; hence, the missile body axes are principal axes and the moments of inertia are I_{xx} , $I_{yy} = I_{zz}$ and $I_{xy} = I_{xz} = I_{yz} = 0$. Consequently, the missile equations of motion are (Ref 3: 2.24)

$$m(\dot{U} - VR + WQ) = -mg \sin\theta + Ax + T \quad (6)$$

$$m(\dot{V} + UR - WP) = mg \sin\phi \cos\theta + A_y \quad (7)$$

$$m(\dot{W} - UQ + VP) = mg \cos\phi \cos\theta + A_z \quad (8)$$

$$I_{xx}\dot{P} = L \quad (9)$$

$$I_{yy}\dot{Q} + (I_{xx} - I_{zz})PR = M \quad (10)$$

$$I_{zz}\dot{R} + (I_{yy} - I_{xx})PQ = N \quad (11)$$

These equations neglect the rate of change of mass and moments of inertia because these rates are small after the first stage burnout, while no flight maneuvering is commanded prior to first stage burnout.

The Retran simulation assumes that the autopilot roll channel operates perfectly in nulling roll rate. Therefore, it is assumed that $P=0$ and $L=0$. Incorporating this assumption, the equations of motion become:

$$\dot{U} = \frac{A_x + T}{m} - g \sin\theta - QW + RV \quad (12)$$

$$\dot{V} = \frac{A_y}{m} + g \cos\theta \sin\phi - RU \quad (13)$$

$$\dot{W} = \frac{A_z}{m} + g \cos\theta \cos\phi + QU \quad (14)$$

$$\dot{P} = 0 \quad (15)$$

$$\dot{Q} = [M + (I_{zz} - I_{xx})PR]/I_{yy} \quad (16)$$

$$\dot{R} = [N + (I_{xx} - I_{yy})PQ]/I_{zz} \quad (17)$$

The aerodynamic forces and moments are determined by the equations:

$$A_x = -[C_{D0} + \Delta C_C + C_C + \Delta C_{Df}] q S \quad (18)$$

$$A_y = -[C_{N2} - C_{N1} \operatorname{sgn}(\delta_C)] q S \quad (19)$$

$$A_z = -[C_{N2} - C_{N1} \operatorname{sgn}(\delta_B)] q S \quad (20)$$

$$M = [C_{mq} \frac{Qd}{2V_M} + C_{M2} - C_{M1} \operatorname{sgn}(\delta_B)] q S d \quad (21)$$

$$N = [C_{mq} \frac{Rd}{2V_M} - C_{M2} + C_{M1} \operatorname{sgn}(\delta_C)] q S d \quad (22)$$

where d is a reference length: $d = 1$ ft.

Aircraft Maneuvering and Rotation of the Line of Sight

Following missile launch, the aircraft is assumed to fly a nearly constant arc about the target, maintaining a horizontal radar gimbal angle of $85^\circ \pm 7^\circ$. The aircraft initially turns away from the target until the commanded gimbal angle is reached, then turns on its arcing maneuver. The aircraft maintains constant airspeed and altitude. Bank and pitch angles are neglected, and the aircraft is assumed to accomplish the turning maneuver through heading change only.

Two parameters which are utilized in the guidance algorithms are the angular orientation of the line of sight and its rotation rate. Angular orientation is determined by first calculating the radar antenna gimbal angles, which could be measured directly in the physical mechanization of the system. These angles are calculated by determining the position of the target relative to the aircraft in the aircraft body frame. This position is located by the position vector

$$\bar{R}_{AT} = X_{AT} \bar{i}_A + Y_{AT} \bar{j}_A + Z_{AT} \bar{k}_A \quad (23)$$

From the geometry of this relationship, as shown in Fig. 14, the gimbal angles can be determined:

$$\theta_{GA} = \sin^{-1} \frac{Z_{AT}}{[R_{AT}]} \quad (24)$$

$$\psi_{GA} = \sin^{-1} \frac{Y_{AT}}{[R_{AT}] \cos \theta_{GA}} \quad (25)$$

Since aircraft bank and pitch angles are assumed to be zero, ψ_{GA} may be added to the aircraft heading ψ_A to obtain the heading of the

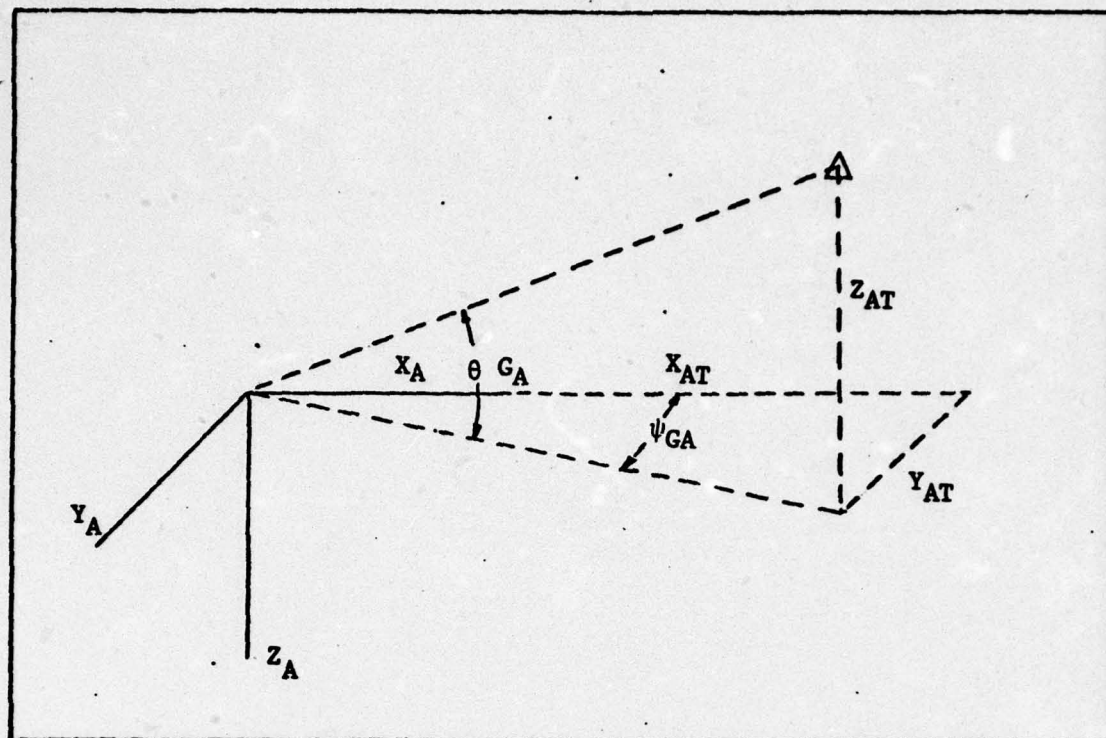


Fig. 14 Gimbal Angles

line of sight in the earth fixed frame:

$$\psi_{LOS} = \psi_A + \psi_{GA} \quad (26)$$

To determine the rotation rate of the line of sight, the antenna gimbal angle rates are determined first, as these rates could be measured in the actual mechanization. The velocity of the target relative to the aircraft in the aircraft body frame is

$$\frac{d}{dt} {}^A(\bar{R}_{AT}) = \frac{d}{dt} \left[{}^G(\bar{R}_{AT}) + \bar{\omega}_{GA} \times \bar{R}_{AT} \right] \quad (27)$$

Since the aircraft is flying a nearly constant radius arc about the target, $\frac{d}{dt} {}^G(\bar{R}_{AT})$ can be neglected. Now the angular velocity of the gimbal frame relative to the aircraft can be determined from the relationship:

$$\bar{\omega}_{GA} \times \bar{R}_{AT} = \frac{d}{dt} {}^A(\bar{R}_{AT}) \quad (28)$$

where $\bar{\omega}_{GA} = \dot{\theta}_{GA} \bar{j}_G + \dot{\psi}_{GA} \bar{k}_A$. The gimbal angle rates are therefore:

$$\dot{\psi}_{GA} = \frac{\dot{Y}_{AT}}{R_{AT} \cos \theta_{GA}} \quad (29)$$

$$\dot{\theta}_{GA} = - \frac{\dot{Z}_{AT}}{R_{AT}} \quad (30)$$

Again, since the aircraft is in level flight, the rotation rate of the line of sight, defined as the vertical component of the angular velocity of the line of sight, can be found by adding the horizontal gimbal angle rate to the turning rate of the aircraft:

$$\omega_Z = \dot{\psi}_{GA} + \dot{\psi}_A \quad (31)$$

Determination of Missile Position and Velocity Errors

The distance of the missile normal to the line of sight and the velocity component of the missile normal to the line of sight are determined for use in the guidance algorithms.

The distance normal to the line of sight is defined by the Y_{AM} and Z_{AM} components of missile position relative to the aircraft in the gimbal frame, as shown in Fig. 15. These are obtained by transformation from the earth fixed frame:

$$\begin{bmatrix} \Delta X \\ \Delta Y \\ \Delta Z \end{bmatrix}_G = [L_{GI}] \begin{bmatrix} X_{AM} \\ Y_{AM} \\ Z_{AM} \end{bmatrix}_I \quad (32)$$

Likewise, the velocity of the missile normal to the line of sight is determined by finding the velocity of the missile relative to the aircraft in the gimbal frame:

$$\frac{d}{dt} {}^G \bar{R}_{AM} = \frac{d}{dt} [{}^I \bar{R}_{AM}] - \bar{\omega}_{GI} \times \bar{R}_{AM} \quad (33)$$

The vertical and horizontal components of this relative velocity, \dot{Y} and $\dot{\Delta Z}$, are then the velocities normal to the line of sight, as shown in Fig. 15:

$$\begin{bmatrix} \dot{\Delta X} \\ \dot{\Delta Y} \\ \dot{\Delta Z} \end{bmatrix}_G = [L_{AI}] \begin{bmatrix} \dot{X}_{AM} - \omega_Z Y_{AM} + \omega_Y Z_{AM} \\ \dot{Y}_{AM} + \omega_Z X_{AM} - \omega_X Z_{AM} \\ \dot{Z}_{AM} - \omega_Y X_{AM} + \omega_X Y_{AM} \end{bmatrix}_I \quad (34)$$

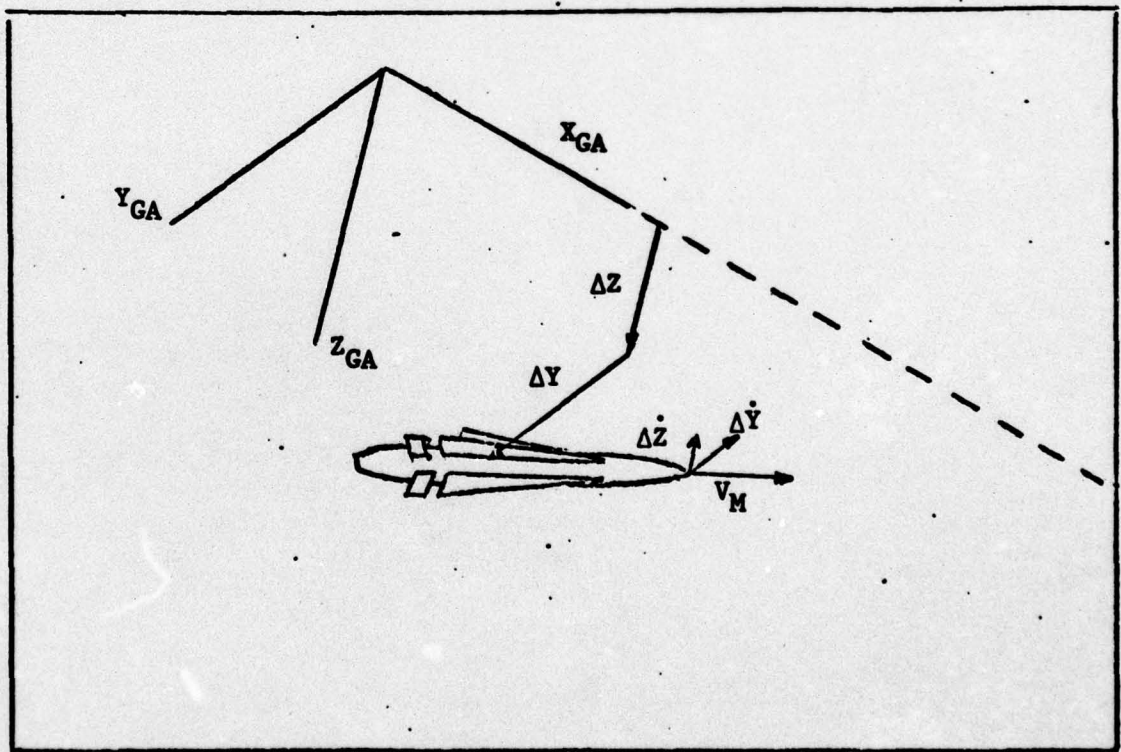


Fig. 15 Missile Position and Velocity Errors

The Guidance Algorithms

The guidance algorithms which were incorporated into the simulation for the launch envelope studies are presented here. Other guidance algorithms which were tested and rejected are discussed in Appendix E. How and why these guidance algorithms were chosen is revealed in Section VI.

Three guidance algorithms were utilized: one to determine acceleration commands in the vertical plane of the gimbal frame and two to determine commands in the horizontal plane of the gimbal frame. These commands were then transformed to the missile body frame before being input to the missile autopilot.

The Vertical Algorithm

In the gimbal frame vertical plane, $X_g Z_g$, the missile is always commanded to intercept and track the line of sight. Acceleration commands are proportional to the missile's vertical distance normal to the line of sight, ΔZ , and to its vertical velocity normal to the line of sight, $\dot{\Delta Z}$. The algorithm is similar to the algorithm for a beam riding missile discussed by J. Clemow in reference 4 (Ref 4: 48). A g-bias was added for trajectory shaping. Note that the vertical acceleration a_v is commanded in the $-\bar{k}_g$ direction. The vertical algorithm is:

$$a_v = 2\zeta \left(k_1 \frac{t_R}{t_{tg}}\right) \Delta \dot{Z} + \left(k_1 \frac{t_R}{t_{tg}}\right)^2 \Delta Z + g_{bias} \quad (35)$$

The term $k_1 \frac{t_R}{t_{tg}}$ is analogous to the natural frequency ω_n of a damped second order system, where k_1 is an arbitrary constant, t_{tg} is the time-to-go to target impact and t_R is an arbitrary reference time which corresponds very roughly to the desired line of sight tracking time. The factor $\frac{t_R}{t_{tg}}$ in effect increases the guidance system gain with decreasing time-to-go in order to speed system response as the target is approached. ζ represents the damping ratio of the system. The values chosen for these parameters are discussed in sections V and VI.

The Horizontal Algorithms

In the early portion of the flight, one of two horizontal algorithms is employed, the choice of algorithm depending upon missile position relative to the line of sight after the first two seconds of flight. If the missile remains ahead of the line of sight ($+\Delta Y$), then the missile is commanded to turn to a heading parallel to the line of sight. Since the line of sight is rotating toward the missile, it will catch up to the missile, at which point the guidance system reverts to command-to-track the line of sight. If the missile falls behind the line of sight ($-\Delta Y$) then the command-to-track algorithm is employed throughout the flight.

The command-to-heading algorithm calculates a commanded acceleration parallel to the earth-fixed XY plane and perpendicular to the missile longitudinal axis. The acceleration commanded is proportional to the angular error between missile heading and the heading of the line of sight:

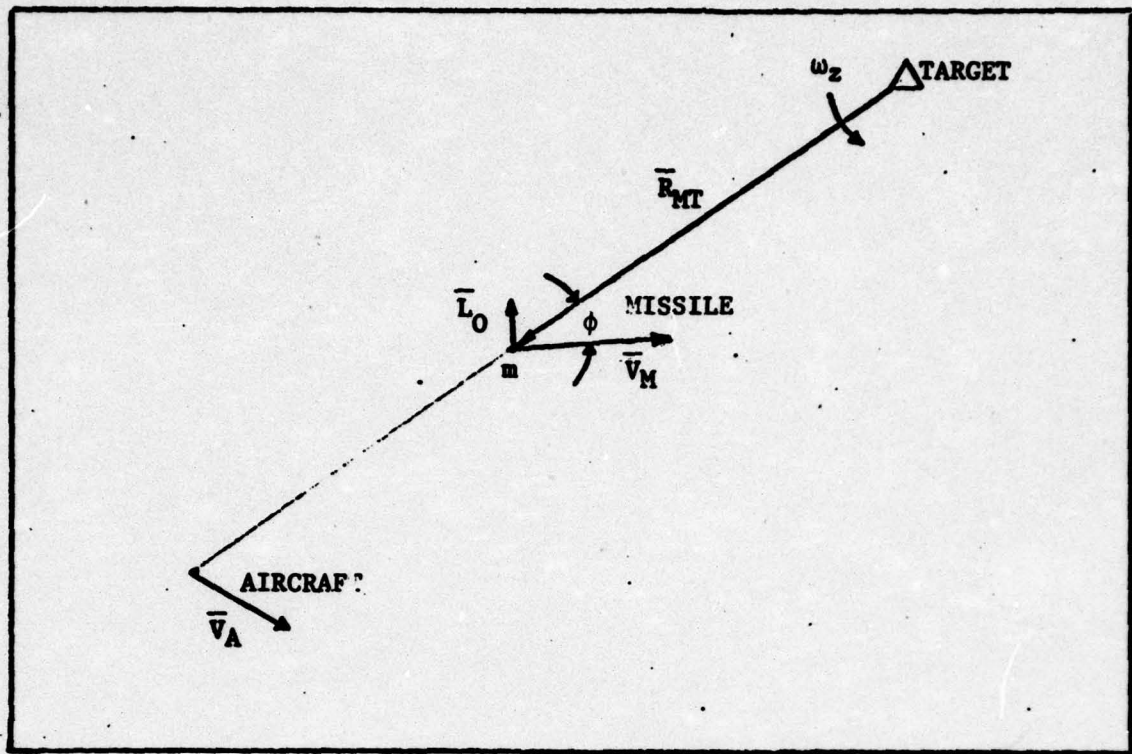
$$a_{hT} = C_T (\psi_{LOS} - \psi) \left[\frac{C_R \cdot T_R}{R_{MT}} \right]^2 \quad (36)$$

C_R is a constant chosen to convert the reference time T_R into an equivalent reference range and R_{MT} is the missile-to-target range, so that system gain in this case increases with decreasing range to the target. C_T is an arbitrary proportionality constant. Again, discussion of the values chosen for the constants is presented in sections V and VI. a_{hT} is transformed into components a_{xg} and a_{hg} in the gimbal frame.

The horizontal command to track algorithm is similar to the vertical algorithm except that in place of a g-bias term a feed-forward rotational bias term is included. This term provides the acceleration required to maintain the missile on the rotating line of sight with zero displacement error. The algorithm is

$$a_h = -2\zeta \left(k_1 \frac{t_R}{t_{tg}} \right) \Delta \dot{Y} - \left(k_1 \frac{t_R}{t_{tg}} \right)^2 \Delta Y + \left(\frac{2\omega_Z V_M}{g} - \frac{R_{MT} \dot{V}_M \omega_Z}{g \cdot V_M} \right) \quad (37)$$

The bias term was determined as follows, assuming that the missile is established on the line of sight in the horizontal ($X_g Y_g$) plane as in Fig. 16. The lateral acceleration required to maintain the rotating line of sight is (Ref 5: 4.d.(1)-3):



$$L_0 = (R_{MT}\dot{\omega}_Z + 2\dot{R}_{MT}\omega_Z) \cos\theta - (\ddot{R}_{MT} - R_{MT}\omega_Z^2) \sin\theta \quad (38)$$

$$L_0 = \frac{R_{MT} \dot{R}_{MT}^{\omega} Z + 2 \dot{R}_{MT}^2 \omega Z - R_{MT} \ddot{R}_{MT}^{\omega} Z + R_{MT}^2 \omega^3 Z}{V_M} \quad (39)$$

$$L_0 = 2V_M \omega_Z - R_{MT} \frac{\dot{V}_M}{V_M} \omega_Z \quad (40)$$

command to slow missile closure on the line of sight so that a smooth interception is accomplished.

Retransmitted Signal Frequency Error

When the missile is displaced from the line of sight, the retransmitted signal travels a path different from the direct reflected path. Because the angular relationships involved in the retransmitted path are different than the direct path, an error is introduced in the doppler shift of the retransmitted signal. These angular relationships are shown in Fig. 17. The error is

$$\Delta f_d = [f_{d1} - f_{d2}] \quad (41)$$

where the doppler frequency of the direct reflected signal is

$$f_{d1} = \frac{1}{\lambda} [2V_A \cos\theta_1] \quad (42)$$

and the doppler frequency of the retransmitted signal is

$$f_{d2} = \frac{1}{\lambda} [V_A \cos\theta_1 + V_M \cos\beta_1 - V_M \cos\beta_2 + V_A \cos\theta_2] \quad (43)$$

The angles θ_1 , θ_2 , β_1 , and β_2 are defined in Fig. 17. A $\lambda = .1$ foot is assumed (X-band radar).

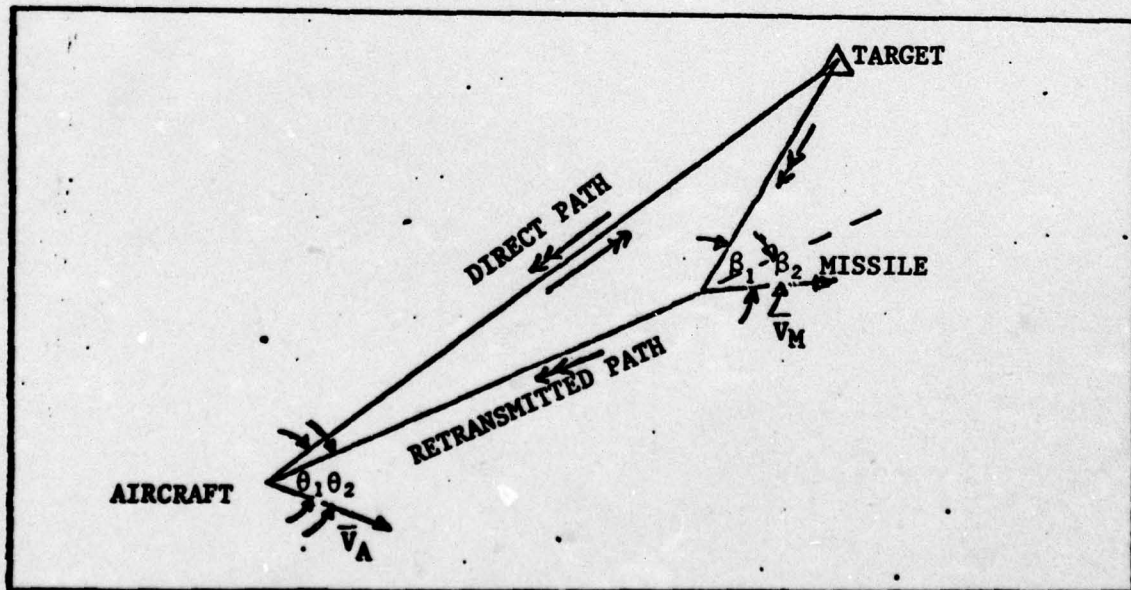


Fig. 17 Retransmitted Radar Signal Path

III. Development of the First Order Gradient Optimization Algorithm

A first order gradient algorithm employing penalty functions was developed in an attempt to optimize the missile trajectory for maximum range. The algorithm is similar to the gradient algorithm employed by Anderson and Smith in reference 6 (Ref 6: 230), which follows the technique described by Kelley in reference 7 (Ref 7: 205-254).

The algorithm, as applied to the SAR-Retran problem, is designed to determine the optimal set of acceleration commands a_h and a_v which produce the trajectory yielding maximum range. The steps used in the algorithm are as follows:

1. The state equations $\dot{\bar{X}}(t)$ are integrated forward, using commands calculated by a guidance algorithm similar to the one employed in the Retran simulation. These commands are stored. Forward integration is terminated when the missile intercepts the line of sight (within 50 feet). This yields $\bar{X}(t)$ and an estimate of the final time t_f .

2. The payoff function J , including penalties, is calculated.

3. The adjoint vector $\bar{\lambda}(t_f)$ is found from

$$\bar{\lambda}^T(t_f) = \partial J / \partial \bar{X}_{t_f} \quad (44)$$

4. The Hamiltonian is calculated:

$$H = \bar{\lambda}^T \cdot \dot{\bar{X}} \quad (45)$$

5. The following differential equation

$$\dot{\bar{\lambda}}^T = - \partial H / \partial \bar{X} \quad (46)$$

is integrated backward to t_0 , using the states obtained from the forward integration. The controls determined from step 1 or the previous step 6 are used. Simultaneously, the gradients $\frac{\partial H}{\partial a_h}(t)$ and $\frac{\partial H}{\partial a_v}(t)$ are calculated and stored.

6. The incremental corrections to the acceleration commands are $\delta a_h(t) = -\alpha \frac{\partial H}{\partial a_h}(t)$ and $\delta a_v(t) = -\alpha \frac{\partial H}{\partial a_v}(t)$. With

$$a_h = a_h(t)_{old} + \delta a_h(t) \quad (47)$$

$$a_v = a_v(t)_{old} + \delta a_v(t) \quad (48)$$

an alpha search is performed to minimize J with respect to α . The new $a_h(t)$ and $a_v(t)$ are stored.

7. Using the new controls resulting from step 6, the state equations are again integrated forward to the stopping condition and steps 2 through 6 are repeated. This process is carried on until J is minimized within the desired tolerance.

The Missile Model

To facilitate the use of the gradient technique, a simplified missile model was developed. Rotational dynamics of the missile were ignored. The missile was assumed to maintain zero bank angle throughout the flight. Aerodynamic coefficient curves were approximated by continuous functions. Small angles were assumed for α and β and control deflections were neglected, except in the determination of ΔC_C .

Equations Of Motion.

Incorporating the above simplifications, the vector equation of the missile is

$$m\dot{\vec{V}}_M = \vec{A}_{x_B} + \vec{A}_{y_B} + \vec{A}_{z_B} + \vec{T} + m\vec{g} \quad (49)$$

which yields the scalar equations

$$\dot{V}_M = \frac{1}{m} [(A_x + T) \cos\alpha \cos\beta + A_y \sin\beta + A_z \sin\alpha \cos\beta] - g \sin\gamma \quad (50)$$

$$\dot{\psi} V_M \cos\alpha = \frac{1}{m} [-(A_x + T) \cos\alpha \sin\beta + A_y \cos\beta - A_z \sin\alpha \sin\beta] \quad (51)$$

$$-\dot{\gamma} V_M = \frac{1}{m} [-(A_x + T) \sin\alpha + A_z \cos\alpha] + g \cos\gamma \quad (52)$$

Aerodynamic Forces

The aerodynamic forces are determined from the relations

$$A_x = -Sq [C_{D0} + C_C + \Delta C_C + \Delta C_{Df}] \quad (53)$$

$$A_y = -Sq [C_{N2} - C_{N1} \operatorname{sgn}(\delta_C)] \quad (54)$$

$$A_z = -Sq [C_{N2} - C_{N1} \operatorname{sgn}(\delta_B)] \quad (55)$$

where S is missile cross-sectional area.

Continuous functions approximating the aerodynamic coefficients were obtained by a least-squares fit to the coefficient curves (using AFITSUBROUTINE PLSQ). These curve fits are illustrated in Figs. 18 through 21. Note that C_C is assumed to be zero (valid for $M = .8$), C_{N1} is assumed to be zero (valid for $\delta = 0$) and the ΔC_C curve selected

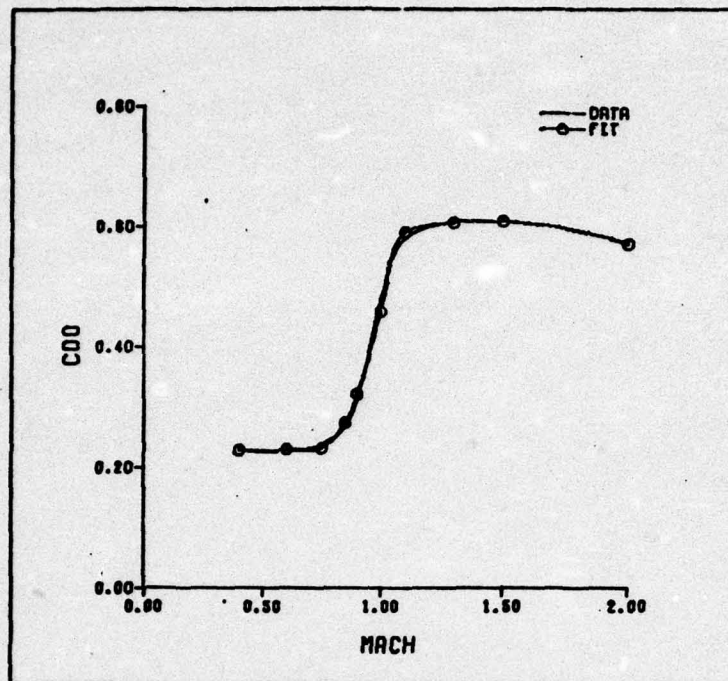


Fig. 18 Least Squares Fit to C_{D0} Curve

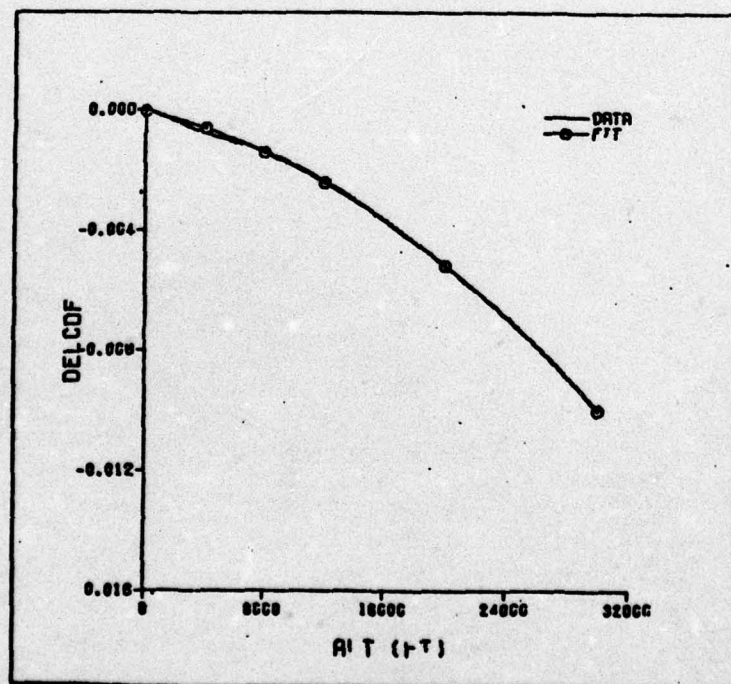


Fig. 19 Least Squares Fit to ΔC_{DF} Curve

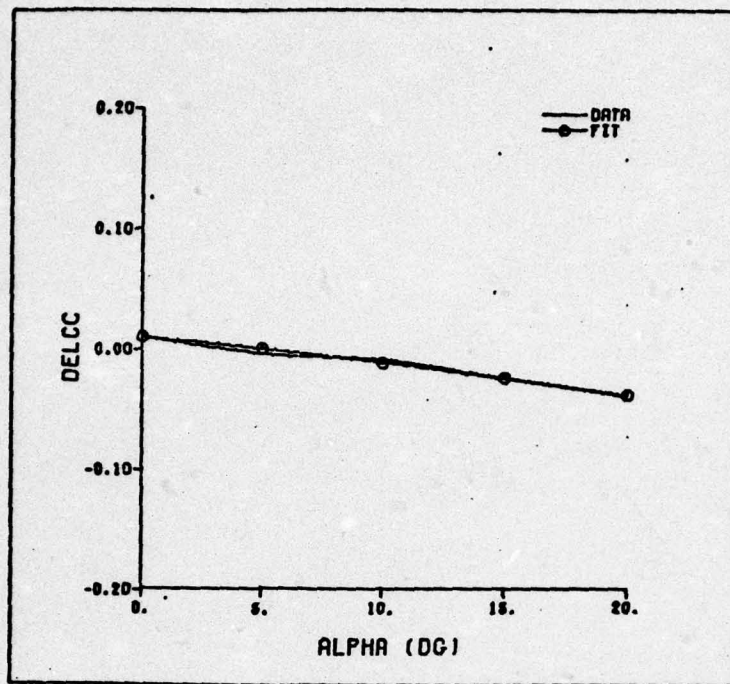


Fig. 20 Least Squares Fit to ΔC_C Curve for $\delta=4^\circ$

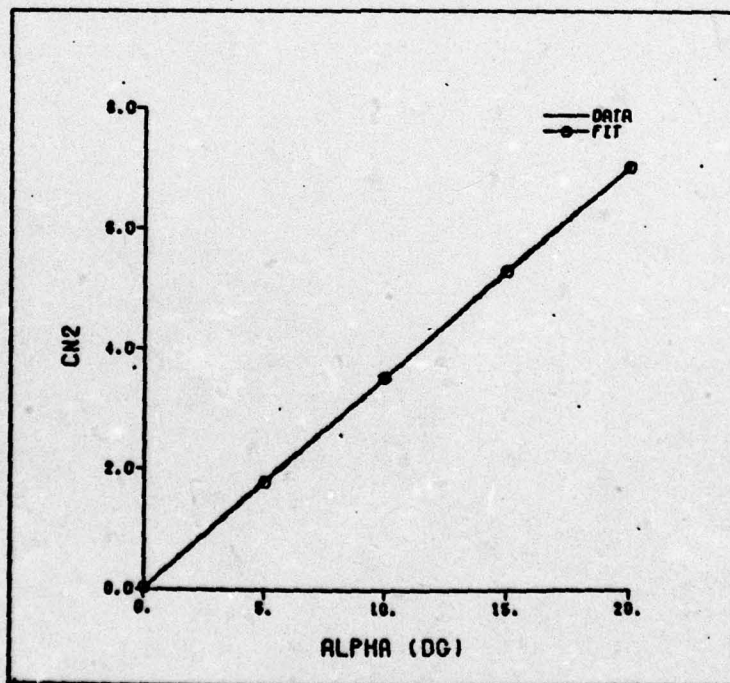


Fig. 21 Least Squares Fit to C_{N2} Curve

is the curve for $\delta = 4^\circ$, which is approximately the average value of control deflection observed in simulated flights. The following functions were obtained:

$$C_{D_0} = -51.658M^7 + 380.974M^6 - 1151.244M^5 + 1844.332M^4 - 1689.781M^3 + 885.882M^2 - 246.298M + 28.250 \quad (56)$$

$$\Delta C_C = -(2.851 \times 10^{-5}) \alpha_T^2 - (1.829 \times 10^{-3}) \alpha_T + 8.571 \times 10^{-3} \quad (57)$$

where $\alpha_T = \sqrt{\alpha^2 + \beta^2}$ (deg)

$$\Delta C_{D_f} = - (7.406 \times 10^{-12}) (-Z)^2 - (1.079 \times 10^{-7}) (-Z) - 8.878 \times 10^{-5} \quad (58)$$

$$C_{N_2} = 20.1 \alpha \quad (59)$$

where α is expressed in radians.

Thrust and Mass.

Thrust is obtained directly from the thrust schedule in section II.

<u>Time of Burn (sec)</u>	<u>Thrust (lb.)</u>
0.0-0.6	9500.
0.6-4.5	2000.

Mass is represented as a linear function between the stage burnout masses.

$$M = M_0 - C_1 t + C_1 \langle t-t_1 \rangle - C_2 \langle t-t_1 \rangle + C_2 \langle t-t_2 \rangle \quad (60)$$

where the stage burnout masses are

time (sec)	0.0	0.6	4.5
mass (slugs)	15.2	14.4	12.4

(Note that $\langle t-t_0 \rangle$ indicates a singularity function which does not become effective until $t \geq t_0$).

Control.

The independent controls in this algorithm are the acceleration commands in the missile body axes, a_h and a_v . In the simplified missile model, it is assumed that the autopilot delivers sufficient control deflection to obtain the commanded accelerations, within the autopilot limit of ± 20 g's. The lateral equations of motion can then be written as

$$a_h = \frac{1}{m} [-(A_x+T)\cos\alpha\sin\beta + A_y \cos\beta - A_z \sin\alpha\sin\beta] \quad (61)$$

$$a_v = \frac{1}{m} [(A_x+T) \sin\alpha - A_z \cos\alpha] - g \cos\gamma \quad (62)$$

Assuming small angles for α and β

$$\sin \alpha \doteq \alpha \quad \cos \alpha \doteq 1$$

$$\sin \beta \doteq \beta \quad \cos \beta \doteq 1$$

and neglecting the terms containing α and β as compared to the other terms, the equations of motion can be approximated as

$$a_h \doteq \frac{F_y}{m} = \frac{-Sq(20.1\beta)}{m} \quad (63)$$

$$a_v \doteq \frac{F_z}{m} - g \cos\gamma = \frac{-Sq(20.1\alpha)}{m} - g \cos\gamma \quad (64)$$

Assuming that the α and β necessary to attain the commanded accelerations may be obtained instantaneously (since the change at each time step is normally very small), α and β may be approximated by the following relationship:

$$\alpha = \frac{(32.2 a_v + g \cos \gamma) m}{20.1 S_q} \quad (65)$$

$$\beta = -\frac{(32.2 a_h) m}{20.1 S_q} \quad (66)$$

α and β are restricted to a maximum of ± 20 degrees, which is consistent with the maximum values observed in simulated flights.

Atmosphere

The atmosphere is modeled according to the 1959 ARDC standard atmosphere.

$$\begin{aligned} \text{Temperature: } \tau &= -\alpha H + C_1 \\ &= .003566Z + 518.69 \quad ^\circ R \end{aligned} \quad (67)$$

$$\begin{aligned} \text{Density: } \rho &= C_2 \tau^{-\left(\frac{g_0}{\alpha R_0}\right)} \\ &= 6.3806 \times 10^{-15} \tau^{4.26} \frac{\text{slug}}{\text{ft}^3} \end{aligned} \quad (68)$$

$$\begin{aligned} \text{Mach No: } M &= \frac{V_M}{\sqrt{\gamma R \tau}} \\ &= .0204 \frac{V_M}{\sqrt{\tau}} \end{aligned} \quad (69)$$

The State Equations.

The state equations consist of the three equations of motion

$$\dot{V}_M = \frac{1}{m} [(A_x + T) \cos \alpha \cos \beta + A_y \sin \beta + A_z \sin \alpha \cos \beta] - g \sin \gamma \quad (70)$$

$$\dot{\psi} = \frac{1}{m V_M \cos \gamma} [-(A_x + T) \cos \alpha \sin \beta + A_y \cos \beta - A_z \sin \alpha \sin \beta] \quad (71)$$

$$\dot{\gamma} = -\frac{1}{m V_M} [-(A_x + T) \sin \alpha + A_z \cos \alpha] - \frac{g}{V_M} \cos \gamma \quad (72)$$

and the three kinematic relationships

$$\dot{X} = V_M \cos\gamma \cos\psi \quad (73)$$

$$\dot{Y} = V_M \cos\gamma \sin\psi \quad (74)$$

$$\dot{Z} = -V_M \sin\gamma \quad (75)$$

The forward integration of the state equations follows this sequence:

1. Flight is initialized at $t = 1.0$ seconds to avoid complications introduced by the safe separation delay. Initial parameter values were obtained from the Retran simulation at the end of the first second of flight for each of the launch positions investigated. a_h and a_v are initialized at zero.
2. Atmospheric, mass and thrust quantities are determined.
3. α and β are determined.
4. Aerodynamic forces are calculated.
5. Missile equations of motion are integrated.
6. Kinematic equations are integrated.
7. The state values are stored
8. A test is made to determine if the stopping condition has been reached. The stopping condition is defined as $(X-X_{LOS})^2 + (Y-Y_{LOS})^2 + (Z-Z_{LOS})^2 \leq (50)^2$ where X_{LOS} , Y_{LOS} and Z_{LOS} are the coordinates of the point on the line of sight at the same range from the target as the missile.
9. If the stopping condition has not been reached, then for the initial forward integration, new guidance commands are calculated using the guidance algorithms. For subsequent forward integrations, the stored values of a_h and a_v are used.

10. Steps 2 through 9 are repeated until the stopping condition is achieved.

Payoff Function and Penalties

Missile range is primarily limited by the necessity of achieving a minimum value of terminal airspeed at target impact. Thus, any trajectory that maximizes range must maximize this terminal airspeed. Consequently, the negative terminal airspeed, $-V_T$, was chosen as the basic payoff function; the algorithm will attempt to minimize $-V_T$, thereby maximizing V_T . However, in order to avoid complications imposed by line of sight tracking in this program, the flight is terminated when the line of sight is intercepted and tracking of the line of sight to the target is assumed. From the results of the Retran simulation, it appears safe to assume that the further decrease in airspeed while tracking the line of sight can be approximated as a function of range from the target; i.e., the terminal velocity can be represented as

$$V_T = V_{M_f} - (k_{01} R_f^2 + k_{02} R_f) \quad (76)$$

where V_{M_f} is the missile airspeed at line of sight intercept and R_f is the range to the target at the point of interception. The basic payoff function is therefore

$$J = -V_{M_f} + k_{01} R_f^2 + k_{02} R_f \quad (77)$$

The values of k_{01} and k_{02} were obtained by a least squares fit of the velocity versus range profile obtained from the Retran simulation for a missile tracking the line of sight. Profiles were obtained for launch altitudes at 35,000 feet and 20,000 feet to account for the change in

inclination of the line of sight with varying altitude. The curve fits to these profiles are illustrated in Figs. 22 and 23. The values of k_{01} and k_{02} obtained were, for the 35,000 foot launch altitude:

$$k_{01} = -2.700 \times 10^{-8}$$

$$k_{02} = 3.395 \times 10^{-3}$$

and for the 20,000 foot launch altitude:

$$k_{01} = 2.815 \times 10^{-8}$$

$$k_{02} = 3.031 \times 10^{-3}$$

Note that the function representing the decrease of airspeed on the line of sight is analagous to a penalty function which penalizes the missile for intercepting the line of sight too early if lower drag could otherwise be achieved.

In order to track the line of sight following intercept, the missile must be generally aligned with the line of sight; otherwise, high g maneuvers are required to align the missile, resulting in increased drag. To account for this extra drag, penalty functions were included to penalize the missile for heading errors at line of sight intercept. The heading tolerances were established as

$$0 \leq \psi_f - \psi_{LOS} \leq 10^\circ$$

$$0 \leq \gamma_f - \theta_{LOS} \leq 10^\circ$$

Likewise, a penalty function was added to penalize the missile for intercepting the line of sight at too short a range to provide adequate

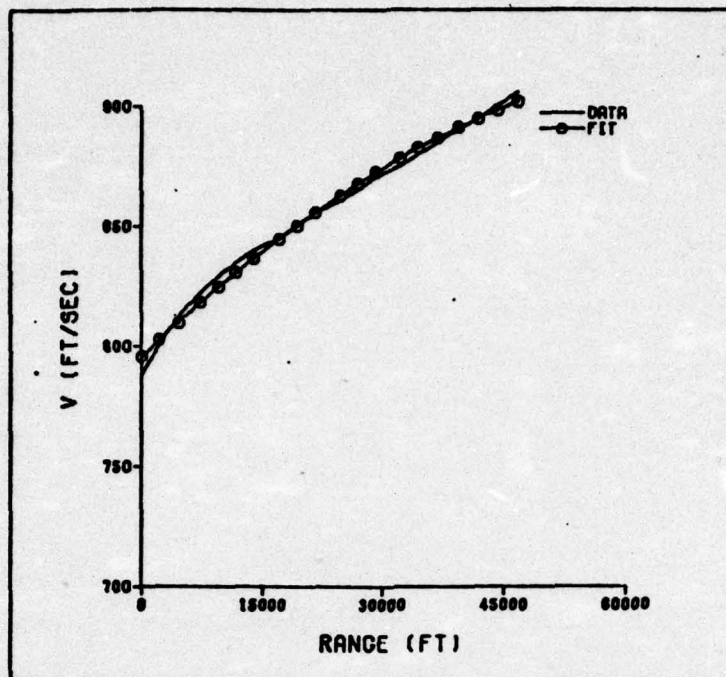


Fig. 22 Least Squares Fit to Velocity vs. Range Profile for Missile Established on Line of Sight - 35,000 ft Launch Altitude

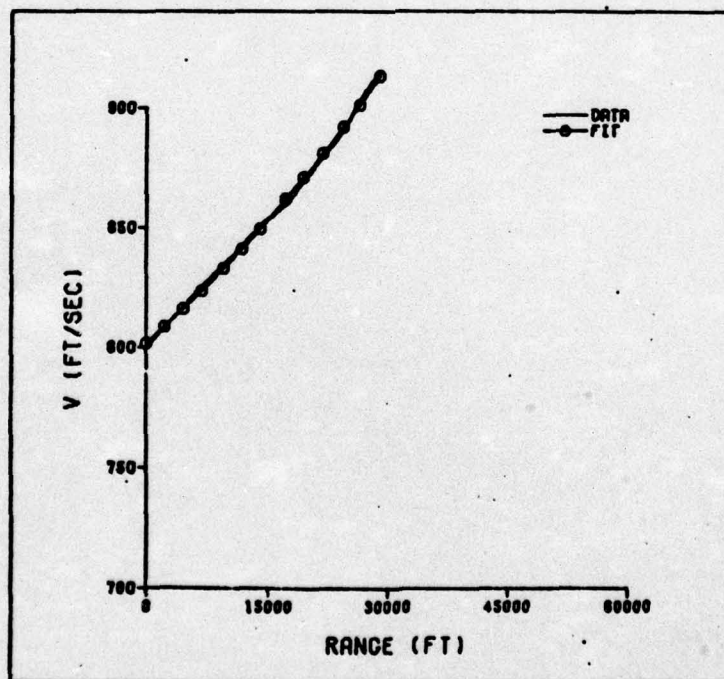


Fig. 23 Least Squares Fit to Velocity vs. Range Profile for Missile Established on Line of Sight - 20,000 ft Launch Altitude

tracking time. The range tolerance was established as

$$R_f \geq 16,000 \text{ ft}$$

to allow a minimum of 20 seconds tracking time at an average missile airspeed of 700 to 800 ft/sec.

The resulting payoff function, including penalties, is

$$J = -V_{M_f} + k_{01}R_f^2 + k_{02}R_f + \frac{1}{2} k_1(\psi_f - \psi_{LOS})^2 + \frac{1}{2} k_2(\gamma_f - \theta_{LOS})^2 + \frac{1}{2} k_3(R_f - 16,000.)^2 \quad (78)$$

The values of k_1 , k_2 , and k_3 were chosen through a sensitivity analysis which is discussed in section V.

Adjoint Vector, Hamiltonian and Backward Integration

The adjoint vector is defined as

$$\bar{\lambda}^T(t_f) = \partial J / \partial \bar{X} \quad t_f \quad (79)$$

where $\partial J / \partial \bar{X} = [\partial J / \partial V \quad \partial J / \partial \psi \quad \partial J / \partial \gamma \quad \partial J / \partial X \quad \partial J / \partial Y \quad \partial J / \partial Z]$

This vector is calculated using the final conditions obtained from forward integration of the state equations.

The Hamiltonian is defined as

$$H = \bar{\lambda}^T \cdot \dot{\bar{X}} \quad (80)$$

The differential equation

$$\dot{\bar{\lambda}}^T = -\partial H / \partial \bar{X} \quad (81)$$

where

$$\partial H / \partial \bar{X} = [\partial H / \partial V \quad \partial H / \partial \psi \quad \partial H / \partial \gamma \quad \partial H / \partial X \quad \partial H / \partial Y \quad \partial H / \partial Z]$$

is integrated backward, along with the state equations, to obtain $\bar{\lambda}(t)$ and $\dot{\bar{X}}(t)$. The $\bar{X}(t)$ and the controls $a_h(t)$ and $a_v(t)$ which were calculated

and stored during the forward integration of the state equations are used in this calculation.

Having found $\bar{\lambda}(t)$ and $\dot{\bar{x}}(t)$, the gradients $\frac{\partial H}{\partial a_h}(t)$ and $\frac{\partial H}{\partial a_v}(t)$ can be determined and stored.

Alpha Search

The adjustments to be made in the controls in order to improve the solution are $\delta a_h(t) = -\alpha \frac{\partial H}{\partial a_h}(t)$ and $\delta a_v(t) = -\alpha \frac{\partial H}{\partial a_v}(t)$. In order to determine the value of α which will minimize the solution at this iteration, a one-dimensional alpha search is performed to minimize J with respect to α . Having determined α , the new acceleration commands are calculated and stored:

$$a_h(t) = a_h(t)_{old} + \delta a_h(t)$$

$$a_v(t) = a_v(t)_{old} + \delta a_v(t)$$

Using these new commands, the state equations are again integrated forward to obtain a new solution and the iteration is repeated.

Algorithm Termination

The algorithm terminates when further iterations will make negligible reductions in the payoff. This point is determined when successive payoffs are within a chosen tolerance of one another; a tolerance of .01% was employed.

IV. Programming

Program Retran

Program Retran is the Retran missile simulation program. It is a modification of a Maverick missile five degree of freedom simulation program which was developed by Mr. Merrill Habbe of the Air Force Avionics Laboratory. The Maverick missile data and parameters were replaced by the Retran missile parameters, and the algorithms necessary to represent the launching aircraft and to incorporate SAR-Retrans guidance were included. A Calcomp plotting routine was added. The program is written in FORTRAN Extended, Version 4, for use on the CDC 6600-CYBER 74 computer system. A source program is attached as Appendix B.

The program employs simple Euler numerical integration. Time steps of less than .05 seconds were found to yield reasonable accuracy (within 5% of results using a very small time step of .005 seconds); the time step is reduced by a factor of 10 in the final 10 seconds of flight for increased accuracy in the critical terminal phase. The program contains an abbreviated ARDC 1959 atmospheric table and tables of aerodynamic coefficients for the missile.

The coefficient tables were obtained from the coefficient curves shown in Figs. 3 through 11. Thrust and mass parameters are also tabularized. A look-up routine employing linear interpolation is used to extract values from these tables.

Flight parameters are initialized at $t_0 = 0$. Data is input on three cards (required input is explained at the beginning of the

program listing in Appendix B) and includes aircraft position coordinates, Euler angles and velocity components at launch, together with target position and velocity (however, the program as listed assumes a stationary target and ignores input target velocity). The missile parameters are initialized to the aircraft parameters at launch.

The program terminates when the missile passes through target altitude or when a specified maximum flight time is exceeded. Output data is printed during the flight; these data are explained at the beginning of the output listing, a sample of which is contained at the end of the program listing in Appendix B. By setting the proper integer flag, aircraft and missile position coordinates are punched on data cards. These can be utilized with a separate plotting routine to produce multiple trajectory plots such as those presented in section V. Setting another integer flag will produce the following Calcomp plots:

1. Plan view of trajectory
2. Vertical profile of trajectory
3. Acceleration commands vs. time
4. α and β vs. time
5. Deceleration due to aerodynamic drag vs. time
6. Retransmitted frequency error vs. time
7. Missile distance normal to the line of sight for the final 20 seconds of flight

Examples of these plots may be seen in Section V and Appendix D.

Multiple flights may be simulated in one input run by including the appropriate number of data cards.

Program Optraj

Program Optraj is the first order gradient optimization program. This program is also written in FORTRAN Extended, Version 4, for use on the CDC 6600-CYBER 74 computer system. A source program listing is attached as Appendix C.

This program utilizes simple Euler numerical integration. Time steps of .5 seconds were found to yield satisfactory results. Flight parameters were initialized at $t_0 = 1.0$ seconds. Data is input on 6 cards (required input is explained at the beginning of the program listing in Appendix C) and includes aircraft and missile position coordinates, Euler angles and velocity components at t_0 , together with initial values of α and β . The penalty function coefficients are also input.

The program terminates when successive payoff values lie within a designated tolerance of each other. The program may also terminate if an initial solution is not obtained or if improvement of the initial solution cannot be made. A message is printed for these abnormal terminations. The following output data is printed during the optimization process:

1. The missile velocity and position, velocity and distance normal to the line of sight and acceleration commands (in missile body axes) are printed for the initial trajectory and again for the optimized trajectory. Only final values are printed for the other forward integrations of the state equations.

2. The value of the payoff function and the calculated terminal velocity are printed for each forward integration. The angular errors and range error at line of sight interception are also printed.

3. The values of $\frac{\partial H}{\partial a_h}$ and $\frac{\partial H}{\partial a_v}$ are printed for each backward integration.

4. The alpha values and payoff values are printed for each alpha search.

Printed output for the Optraaj program can be seen in Appendix F.

A number of Calcomp plots are drawn at the completion of the optimization process. These plots present the initial curves and optimized curves for the following parameters:

1. Trajectory plan view
2. Trajectory vertical profile
3. a_{hG}
4. a_{vG}
5. α
6. β
7. \dot{V}_M
8. ΔY
9. ΔZ

Examples of these plots may be seen in section V.

Only one trajectory may be optimized on an input run.

Validity of Program Results

Retran Simulation. Because the Retran missile is a hypothetical vehicle, no flight data is available to validate the results of the simulation. However, the Maverick missile 5 degree of freedom simulation upon which this program is based has been successfully validated against flight test data. While the performance of the Retran missile differs

from that of the Maverick, the simulation results appear to be reasonable in the light of the Maverick simulation results. Unfortunately, the Maverick simulation results are classified; therefore, a direct comparison cannot be presented in this report.

OptraJ Optimization. An attempt was made to validate the performance of the OptraJ program by obtaining the same optimal solution from two widely differing initial solutions. However, it became apparent from these attempts that numerous, relatively closely spaced local minimums were encountered in the payoff function. Since the first order gradient technique will converge on the local minimum within the same range as the initial solution, the program converged on different optimal solutions for widely differing initial solutions. In order to obtain convergence on the same optimal solution, the initial solutions could differ only slightly.

Because the trajectory changes made by the optimization algorithm were too slight to duplicate in the Retran simulation, the effects of the optimization could not be validated in the simulation.

V. Results

Guidance Algorithm Selection

Several guidance algorithms were tested in the Retran simulation in order to select the algorithms most suitable for employment of the missile with SAR-Retrans guidance. The algorithms which were rejected are discussed in Appendix E, while discussion of the algorithms presented here may be found in section II. The algorithms selected were:

vertical command-to-track:

$$a_v = 2\zeta \left(k_1 \frac{t_R}{t_{tg}} \right) \Delta \dot{Z} + \left[\left(k_1 \frac{t_R}{t_{tg}} \right)^2 \Delta Z + g_{bias} \right]$$

horizontal command-to-heading:

$$a_{h_T} = C_T (\psi_{cos} - \psi) \left[\frac{C_R \cdot t_R}{R_{MT}} \right]^2$$

horizontal command-to-track:

$$a_h = -2\zeta \left(k_1 \frac{t_R}{t_{tg}} \right) \Delta \dot{Y} - \left(k_1 \frac{t_R}{t_{tg}} \right) \Delta Y + \frac{2\omega_Z V_M}{g} - \frac{R_{MT} V_M \omega_Z}{g V_M}$$

The coefficient values selected for these algorithms were

$$\begin{aligned} t_R &= 20.0 \text{ seconds} \\ k_1 &= .249 \\ \zeta &= .50 \\ g_{bias} &= 1.0 \\ C_T &= 25.0 \\ C_R &= 1000. \text{ ft/sec} \end{aligned}$$

Horizontal and vertical trajectories produced by these algorithms are presented in Figs. 24 and 25 for a long range medium squint angle launch (squint angle is the angle between the aircraft velocity vector and the line of sight).

Performance parameters which were considered important in the selection of the guidance algorithms were the schedule of accelerations commanded by the algorithms, the time histories of angle of attack α and sideslip angle β , the profile of deceleration due to aerodynamic drag and the missile distance errors in the terminal phase. The retransmitted frequency error was also considered, as maintenance of this error below 8 hz was the criteria for line of sight tracking. These performance parameters are presented in Figs. 26 thru 30 for the long range medium squint angle launch. Parameter plots for launches from different altitudes and ranges may be seen in Appendix D.

Trajectory Optimization

An attempt was made to optimize the acceleration command schedule to produce a trajectory yielding maximum range. An initial squint angle of 45 degrees was chosen for the optimization, with launches made from altitudes of 35,000 ft. and 20,000 ft. Initial trajectories were obtained using essentially the same guidance algorithms employed in the Retran simulation, although the values of C_T , t_R , ζ , and g_{bias} were varied slightly in order to achieve trajectory shapes similar to those obtained from the simulation.

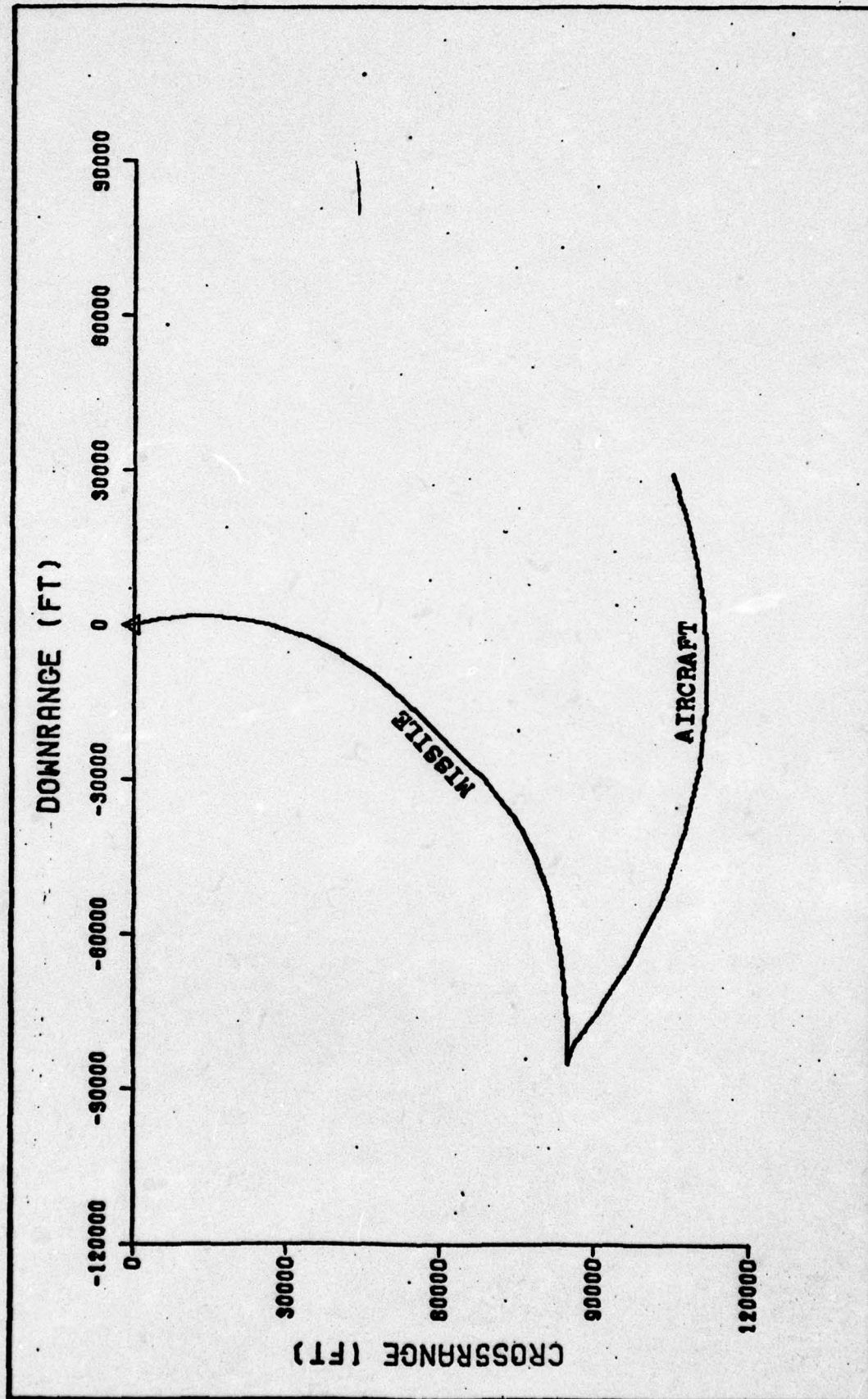


Fig. 24 Trajectory Planview - 45°, 35,000 ft Launch

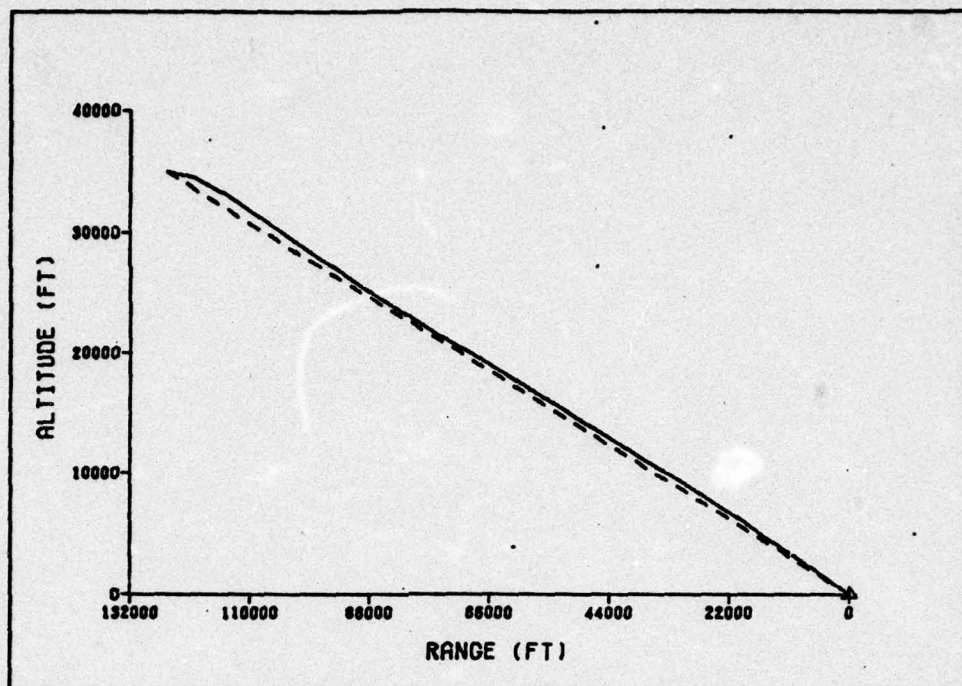


Fig. 25 Trajectory Vertical Profile - 45°, 35,000 ft Launch

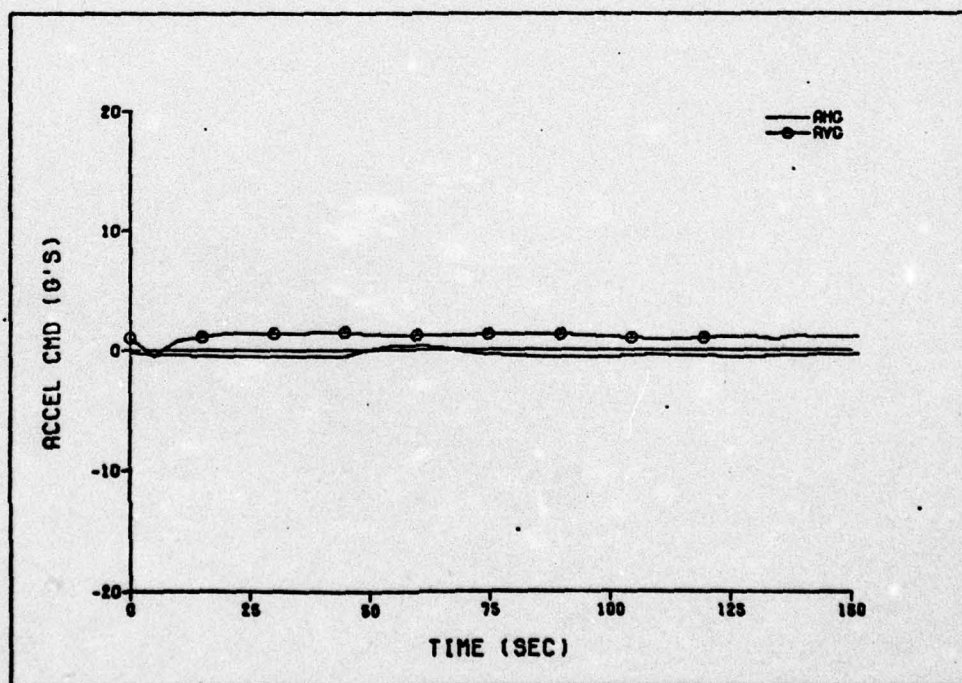


Fig. 26 Accelerations Commands vs. Time - 45°, 35,000 ft Launch

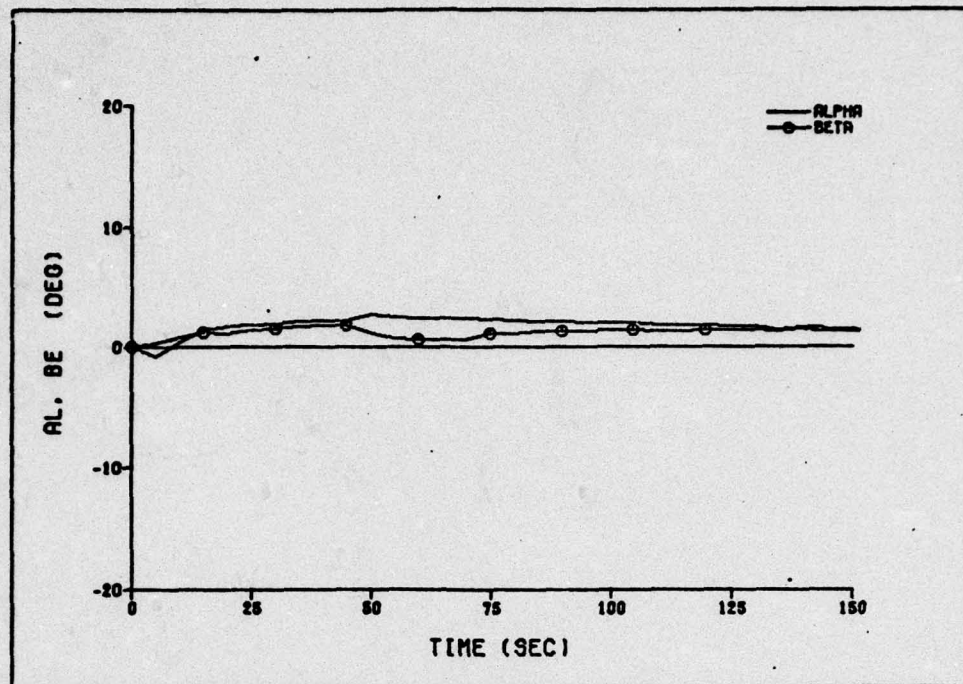


Fig. 27 Alpha and Beta vs. Time - 45°, 35,000 ft Launch

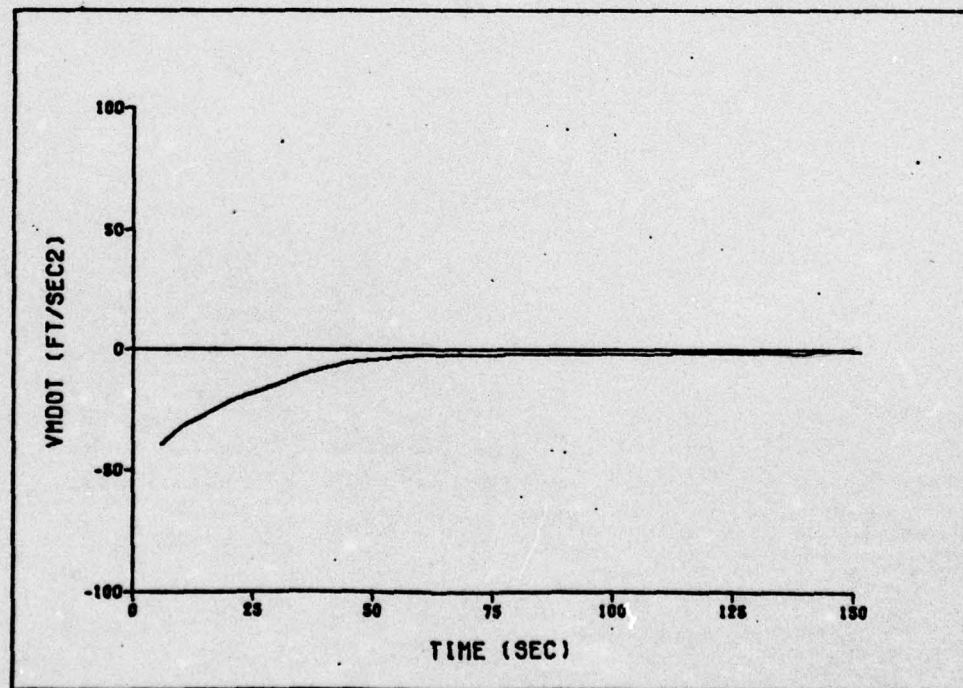


Fig. 28 Deceleration Due to Aerodynamic Drag vs. Time - 45°, 35,000 ft Launch

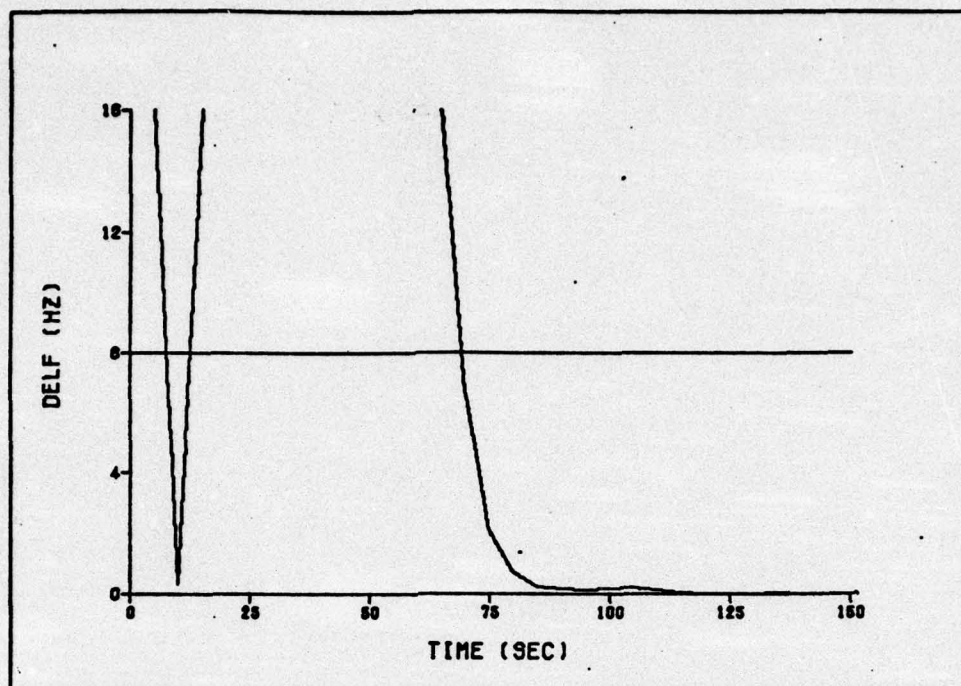


Fig. 29 Retrmitted Frequency Error vs. Time - 45°, 35,000 ft Launch

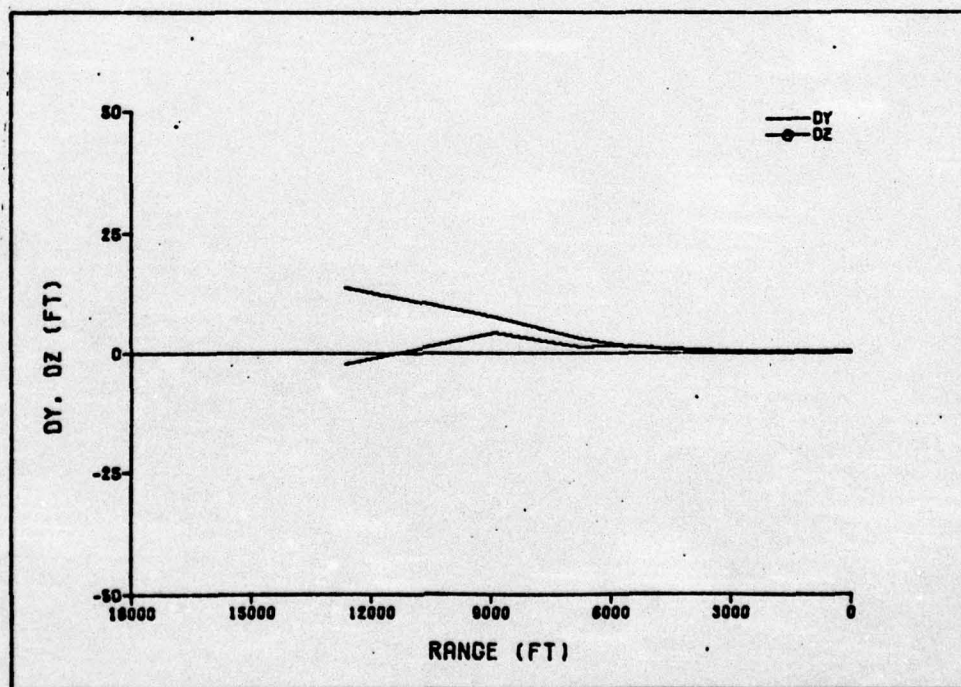


Fig. 30 Missile Distance Errors, Terminal Phase - 45°, 35,000 ft Launch

A sensitivity analysis determined that penalty function values of $k_1 = 1000.$, $k_2 = 1000.$, and $k_3 = 1.0 \times 10^{-6}$ would yield satisfactory solutions.

The first order gradient algorithm directed only small changes in the acceleration command schedule before reaching a local minimum of the payoff function. The resulting trajectory changes were negligible, as were changes in the performance parameters. Plots of the initial and optimized trajectories and performance parameters for the 35,000 ft. launch are presented in Figs. 31-39. For this launch, the payoff function was improved from $J = -731.88$ to $J = -731.89$, with terminal velocities of 771.78 for the initial trajectory and 771.79 for the optimized trajectory. The trajectories and performance parameters for the 20,000 ft. launch are presented in Figs. 40-48; here, the payoff function went from $J = -307.49$ to $J = -307.57$, with terminal velocities of 452.89 and 452.96.

Because the trajectory and performance parameter changes were too small to be distinguishable on the Calcomp plots, the output listings for these two program runs are included in Appendix F.

Launch Envelope Determination

Using the algorithms selected through the simulation investigation, the launch envelope for the Retran missile was determined. The criteria used in determining a successful launch were:

1. Minimum terminal airspeed of 700 ft/sec.
2. Minimum tracking time on the line of sight ($\Delta f_d \leq 8$ Hz) of 20 seconds.

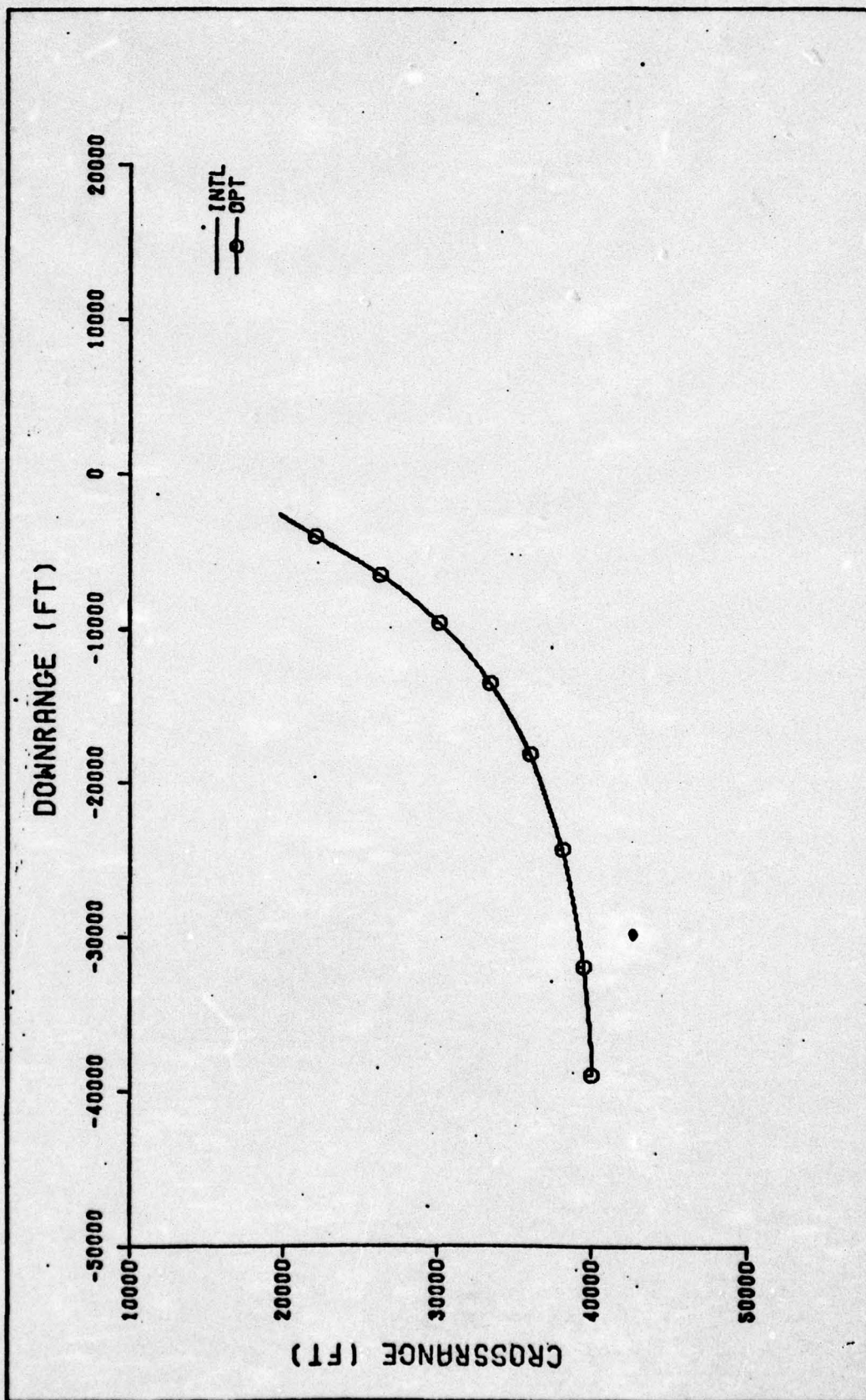


Fig. 31 Trajectory Plan View, Optraj Optimization - 35,000 ft Launch

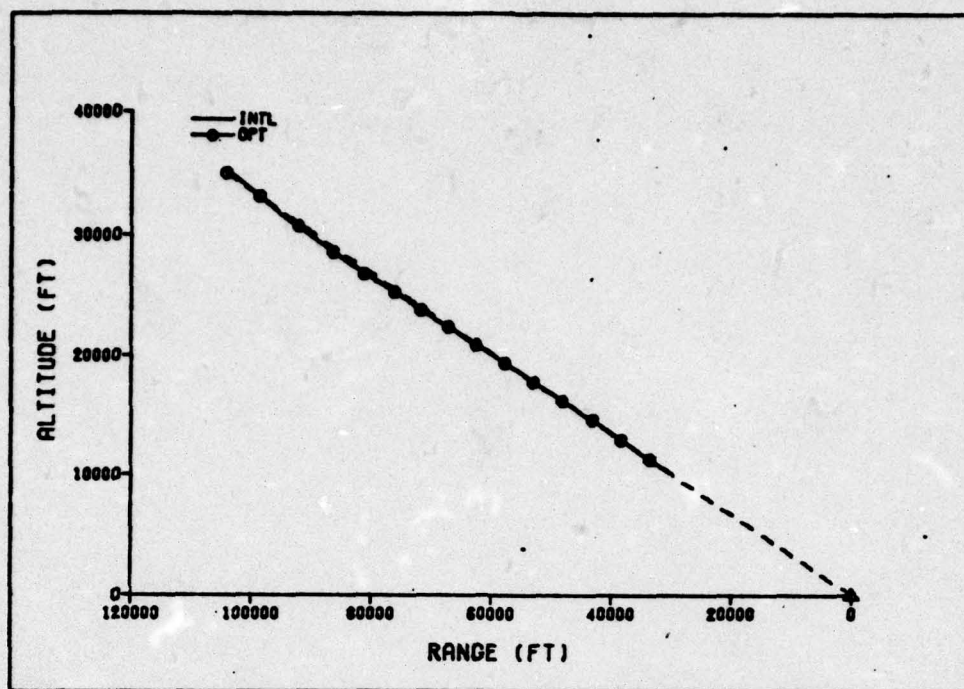


Fig. 32 Trajectory Vertical Profile, Optraaj Optimization - 35,000 ft Launch

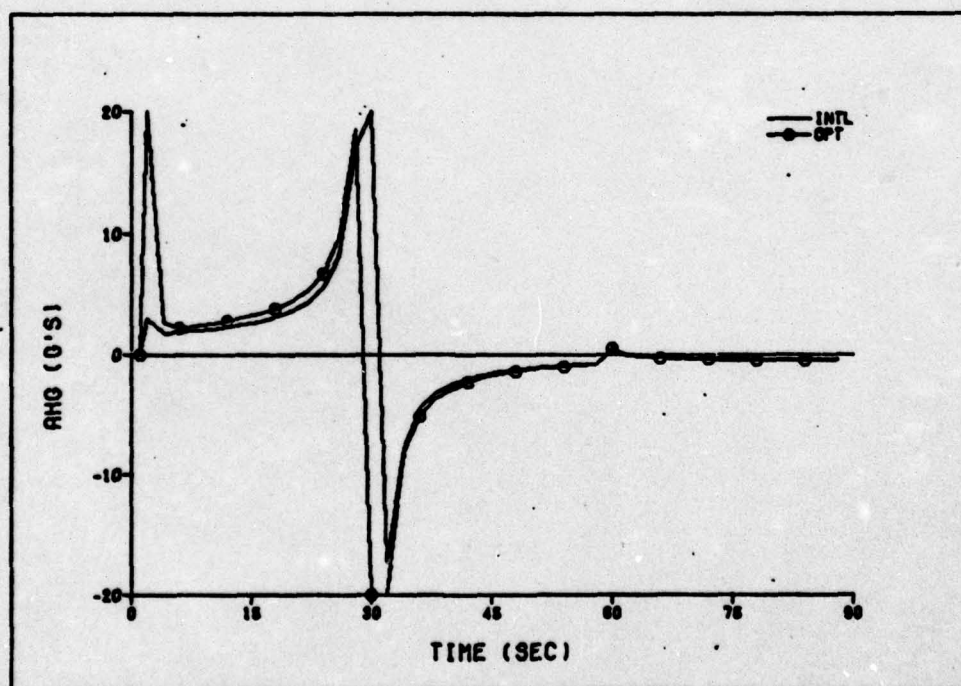


Fig. 33 Horizontal Acceleration Commands, Optraaj Optimization - 35,000 ft Launch

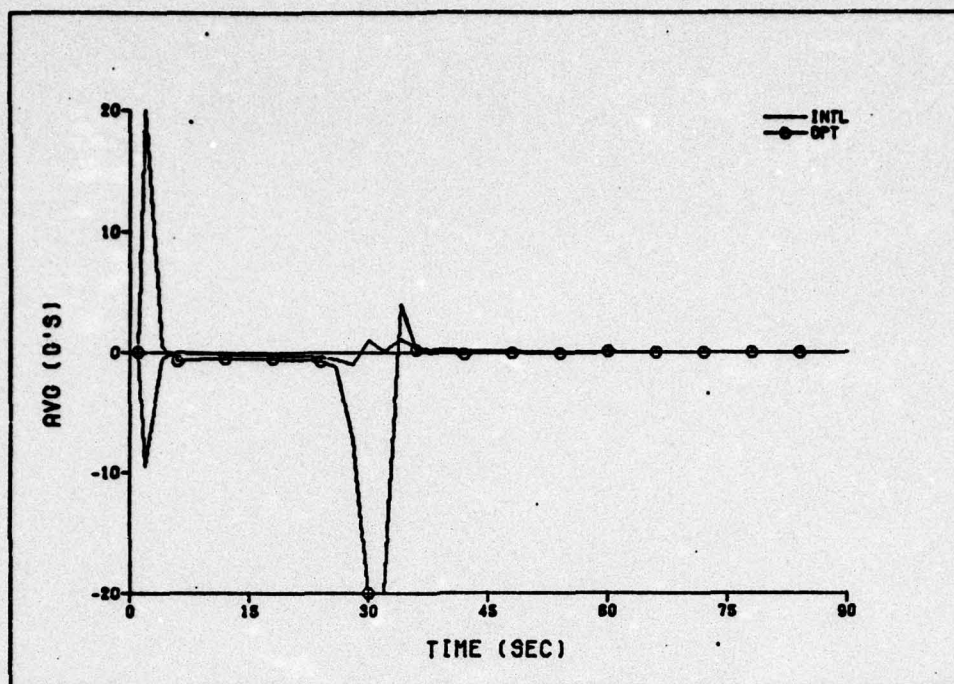


Fig. 34 Vertical Acceleration Commands, Optraj Optimization - 35,000 ft Launch

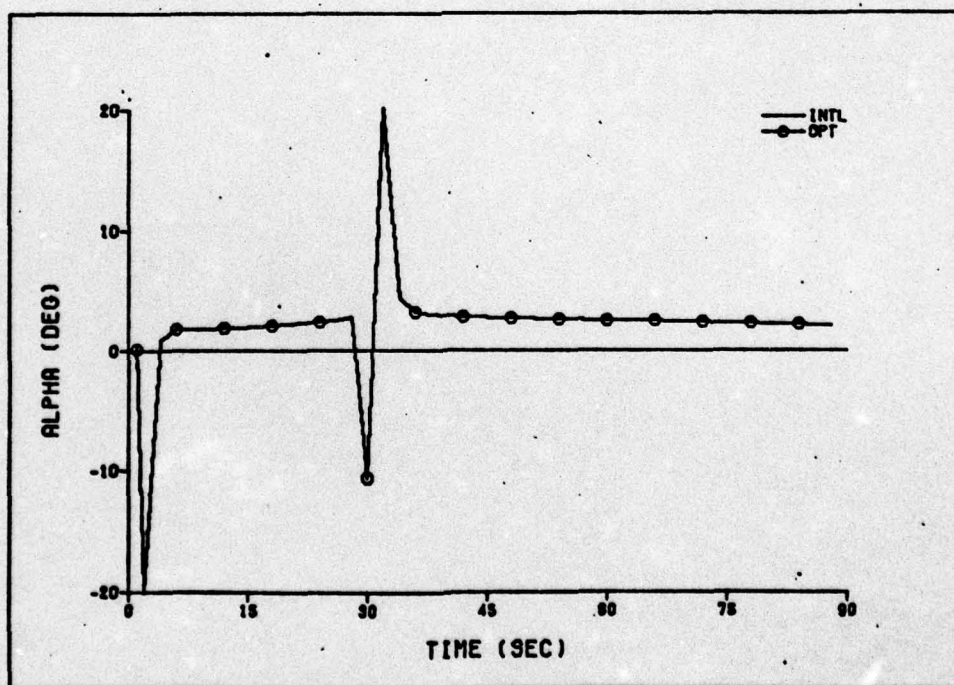


Fig. 35 Angle of Attack, Optraj Optimization - 35,000 ft Launch

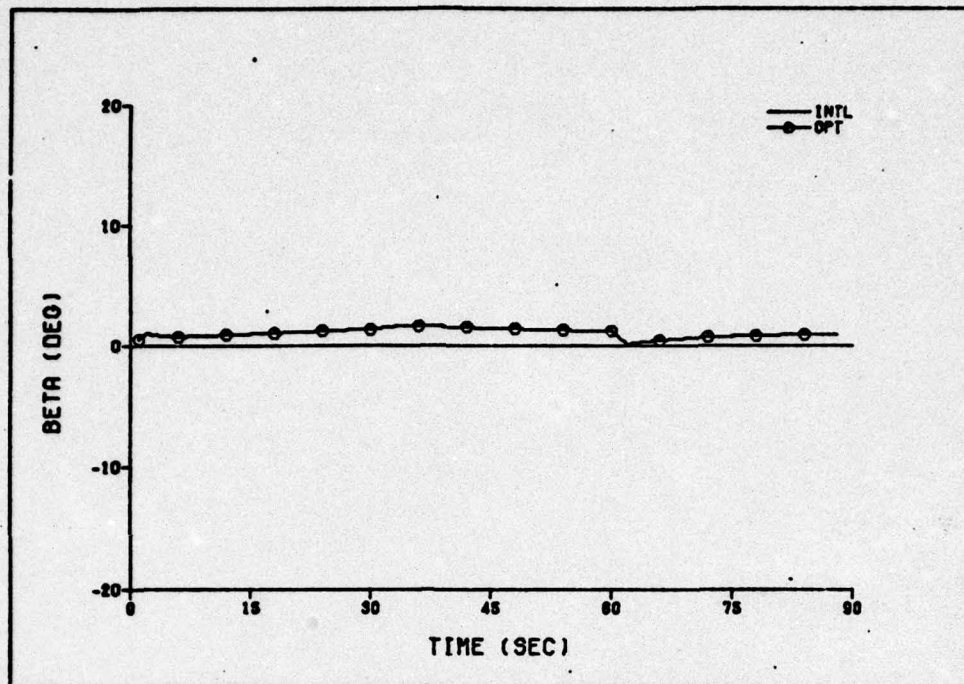


Fig. 36 Sideslip Angle, Optraaj Optimization - 35,000 ft Launch

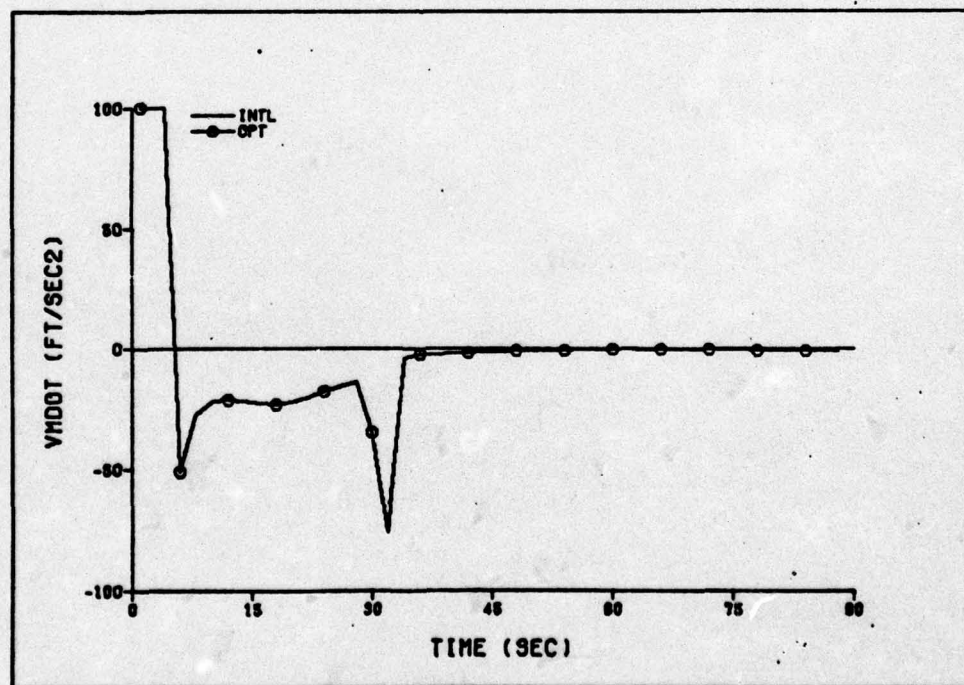


Fig. 37 \dot{V}_m , Optraaj Optimization - 35,000 ft Launch

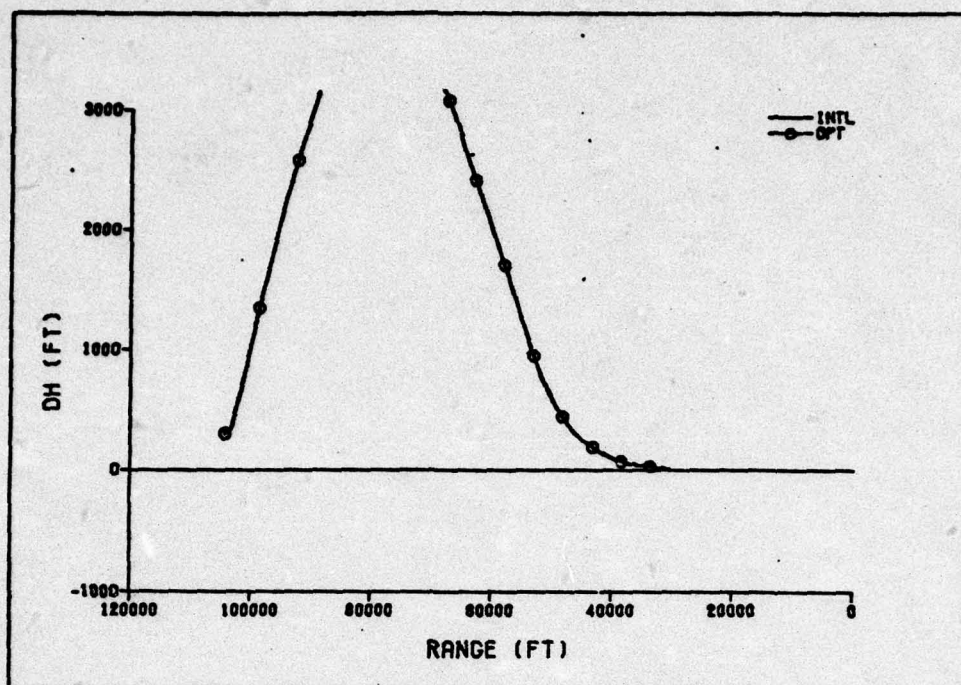


Fig. 38 ΔY Distance Error, Optraaj Optimization - 35,000 ft Launch

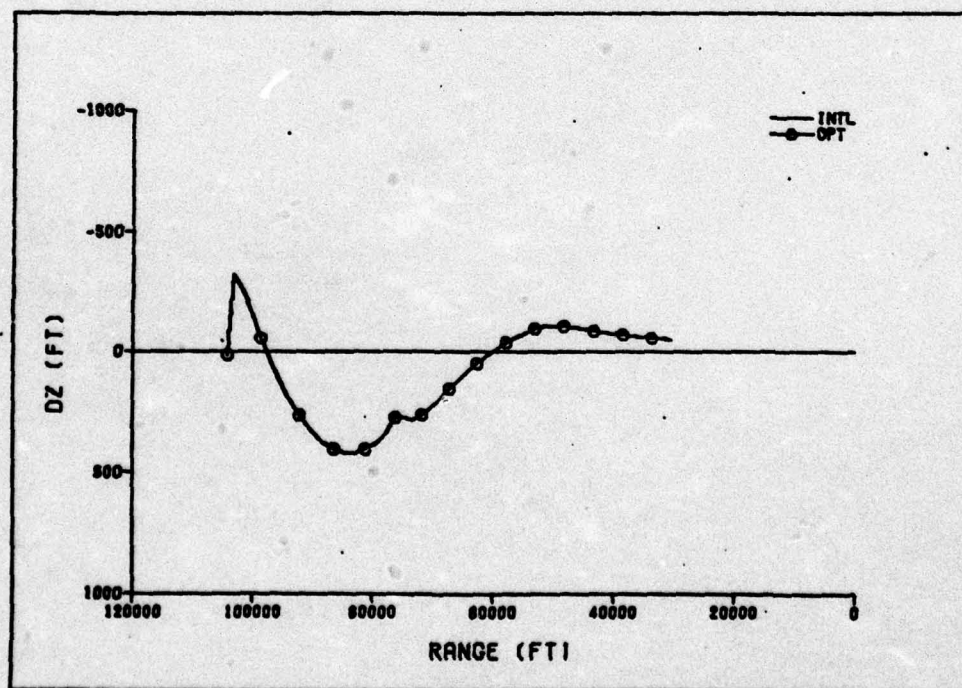


Fig. 39 ΔZ Distance Error, Optraaj Optimization - 35,000 ft Launch

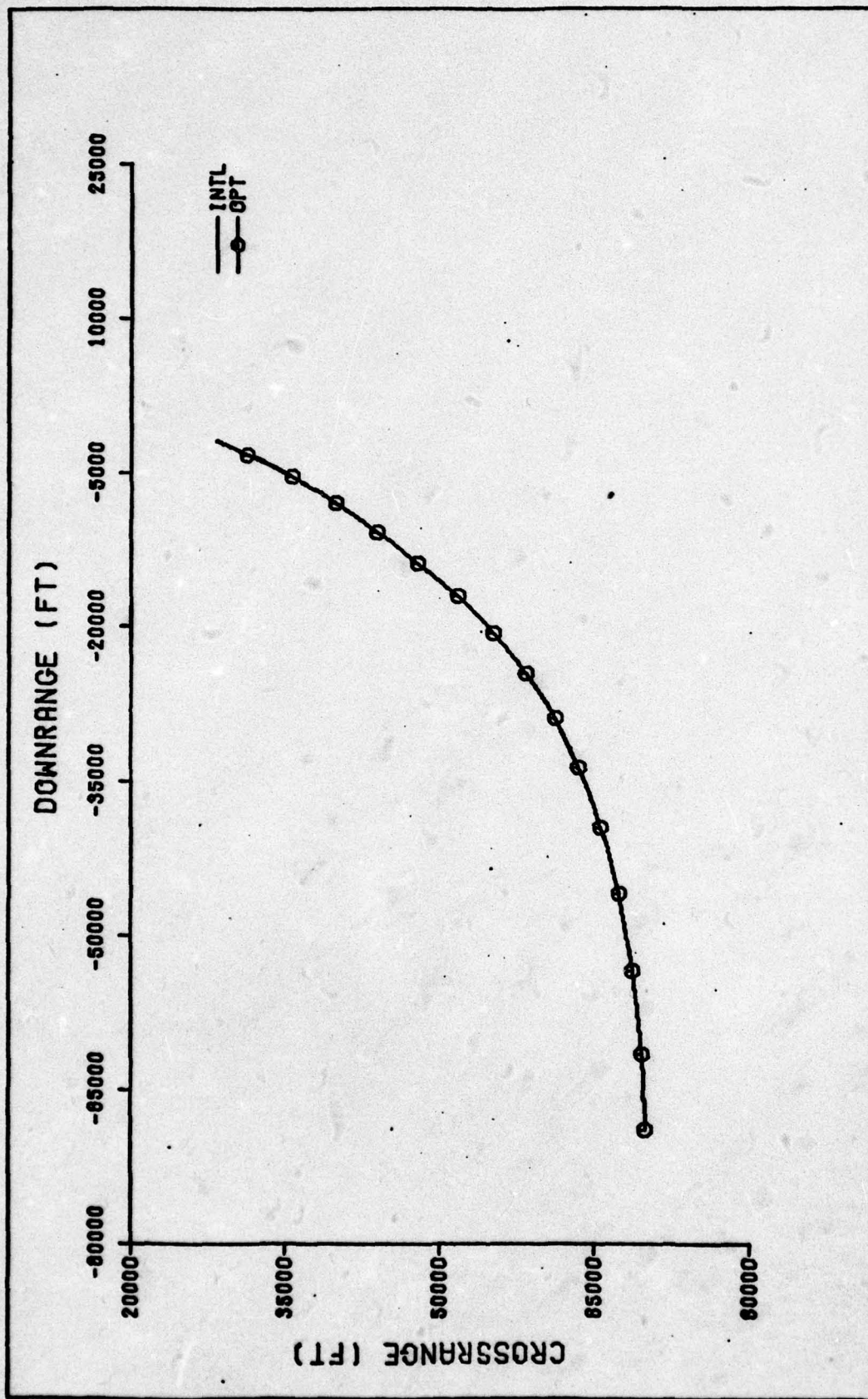


Fig. 40 Trajectory Plan View, Optraj Optimization - 20,000 ft Launch

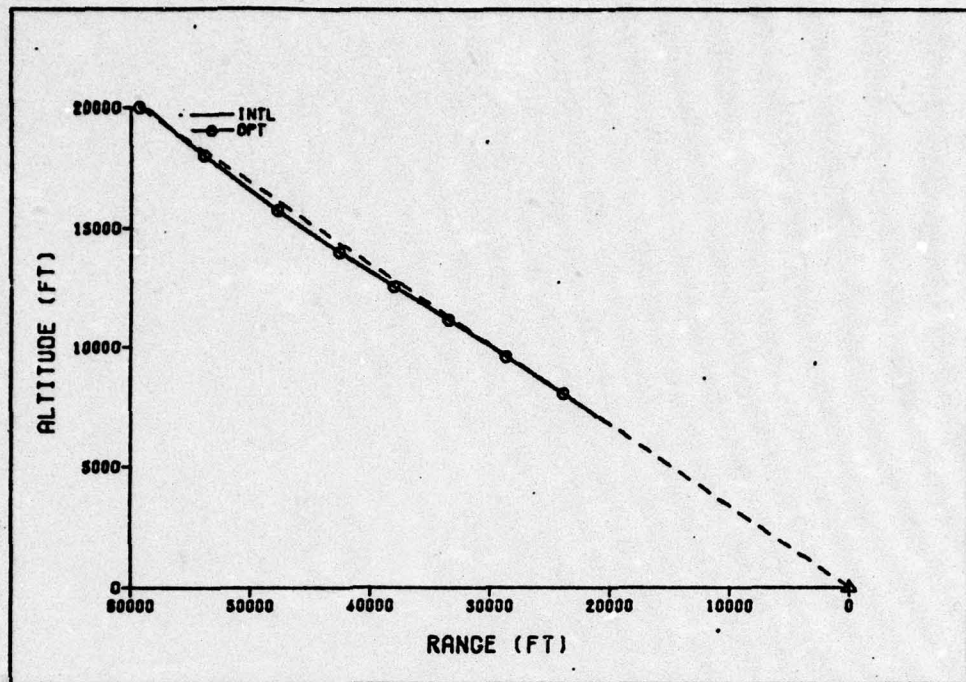


Fig. 41 Trajectory Vertical Profile, Optraj Optimization - 20,000 ft Launch

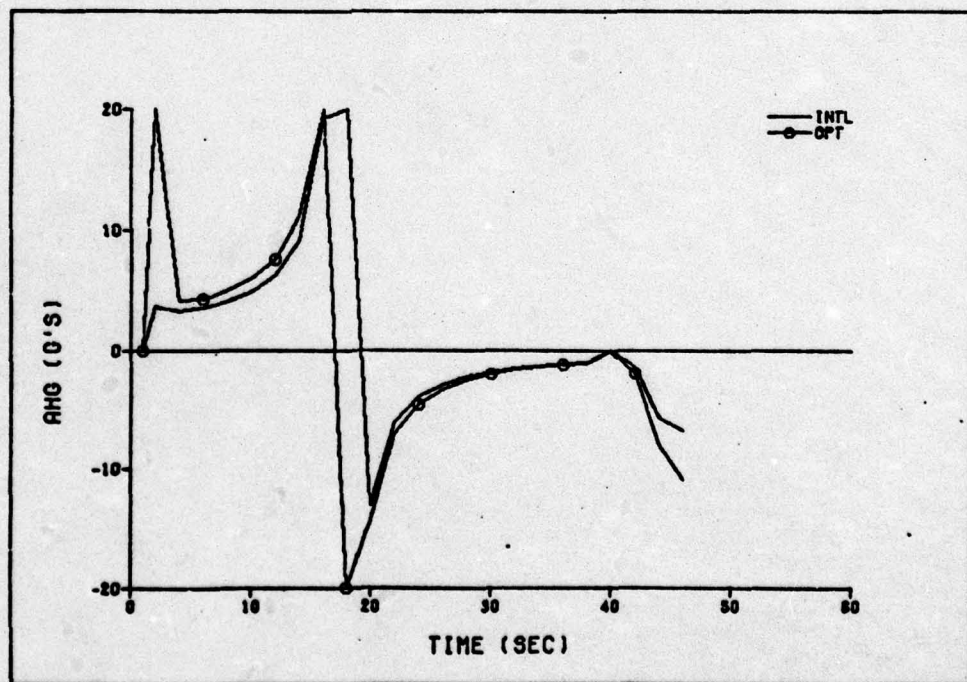


Fig. 42 Horizontal Acceleration Commands, Optraj Optimization - 20,000 ft Launch

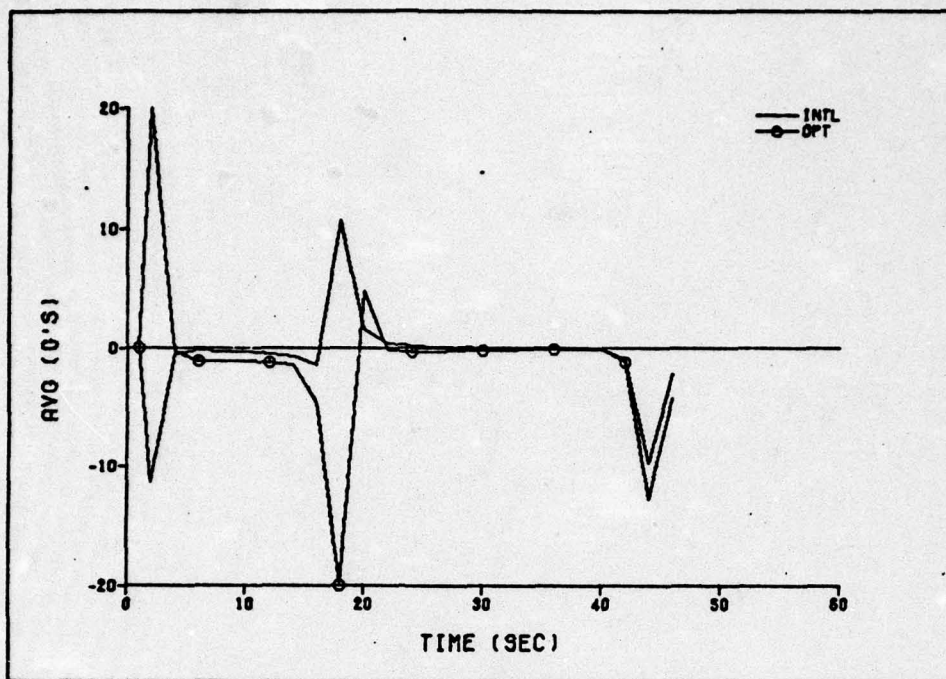


Fig. 43 Vertical Acceleration Commands, Optraj Optimization - 20,000 ft Launch

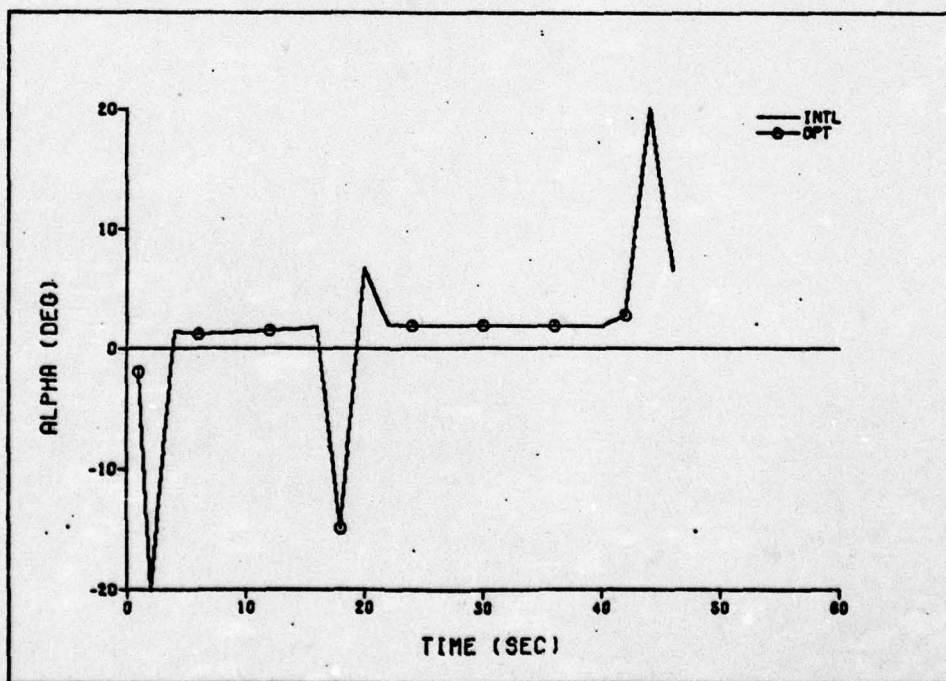


Fig. 44 Angle of Attack, Optraj Optimization - 20,000 ft Launch

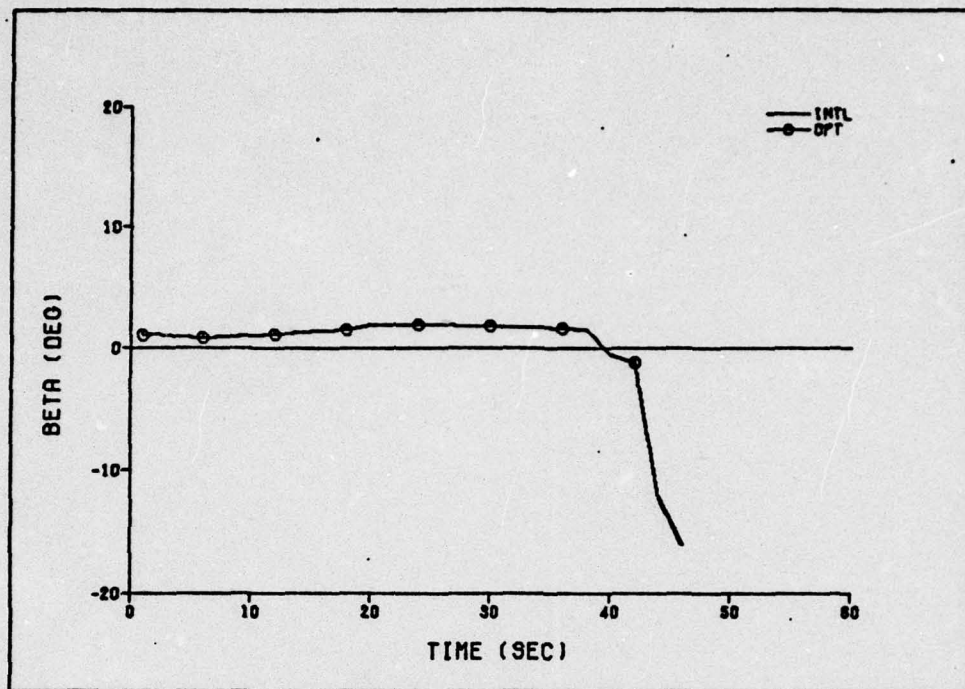


Fig. 45 Sideslip Angle, Optraaj Optimization - 20,000 ft Launch

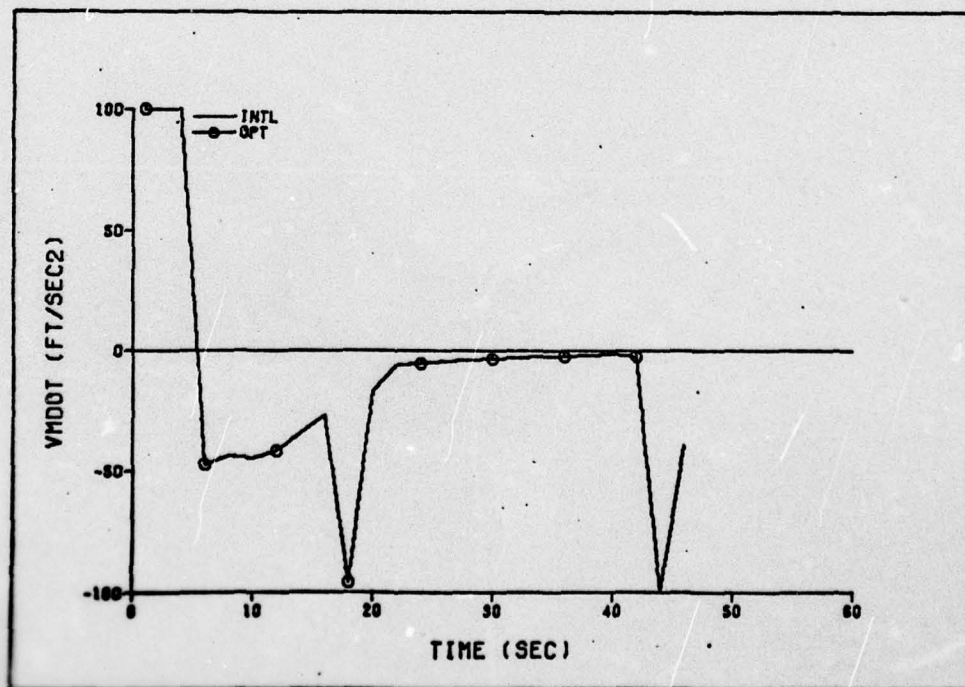


Fig. 46 \dot{V}_H , Optraaj Optimization - 20,000 ft Launch

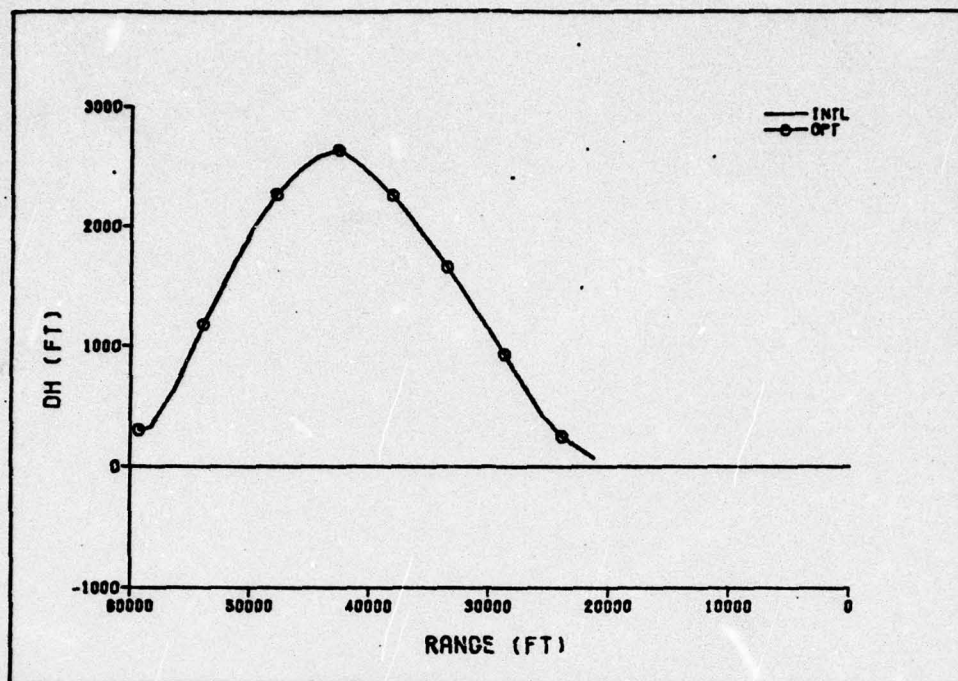


Fig. 47 ΔY Distance Error, Optraaj Optimization - 20,000 ft Launch

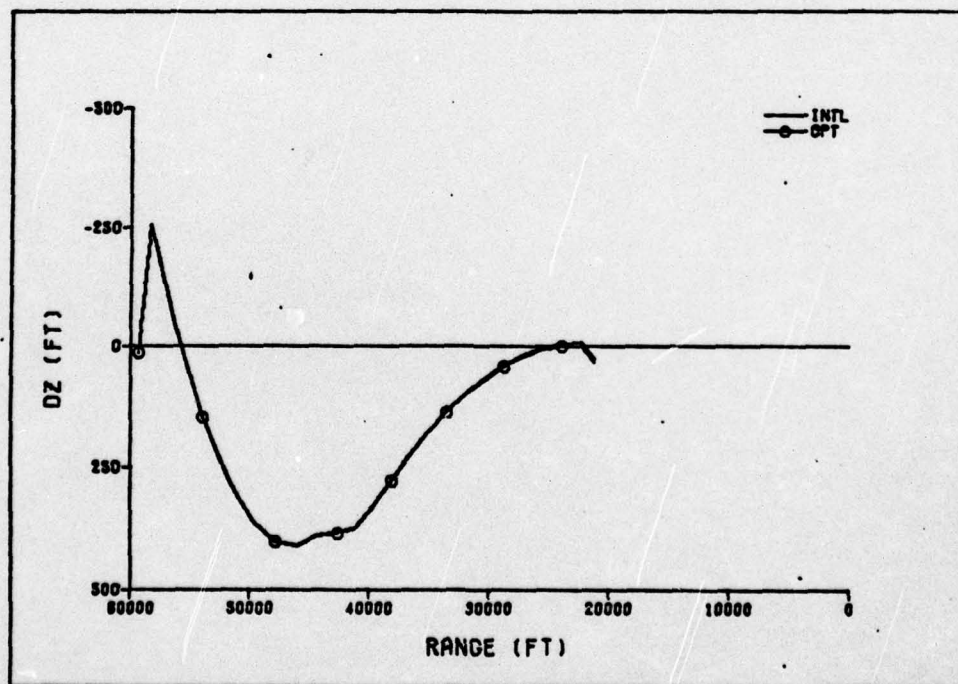


Fig. 48 ΔZ Distance Error, Optraaj Optimization - 20,000 ft Launch

Simulated flights were made to determine the maximum and minimum ranges obtainable at a given initial squint angle. Squint angles of 15°, 30°, 45°, 60°, 75°, and 90° were investigated, with launches made from altitudes of 5,000 ft, 20,000 ft and 35,000 ft. Thus, three sets of planview launch envelopes were obtained - one for each launch altitude. The launch envelopes are shown in Figs. 49-51 as they would appear relative to the aircraft; these figures indicate that any target lying within the envelope corresponding to aircraft altitude could be successfully struck by a Retran missile. A different view of the launch envelope is presented through Figs. 52-57. These show the planview trajectories for maximum and minimum range launches at each of the three launch altitudes, thus together they indicate the size and shape of one-half of the launch envelope relative to the target.

Note that the minimum squint angle of 15 degrees was chosen as a practical minimum value at which target acquisition and tracking would be accomplished by the SAR-Retran system. This is not necessarily a missile limitation, although no launches were attempted from lower squint angles. Likewise, 90 degrees was the maximum practical squint angle obtainable with the aircraft gimbal system. 35,000 ft was taken as the maximum operational altitude for a loaded fighter aircraft, while 5000 ft appears to be the minimum altitude from which a useful launch envelope can be obtained due to missile range limitations.

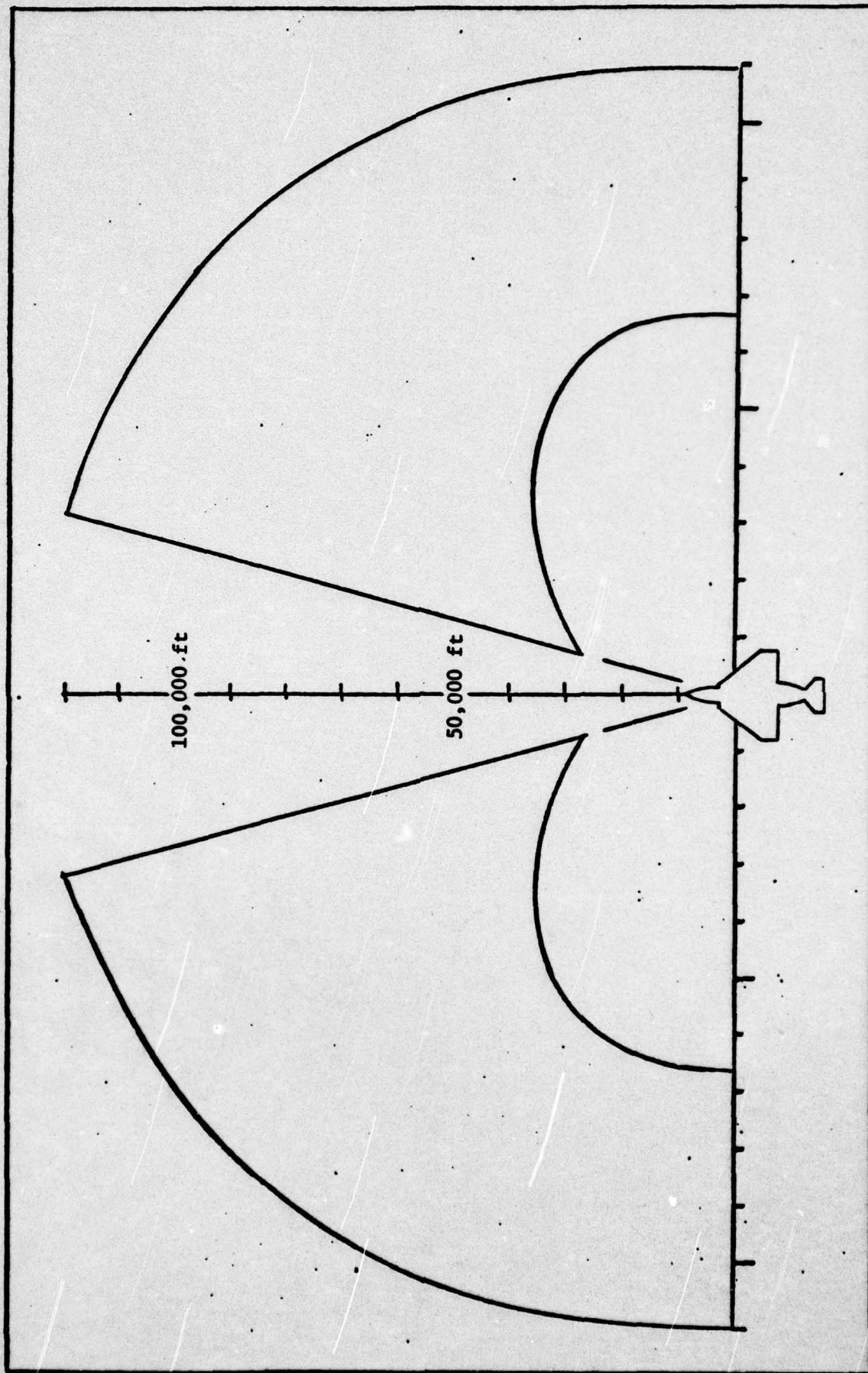


Fig. 49 Retran Missile Launch Envelopes Relative to Aircraft - 35,000 ft Launch Altitude

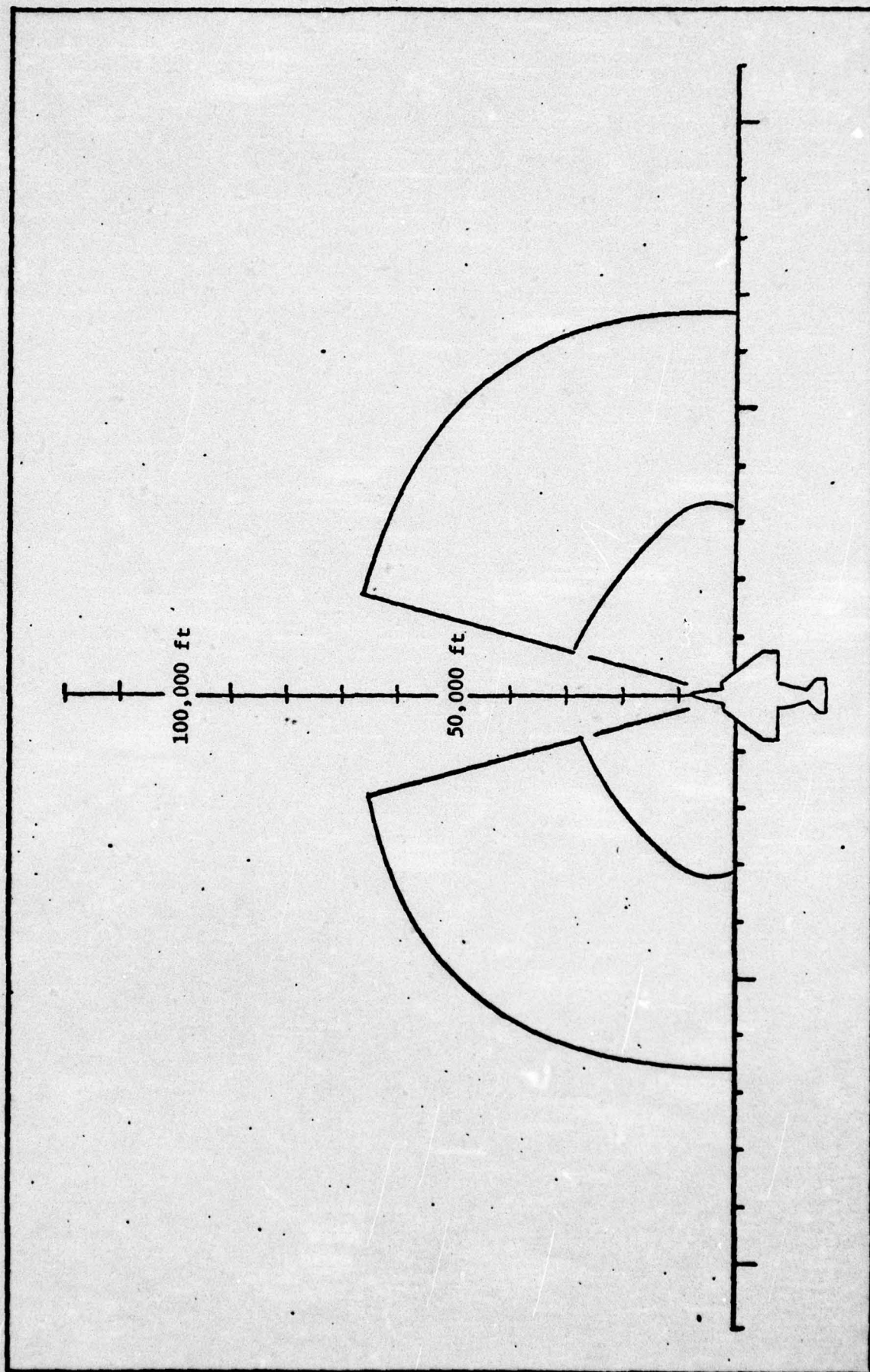


Fig. 50 Retran Missile Launch Envelopes Relative to Aircraft - 20,000 ft Launch Altitude

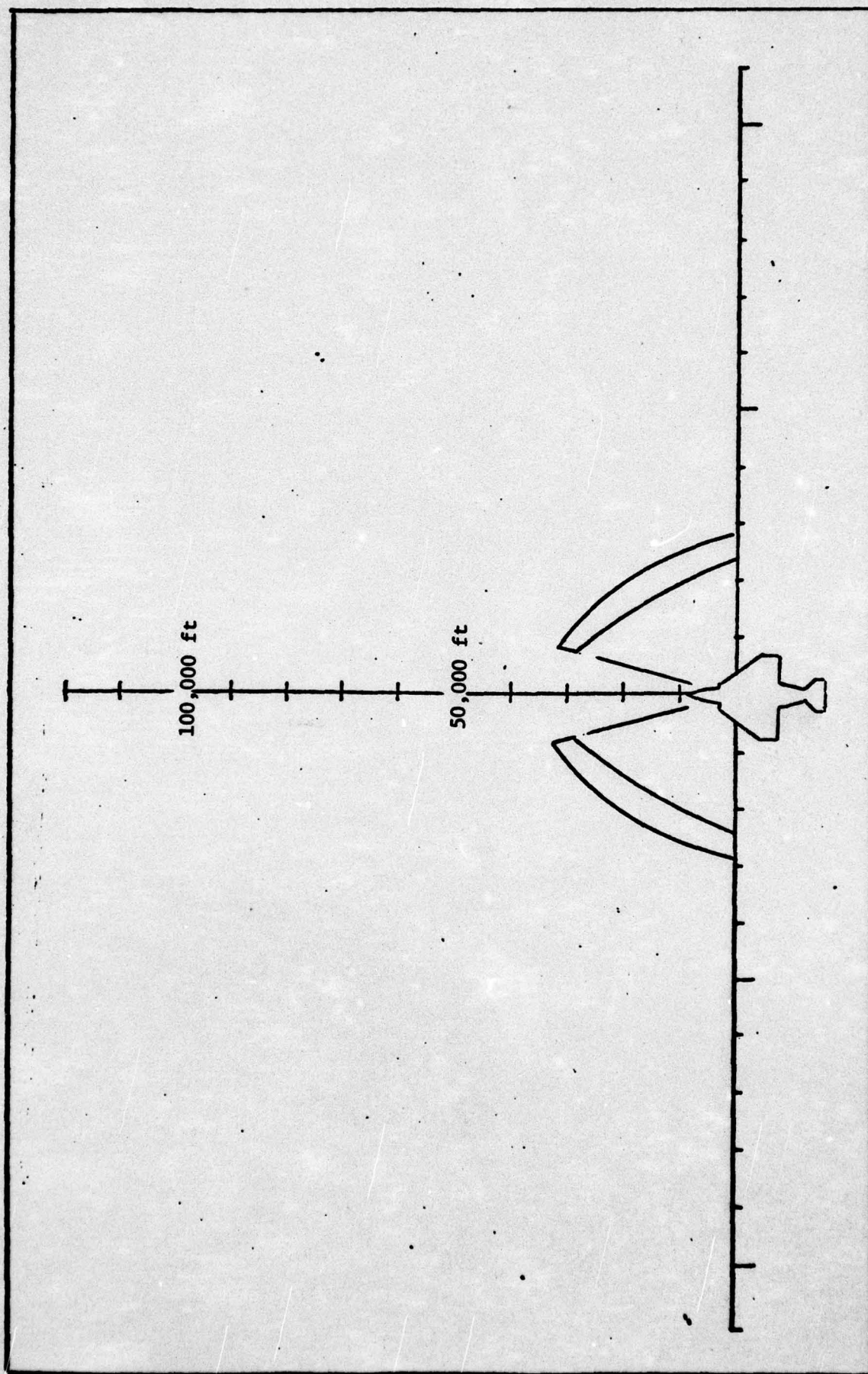


Fig. 51 Retran Missile Launch Envelope Relative To Aircraft - 5,000 ft Launch Altitude

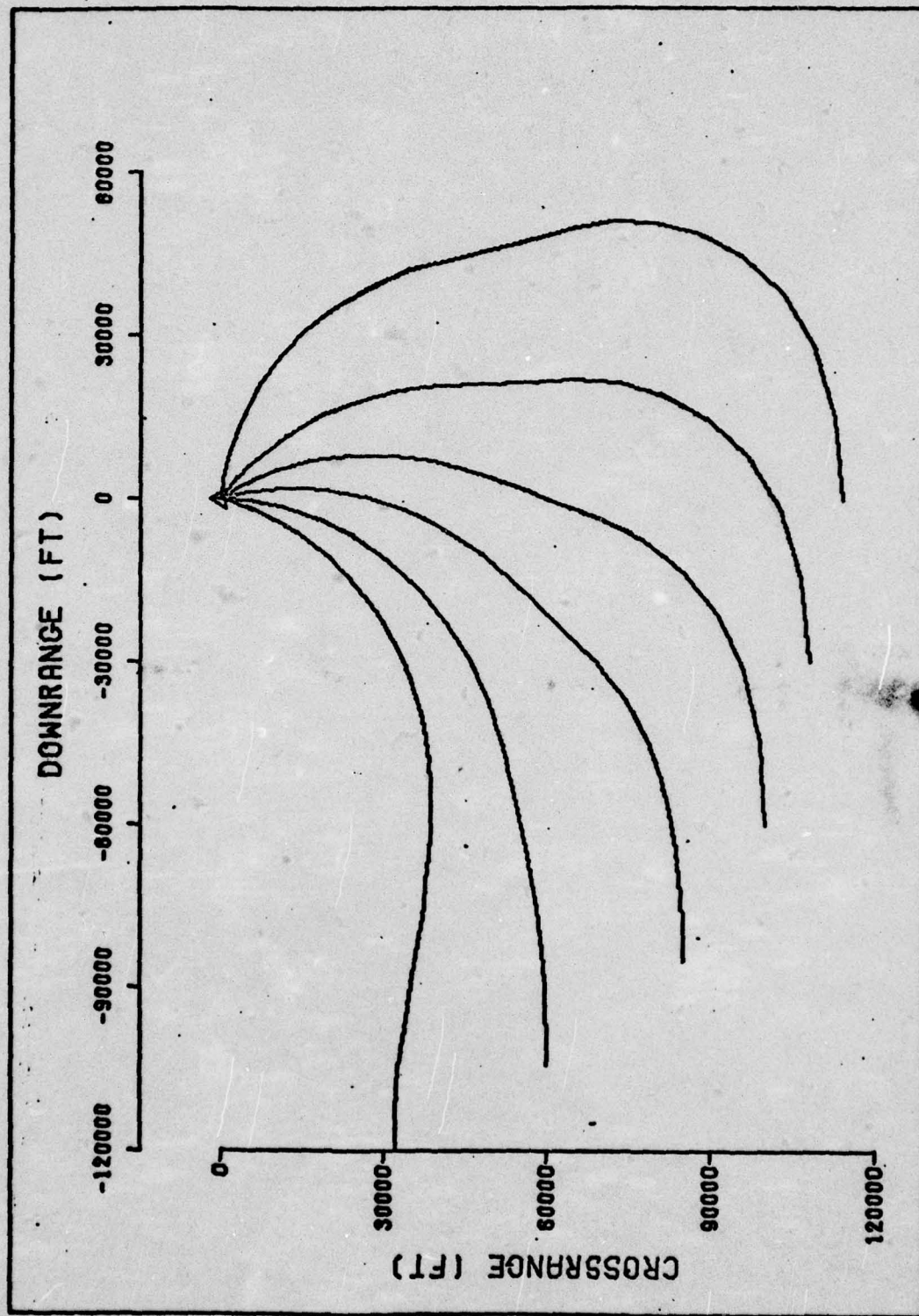


Fig. 52 Trajectory Plan Views, 35,000 ft Maximum Range Launches

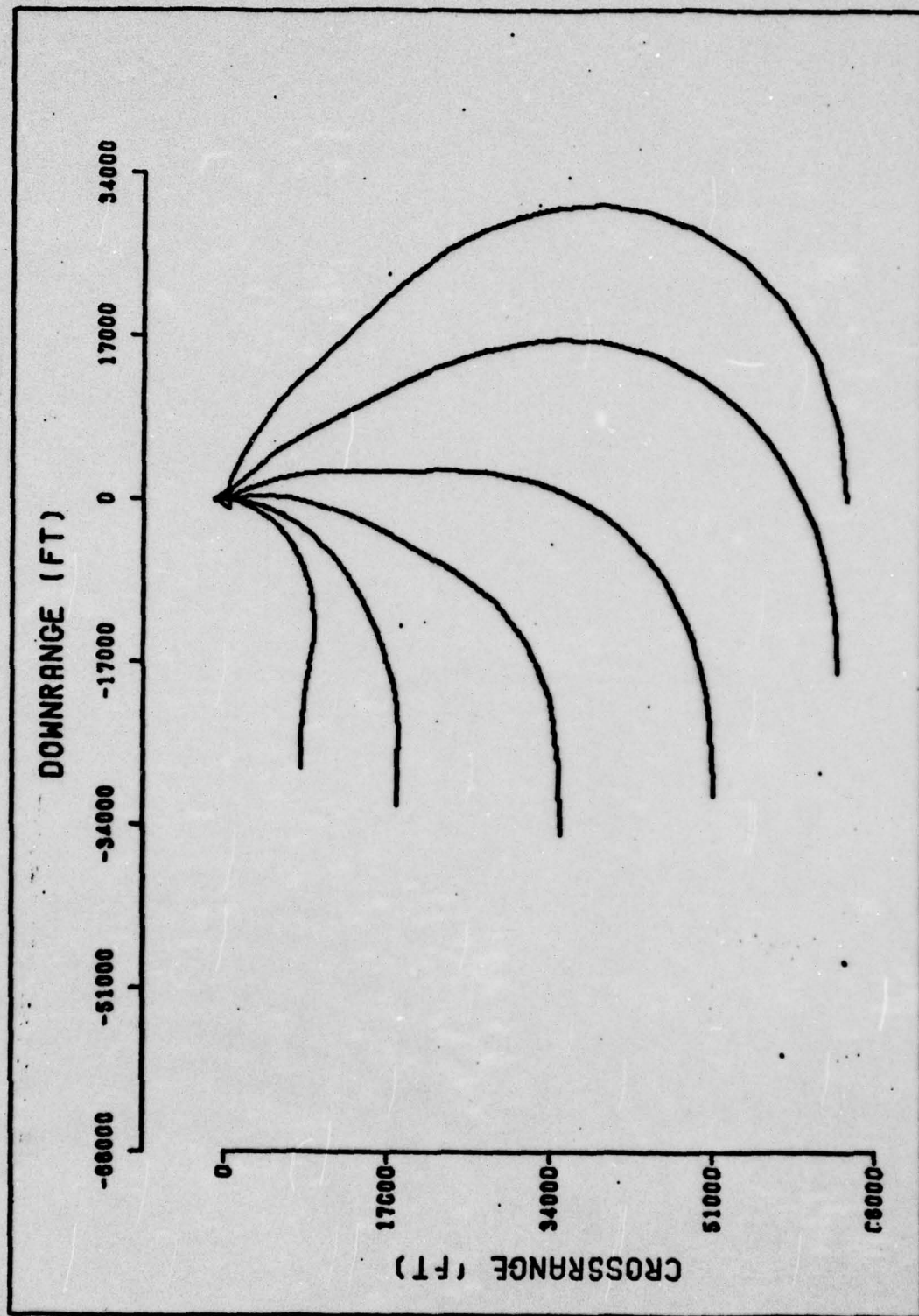


Fig. 53 Trajectory Plan Views, 35,000 ft Minimum Range Launches

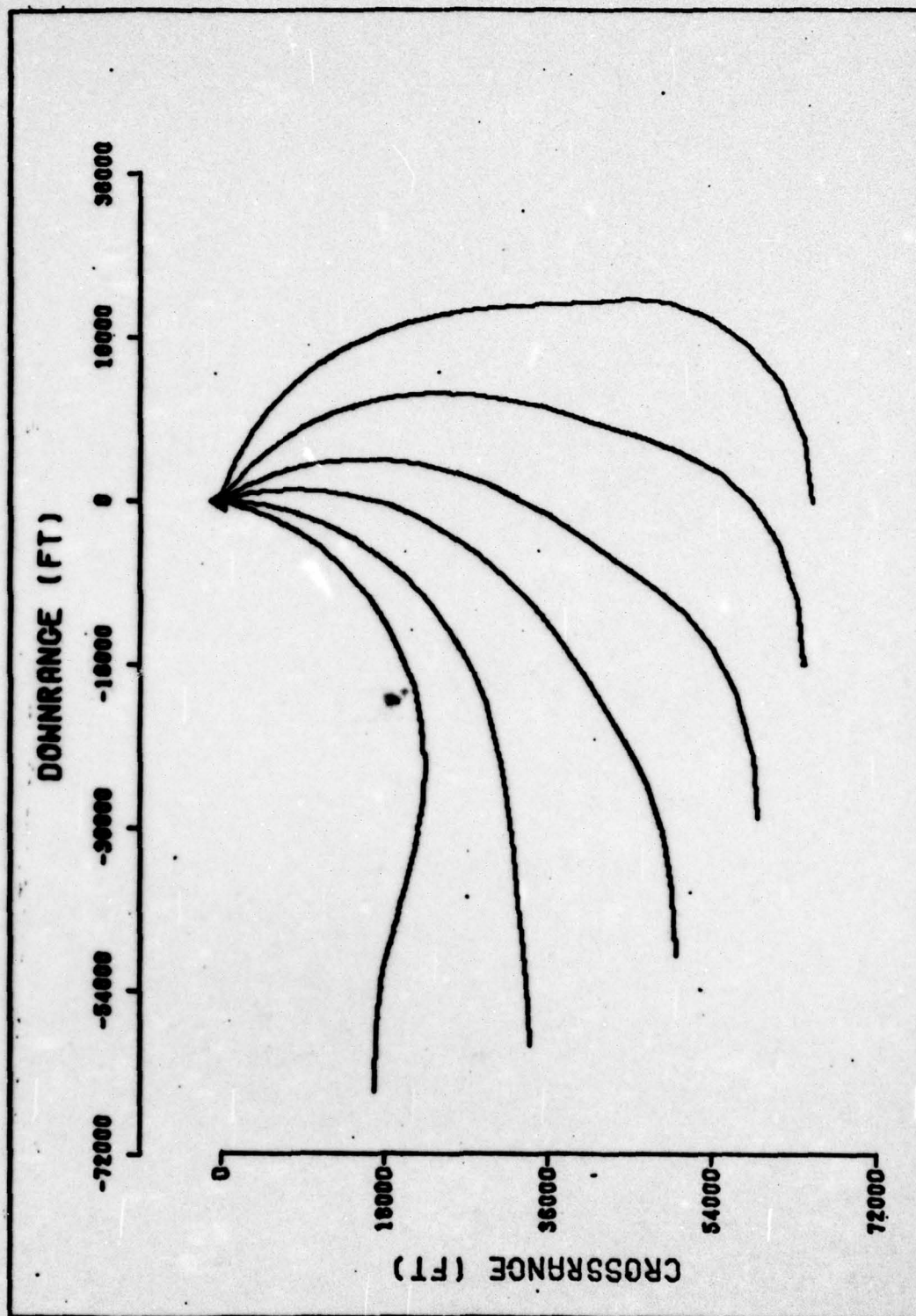


Fig. 54 Trajectory Plan Views, 20,000 ft Maximum Range Launches

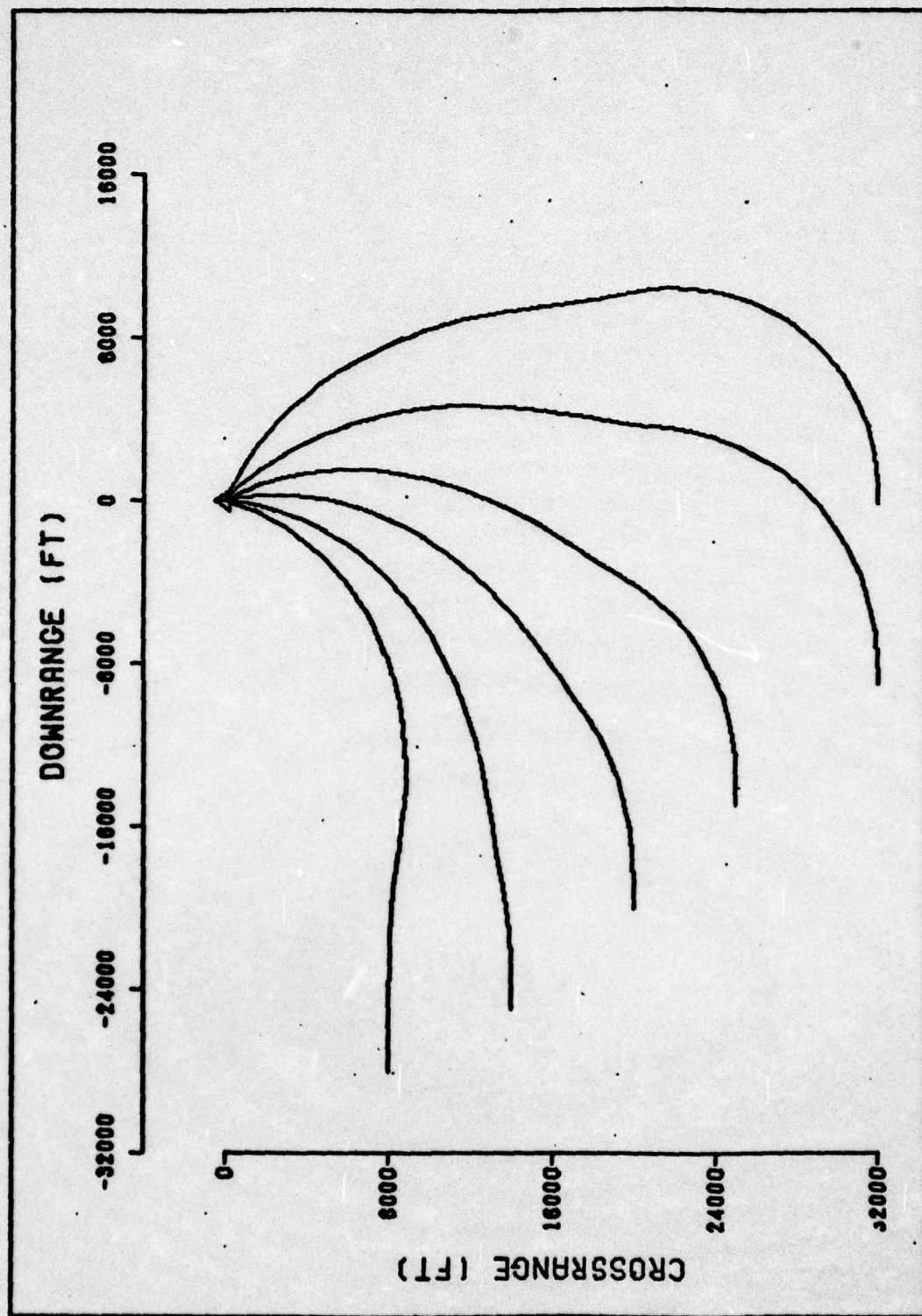


Fig. 55 Trajectory Plan Views, 20,000 ft Minimum Range Launches

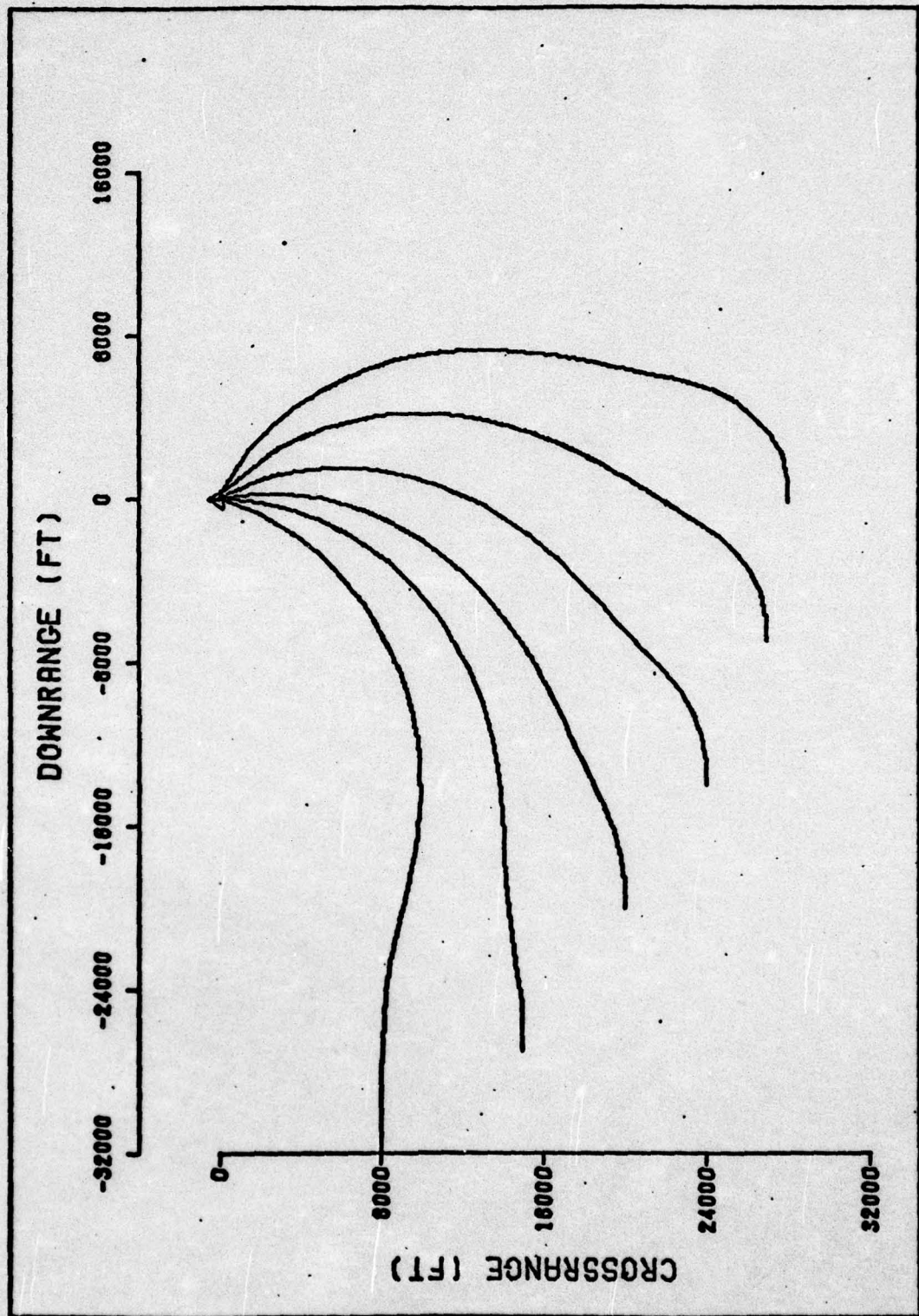


Fig. 56 Trajectory Plan Views, 5,000 ft Maximum Range Launches

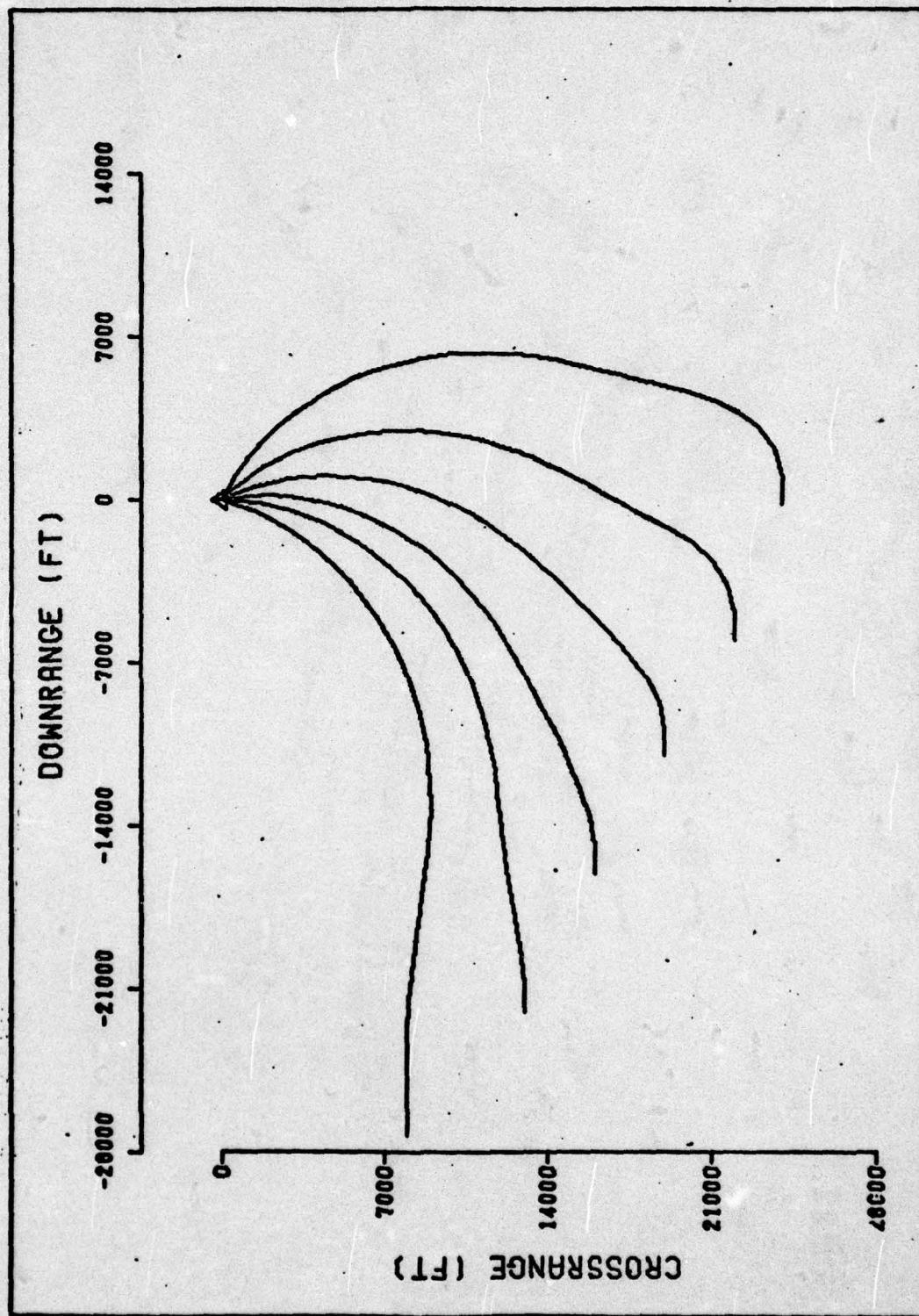


Fig. 57 Trajectory Plan Views, 5,000 ft Minimum Range Launches

VI. Discussion of Results

Guidance Algorithm Selection

The guidance algorithms were selected on the basis of missile performance obtained in the Retran simulation. Several algorithms were studied, with primary emphasis placed on obtaining maximum range. Preliminary investigations had been made by the Air Force Avionics Laboratory utilizing algorithms that were similar to the command-to-track algorithms. At low initial squint angles (below 30 degrees), where the missile initially falls behind the line of sight, these algorithms produced a long curving flight path, as can be seen in Fig. 97. The first algorithms tested in this study produced a straight line path to the line of sight intercept, then a relatively high-g (4 g's) turn onto the line of sight (these algorithms are discussed in Appendix E). Flight time and flight distance were reduced; however, the drag penalty incurred during the intercept turn resulted in lower terminal velocities than had been obtained with the command-to-track algorithms. The algorithms were modified to reduce the turning angle required at line of sight intercept, but terminal velocities were still low.

The desirable feature of the command-to-track algorithm for low to medium squint angle launches is that, with proper selection of frequency coefficient and damping ratio, a fairly uniform schedule of low-g commands can be achieved, keeping angle of attack and sideslip angle low throughout the flight. Consequently, a smooth deceleration due to drag was maintained, with no sharp airspeed losses (see the

parameter plots in Appendix D). However, at high initial squint angles (greater than 45 degrees) where the missile accelerates out ahead of the line of sight, the command-to-track algorithm commands large accelerations (6-9 g's) in the initial turn, then directs a fairly large intercept angle back to the line of sight which necessitates a high-g (10-15 g's) turn onto the line of sight. At very high squint angles, the accelerations required can exceed missile maneuvering capability.

To achieve satisfactory trajectories from high squint angles, the command-to-heading algorithm was added. With proper choice of the turning coefficient C_T , the schedule of acceleration commands can be kept uniformly low. The missile is commanded to turn to parallel the line of sight, with line of sight rotation toward the missile providing the closure rate. Since this closure rate is relatively low, a smooth transition to the command-to-track algorithm can be made, with no large accelerations required.

Launches from minimum ranges present a different problem. Here, large accelerations are required to achieve early interception to the line of sight so that minimum tracking time can be attained. These large accelerations are obtained by scheduling the gain of the command-to-heading algorithm proportional to the inverse square of missile-to-target range. Likewise, the frequency of the command-to-track algorithm is calculated proportional to the inverse of time-to-go to target impact, thus speeding response at shorter ranges. Range was chosen for gain scheduling of the command-to-heading algorithm because the large angle between missile velocity and the line of sight during

AD-A034 941

AIR FORCE INST OF TECH WRIGHT-PATTERSON AFB OHIO SCH--ETC F/G 17/9
PERFORMANCE OF AN AIR-TO-GROUND MISSILE EMPLOYING SAR-RETRAN GU--ETC(U)
DEC 76 E H JESSUP
6AE/MC/76D-6

UNCLASSIFIED

NL

2 OF 3

AD
A034941



initial employment of this algorithm makes time-to-go an unreliable indicator.

The coefficient values t_R , K , and C_T were chosen to yield a fairly uniform schedule of acceleration commands throughout the flight. The value of the range conversion coefficient, C_R , was chosen as 1000 ft/sec, which corresponds roughly to the average missile airspeed during the initial turning portion of the flight.

The damping ratio $\zeta = .5$ was the highest damping ratio that did not produce large acceleration commands during the transition to the horizontal command-to-track algorithm. This same damping ratio was utilized in the vertical algorithm and produced smooth convergence to the line of sight after only one overshoot in both the vertical and horizontal planes (this can be seen from the distance error plots in Appendix D). This smooth convergence was obtained by not allowing the algorithm frequency to increase beyond 5 seconds time-to-go; if frequency were allowed to increase without bound, the missile trajectory became erratic in the final seconds of flight. In the actual guidance system, a larger damping ratio would probably be desired in the terminal phase, with no limitation on maximum frequency in the algorithm. However, it was felt that the terminal accuracy obtained with $\zeta = .5$ was sufficient for the purpose of this study.

A g-bias of 1g produced the desired trajectory shaping for terrain clearance, as can be seen in the vertical trajectory profiles.

Autopilot Compatibility

One of the goals of this study was to determine the stability of the guidance loop with the roll stabilized autopilot of the Retran

missile. Initially, the autopilot g-bias was set at 1g and guidance commands were not transformed to the missile body frame; that is, it was assumed that the missile body frame was sufficiently aligned with the gimbal frame. This is the configuration in which the Retran missile autopilot would be employed with conventional sensors and guidance (laser, electro-optical, etc.). However, in the turning trajectories required by SAR-Retran, missile bank angles greater than 30 degrees were frequently encountered. These large bank angles caused sizeable errors in the orientation of the resulting missile acceleration. Thus, missile response to guidance commands was erratic and sometimes uncontrollable.

To eliminate this erratic behavior, the autopilot g-bias was set to zero and a g-bias was included in the vertical guidance algorithm. Guidance commands calculated by the algorithms in the gimbal frame were transformed to the missile body frame, so that no matter what missile bank angle was, the resulting accelerations were properly oriented in the gimbal frame. With these modifications, no further problems were encountered with the missile autopilot.

Trajectory Optimization

The attempt at trajectory optimization using the first order gradient algorithm was largely inconclusive. The problems which were encountered are enumerated here.

Obtaining satisfactory initial trajectories was difficult with the simplified missile model. Since instantaneous response was assumed, missile performance and, hence, accelerations commanded by the guidance

algorithm fluctuated extensively. Trajectories achieved in the simulation could not be duplicated in the initial solution, but reasonably shaped trajectories were obtained.

A sensitivity analysis was carried out to determine what values should be assigned for the penalty function coefficients. It was found that a value of $K_3 > 1.0 \times 10^{-6}$ caused the values of $\frac{\partial H}{\partial a_h}(t)$ and $\frac{\partial H}{\partial a_v}(t)$ to become very large, while values smaller than 1.0×10^{-6} had little effect on moving the solution toward longer range intercept points. Thus, $K_3 = 1.0 \times 10^{-6}$ was chosen. Similarly, it was determined that values of K_1 and K_2 larger than 1000. had little increasing effect on the heading error; in fact, an improvement of 10% in heading error was the maximum which could be achieved and this was obtained using K_1 and K_2 equal to 1000.

In the first order gradient algorithm, the solution converges to a local minimum. In the Retran problem, local minima of the payoff function were encountered with only minor trajectory changes. Widely differing initial solutions converged to different optimal solutions, with similarly small trajectory modifications. Because of the occurrence of numerous local minima in the function, it could not be concluded that any of the resulting trajectories were optimum, indeed, the optimal trajectory could only have been obtained by inputting an initial solution already very close to the optimum solution.

Since the guidance algorithms and coefficient values previously selected yielded highly satisfactory results, these algorithms were used unchanged for the launch envelope determination.

Launch Envelope Determination

The extent of the usable launch envelope was determined by finding the maximum and minimum range launch points from which the missile could satisfy the constraints of minimum terminal airspeed and minimum line of sight tracking time. Maximum launch range was limited by the airspeed constraint; a terminal airspeed between 700 ft/sec and 750 ft/sec was chosen as criteria for a maximum range launch. The tracking time constraint was always satisfied for maximum range launches. Minimum launch range was limited by the tracking time constraint. Terminal airspeed was sufficient in all minimum range launches.

It was felt that launch points can safely be interpolated between the test points used to determine the launch envelope boundaries, although no thorough investigations of launches from points within the envelope was undertaken. This hypothesis was never contradicted by any of the intermediate range launches that were attempted in the process of determining the launch envelope boundaries.

One common feature among the 20,000 ft and 35,000 ft launch envelopes is that missile flight path angles were such that the missile maintained an almost constant airspeed of 750 ft/sec - 775 ft/sec during the latter tracking phase of the trajectory.

VII. Conclusions and Recommendations

Conclusions

Based on the performance of the hypothetical Retran missile, it appears that the SAR-Retrans guidance system could be demonstrated using an existing boost-glide air-to-ground missile. A large launch envelope is achievable at high altitude, thus providing good stand-off capability. However, the launch envelope becomes very narrow at a launch altitude of 5000 ft; thus, this appears to be the minimum altitude for successful operation.

The missile autopilot can be made compatible with SAR-Retrans guidance by eliminating the g-bias from the autopilot and, instead, including this bias in the guidance algorithm. The guidance commands must be resolved into the missile body frame before being input to the autopilot.

The first order gradient technique, as applied to this problem, produced inconclusive results. Although it indicated that only minute trajectory changes were required to achieve a local minimum in the payoff function, the solution to which it converged was not necessarily an absolute minimum.

Recommendations

The effect of aircraft post-launch tactical maneuvering on missile performance and launch envelope should be studied. A maneuvering aircraft could be included in the Retran simulation.

The effect of maneuvering targets, such as a tank or truck, should be investigated.

A higher order optimization technique might be employed to optimize missile trajectories for maximum range.

In view of the range limitation of present air-to-ground missile, as represented by the Retran missile, particularly at low altitude, performance specifications should be developed for new tactical missiles to be employed with SAR-Retran.

Bibliography

1. Zuerndorfer, H. et al. "Pulse Doppler Missile Guidance." AGARD Lecture Series, 52: 4.d.(2). 1-10. Nevilly-Sur-Seine, France: NATO Advisory Group for Aerospace Research and Development, May 1972.
2. Habbe, M., and E. Mirmac. SAR Guidance Capability of the AGM-~~129~~ Maverick Missile. Thesis Topic Proposal. Wright-Patterson Air Force Base, Ohio: Air Force Avionics Laboratory, March 1976.
3. Roskam, Jan. Flight Dynamics of Rigid and Elastic Airplanes, Part One. Lawrence Kansas: Roskam Aviation and Engineering Corporation, 1972.
4. Clemow, J. Short-Range Guided Weapons. London: Temple Press, 1961.
5. Heap, E. "Methodology of Research Into Command-Line-of-Sight and Homing Guidance." AGARD Lecture Series, 52: 4.d.(1). 1-9. Nevilly-Sur-Seine, France: NATO Advisory Group for Aerospace Research and Development, May 1972.
6. Anderson, G. M., and E. A. Smith. "A Combined Gradient/Neighboring Extremal Algorithm for the Calculation of Optimal Transfer Trajectories Between Noncoplanar Orbits Using a Constant Low Thrust Rocket." The Journal of the Astronautical Sciences, XXIII: 3,225-239 (July-September 1975).
7. Kelly, H. J. "Method of Gradients." Optimization Techniques, edited by George Leitmann. New York: Academic Press, 1962.

Appendix A

Coordinate Transformations

The following coordinate transformations are utilized in both the Retran simulation and the OptraJ optimization program. The order of rotation from the earth fixed frame to the missile and aircraft body frames is (Ref 1: 2.16)

1. Yaw (ψ, ψ_A)
2. Pitch (θ, θ_A)
3. Roll (ϕ, ϕ_A)

The order of rotation from the aircraft body frame to the gimbal frame is

1. Yaw (ψ_{GA})
2. Pitch (θ_{GA})

Earth Frame to Aircraft Body Frame

$$\begin{bmatrix} X_A \\ Y_A \\ Z_A \end{bmatrix} = [\phi_A][\theta_A][\psi_A] \begin{bmatrix} X \\ Y \\ Z \end{bmatrix} \quad (85)$$

$$= [L_{AI}] \begin{bmatrix} X \\ Y \\ Z \end{bmatrix} \quad (86)$$

where

$$[L_{AI}] = \begin{bmatrix} C\psi_A C\phi_A & S\psi_A C\phi_A & -S\theta_A \\ C\psi_A S\theta_A S\phi_A - S\psi_A C\phi_A & S\psi_A S\theta_A S\phi_A + C\psi_A C\phi_A & C\theta_A S\phi_A \\ C\psi_A S\theta_A C\phi_A + S\psi_A S\phi_A & S\psi_A S\theta_A C\phi_A - C\psi_A S\phi_A & C\theta_A C\phi_A \end{bmatrix} \quad (87)$$

Aircraft Body Frame to Earth Frame

$$\begin{bmatrix} X \\ Y \\ Z \end{bmatrix} = [\psi_A]^{-1} [\theta_A]^{-1} [\phi_A]^{-1} \begin{bmatrix} X_A \\ Y_A \\ Z_A \end{bmatrix} \quad (88)$$

$$= [L_{IA}] \begin{bmatrix} X_A \\ Y_A \\ Z_A \end{bmatrix} \quad (89)$$

where

$$[L_{IA}] = \begin{bmatrix} C\psi_A C\theta_A & C\psi_A S\theta_A S\phi_A - S\psi_A C\phi_A & C\psi_A S\theta_A C\phi_A + S\psi_A S\phi_A \\ S\psi_A C\theta_A & S\psi_A S\theta_A S\phi_A + C\psi_A C\phi_A & S\psi_A S\theta_A C\phi_A - C\psi_A S\phi_A \\ S\theta_A & C\theta_A S\phi_A & C\theta_A C\phi_A \end{bmatrix} \quad (90)$$

Earth Frame to Missile Body Frame

$$\begin{bmatrix} X_M \\ Y_M \\ Z_M \end{bmatrix} = [\phi][\theta][\psi] \begin{bmatrix} X \\ Y \\ Z \end{bmatrix} \quad (91)$$

$$= [L_{MI}] \begin{bmatrix} X \\ Y \\ Z \end{bmatrix} \quad (92)$$

$[L_{MI}]$ is identical to $[L_{AI}]$ except for deletion of the subscripts.

Missile Body Frame to Earth Frame

$$\begin{bmatrix} X \\ Y \\ Z \end{bmatrix} = [\psi]^{-1} [\theta]^{-1} [\phi]^{-1} \begin{bmatrix} X_M \\ Y_M \\ Z_M \end{bmatrix} \quad (93)$$

$$= [L_{IM}] \begin{bmatrix} X_M \\ Y_M \\ Z_M \end{bmatrix} \quad (94)$$

$[L_{IM}]$ is identical to $[L_{IA}]$ except for deletion of the subscripts.

Aircraft Body Frame to Gimbal Frame

$$\begin{bmatrix} X_G \\ Y_G \\ Z_G \end{bmatrix} = [\theta_{GA}] [\psi_{GA}] \begin{bmatrix} X_A \\ Y_A \\ Z_A \end{bmatrix} \quad (95)$$

$$= [L_{GA}] \begin{bmatrix} X_A \\ Y_A \\ Z_A \end{bmatrix} \quad (96)$$

where

$$[L_{GA}] = \begin{bmatrix} c\theta_{GA} c\psi_{GA} & c\theta_{GA} s\psi_{GA} & -s\theta_{GA} \\ -s\psi_{GA} & c\psi_{GA} & 0 \\ s\theta_{GA} c\psi_{GA} & s\theta_{GA} s\psi_{GA} & c\theta_{GA} \end{bmatrix} \quad (97)$$

Gimbal Frame to Aircraft Body Frame

$$\begin{bmatrix} X_A \\ Y_A \\ Z_A \end{bmatrix} = [\psi_{GA}]^{-1} [\theta_{GA}]^{-1} \begin{bmatrix} X_G \\ Y_G \\ Z_G \end{bmatrix} \quad (98)$$

$$= [L_{AG}] \begin{bmatrix} X_G \\ Y_G \\ Z_G \end{bmatrix} \quad (99)$$

where

$$[L_{AG}] = \begin{bmatrix} C\psi_{GA}C\theta_{GA} & -S\psi_{GA} & C\psi_{GA}S\theta_{GA} \\ S\psi_{GA}C\theta_{GA} & C\psi_{GA} & S\psi_{GA}S\theta_{GA} \\ -S\theta_{GA} & 0 & C\theta_{GA} \end{bmatrix} \quad (100)$$

Earth Frame to Gimbal Frame

$$\begin{bmatrix} X_G \\ Y_G \\ Z_G \end{bmatrix} = [L_{GI}] \begin{bmatrix} X \\ Y \\ Z \end{bmatrix} \quad (101)$$

where $[L_{GI}] = [L_{GA}][L_{AI}]$

Gimbal Frame to Missile Body Frame

$$\begin{bmatrix} X_M \\ Y_M \\ Z_M \end{bmatrix} = [L_{MG}] \begin{bmatrix} X_G \\ Y_G \\ Z_G \end{bmatrix} \quad (102)$$

where $[L_{MG}] = [L_{MI}][L_{IA}][L_{AG}]$

Appendix B

Program Retran Listing and Sample Output

PROGRAM RETRAN(INPUT,OUTPUT,TAPES=INPUT,TAPES=OUTPUT,PLOT,PUNCH)

RETRAN MISSILE SIMULATION

DEFINITION OF INPUT VARIABLES

XEA, YEA, ZEA - INITIAL AIRCRAFT POSITION IN EARTH-FIXED COORDINATES (FT).

XEAD, YEAD, ZEAD - INITIAL AIRCRAFT VELOCITY IN EARTH-FIXED COORDINATES (FT/SEC).

THADG, PSADG, PHADG - INITIAL AIRCRAFT PITCH, HEADING, AND ROLL ANGLES IN DEGREES WHICH ARE CONVERTED TO RADIANS (TH,PS,PH)

XET, YET, ZET - TARGET POSITION IN EARTH-FIXED COORDINATES (FT)

Δ - INTEGRATION STEP SIZE IN SECONDS.

GBIAS - BIAS COMMAND IN VERTICAL CHANNEL IN G'S

GHBias - BIAS COMMAND IN HORIZONTAL CHANNEL IN G'S

TIME - MAXIMUM FLIGHT TIME (SEC). (PROGRAM TERMINATES WHEN MISSLE GOES THROUGH TARGET ALTITUDE OR WHEN TIME IS EXCEEDED.)

ITABL - INTEGER SWITCH CONTROLLING PRINTING OF AERODYNAMIC TABLES. PRINTING TAKES PLACE ONLY IF ITABL = 1.

IPR - THE NUMBER OF SECONDS BETWEEN PRINT CYCLES (INTEGER)

PBIAS - BIAS ON AUTOPILOT ROLL RATE BYRD IN RADIANS / SECOND.

TR - ACCELERATION COMMAND COEFFICIENT REFERENCE TIME (SEC).

ZI - DAMPING RATIO IN COMMAND TO LOS GUIDANCE ALGORITHMS

CT - GAIN COEFFICIENT FOR COMMAND TO HEADING GUIDANCE ALGORITHM

F - PLOTTING SIZE FACTOR F = 1.0 YIELDS 6IN BY 9IN PLOTS.

IPU - INTEGER SWITCH CONTROLLING PUNCH OUTPUT. PUNCHING TAKES PLACE ONLY IF IPU = 1.

IPT - INTEGER SWITCH CONTROLLING PLOTTING. PLOTTING TAKES PLACE ONLY IF IPT = 1.

ILEG - INTEGER SWITCH CONTROLLING PRINTING OF LEGEND OF OUTPUT


```

C*          VARIABLES.  LEGEND IS PRINTED ONLY IF ILEG = 1.
C*
C*****
C
COMMON /ACC/ AXB,AYB,ABY,AXE,AYE,AZE,PDOT,QDOT,RDOT
COMMON /AEJLER/ PHADOT,THADOT,PSADOT
COMMON /AER/ DEL,DCC,CN1,CN1,CC,CM2,CN2,CN,DDO,DELDD,AYACH,ALPHA
1  ,ALT,BETA,CCY,CN2Y,CN2Y,CN1Y,CN1Y,DDCY,DD,CN,CN1
COMMON /ANG/ PS, T1, P1, PSDG, T1D, P1D, P1, T1, P1A,
1  PSDG, THADG, PHADG, PSADG, THADG, 1GADG
COMMON /BJCK1/ XXI,YYI,ZZI,AMASS,CG,CG,PBIAS,XX
COMMON /BJCK2/ A4G,AVG,TTG,DELF,ISUID,TR,UA,RANGE,ZI,CT,VDOT
COMMON /CMJ/ AV,AH,WY,WZ
COMMON /CNT_1/ DB,DC,DT,ACZ,ACY,ACK,SBIAS,GHBIAS,IJK
COMMON /CNT_2/ R,Q,S,J,C,B1,P1,P2,K,P
COMMON /DER/ D,RL,CN1D,CMCG,QQ,S,VEL,THR,CN1Y,CMCGY,RV
COMMON /INITL/ H,TIME,ITABL,IPR,ILEG
COMMON /MATRIX/ CET1,CET2,CET3,CET4,CET5,CET6,CET7,CET8,CET9,
1  CIG1,CIG2,CIG3,CIG4,CIG5,CIG6,CIG7,CIG8,CIG9,
1  CMG1,CMG2,CMG3,CMG4,CMG5,CMG6,CMG7,CMG8,CMG9,
1  SPSGA,CPSGA,STHGA,CTHGA
COMMON /OLJAT1/ PXET( 52),PYET( 52),PXE( 52),PXE( 52),PXE( 52),
1  PYEA( 52),PZE( 52),PZEA( 52),F
COMMON /OLJAT2/ PAHG( 52),PAVG( 52),PT( 52),PJF( 52),
1  PR( 52),PAL( 52),PBE( 52),PVD( 52),PDY( 52),PDZ( 52)
COMMON /OLJAT3/ PAVS( 32),PBES( 32),PTS( 32),PR3( 32) , IPR0
COMMON /POS/ XET,YET,ZET,XEA,YEA,ZEA,RANAT,XE,YE,ZE
COMMON /PRNT1/ DY,DZ,DVY,DVZ,AYP,AZP
COMMON /VTARGET/ XETD,YETD,ZETD,XBD,YBD,ZBD
COMMON /THRST/ TIMES(21),THSTLB(21)
COMMON /VELJ/ XED,YED,ZED,XEAD,YEAD,ZEAD,JB,V3,W3
C
C
C*****
C*
C*          FLIGHT INITIALIZATION
C*
C*****
C
10 CONTINUE
C
C***** INITIALIZE INTEGRATION STEP COUNTER
C
IJK = -1
C
C***** INITIALIZE PLOT COUNTER
C
NPTS=0
NPT2 = 0
NPT3 = 0
C
C***** READ INITIAL FLIGHT CONDITIONS
C
READ(5,9010) XEA, YEA, ZEA, XEAD, YEAD, ZEAD, THADG, PSADG, PHADG
1  ,XET, YET, ZET, H, SBIAS, GHBIAS, TIME, ITABL, IPR, PBIAS,TR,
1  ZI,CT,F,I,J,IPT,ILEG
C
9010 FORMAT( 9F10.2, / 5F3.?, 2F6.2, F5.2, I2, I4, F5.3 , F4.1 /3F10.0,

```

```

      12,IX,IY,IX,IY)
C
C***** TEST FOR END OF JOB
C
      IF(EOF(5)) 75,15
C
C***** SET COMMANDED AZIMUTH GIMBAL ANGLE OF AIRCRAFT (PSGC)
C
      15  PSGC = -95.
C
C***** DEFINE AIRCRAFT VELOCITY (UA)
C
      UA = XEAD
C
C***** PRINT INITIAL CONDITIONS AND AERODYNAMIC TABLES
C
      CALL OUTPR.
      IF(IPU.EQ.1) PUNCH 12,XEA,YEA,ZEA
      12  FORMAT(3F10,2)
C
C***** INITIALIZE FLIGHT PARAMETERS
C
      CALL INTFL.
      IPR0 = IPR
      IPR = IPR/4
      H0 = H.
C
C*****
C*
C*          THIS SEQUENCE IS FOLLOWED FOR EACH INTEGRATION STEP
C*
C*****
C
      20 CONTINUE
C
C***** INCREMENT INTEGRATION STEP COUNTER
C
      IJK = IJK + 1
C
C***** OBTAIN TARGET VELOCITY
C
      CALL TARGET(X)
C
C***** COMPUTE COORDINATE TRANSFORMATIONS
C
      CALL EULER(1)
C
C***** COMPUTE GUIDANCE COMMANDS AND CONTROL DISPLACEMENTS
C
      CALL COMMAND
      CALL CONTROL
C
C***** COMPUTE AIR DENSITY AND SPEED OF SOUND
C
      ALT = -7E
      CALL ATMOS (ALT,RHO,SOS)
C
C***** COMPUTE ANGLE OF ATTACK, SIDE-SLIP AIR SPEED, MACH NUMBER, AND

```



```

C          DYNAMIC PRESSURE
C
C          ALPHA = ATAN(W3/U3)*57.3
C          BETA = ATAN(V3/U3)*57.3
C          VEL = SQRT(XED*XED + YED*YED + ZED*ZED)
C          AMACH = VEL/SOS
C          QQ = 5*VEL*VEL*RHO
C
C***** COMPUTE THRUST, MOMENTS OF INERTIA, AND CENTER OF GRAVITY
C
C          IF(X.LT.4.5)CALL THRJST(X)
C
C***** FOR AERODYNAMIC FORCES AND MOMENTS ON MISSILE AND
C          COMPUTE THE ACCELEROMETER OUTPUTS IN BODY FRAME AXES.
C
C          CALL AERO
C
C***** COMPUTE MISSILE AIRSPEED ACCELERATION/DECELERATION
C
C          VDOT = (AX3)*COS(ALPHA/57.295)*COS(BETA/57.295)+AY3*SIN(
1 BETA/57.295)+AZ3*SIN(ALPHA/57.295)*COS(BETA/57.295)-32.2*SIN(T4-
1 ALPHA/57.295)
C
C***** TRANSFORM ACCELERATION COMPONENTS OF MISSILE FROM BODY AXES TO
C          EARTH SYSTEM. (AX3,AY3,AZ3) TO (AXE,AYE,AZE)
C
C          CALL EULER(2)
C
C***** INTEGRATE ACCELERATION COMPONENTS OF MISSILE (AXE,AYE,AZE)
C          GIVING VELOCITIES (XED,YED,ZED)
C
C          YED = YED + AYE*H
C          ZED = ZED + AZE*H
C          XED = XED + AXE*H
C
C***** INTEGRATE ANGULAR ACCELERATIONS OF MISSILE (QDOT, RDOT)
C          GIVING BODY ANGULAR RATES (Q, R)
C
C          Q = Q + QDOT*H
C          R = R + RDOT*H
C
C***** COMPUTE EULER ANGLE RATES (PSDOT, THDOT, PHDOT)
C
C          PSDOT = (Q*SIN(PH) + R*COS(PH)) / COS(TH)
C          THDOT = Q*COS(PH) - R*SIN(PH)
C          PHDOT = PSDOT*SIN(TH) + PBIAS
C
C***** INTEGRATE EULER ANGLE RATES (PSDOT, THDOT, PHDOT)
C          GIVING MISSILE ATTITUDES (PS, TH, PH)
C
C          PS = PS + PSDOT*H
C          TH = TH + THDOT*H
C          PH = PH + PHDOT*H
C
C***** COMMAND AIRCRAFT TURNING RATE
C
C          PSERR IS THE ERROR BETWEEN THE COMMANDED AIRCRAFT GIMBAL ANGLE
C          AND THE ACTUAL GIMBAL ANGLE. THIS ERROR IS LIMITED TO PLUS OR

```

```

C      MINUS 7 DEGREES AND IS USED TO COMMAND AN AIRCRAFT TURNING RATE
C      PSAJOT.
C
C      PSGERR = PS33 - PSGA33
C      IF(PSGERR.GT.7.)PSGERR=7.
C      IF(PSGERR.LT.-7.)PSGERR=-7.
C      PSADOT = -PSGERR/37.295
C      PSAJG = PSAJG - PSGERR*4
C      PSA = PSAJG/37.295
C
C***** INTEGRATE AIRCRAFT VELOCITIES(XEAD,YEAD) GIVING
C      AIRCRAFT POSITION (XEA,YEA)
C
C      30  XEAD = JA*COS(THA)*COS(PSA)
C          YEAD = JA*COS(THA)*SIN(PSA)
C          ZEAD = JA*SIN(THA)
C          XEA = XEA + XEAD*H
C          YEA = YEA + YEAD*H
C          ZEA = ZEA + ZEAD*H
C
C***** INTEGRATE MISSILE VELOCITIES (XED,YED,ZED)
C      GIVING MISSILE POSITION (XE,YE,ZE)
C
C      XE = XE + XED*H
C      YE = YE + YED*H
C      ZE = ZE + ZED*H
C
C***** INTEGRATE TARGET VELOCITIES (XETD,YETD,ZETD)
C      GIVING TARGET POSITION (XET,YET,ZET)
C
C      XET = XET + XETD*H
C      YET = YET + YETD*H
C      ZET = ZET + ZETD*H
C
C***** TEST FOR IMPACT
C
C      IF(ZE.GT.ZET) GO TO 40
C
C***** INCREMENT TIME
C
C      IF(TTG.LT.10.) H=40/10
C      IF(TTG.LT.10.) IPR = 1 /H
C      X = X + H
C
C***** TEST INTEGRATION STEP COUNTER FOR PRINTING
C
C      IF(MOD(IJK,IPR).NE.0) GO TO 50
C
C      40 CONTINUE
C
C***** UPDATE PLOT ARRAY
C
C      NPTS=NPTS+1
C      PXEA(NPTS)=XEA
C      PYEA(NPTS)=YEA
C      PZEA(NPTS) = -ZEA
C      PXET(NPTS)=XET
C      PYET(NPTS)=YET

```



```

PX(NPTS) = X
PY(NPTS) = Y
PZ(NPTS) = -ZE
PT(NPTS) = X
PR(NPTS) = RANGE
PAHG(NPTS) = AHG
IF(PAHG(NPTS).GE. 20.) PAHG(NPTS) = 20.
IF(PAHG(NPTS).LE.-20.) PAHG(NPTS) = -20.
PAVG(NPTS) = AVG
IF(PAVG(NPTS).GE. 20.) PAVG(NPTS) = 20.
IF(PAVG(NPTS).LE.-20.) PAVG(NPTS) = -20.
PAL(NPTS) = ALPHA
PBE(NPTS) = BETA
PDF(NPTS) = DELF
IF(PDF(NPTS).GT. 15.) PDF(NPTS) = 15.
PVDOT(NPTS) = VDOT
IF(PVDOT(NPTS).GE. 100.) PVOT(NPTS) = 100.
IF(PVDOT(NPTS).LE.-100.) PVOT(NPTS) = -100.
IF(X.GT.12.) GO TO 41
NPT2 = NPT2+1
PAVS(NPT2) = AVG
IF(PAVS(NPT2).LE.-20.) PAVS(NPT2) = -20.
IF(PAVS(NPT2).GE. 20.) PAVS(NPT2) = 20.
PBES(NPT2) = BETA
PTS(NPT2) = X
GO TO 43
41 NPT3 = NPT3+1
PDY(NPT3) = DY
PDZ(NPT3) = DZ
PR3(NPT3) = RANGE
43 IF(IPU.EQ.1) PUNCH 42,XE,YE,ZE,XEA,YEA,ZEA
42 FORMAT(3F10.2/3F10.2)
C
C***** PRINT FLIGHT VARIABLES
C
C      CALL OJFLT
C
C      50 CONTINUE
C
C***** TEST FOR CONTINUATION OF FLIGHT
C
C      IF(X.LT.TIME.AND.ZE.LT.ZET) GO TO 20
C
C***** END OF FLIGHT
C
C***** PLOT TRAJECTORY
C
C      IF(IPT.EQ.1) CALL PIK(NPTS,NPT2,NPT3)
C
C      GO TO 10
C
C      75 CONTINUE
C
C***** END OF JOB
C
C      STOP 1
C
C      END

```

SUBROUTINE AERO

```

C
C*****
C* THIS ROUTINE COMPUTES FORCES AND MOMENTS GIVEN ANGLES OF ATTACK,
C* CONTROL DEFLECTIONS, AND MACH NUMBER.  OUTPUT IS TRANSLATIONAL AND
C* ROTATIONAL ACCELERATION COMPONENTS IN BODY AXES.
C*****
C
COMMON /ACC/ AXR,AYR,AZR,AXE,AYE,AZE,PDOT,QDOT,RDOT
COMMON /AER/ DEL,DCC,DN1,CM1,CC,CM2,DN2,CM,CCO,DELCD,AMACH,ALPHA
1  ,ALT,BETA,DZY,DZ2Y,CN2Y,CMY,CN1Y,CM1Y,DCCY,CD,CN,CNY
COMMON /AERTBL/ DCC(8,5,6),CMT(8,5,5),CNT(8,5,5),X1(16),
1  DDT(10,6),DMT(10,6),CN2T(10,6),CMTT(10,5),X2(16),
2  DDT(10),DMT(10),H(6),DELCDT(6)
COMMON /A45/ RH02(12),SDS2(12),ALTT(12)
COMMON /BLOCK1/ XXI,YYI,ZZI,AMASS,CG,WG,PBIAS,XX
COMMON /CNT1/ DB,DC,DT,ACZ,ACY,ACK,GBIAS,G4BIAS,IJK
COMMON /CNT2/ R,Q,G,U,C,B1,P1,P2,X,P
COMMON /DER/ D,RL,C4D,CMDG,QQ,S,VEL,THR,CMADY,CMDSY,RY
COMMON /T4RST/ TIMES(21),T4STLB(21)
COMMON /VELD/ XED,YED,ZED,XEAD,YEAD,ZEAD,UB,V3,W3

```

DIMENSION VA(2),XA(2),VA1(3),XA1(3)

AERODYNAMIC TABLES

DATA (((DCC(I,J,K),I=1,8),J=1,5),K=1,3) /

1	0.00	, .010	, .045	, .110	, .200	, .300	, .300	, .300	,
2	-.01	, 0.000	, .033	, .090	, .150	, .250	, .250	, .250	,
3	-.02	, -.010	, .020	, .075	, .140	, .200	, .200	, .200	,
4	-.03	, -.025	, 0.00	, .040	, .090	, .130	, .130	, .130	,
5	-.04	, -.040	, -.12	, .005	, .030	, .050	, .050	, .050	,

6	0.00	, .010	, .045	, .110	, .200	, .300	, .300	, .300	,
7	-.01	, 0.000	, .033	, .090	, .150	, .250	, .250	, .250	,
8	-.02	, -.010	, .020	, .075	, .140	, .200	, .200	, .200	,
9	-.03	, -.025	, 0.00	, .040	, .090	, .130	, .130	, .130	,
A	-.04	, -.040	, -.12	, .005	, .030	, .050	, .050	, .050	,

B	0.00	, .010	, .045	, .110	, .200	, .300	, .300	, .300	,
C	-.01	, 0.000	, .033	, .090	, .150	, .250	, .250	, .250	,
D	-.02	, -.010	, .020	, .075	, .140	, .200	, .200	, .200	,
E	-.03	, -.025	, 0.00	, .040	, .090	, .130	, .130	, .130	,
F	-.04	, -.040	, -.12	, .005	, .030	, .050	, .050	, .050	/

DATA (((DCC(I,J,K),I=1,8),J=1,5),K=4,6) /

1	0.00	, .010	, .045	, .110	, .200	, .300	, .300	, .300	,
2	-.01	, 0.000	, .033	, .090	, .150	, .250	, .250	, .250	,
3	-.02	, -.010	, .020	, .075	, .140	, .200	, .200	, .200	,
4	-.03	, -.025	, 0.00	, .040	, .090	, .130	, .130	, .130	,

	5	-0.04	, -0.040	, -0.12	, .005	, .030	, .050	, .050	,
C	6	0.00	, .010	, .045	, .110	, .200	, .300	, .300	,
	7	-0.01	, 0.000	, .033	, .090	, .150	, .250	, .250	,
	8	-0.02	, -.010	, .020	, .075	, .140	, .200	, .200	,
	9	-0.03	, -.025	, 0.00	, .040	, .090	, .130	, .130	,
	A	-0.04	, -.040	, -.12	, .005	, .030	, .050	, .050	,
C									
	B	0.00	, .010	, .045	, .110	, .200	, .300	, .300	,
	C	-0.01	, 0.000	, .033	, .090	, .150	, .250	, .250	,
	D	-0.02	, -.010	, .020	, .075	, .140	, .200	, .200	,
	E	-0.03	, -.025	, 0.00	, .040	, .090	, .130	, .130	,
	F	-0.04	, -.040	, -.12	, .005	, .030	, .050	, .050	/

C
C*****

	DATA (((C4T (I,J,K),I=1,8),J=1,5),K=1,3) /								
C									
	1	.0	, 1.0	, 2.0	, 3.0	, 4.0	, 5.0	, 5.0	,
	2	.0	, 1.0	, 2.0	, 3.0	, 4.0	, 5.0	, 5.0	,
	3	.0	, 1.0	, 2.0	, 3.0	, 4.0	, 5.0	, 5.0	,
	4	.0	, 1.0	, 2.0	, 3.0	, 4.0	, 5.0	, 5.0	,
	5	.0	, 1.0	, 2.0	, 3.0	, 4.0	, 5.0	, 5.0	,
C									
	6	.0	, 1.0	, 2.0	, 3.0	, 4.0	, 5.0	, 5.0	,
	7	.0	, 1.0	, 2.0	, 3.0	, 4.0	, 5.0	, 5.0	,
	8	.0	, 1.0	, 2.0	, 3.0	, 4.0	, 5.0	, 5.0	,
	9	.0	, 1.0	, 2.0	, 3.0	, 4.0	, 5.0	, 5.0	,
	A	.0	, 1.0	, 2.0	, 3.0	, 4.0	, 5.0	, 5.0	,
C									
	B	.0	, 1.0	, 2.0	, 3.0	, 4.0	, 5.0	, 5.0	,
	C	.0	, 1.0	, 2.0	, 3.0	, 4.0	, 5.0	, 5.0	,
	D	.0	, 1.0	, 2.0	, 3.0	, 4.0	, 5.0	, 5.0	,
	E	.0	, 1.0	, 2.0	, 3.0	, 4.0	, 5.0	, 5.0	,
	F	.0	, 1.0	, 2.0	, 3.0	, 4.0	, 5.0	, 5.0	/

	DATA (((C4T (I,J,K),I=1,8),J=1,5),K=4,6) /								
C									
	1	.0	, 1.0	, 2.0	, 3.0	, 4.0	, 5.0	, 5.0	,
	2	.0	, 1.0	, 2.0	, 3.0	, 4.0	, 5.0	, 5.0	,
	3	.0	, 1.0	, 2.0	, 3.0	, 4.0	, 5.0	, 5.0	,
	4	.0	, 1.0	, 2.0	, 3.0	, 4.0	, 5.0	, 5.0	,
	5	.0	, 1.0	, 2.0	, 3.0	, 4.0	, 5.0	, 5.0	,
C									
	6	.0	, 1.0	, 2.0	, 3.0	, 4.0	, 5.0	, 5.0	,
	7	.0	, 1.0	, 2.0	, 3.0	, 4.0	, 5.0	, 5.0	,
	8	.0	, 1.0	, 2.0	, 3.0	, 4.0	, 5.0	, 5.0	,
	9	.0	, 1.0	, 2.0	, 3.0	, 4.0	, 5.0	, 5.0	,
	A	.0	, 1.0	, 2.0	, 3.0	, 4.0	, 5.0	, 5.0	,
C									
	B	.0	, 1.0	, 2.0	, 3.0	, 4.0	, 5.0	, 5.0	,
	C	.0	, 1.0	, 2.0	, 3.0	, 4.0	, 5.0	, 5.0	,
	D	.0	, 1.0	, 2.0	, 3.0	, 4.0	, 5.0	, 5.0	,
	E	.0	, 1.0	, 2.0	, 3.0	, 4.0	, 5.0	, 5.0	,
	F	.0	, 1.0	, 2.0	, 3.0	, 4.0	, 5.0	, 5.0	/

C
C*****
C

```

DATA (((CNT (I,J,K),I=1,8),J=1,5),K=1,3) /
C
1 0. , -20 , -10 , -60 , -80 , -1.00 , -1.00 , -1.00 ,
2 0. , -20 , -10 , -50 , -90 , -1.00 , -1.00 , -1.00 ,
3 0. , -20 , -10 , -60 , -80 , -1.00 , -1.00 , -1.00 ,
4 0. , -20 , -10 , -60 , -80 , -1.00 , -1.00 , -1.00 ,
5 0. , -20 , -10 , -60 , -80 , -1.00 , -1.00 , -1.00 ,
C
6 0. , -20 , -10 , -60 , -80 , -1.00 , -1.00 , -1.00 ,
7 0. , -20 , -10 , -60 , -80 , -1.00 , -1.00 , -1.00 ,
8 0. , -20 , -10 , -60 , -80 , -1.00 , -1.00 , -1.00 ,
9 0. , -20 , -10 , -60 , -80 , -1.00 , -1.00 , -1.00 ,
A 0. , -20 , -10 , -60 , -80 , -1.00 , -1.00 , -1.00 ,
C
B 0. , -20 , -10 , -60 , -80 , -1.00 , -1.00 , -1.00 ,
C 0. , -20 , -10 , -60 , -80 , -1.00 , -1.00 , -1.00 ,
D 0. , -20 , -10 , -60 , -80 , -1.00 , -1.00 , -1.00 ,
E 0. , -20 , -10 , -60 , -80 , -1.00 , -1.00 , -1.00 ,
F 0. , -20 , -10 , -60 , -80 , -1.00 , -1.00 , -1.00 /

```

```

DATA (((CNT (I,J,K),I=1,8),J=1,5),K=4,6) /
C
1 0. , -20 , -10 , -60 , -80 , -1.00 , -1.00 , -1.00 ,
2 0. , -20 , -10 , -60 , -80 , -1.00 , -1.00 , -1.00 ,
3 0. , -20 , -10 , -60 , -80 , -1.00 , -1.00 , -1.00 ,
4 0. , -20 , -10 , -60 , -80 , -1.00 , -1.00 , -1.00 ,
5 0. , -20 , -10 , -60 , -80 , -1.00 , -1.00 , -1.00 ,
C
6 0. , -20 , -10 , -60 , -80 , -1.00 , -1.00 , -1.00 ,
7 0. , -20 , -10 , -60 , -80 , -1.00 , -1.00 , -1.00 ,
8 0. , -20 , -10 , -60 , -80 , -1.00 , -1.00 , -1.00 ,
9 0. , -20 , -10 , -60 , -80 , -1.00 , -1.00 , -1.00 ,
A 0. , -20 , -10 , -60 , -80 , -1.00 , -1.00 , -1.00 ,
C
B 0. , -20 , -10 , -60 , -80 , -1.00 , -1.00 , -1.00 ,
C 0. , -20 , -10 , -60 , -80 , -1.00 , -1.00 , -1.00 ,
D 0. , -20 , -10 , -60 , -80 , -1.00 , -1.00 , -1.00 ,
E 0. , -20 , -10 , -60 , -80 , -1.00 , -1.00 , -1.00 ,
F 0. , -20 , -10 , -60 , -80 , -1.00 , -1.00 , -1.00 /

```

C *****

```

C
DATA X1 /
C

```

```

1 0 0 , 4.0 , 8.0 , 12.0 , 16.0 , 20.0 , 24. , 28. ,
2 0 0 , 3.0 , 10.0 , 15.0 , 20.0 ,
3 0.5 , 0.8 , .950 , 1.14 , 1.3 , 1.6 /

```

C *****

```

C
DATA COT /
C

```

```

1 -.020 , -.013 , -.004 , -.002,0. , -.002 , -.004 , -.011 , -.015 , -.020 ,
2 0. , 0. , 0. , 0. , 0. , 0. , 0. , 0. , 0. , 0. ,
3 .030 , .022 , .008 , .004 , 0. , .014 , .008 , .015 , .022 , .030 ,
4 .003 , .008 , -.020 , -.010,0. , -.010 , -.020 , .003 , .008 , .008 ,
5 .008 , .003 , -.020 , -.010,0. , -.011 , -.020 , .008 , .008 , .003 ,
6 .008 , .075 , .024 , .012 , 0. , .012 , .024 , .050 , .076 , .100 /

```


C
C*****
C

DATA 342T /

C

1	3.00	2.25	.70	.35	0.00	-.35	-.70	-1.50	-2.25	-3.00	,
2	3.00	2.25	.70	.35	0.00	-.35	-.70	-1.50	-2.25	-3.00	,
3	3.00	2.25	.70	.35	0.00	-.35	-.70	-1.50	-2.25	-3.00	,
4	3.00	2.25	.70	.35	0.00	-.35	-.70	-1.50	-2.25	-3.00	,
5	3.00	2.25	.70	.35	0.00	-.35	-.70	-1.50	-2.25	-3.00	,
6	3.00	2.25	.70	.35	0.00	-.35	-.70	-1.50	-2.25	-3.00	/

C
C*****
C

DATA 342T /

C

1	-7 0	,-5.2	,-1.8	,-1.0	,0.0	,1.0	,1.8	,3.5	,5.2	,7.0	,
2	-7 0	,-5.2	,-1.8	,-1.0	,0.0	,1.0	,1.8	,3.5	,5.2	,7.0	,
3	-7 0	,-5.2	,-1.8	,-1.0	,0.0	,1.0	,1.8	,3.5	,5.2	,7.0	,
4	-7 0	,-5.2	,-1.8	,-1.0	,0.0	,1.0	,1.8	,3.5	,5.2	,7.0	,
5	-7 0	,-5.2	,-1.8	,-1.0	,0.0	,1.0	,1.8	,3.5	,5.2	,7.0	,
6	-7 0	,-5.2	,-1.8	,-1.0	,0.0	,1.0	,1.8	,3.5	,5.2	,7.0	/

C
C*****
C

DATA 34TT /

C

1	-8 0	,-9 0	,-6.5	,-5 5	,-6.5	,-6.5	,-6.5	,-7.5	,-8.0	,-9.0	,
2	-9 0	,-9.0	,-8.0	,-9 0	,-8.0	,-8.0	,-8.0	,-9.0	,-8.0	,-8.0	,
3	-9 0	,-9.0	,-7.5	,-7 5	,-7.5	,-7.5	,-7.5	,-9.0	,-8.0	,-8.0	,
4	-9 0	,-9.0	,-7.0	,-7 0	,-7.0	,-7.0	,-7.0	,-9.0	,-8.0	,-8.0	,
5	-8.0	,-9.0	,-7.0	,-7 0	,-7.0	,-7.0	,-7.0	,-9.0	,-9.0	,-9.0	,
6	-8.0	,-9.0	,-6.0	,-5 0	,-6.0	,-5.0	,-6.0	,-7.0	,-8.0	,-8.0	/

C
C*****
C

DATA K2. /

C

1	-20.	,-13.	,-5.	,-2.5	,0.0	,2.5	,5.0	,10.	,
2	15 0	,20.	,	,	,	,	,	,	,
3	5	,8	,.95	,1.14	,1.3	,1.5	,	,	/

C
C*****
C

DATA TIMES /

C

1	0.0	,.04	,.05	,.1	,.15	,.21	,.37	,
2	.52	,.54	,.57	,.59	,.65	,.8	,1.1	,
3	1.3	,2.2	,3.1	,3.88	,4.49	,4.50	,1000.	/

C
C*****
C

DATA T4STL3 /

C

1	0.	,3500.	,9500	,9500.	,9500.	,9500.	,9500.	,
2	9500.	,3500.	,9500	,9500.	,8600.	,5600.	,2000.	,
3	2000.	,2000.	,2000	,2000.	,2000.	,0.	,0.	/

```

C
C*****
C
  DATA ALTT /
C
  1  0      , 1500. , 3000. , 6000. , 10000. , 15800. ,
  2 19890. , 24000. , 28000. , 32000. , 35000. , 40000. /
C
C*****
C
  DATA SJS2 /
C
  1 1115.4 , 1110.5 , 1104.8 , 1093.2 , 1077.4 , 1054.1 ,
  2 1037.7 , 1020.3 , 1003.3 , 996.2 , 972.1 , 973.1 /
C
C*****
C
  DATA R402 /
C
  1 .23770 , .22793 , .21796 , .19336 , .17550 , .14534 ,
  2 .12762 , .11052 , .09608 , .08297 , .0708 , .05872 /
C
C*****
C
  DATA C30T /
C
  1 .228, .229, .239, .256, .314, .475, .580, .508, .609, .573 /
C
C*****
C
  DATA MCHC3T /
C
  1 .4 , .6 , .75 , .95 , .9 , 1.0 , 1.1 , 1.3, 1.5, 2.0 /
C
C*****
C
  DATA H /
C
  1 0.0 , 4000. , 8000. , 12000. , 20000. , 30000. /
C
C*****
C
  DATA DELC3T /
  1 0 0 , -.0008 , -.0014 , -.0024 , -.0052 , -.0100 /
C
C*****
C
  DATA N1 / 10, 6 /
C
C*****
C
  DATA N41 / 8, 5, 5 /
C
C
C*****
C
COMPUTATIONS BEGIN HERE
C
C

```



```

C*****
C
C***** FIND AXIAL FORCE COEFFICIENTS
C
      CALL NDTLJ(2, 6, H, DELCOT, ALT, DELCD, IE, 0)
      CALL NDTLJ(2, 10, MC4COT, CDOOT, AMACH, CDO, IE, 1)
C
C***** FIND YAW MOMENT COEFFICIENTS
C
      XA(1) = BETA
      XA(2) = AMACH
      CALL NDTLJ(3, NA, X2, C42T, XA, CM2Y, IE, 1)
      CALL NDTLJ(3, NA, X2, C42T, XA, CN2Y, IE, 1)
      CALL NDTLJ(3, NA, X2, C4TT, XA, CMY, IE, 1)
C
C***** FIND PITCH MOMENT COEFFICIENTS
C
      XA(1) = ALPHA
      CALL NDTLJ(3, NA, X2, C42T, XA, CM2, IE, 1)
      CALL NDTLJ(3, NA, X2, C42T, XA, CN2, IE, 1)
      CALL NDTLJ(3, NA, X2, C4TT, XA, CM, IE, 1)
C
C***** FIND INDUCED DRAG COEFFICIENT
C
      ALPHAT = ATAN( SQRT( W3*WB + VB*VB ) / U3 ) * 57.3
      XA(1) = ALPHAT
      CALL NDTLJ(3, NA, X2, COT, XA, CC, IE, 1)
C
C***** FIND YAW FORCE AND MOMENT COEFFICIENTS
C
      XA1(1) = ABS(DC)
      XA1(2) = ABS(BETA)
      XA1(3) = AMACH
      CALL NDTLJ(4, NA1, X1, CMT, XA1, CM1Y, IE, 1)
      CALL NDTLJ(4, NA1, X1, CNT, XA1, CN1Y, IE, 1)
C
C***** FIND PITCH FORCE AND MOMENT COEFFICIENTS
C
      XA1(1) = ABS(DB)
      XA1(2) = ABS(ALPHA)
      CALL NDTLJ(4, NA1, X1, CMT, XA1, CM1, IE, 1)
      CALL NDTLJ(4, NA1, X1, CNT, XA1, CN1, IE, 1)
C
C***** FIND INDUCED DRAG COEFFICIENT
C
      XA1(1) = ABS(DB)
      XA1(2) = ABS(ALPHA)
      CALL NDTLJ(4, NA1, X1, JCOOT, XA1, DCC, IE, 1)
      XA1(1) = ABS(DC)
      XA1(2) = ABS(BETA)
      CALL NDTLJ(4, NA1, X1, JCOOT, XA1, DCC1, IE, 1)
      DCC = JCC + DCC1
C
C***** COMBINE COEFFICIENTS
C
      CD = CDD + JCC + CC + DELCD
      SINDCL = SIGN(1., D9)
      SINDCR = SIGN(1., DC)

```

```

      CN = CN2-CN1*SINDEL
      CMA0 = CM2-CM1*SINDEL
      CMCG=(43.7-CG)*CN/12.
      CNY = CN2Y-CN1Y*SINDEL
      CMA0Y = CM2Y-CM1Y*SINDEL
      CMCGY = (43.7-CG)*CN/12.
C
C***** LINEAR ACCELERATION COMPONENTS OF MISSILE IN BODY AXES DUE TO
C      AERODYNAMIC FORCES AND THRUST
C
      AXR = (THR-S*Q2*CD)/AMASS
      AYR = -S*Q2*CNY/AMASS
      AZR = -S*Q2*CN/AMASS
      ACX = AXR/32.2
      ACY = AYR/32.2
      ACZ = AZR/32.2
C
C***** ANGULAR ACCELERATION COMPONENTS OF MISSILE IN BODY AXES DUE TO
C      AERODYNAMIC MOMENTS
C
      PDOT = 0.
      QDOT = S*Q2*( (CM*Q/(2.*VEL)) + (CMA0-CMCG) ) / YYI + XX*R
      RDOT = S*Q2*( (CMY*R/(2.*VEL)) - (CMA0Y-CMCGY) ) / ZZI - XX*Q
C
      RETURN
C
      END
      SUBROUTINE ATMOS (ALT,RHO,SOS)
C
C*****
C*
C* THIS ROUTINE COMPUTES AIR DENSITY AND SPEED OF SOUND AS
C* A FUNCTION OF ALTITUDE.
C*
C*****
C
      COMMON /AMS/ R402(12),SOS2(12),ALT(12)
C
      DIMENSION NA(1),XA(1)
C
      NA(1)=12
      XA(1)=ALT
C
C***** AIR DENSITY
C
      CALL NOTLJ(2,NA,ALT,R402,XA,RHO,IE,0)
      RHO=.01*R40
C
C***** SPEED OF SOUND
C
      CALL NOTLJ(2,NA,ALT,SOS2,XA,SOS,IE,0)
C
      RETURN
C
      END
      SUBROUTINE COMMAND
C
C*****

```


C* THIS ROUTINE COMPUTES THE POSITION AND VELOCITY OF THE MISSILE WITH
 C* RESPECT TO THE AIRCRAFT-TO-TARGET LINE-OF-SIGHT AND ISSUES
 C* ACCELERATION COMMANDS (AV, AH) TO GUIDE THE MISSILE DOWN THE
 C* LINE-OF-SIGHT.

C*****

C
 COMMON /ACC/ AXB,AYB,ABZ,AXE,AYE,AZE,POOT,QOOT,ROOT
 COMMON /ACCELER/ PHADOT,THADOT,PSADOT
 COMMON /ANG/ PS, TH, PH, PSDG, THDG, PHDG, PSA, THA, PHA,
 1 PSDG, THDG, PHDG, PSSADG, THSADG, HGSADG
 COMMON /BLCK2/ AIG,AVG,TTG,DELF,ISUID,TR,UA,RANGE,ZI,CT,VOT
 COMMON /CMD/ AV,AH,WY,WZ
 COMMON /CNFL1/ DB,DC,DT,ACZ,ACY,ACX,GBIAS,GHBIAS,IJK
 COMMON /CNFL2/ R,D,G,J,C,B1,P1,P2,X,?
 COMMON /DER/ D,RL,CMAD,CMCG,QQ,S,VEL,THR,CMADY,CMDSY,RY
 COMMON /INITL/ H,TIME,ITABL,IPR,ILEG
 COMMON /MATRIX/ CET1,CET2,CET3,CET4,CET5,CET6,CET7,CET8,CET9,
 1 CIG1,CIG2,CIG3,CIG4,CIG5,CIG6,CIG7,CIG8,CIG9,
 1 CMG1,CMG2,CMG3,CMG4,CMG5,CMG6,CMG7,CMG8,CMG9,
 1 SPSSA,CPSGA,STHGA,CTHGA
 COMMON /POS/ XET,YET,ZET,XEA,YEA,ZEA,RANAT,XE,YE,ZE
 COMMON /PRNT1/ DY,DZ,DVY,DVZ,AYP,AZP
 COMMON /VELD/ XED,YED,ZED,XEAD,YEAD,ZEAD,UB,VB,WB
 COMMON /VTARGET/ XETD,YETD,ZETD,XBTD,YBTD,ZBTD

C
 C***** FIND POSITION OF TARGET RELATIVE TO AIRCRAFT (EARTH AXES)

C
 XAT = XET - XEA
 YAT = YET - YEA
 ZAT = ZET - ZEA

C
 C***** FIND VELOCITY OF TARGET RELATIVE TO AIRCRAFT IN EARTH FRAME
 C (EARTH AXES)

C
 XTADI = XETD-XEAD
 YTADI = YETD-YEAD
 ZTADI = ZETD-ZEAD

C
 C***** FIND ANGULAR VELOCITY OF AIRCRAFT FRAME RELATIVE TO EARTH FRAME
 C (WA) (EARTH AXES)

C
 WAX = PHADOT*COS(THA)*COS(PSA)-THADOT*SIN(PSA)
 WAY = PHADOT*COS(THA)*SIN(PSA)+THADOT*COS(PSA)
 WAZ = -PHADOT*SIN(THA)+PSADOT

C
 C***** FIND VELOCITY OF TARGET RELATIVE TO AIRCRAFT IN AIRCRAFT FRAME
 C (EARTH AXES)

C
 XTADA = XTADI-WAY*ZAT+WAZ*YAT
 YTADA = YTADI-WAZ*XAT+WAX*ZAT
 ZTADA = ZTADI-WAX*YAT+WAY*XAT

C
 C***** TRANSFORM VELOCITY OF TARGET RELATIVE TO AIRCRAFT TO
 C GIMBAL AXES

C
 YTADAG = CET4*XTADA+CET5*YTADA+CET6*ZTADA

```

      ZTADAG = CET7*XTADA+CET8*YTADA+CET9*ZTADA
C
C***** COMPUTE GIMBAL ANGLE RATES (GIMBAL AXES)
      PSGADOT = YTADAG/(RANAT*CTHGA)
      THGADOT = -ZTADAG/RANAT
C
C***** TRANSFORM ANGULAR VELOCITY OF GIMBAL FRAME RELATIVE TO AIRCRAFT
C      FRAME (AGA) TO EARTH AXES
C
      WGAX = -CIG1*PSGADOT*STHGA+CIG2*THGADOT+CIG3*PSGADOT*CTHGA
      WGAY = -CIG4*PSGADOT*STHGA+CIG5*THGADOT+CIG6*PSGADOT*CTHGA
      WGAZ = -CIG7*PSGADOT*STHGA+CIG8*THGADOT+CIG9*PSGADOT*CTHGA
C
C***** FIND ANGULAR VELOCITY OF GIMBAL FRAME RELATIVE TO EARTH FRAME
C      (WGI) (EARTH AXES)
C
      WGIY = WGAX+WAX
      WGIY = WGAY+WAY
      WGIY = WGAZ+WAZ
C
C***** * FIND ANGULAR VELOCITY OF LINE OF SIGHT (WLOS) (EARTH AXES)
C
      WX = WGIY
      WY = WGIY
      WZ = WGIY
C
C***** FIND POSITION OF MISSILE RELATIVE TO AIRCRAFT (EARTH AXES)
C
      RAMX = XE - XEA
      RAMY = YE - YEA
      RAMZ = ZE - ZEA
C
C***** FIND VELOCITY OF MISSILE RELATIVE TO AIRCRAFT IN EARTH FRAME
C      (EARTH AXES)
C
      VAMX = XED - XEAD
      VAMY = YED - YEAD
      VAMZ = ZED - ZEAD
C
C***** FIND DISTANCE OF MISSILE NORMAL TO LINE OF SIGHT
C
      DY=CET4*RAMX + CET5*RAMY + CET6*RAMZ
      DZ=CET7*RAMX + CET8*RAMY + CET9*RAMZ
C
C***** FIND VELOCITY OF MISSILE NORMAL TO LINE OF SIGHT (EARTH AXES)
C
      DELXD = VAMX+WZ*RAMY-WY*RAMZ
      DELYD = VAMY+WZ*RAMX+WY*RAMZ
      DELZD = VAMZ+WY*RAMX-WY*RAMY
C
C***** TRANSFORM VELOCITY OF MISSILE NORMAL TO LINE OF SIGHT
C      TO AIRCRAFT GIMBAL AXES
C
      DVY=CET4*DELXD + CET5*DELYD + CET6*DELZD
      DVZ=CET7*DELXD + CET8*DELYD + CET9*DELZD
C
C***** FIND RANGE FROM MISSILE TO TARGET
C

```



```

      RANGE=SQRT((XET-XE)**2+(YET-YE)**2+(ZET-ZE)**2)
C
C***** FIND VELOCITY OF MISSILE RELATIVE TO TARGET (EARTH AXES)
C
      VTMX = XEJ-XETO
      VTMY = YEJ-YETO
      VTMZ = ZEJ-ZETO
C
C***** COMPUTE RETRAN FREQUENCY ERROR
C
      IF(X LT.2.) GO TO 2
      ALAM = .1
      SIGI1 = ATAN2(SIGN(SQRT(YAT**2+ZAT**2),YAT),XAT)
      SIGI2 = ATAN2(SIGN(SQRT(RAMY**2+RAYZ**2),RAMY),RAMX)
      SIGI3 = ATAN2(SIGN(SQRT(YEAD**2+ZEAD**2),YEAD),XEAD)
      EPSI1 = ATAN2(SIGN(SQRT((YET-YE)**2+(ZET-ZE)**2),YET-YE),XET-XE)
      EPSI2 = ATAN2(SIGN(SQRT(YED**2+ZED**2),YED),XED)
      SIG1 = ABS(SIGI1-SIGI3)
      SIG2 = ABS(SIGI2-SIGI3)
      EPS1 = ABS(EPSI1-EPSI2)
      EPS2 = ABS(EPSI2-SIGI2)
      DELF = ABS(JA*(COS(SIG1)-COS(SIG2))+VEL*(COS(EPS2)-COS(EPS1)))/
1ALAM
C
C***** COMPUTE HEADING OF GIMBAL X AXIS (EARTH AXES)
C
      2   PSGAP = ASIN(PSGSA*COS(PHA)/COS(THA))
      HGA = PSGAP+PSA
      HGA0G = HGA*57.295
C
C***** TRANSFORM VELOCITY OF MISSILE RELATIVE TO TARGET TO GIMBAL AXES
C      TO FIND APPROXIMATE CLOSURE RATE
C
      VC = CET1*VTMX+CET2*VTMY+CET3*VTMZ
C
C***** FIND APPROXIMATE MISSILE TIME TO GO
      TTG = RANGE/ABS(VC)
C
C***** COMPUTE ACCELERATION COMMAND COEFFICIENTS
C
      IF(TTG.LT.(TR/4.)) TTG = TR/4.
      RR = 1000.
      CH = CT*(TR*RR/RANGE)**2
      C1 = .0155*(TR/TTG)**2
      C2 = ZI*.125*(TR/TTG)
      GGBIAS = 1.
      CB = (2.*WZ*VEL/32.2-RANGE*VDOOT*WZ/(32.2*VEL))
C
C***** ACCOUNT FOR GUIDANCE DELAY
C
      IF((X GT..7) OR.(ACX.LT.9.5)) GO TO 5
      AH = 0.
      AV = 0.
      GO TO 100
C
C***** IF MISSILE IS AHEAD OF LOS, COMMAND TURN TO PARALLEL LOS
C
      5   IF(IGUID.EQ.1) GO TO 10

```

```

      AHT = C1*(13A-PS)
      AXI = -AHT*SIN(PS)
      AYT = AHT*COS(PS)
      AXG = CET1*AXI+CET2*AYT
      AHG = CET4*AXI+CET5*AYT
      AVG = (C1*JZ+C2*DVZ)+GGBIAS
C
C***** TRANSFORM ACCELERATION COMMANDS TO MISSILE BODY AXES
C
      AH = CMG4*AXG+CMG5*AYG-CMG6*AVG
      AV = -CMG7*AXG-CMG8*AHG+CMG9*AVG
C
C***** TRANSITION TO COMMAND TO LOS
C
      AHTEST = (-C1*DY-C2*JY)
      IF(HGA*AHTEST.GT.0.) GO TO 100
      IF(X.GT.2.) IGUID = 1
C
C***** COMMAND ACCELERATION TO LINE OF SIGHT
C
10    AHG = (-C1*DY-C2*JY+C3)
      AVG = (C1*JZ+C2*DVZ)+GGBIAS
C
C***** TRANSFORM ACCELERATION COMMANDS TO MISSILE BODY AXES
C
97    AH = CMG5*AHG-CMG6*AVG
      AV = -CMG7*AHG+CMG9*AVG
C
100   RETURN
C
      END
      SUBROUTINE CONTROL
C
C*****
C*
C* THIS ROUTINE SIMULATES THE ACCELERATION AUTOPILOT AND CONTROL
C* SURFACE DYNAMICS AND DETERMINES THE EFFECTIVE CONTROL SURFACE
C* DEFLECTIONS (DB, DC) GIVEN THE ACCELERATION COMMANDS (AV, AH).
C*
C*****
C
      COMMON /CM1/ AV,AH,WY,AZ
      COMMON /CNTL1/ DB,DC,DT,ACZ,ACY,ACX,GBIAS,GHBias,IJK
      COMMON /CNTL2/ R,Z,G,U,C,B1,P1,P2,X,P
C
C*****
C*
C* VERTICAL CHANNEL AMPLIFIER
C*
C*  $C = B(3.11(.03S + 1)/(0.1S + 1))$ , WHERE S = JW
C*
C*****
C
C***** TOTAL COMMANDED VERTICAL ACCELERATION (LIMITED TO 20 G'S)
C
      A=AV+GBIAS
      IF(A.GT.20.)A=20.
      IF(A.LE.-20.)A=-20.

```



```

C
C***** ADD VERTICAL ACCELEROMETER DAMPING COMMAND
C
      B = A + ACZ
C
C***** ACCOUNT FOR GUIDANCE DELAY
C
      IF(X.LT..7.DR.ACX.GT.9.5)B=0.0
C
C***** COMPUTE VERTICAL CHANNEL OUTPUT (LIMITED TO 9 DEGREES)
C
      B1=(31.1*3-10.*C)*DT+31
      C=B1+.933*3
      IF(C.GT.11.1)C=11.1
      IF(C.LE.-11.1)C=-11.1
C
C***** ADD PITCH BODY RATE DAMPING COMMAND
C
      D = C -11.45*Q
C
C*****
C*
C* HORIZONTAL CHANNEL AMPLIFIER
C*
C* P2 = 0( 3.11(.03 S +1)/(1.1 S + 1) ), WHERE S = JH
C*
C*****
C
C***** TOTAL COMMANDED HORIZONTAL ACCELERATION (LIMITED TO 20 G'S)
C
      H=AH
      IF(H.GT.20.)H=20.
      IF(H.LE.-20.)H=-20.
C
C***** ADD HORIZONTAL ACCELEROMETER DAMPING COMMAND
C
      O=H-ACX
C
C***** ACCOUNT FOR GUIDANCE DELAY
C
      IF(X.LT..7.DR.ACX.GT.9.5)O=0.0
C
C***** COMPUTE HORIZONTAL CHANNEL OUTPUT (LIMITED TO 3 DEGREES)
C
      P1=(31.1*3-10.*P2)*DT+31
      P2=P1+.933*3
      IF(P2.GT.11.1)P2=11.1
      IF(P2.LE.-11.1)P2=-11.1
C
C***** ADD YAW BODY RATE DAMPING COMMAND
C
      QP=P2-11.45*R
C
C***** ADD HORIZONTAL CROSSOVER AND FEEDBACK TO VERTICAL CHANNEL
C
      E=-G+R+D
C
C***** COMPUTE VERTICAL CONTROL SURFACE RATE (LIMITED TO 300 DEGREES

```

```

C      PER SECOND)
C
C      FF=66.7*E
C      IF(FF.GT.300.)FF=300.
C      IF(FF.LE.-300.)FF=-300
C
C***** INTEGRATE VERTICAL CONTROL SURFACE RATE
C
C      G=FF*DT+G
C
C***** ADD VERTICAL CROSSOVER AND FEEDBACK TO HORIZONTAL CHANNEL
C
C      S1=-D+RP-U
C
C***** COMPUTE HORIZONTAL CONTROL SURFACE RATE (LIMITED TO 300 DEGREES
C      PER SECOND)
C
C      T=66.7*S1
C      IF(T.GT.300.)T=300.
C      IF(T.LT.-300.)T=-300.
C
C***** INTEGRATE HORIZONTAL CONTROL SURFACE RATE
C
C      U=T*DT+U
C
C***** CALCULATE EFFECTIVE VERTICAL CONTROL SURFACE DEFLECTION (DB)
C      (LIMITED TO 15 DEGREES)
C
C      DB=(-G+U)/2.
C      IF(DB.GT.15.)DB=15.
C      IF(DB.LT.-15.)DB=-15.
C
C***** CALCULATE EFFECTIVE HORIZONTAL CONTROL SURFACE DEFLECTION (DC)
C      (LIMITED TO 15 DEGREES)
C
C      DC=(U+S)/2.
C      IF(DC.GT.15.)DC=15.
C      IF(DC.LT.-15.)DC=-15.
C
C      RETURN
C
C      END
C      SUBROUTINE EULER(IFLAG)
C
C*****
C*
C* THIS ROUTINE COMPUTES THE AIRCRAFT GIMBAL ANGLES PS3A AND TH3A
C* (ASSUMING PERFECT TARGET TRACKING) AND COMPUTES THE TRANSFORMATION
C* MATRICES WHICH RELATE THE EARTH AXES, AIRCRAFT AXES, GIMBAL AXES
C* AND MISSILE AXES.
C*
C*****
C
COMMON /ACC/ AX9,AY9,AZ9,AXE,AYE,AZE,PDOT,QDOT,RDOT
COMMON /ANG/ PS, TH, PH, PSOG, THOG, PHOG, PSA, THA, PHA,
1          PSAOG, THOG, PHOG, PS3AOG, TH3AOG, PH3AOG
COMMON /MATRIX/ CET1,CET2,CET3,CET4,CET5,CET6,CET7,CET8,CET9,
1          CIG1,CIG2,CIG3,CIG4,CIG5,CIG6,CIG7,CIG8,CIG9,

```



```

1      CMG1,CMG2,CMG3,CMG4,CMG5,CMG6,CMG7,CMG8,CMG9,
1      SPSSA,CPSGA,STHGA,CTHGA
COMMON /PCS/ XET,YET,ZET,XEA,YEA,ZEA,RANAT,XE,YE,ZE
COMMON /VELD/ XED,YED,ZED,XEAD,YEAD,ZEAD,UB,V3,M3
COMMON /VTARGET/ XETD,YETD,ZETD,XETD,YETD,ZETD
REAL L1P,L2P,L3P,M1P,M2P,M3P,N1P,N2P,N3P
REAL L1,L2,L3,M1,M2,M3,N1,N2,N3

C
      IF(IFLAG.E2,2)GO TO 20

C
C***** TRANSFORMATION FROM EARTH TO AIRCRAFT AXES
C
      L1P=COS(THA)*COS(PSA)
      L2P=SIN(PSA)*COS(THA)
      L3P=-SIN(THA)
      M1P=COS(PSA)*SIN(THA)*SIN(PHA)-SIN(PSA)*COS(PHA)
      M2P=SIN(PSA)*SIN(THA)*SIN(PHA)+COS(PSA)*COS(PHA)
      M3P=COS(THA)*SIN(PHA)
      N1P=COS(PSA)*SIN(THA)*COS(PHA)+SIN(PSA)*SIN(PHA)
      N2P=SIN(PSA)*SIN(THA)*COS(PHA)-COS(PSA)*SIN(PHA)
      N3P=COS(THA)*COS(PHA)

C
C***** TRANSFORMATION FROM EARTH TO MISSILE AXES
C
      L1 = COS(TH)*COS(PS)
      L2 = SIN(PS)*COS(TH)
      L3 = -SIN(TH)
      M1 = COS(PS)*SIN(TH)*SIN(PH) - SIN(PS)*COS(PH)
      M2 = SIN(PS)*SIN(TH)*SIN(PH) + COS(PS)*COS(PH)
      M3 = COS(TH)*SIN(PH)
      N1 = COS(PS)*SIN(TH)*COS(PH) + SIN(PS)*SIN(PH)
      N2 = SIN(PS)*SIN(TH)*COS(PH) - COS(PS)*SIN(PH)
      N3 = COS(TH)*COS(PH)

C
C***** FIND RANGE FROM AIRCRAFT TO TARGET
C
      RANAT=SQRT((XET-XEA)**2 + (YET-YEA)**2 + (ZET-ZEA)**2)

C
C***** COMPUTE AIRCRAFT GIMBAL ANGLES (LIMITED TO 90 DEGREES)
C
      THE COMPUTATION OF CTHGA AND CPSGA IS VALID ONLY IF THA IS
      BETWEEN -90 DEG AND + 90 DEG
C
      STHGA=-(M1P*(XET-XEA)+M2P*(YET-YEA)+M3P*(ZET-ZEA))/RANAT
      IF(STHGA.GT.1.)STHGA=.9999
      IF(STHGA.LT.-1.)STHGA=-.9999
      CTHGA=SQRT(1-STHGA**2)
      THGADG = ASIN(STHGA)*57.295

C
      SPSSA=1./(RANAT*CTHGA)*((XET-XEA)*M1P+(YET-YEA)*M2P+(ZET-ZEA)*M3P)
      IF(SPSSA.GT.1.)SPSSA=.9999
      IF(SPSSA.LT.-1.)SPSSA=-.9999
      CPSGA = (L1P*(XET-XEA)+L2P*(YET-YEA)+L3P*(ZET-ZEA))/(CTHGA*RANAT)
      PSGADG = ASIN(SPSSA)*57.295

C
C***** TRANSFORMATION FROM AIRCRAFT AXES TO GIMBAL AXES
C
      CAT1=CTHGA*CPSGA

```

CAT2=CTHGA*SPSGA
 CAT3=-STHGA
 CAT4=-SPSGA
 CAT5=CPSGA
 CAT6=0.0
 CAT7=STHGA*SPSGA
 CAT8=STHGA*SPSGA
 CAT9=CTHGA

C
 C***** TRANSFORMATION FROM EARTH AXES TO GIMBAL AXES
 C

CET1=CAT1*_1P+CAT2*_41P+CAT3*_N1P
 CET2=CAT1*_2P+CAT2*_42P+CAT3*_N2P
 CET3=CAT1*_3P+CAT2*_43P+CAT3*_N3P
 CET4=CAT4*_1P+CAT5*_41P+CAT6*_N1P
 CET5=CAT4*_2P+CAT5*_42P+CAT6*_N2P
 CET6=CAT4*_3P+CAT5*_43P+CAT6*_N3P
 CET7=CAT7*_1P+CAT8*_41P+CAT9*_N1P
 CET8=CAT7*_2P+CAT8*_42P+CAT9*_N2P
 CET9=CAT7*_3P+CAT8*_43P+CAT9*_N3P

C
 C***** TRANSFORMATION FROM AIRCRAFT AXES TO EARTH AXES
 C

CIA1 = COS(PSA)*COS(THA)
 CIA2 = -COS(PSA)*SIN(THA)*SIN(PHA)-SIN(PSA)*COS(PHA)
 CIA3 = -COS(PSA)*SIN(THA)*COS(PHA)+SIN(PSA)*SIN(PHA)
 CIA4 = SIN(PSA)*COS(THA)
 CIA5 = -SIN(PSA)*SIN(THA)*SIN(PHA)+COS(PSA)*COS(PHA)
 CIA6 = -SIN(PSA)*SIN(THA)*COS(PHA)-COS(PSA)*SIN(PHA)
 CIA7 = SIN(THA)
 CIA8 = COS(THA)*SIN(PHA)
 CIA9 = COS(THA)*COS(PHA)

C
 C***** TRANSFORMATION FROM GIMBAL AXES TO AIRCRAFT AXES
 C

CAG1 = CPSGA*CTHGA
 CAG2 = -SPSGA
 CAG3 = CPSGA*STHGA
 CAG4 = SPSGA*CTHGA
 CAG5 = CPSGA
 CAG6 = SPSGA*STHGA
 CAG7 = -STHGA
 CAG8 = 0.0
 CAG9 = CTHGA

C
 C***** TRANSFORMATION FROM GIMBAL AXES TO EARTH AXES
 C

CIG1 = CIA1*CAG1+CIA2*CAG4+CIA3*CAG7
 CIG2 = CIA1*CAG2+CIA2*CAG5+CIA3*CAG8
 CIG3 = CIA1*CAG3+CIA2*CAG6+CIA3*CAG9
 CIG4 = CIA4*CAG1+CIA5*CAG4+CIA6*CAG7
 CIG5 = CIA4*CAG2+CIA5*CAG5+CIA6*CAG8
 CIG6 = CIA4*CAG3+CIA5*CAG6+CIA6*CAG9
 CIG7 = CIA7*CAG1+CIA8*CAG4+CIA9*CAG7
 CIG8 = CIA7*CAG2+CIA8*CAG5+CIA9*CAG8
 CIG9 = CIA7*CAG3+CIA8*CAG6+CIA9*CAG9

C
 C***** TRANSFORMATION FROM GIMBAL AXES TO MISSILE BODY AXES


```

C
CMG1 = L1*CI31+L2*CI34+L3*CI67
CMG2 = L1*CI32+L2*CI35+L3*CI68
CMG3 = L1*CI33+L2*CI36+L3*CI69
CMG4 = M1*CI31+M2*CI34+M3*CI67
CMG5 = M1*CI32+M2*CI35+M3*CI68
CMG6 = M1*CI33+M2*CI36+M3*CI69
CMG7 = N1*CI31+N2*CI34+N3*CI67
CMG8 = N1*CI32+N2*CI35+N3*CI68
CMG9 = N1*CI33+N2*CI36+N3*CI69

C
C***** TRANSFORM VELOCITY COMPONENTS IN EARTH AXES (XED,YED,ZED)
C      TO MISSILE AXES (UB,VB,WB)
C
      UB = L1*XED + L2*YED + L3*ZED
      VB = M1*XED + M2*YED + M3*ZED
      WB = N1*XED + N2*YED + N3*ZED

C
      RETURN

C
C***** TRANSFORM ACCELERATION COMPONENTS IN MISSILE AXES (AXB,AYB,AZB)
C      TO EARTH AXES (AXE,AYE,AZE)
C
      20 CONTINUE
      AXE = L1*AXB + M1*AYB + N1*AZB
      AYE = L2*AXB + M2*AYB + N2*AZB
      AZE = L3*AXB + M3*AYB + N3*AZB

C
C***** ADD ACCELERATION DUE TO GRAVITY
C
      AZE = AZE + 32.2

C
      RETURN

C
      END
      SUBROUTINE INTFLT

C
C*****
C*
C* THIS ROUTINE SETS FLIGHT PARAMETERS TO THEIR INITIAL VALUES.
C*
C*****
C
      COMMON /AEJLER/ PHADOT,THADOT,PSADOT
      COMMON /ANG/ PS, TH, PA, PSDG, THDG, PHDG, PSA, THA, PA,
1      PSDG, THDG, PHDG, PSADG, THADG, PHADG
      COMMON /ALOCK1/ XXI,YYI,ZZI,AMASS,CG,WG,PBIAS,XX
      COMMON /ALOCK2/ AHG,AVG,TTG,DELF,IGUID,TR,UA,RANGE,ZI,CT,VDDT
      COMMON /CMJ/ AV,AH,WY,WZ
      COMMON /CNFL1/ DB,DC,DT,ACZ,ACY,ACX,BBIAS,GHBIAS,IJK
      COMMON /CNFL2/ R,Q,S,J,C,B1,P1,P2,X,P
      COMMON /DER/ D,RL,CHAD,CMCG,QQ,S,VEL,THR,CHAJY,CHCSY,RV
      COMMON /FIV/ DOND, DEVN
      COMMON /INITL/ H,TIME,ITABL,IPR,ILEG
      COMMON /POS/ XET,YET,ZET,XEA,YEA,ZEA,RANAT,XE,YE,ZE
      COMMON /VEL/ XED,YED,ZED,XEAD,YEAD,ZEAD,UB,VB,WB

```

C***** CONVERT AIRCRAFT ATTITUDE FROM DEGREES TO RADIANS

C

THA = THADG / 57.295

PHA = PHADG / 57.295

PSA = PSADG / 57.295

C

C***** SET INITIAL GUIDANCE FLAG

C

IGUID = 0

C

C***** INITIALIZE MISSILE PARAMETERS TO AIRCRAFT PARAMETERS AT LAUNCH

C

TH=THA

PS=PSA

PH=PHA

XE=XEA

YE=YEA

ZE=ZEA

XED=XEAD

YED=YEAD

ZED=ZEAD

VEL = JA

C

C***** INITIALIZE ACCELERATION COMMANDS

C

AH = 0.

AV = 0.

C

C***** SET INITIAL VALUES ON INTEGRATORS IN CONTROL SUBROUTINE

C

DT = H

Q1 = 0.

B2 = 0.

P1 = 0.

P2 = 0.

C = 0.

G = 0.

U = 0.

C

C***** SET INITIAL VALUES OF MISSILE ANGULAR VELOCITY

C

P = 0.

Q = 0.

R = 0.

C

C***** SET INITIAL VALUES OF AIRCRAFT EULER RATES

C

PHADOT=0.

THADOT=0.

PSADOT=0.

C

C***** SET INITIAL MASS PARAMETERS AND REFERENCE AREA OF MISSILE

C

AMASS = 500./32.2

XXI = 2.5

YYI = 57.0

ZZI = 57.0

S = .875


```

C
C***** SET INITIAL VALUES ON ACCELEROMETER OUTPUTS
C

```

```

    ACX = 0.
    ACY = 0.
    ACZ = 0.
    VDOT = 0.

```

```

C
C***** INITIALIZE TIME
C

```

```

    X = 0.

```

```

    RETURN

```

```

C
    END
    SUBROUTINE VDTLU(ND,NA,X,Z,XA,ZR,IE,NEXTR)

```

```

C
C*****
C
C***** N-DIMENSIONAL TABLE LOOK-UP *****
C
C***** GIVEN THE ARGUMENTS X(1),X(2),...X(N-1), *****
C***** COMPUTES Y = F(X(1),X(2),...X(N-1)) BY *****
C***** LINEAR INTERPOLATION FROM A TABLE. *****
C
C***** ACCURACY REAL SINGLE PRECISION *****
C
C***** CALLING SEQUENCE *****
C
C***** CALL LOOKUP(ND,NA,X,Z,XA,ZR,IE,NEXTR) *****
C***** WHERE *****
C*****
C***** ND = DIMENSION OF LOOK-UP *****
C***** WHEN Y=F(X) ND = 2 *****
C
C***** NA = AN ARRAY OF LENGTH ND-1 *****
C***** NUMBERS OF VALUES OF EACH TABLE OF X *****
C***** THE TABLES ARE LISTED BY SIZE, THE LARGEST FIRST. *****
C
C***** X = TABLES OF EACH X IN ORDER *****
C***** Z = FUNCTION VALUES *****
C***** IF A = F(X,Y,Z) THE DEPENDENT VARIABLE ARRAY *****
C***** MUST BE IN THE FOLLOWING ORDER. *****
C***** ASSUME X=4,4=3,Z=2 *****
C*****
C***** Z(1)= F(X1,Y1,Z1) Z(13)= F(X1,Y1,Z2) *****
C***** Z(2)= F(X2,Y1,Z1) Z(14)= F(X2,Y1,Z2) *****
C***** Z(3)= F(X3,Y1,Z1) Z(15)= F(X3,Y1,Z2) *****
C***** Z(7)= F(X3,Y2,Z1) Z(19)= F(X3,Y2,Z2) *****
C***** Z(8)= F(X4,Y2,Z1) Z(20)= F(X4,Y2,Z2) *****
C***** Z(9)= F(X1,Y3,Z1) Z(21)= F(X1,Y3,Z2) *****
C***** Z(10)= F(X2,Y3,Z1) Z(22)= F(X2,Y3,Z2) *****
C***** Z(11)= F(X3,Y3,Z1) Z(23)= F(X3,Y3,Z2) *****
C***** Z(12)= F(X4,Y3,Z1) Z(24)= F(X4,Y3,Z2) *****
C
C***** ZR = RESULT *****
C
C***** NEXTR = 1 EXTRAPOLATE *****
C***** = 0 NO EXTRAPOLATION *****
C

```

```

C*
C*          IE  =  ERROR CODE
C*          0  NO ERROR
C*          -1  X ARRAY TOO SMALL
C*          1  X ARRAY TOO LARGE
C*          2  ARRAY NOT IN ASCENDING ORDER
C*
C*-----
C

```

```

C      DIMENSION X(1),Z(1),NA(1),XA(1),NS(5),WJ(32)
C      EQUIVALENCE (XMM,MM) , (XMM,MH)
C      L1=2
C      LF=ND-1
C      DO 3 I=1,LF
C      L2=L1+NA(I)-2
C      FOUND=J.
C      DO 4 J=L1,L2
C      IF(X(J).GT,X(J-1)) GO TO 6
C      IE=2
C      RETURN
6      IF(FOUND.NE.0.) GO TO 4
C      IF(XA(I)-X(J-1)) 3,4,4
8      IF(J.GT.L1) GO TO 10
C      IF(NEXTR.EQ.0) GO TO 37
C      FOUND=1.
C      NS(I)=-1-1
C      GO TO 4
37      IE=-1
C      RETURN
10      FOUND=1.
C      NS(I)=J-2
4      CONTINUE
C      IF(FOUND) 11,12,11
12      IF(XA(I)-X(L2)) 13,13,14
14      IF(NEXTR.NE.0) GO TO 13
C      IE=1
C      RETURN
13      NS(I)=-2-1
11      L1=L2+2
3      CONTINUE
C      KF=2**LF
C      MH=-2
C      DO 15 I=1,KF,2
C      L1=0
C      IZ=0
C      MH=MH+2
C      NPT=1
C      DO 19 J=1,MH
C      MH=2** (J-1)
C      IF(AND(XMM,XMH).EQ.0) GO TO 22
C      N=NS(J)+1
C      GO TO 23
22      N=NS(J)
23      N=N-L1
C      L1=L1+NA(J)
C      IZ=NPT*(N-1)+IZ
19      NPT=NPT*NA(J)

```



```

      WJ(I)=7(IZ+1)
18    WJ(I+1)=7(IZ+2)
      DO 32 J=1,LF
      M = NS(I)
      KF=KF/?
      RATIO=(XA(I)-X(M))/(X(I+1)-X(M))
      DO 32 J=1,LF
32    WJ(J)=WJ(2*J-1)+(WJ(2*J)-WJ(2*J-1))*RATIO
      ZR=WJ(1)

C
      RETURN
C
      END
      SUBROUTINE OUTFLT
C
C*****
C*
C* THIS ROUTINE PRINTS THE OUTPUT DURING THE FLIGHT
C*
C*****
C
      COMMON /AER/ DEL,DCG,CN1,CN1,CC,CN2,CN2,C4,DDG,DELDD,AMACH,ALPHA
1      ,ALT,BETA,CCY,CN2Y,CN2Y,CN1Y,CN1Y,DDCY,DO,CN,CNY
      COMMON /ANG/ PS, TH, PH, PSDG, THDG, PHDG, PS1, TH1, PH1,
1      ,PSADG, THADG, PHADG, PSADG, THADG, HGADG
      COMMON /B-DCK2/ AHG,AVG,TTG,DELF,IGUID,TR,UA,RANGE,ZI,CT,VDDT
      COMMON /C4/ AV,A1,M1,M2
      COMMON /CN1L1/ DB,DC,DT,ACZ,ACY,ACX,GBIAS,G4BIAS,IJK
      COMMON /CN1L2/ R,Q,G,U,C,B1,P1,P2,X,P
      COMMON /DER/ D,RL,CN1D,CN1D,QQ,S,VEL,THR,CN1DY,CN1DY,RY
      COMMON /DJS/ XET,YET,ZET,XEA,YEA,ZEA,RANAT,KE,YE,ZE
      COMMON /PRNT1/ DY,DZ,DVY,DVZ

C
C***** CONVERT MISSILE ATTITUDE FROM RADIANS TO DEGREES
C
      PSDG=57.295*PS
      THDG=57.295*TH
      PHDG=57.295*PH

C
C***** OUTPUT
C
      WRITE(3,900)
      WRITE(3,905)X,TTG
      WRITE(3,910) VEL,AMACH,DELF,IGUID
      WRITE(3,915)DY,DVY,A1G,AM,BETA,DC,ACY
      WRITE(3,920) DZ,DVZ,AVG,AV,ALPHA,DB,DCZ
      WRITE(3,925) XE,PSDG,XEA,PSADG,HGADG
      WRITE(3,930) YE,THDG,YEA,THADG
      WRITE(3,935) ZE,PHDG,ZEA,PHZ

C
      RETURN
C
900  FORMAT(/)
905  FORMAT(1X,5HTIME ,F8.2,3X,4HTTG ,F9.2)
910  FORMAT(1X,4HVEL ,F9.2,3X,5HAMACH ,F3.2,3X,5HDELF ,F9.2,3X,6HIGUID ,
115)
915  FORMAT(1X,2HDY,F11.1,3X,4HDVY ,F9.2,3X,3HAM1G,F11.2,3X,3HAM ,F8.2,
13X,5HBETA ,F7.2,3X,3HDC ,F9.2,3X,4HACY ,F8.2)

```

```

920 FORMAT( 1X,2407,F11.1,3X,440VZ ,F9.2,3X,34AVS,F11.2,3X,3HAV ,F8.2,
13X,5HALPHA,F9.2,3X,3403 ,F9.2,3X,44ACZ ,F9.2)
925 FORMAT(1X,24XE,F11.2,3X,3HPS ,F10.2,3X,34XEA,F11.2,3X,4HPSSA,F7.2
1,3X,4H4GA ,F9.2)
930 FORMAT( 1X,24YE,F11.2,3X,34TH ,F10.2,3X,34YEA,F11.2,3X,5HTHGA ,
1F6.2)
935 FORMAT( 1X,24ZE,F11.2,3X,3HPH ,F10.2,3X,34ZEA,F11.2,3X,3HWZ ,F8.2)
C
END
SUBROUTINE OUTINTL
C
C*****
C*
C* THIS ROUTINE PRINTS THE INITIAL INPUT VALUES. THE AERODYNAMIC
C* TABLES ARE ALSO PRINTED IF ITABL = 1.
C*
C*****
C
COMMON /ANG/ PS, TH, P4, PSDG, THDG, PHDG ,PSA, THA, PHA,
1 PSDAG, THADG, PHADG, PSADG, THSADG , HSADG
COMMON /BLOCK1/ XXI,YYI,ZZI,AMASS,CG,W3,PBIAS,XX
COMMON /BLOCK2/ AHG,AVG,TTG,DELTA,ISUID,TR,UA,RANGE,ZI,CT,VOGT
COMMON /CNFL1/ DB,OC,OT,ACZ,ACY,ACX,BBIAS,GHBIAS,IJK
COMMON /INITL/ H,TIME,ITABL,IPR,ILEG
COMMON /POS/ XET,YET,ZET,XEA,YEA,ZEA,RANAT,XE,YE,ZE
COMMON /VELD/ XED,YED,ZED,XEAD,YEAD,ZEAD,UB,V8,W8
C
C***** PRINT INITIAL INPUT VALUES
C
WRITE(5,9000)
8000 FORMAT("1"//40X,"RETRAN MISSILE SIMULATION")
WRITE(5,9000) XEA, YEA, ZEA, XEAD, YEAD, ZEAD, THADG, PSDAG, PHADG
1 ,XET, YET, ZET, H, BBIAS, GHBIAS, TIME, PBIAS , CT , TR , ZI
C
C***** OPTIONAL PRINTING OF AERODYNAMIC TABLES
C
IF(ITABL.EQ.1) CALL OUTTBL
C
C***** OPTIONAL PRINTING OF VARIABLE LEGEND
C
IF(ILEG.EQ.1) WRITE(5,7000)
IF(ILEG.EQ.1) WRITE(5,7500)
C
RETURN
C
7000 FORMAT(//45X,"OUTPUT LEGEND"/
1"TIME - ELAPSED FLIGHT TIME (SEC)
1"TTG - TIME REMAINING TO TGT IMPACT (SEC)
1"VEL - MISSILE AIRSPEED (FT/SEC)
1"MACH - MISSILE MACH NUMBER
1"DELTA - RETRANSMITTED FREQUENCY ERROR (HZ)
1"OY - HORIZONTAL DISTANCE ERROR (FT)
1"OVY - HORIZONTAL VELOCITY ERROR (FT/SEC)
1"OZ - VERTICAL DISTANCE ERROR (FT)
1"OVZ - VERTICAL VELOCITY ERROR (FT/SEC)
1"ANG - HOR. ACCELERATION COMMAND - GIMBAL FRAME (G'S)
1"AH - HOR. ACCEL. COMMAND - MISSILE FRAME (G'S)
1"AVG - VERT. ACCEL. COMMAND - GIMBAL FRAME (G'S)

```



```

1"AV - VERT. ACCEL. COMMAND - MISSILE FRAME (G'S)      "/"
1"BETA - SIDESLIP ANGLE (DEG)                          ",
1"ALPHA - ANGLE OF ATTACK (DEG)                         ",
1"OC - EFFECTIVE YAW CONTROL DEFLECTION (DEG)          ",
1"OB - EFFECTIVE PITCH CONTROL DEFLECTION (DEG)        "/"
1"ACY - MISSILE ACCELEROMETER OUTPUT (G'S)             ",
1"ACZ - MISSILE ACCELEROMETER OUTPUT (G'S)             ")
7500 FORMAT("X",58X,
1"XEA
1"YEA - MISSILE POSITION COORDINATES (FT)               ",
1"YEA - AIRCRAFT POSITION COORDINATES (FT)              "/"
1"ZEA
1"ZEA
1"PS - MISSILE HEADING (DEG)                           ",
1"PSGA - HORIZONTAL GIMBAL ANGLE (DEG)                  "/"
1"TH - MISSILE PITCH ANGLE (DEG)                        ",
1"THGA - VERTICAL GIMBAL ANGLE (DEG)                    "/"
1"PH - MISSILE BANK ANGLE (DEG)                         ",
1"WZ - ROTATION RATE OF LINE OF SIGHT (RAD/SEC)        "/"
1"MG - HEADING OF LINE OF SIGHT (DEG)                  ",
1"IGUID - HORIZONTAL ALGORITHM MODE                     "/"
169X,"IGUID = 0 : COMMAND TO HEADING"/
169X,"IGUID = 1 : COMMAND TO TRACK"/
9000 FORMAT( * INITIAL FLIGHT CONDITIONS* /
12X,4HXEA ,F13.2,3X,4HYEA ,F10.2,3X,4IZEA ,F10.2,3X,5HXEAD ,F13.2,
13X,5HYEAD ,F10.2,3X,5HZEAD ,F10.2/2X,4HTHA ,F13.2,3X,4HPSA ,F10.2,
13X,4HPHA ,F10.2,3X,4HRET ,F14.2,3X,4HYET ,F11.2,3X,4HZET ,F11.2/
12X,2HH ,F4.2,3X,6HGBIAS ,F2.0,3X,7HGBIAS ,F7.0,3X,5HTIME ,F9.1,
13X,6HPIAS ,F12.2,3X,3HCT ,F5.2,3X,3HTR ,F6.2,4X,3HZI ,F6.2)
C
END
SUBROUTINE OUTTBL
C
C*****
C*
C* THIS ROUTINE PRINTS THE AERODYNAMIC TABLE GENERATED IN SUBROUTINE *
C* AERO. *
C*
C*****
C
COMMON /AERTBL/ OCCT(8,5,6), CMT(8,5,5), CNT(8,5,5), X1(19),
1 OCCT(10,5), Y2T(10,5), CY2T(10,6), CMTT(10,5), X2(15),
2 OCCT(10), MCHOCCT(10), H(5), DELCCT(6)
COMMON /A45/ RH02(12), SOS2(12), ALTT(12)
COMMON /THRST/ TIMES(21), THSTLB(21)
C
WRITE(6,50)
50 FORMAT(1X//44X,"AERODYNAMIC TABLE"/)
WRITE(5,51)
51 FORMAT(10X,"OCCT")
WRITE(5,100)OCCT
WRITE(5,52)
52 FORMAT(10X,"CMT")
WRITE(5,100)CMT
WRITE(5,53)
53 FORMAT(10X,"CNT")
WRITE(5,100)CNT
WRITE(6,65)

```

```

66  FORMAT(10X,*X1*)
    WRITE(5,100)X1
    WRITE(5,54)
54  FORMAT(10X,*CCT*)
    WRITE(5,110)CCT
    WRITE(6,55)
55  FORMAT(10X,*CM2T*)
    WRITE(5,110)CM2T
    WRITE(6,55)
56  FORMAT(10X,*CN2T*)
    WRITE(5,110)CN2T
    WRITE(6,57)
57  FORMAT(10X,*CMTT*)
    WRITE(5,110)CMTT
    WRITE(6,58)
58  FORMAT(10X,*X2*)
    WRITE(5,110)X2
    WRITE(5,59)
59  FORMAT(10X,*TIMES*)
    WRITE(5,120)TIMES
    WRITE(5,50)
60  FORMAT(10X,*THSTLB*)
    WRITE(5,120)THSTLB
    WRITE(5,51)
61  FORMAT(10X,*ALTT*)
    WRITE(5,130)ALTT
    WRITE(5,52)
62  FORMAT(10X,*SOS2*)
    WRITE(5,130)SOS2
    WRITE(5,53)
63  FORMAT(10X,*RH02*)
    WRITE(5,140)RH02
    WRITE(5,54)
64  FORMAT(10X,*CDDT*)
    WRITE(5,105)CDDT
    WRITE(6,55)
65  FORMAT(10X,*MCHCOT*)
    WRITE(5,105)MCHCOT
    WRITE(5,57)
67  FORMAT(10X,*H*)
    WRITE(5,100)H
    WRITE(5,58)
    WRITE(6,59)
68  FORMAT(10X,*DELCOT*)
    WRITE(5,140)DELCOT
C
    RETURN
C
110  FORMAT(10F9,4)
100  FORMAT(9F10,4)
105  FORMAT(10E9,3)
120  FORMAT(7E10,2)
130  FORMAT(5E10,2)
140  FORMAT(5F10,5)
C
    END
    SUBROUTINE TARGET (X)
C

```



```

C*****
C*
C* THIS ROUTINE SUPPLIES TARGET VELOCITY IN EARTH-FIXED INERTIAL
C* COORDINATES AS A FUNCTION OF TIME (X).
C*
C*****
C
C      COMMON /VTARGET/ XETO, YETO, ZETO, XBTO, YBTO, ZBTO
C
C***** TARGET IS STATIONARY IN THIS SIMULATION
C
C      XETO = 0.
C      YETO = 0.
C      ZETO = 0.
C
C      RETURN
C
C      END
C      SUBROUTINE THRUST(T)
C
C*****
C*
C* THIS ROUTINE COMPUTES THE MASS PARAMETERS AND THRUST DURING BOOST.
C*
C*****
C
C      COMMON /BLOCK1/ XXI,YYI,ZZI,AMASS,CG,WC,PSIAS,XX
C      COMMON /DER/ D,RL,CMAD,CMCG,QQ,S,VEL,THR,CMADY,CMCZY,RY
C      COMMON /THRST/ TIMES(21),THSTLB(21)
C
C      DIMENSION NA(1),XA(1)
C      DIMENSION ST(3),WT(3),XXIT(3),ZZIT(3),CST(3)
C
C      DATA CST / 55.0, 54.3, 52.0 /
C      DATA ST / 0., .60, 4.5 /
C      DATA WT / 500., 450., 400. /
C      DATA XXIT / 3*2.5 /
C      DATA ZZIT / 57.0, 54.0, 58.0 /
C
C      NA(1)=3
C      XA(1)=T
C
C***** CENTER OF GRAVITY OF THE MISSILE
C
C      CALL NDTLJ(2,NA,ST,CST,XA,CG,IE,0)
C
C***** HEIGHT OF THE MISSILE
C
C      CALL NDTLJ(2,NA,ST,WT,XA,WC,IE,0)
C
C***** MOMENT OF INERTIA ABOUT THE LONGITUDINAL AXES
C
C      CALL NDTLJ(2,NA,ST,XXIT,XA,XXI,IE,0)
C
C***** MOMENTS OF INERTIA ABOUT THE TRANSVERSE AXES
C
C      CALL NDTLJ(2,NA,ST,ZZIT,XA,ZZI,IE,0)
C      YYI=ZZI

```



```

PX(N+1)=X4
PX(N+2)=X3
PY(N+1)=Y4
PY(N+2)=Y3
CALL PLOTS(30)
CALL PLOT(5.,-5.,-3)
CALL PLOT(1.5,2.0,-3)
CALL FACTOR(F)
CALL SPAXIS(0.,0.,15+DROSSRANGE (FT),15,4.0,30.,Y4,Y3,-.65,1.20,
1 1130,30.,1.,-1.,.0905)
CALL SPAXIS(0.,4.0,14+DOWNRANGE (FT),14,7.0,0.0,X4,X3,2.80,4.50,
1 1130,0.,1.,-1.,.0805)
CALL LINE(PXE4,PYE4,N,1,0,0)
CALL LINE(PXE,PYE,N,1,0,0)
CALL LINE(PXET,PYET,N,1,0,0)
CALL SYMBO(4.00,4.00,126,2,0.,-1)
CALL PLOT(-1,-.8,3)
CALL PLOT(3.0,-.8,2)
CALL PLOT(3.0,4.8,2)
CALL PLOT(-1,4.8,2)
CALL PLOT(-1,-.8,2)

```

```

C
C
C***** DRAW VERTICAL TRAJECTORY PLOT
C

```

```

IF(PZE4(1).GT.5000.) GO TO 25
RM = 35000.
RD = -5000.
ZM = 0.
ZD = 1500.
GO TO 35
25 IF(PZE4(1).GT.20000.) GO TO 30
RM = 90000.
RD = -15000.
ZM = 0.
ZD = 5000.
GO TO 35
30 RM = 132000.
RD = -22000.
ZM = 0.
ZD = 10000.
35 PR(N+1) = RM
PR(N+2) = RD
PZE(N+1) = ZM
PZE(N+2) = ZD
R0(1) = PR(1)
Z0(1) = PZE4(1)
R0(2) = 0.
Z0(2) = 0.
R0(3) = RM
R0(4) = RD
Z0(3) = ZM
Z0(4) = ZD
CALL PLOT(14.,0.,-3)
CALL SPAXIS(0.,0.,134+ALTITUDE (FT),13,4.0,90.,Z4,Z3,-.65,1.30,
1 1130,30.,1.,-1.,.0905)
CALL SPAXIS(0.,0.,10+RANGE (FT),-10,5.0,0.0,R4,RD,2.50,-.5230,
1 1130,0.,1.,-1.,.0905)

```

```

CALL LINE(PR,PZE,N,1,0,0)
CALL DASH_V(R0,Z0,2,1)
CALL SYMBO_(5.,0.,.125,2,0.,-1)
CALL PLOT(-1.,-.8,3)
CALL PLOT(7.0,-.8,2)
CALL PLOT(7.0,4.8,2)
CALL PLOT(-1.,4.8,2)
CALL PLOT(-1.,-.8,2)

```

C

C***** DRAW ANG AND AVG VS TIME PLOT

C

```

IF(PZEA(1),3T.5000.) GO TO 45
TH = 0.
TO = 10.
GO TO 55
45 IF(PZEA(1),3T.20000.) GO TO 50
TH = 0.
TO = 22.
GO TO 55
50 TH = 0.
TO = 35.
35 AM = -20.
AD = 10.
PT(N+1) = TM
PT(N+2) = TO
PAHG(N+1) = AM
PAHG(N+2) = AD
PAVG(N+1) = AM
PAVG(N+2) = AD
PTS(N2+1) = TM
PTS(N2+2) = TO
PAVS(N2+1) = AM
PAVS(N2+2) = AD
CALL PLOT(14.,0.,-3)
CALL SPAXIS(0.,0.,15+ACCEL CMD (G'S),15,4.0,30.,44,AD,-.60,1.20,
1 1190,30.,1.,-1.,.0305)
CALL SPAXIS(0.,0.,10+TIME (SEC),-10,5.0,0.0,T4,TO,2.50,-.5230,
1 1190,0.,1.,-1.,.0305)
CALL LINE(PT,PAHG,N,1,0,0)
CALL LINE(PT,PAVG,N,1,0,0)
CALL LINE(PTS,PAVS,N2,1,-3,1)
CALL PLOT(0.,2.,3)
CALL PLOT(5.,2.,2)
CALL PLOT(5.30,3.94,3)
CALL PLOT(5.55,3.94,2)
CALL SYMBO_(5.70,3.93, 0805,3HAHG,0.,3)
CALL PLOT(5.30,3.91,3)
CALL PLOT(5.55,3.91,2)
CALL SYMBO_(5.70,3.77, 0805,3HAVG,0.,3)
CALL SYMBO_(5.47,3.807,.0700,1,0.,-1)
CALL PLOT(-1.,-.8,3)
CALL PLOT(7.0,-.8,2)
CALL PLOT(7.0,4.8,2)
CALL PLOT(-1.,4.8,2)
CALL PLOT(-1.,-.8,2)

```

C

C***** DRAW ALPHA AND BETA VS.TIME PLOT

C


```

PAL(N+1) = AM
PAL(N+2) = AD
PBE(N+1) = AM
PBE(N+2) = AD
PBES(N2+1) = AM
PBES(N2+2) = AD
CALL PLOT(14.,0.,-3)
CALL SPAXIS(0.,0.,1344., BE (DES),13,4.0,90.,44,4),-.50,1.30,
1 1190,90,1.,-1.,.0805)
CALL SPAXIS(0.,0.,104TIME (SEC),-10,5.0,0.0,T4,TD,2.50,-.5230,
1 1190,0.,1.,-1.,.0805)
CALL LINE(PT,PAL,N,1,0,0)
CALL LINE(PT,PBE,N,1,0,0)
CALL LINE(PTS,PBES,N2,1,-3,1)
CALL PLOT(0.,2.,3)
CALL PLOT(5.,2.,2)
CALL PLOT(5.30,3.94,3)
CALL PLOT(5.55,3.94,2)
CALL SYMBO_(5.70,3.90, 0805,5HALPHA,0.,5)
CALL PLOT(5.30,3.81,3)
CALL PLOT(5.55,3.81,2)
CALL SYMBO_(5.70,3.77, 0805,4HBETA,0.,4)
CALL SYMBO_(5.47,3.807,.0700,1,0.,-1)
CALL PLOT(-1.,-.8,3)
CALL PLOT(7.0,-.8,2)
CALL PLOT(7.0,4.8,2)
CALL PLOT(-1.,4.8,2)
CALL PLOT(-1.,-.8,2)

```

```

C
C***** DRAW VMDDT VS. TIME PLOT
C

```

```

VM = -100.
VD = 50.
IF(PVDT(4).GE.0.) PVDT(4) = PVDT(5)
IF(PVDT(3).GE.0.) PVDT(3) = PVDT(4)
IF(PVDT(2).GE.0.) PVDT(2) = PVDT(3)
PVDT(1) = PVDT(2)
PVDT(N+1) = VM
PVDT(N+2) = VD
CALL PLOT(14.,0.,-3)
CALL SPAXIS(0.,0.,154VMDDT (FT/SEC2),15,4.0,90.,V4,VD,-.60,1.20,
1 1190,90.,1.,-1.,.0805)
CALL SPAXIS(0.,0.,104TIME (SEC),-10,5.0,0.0,T4,TD,2.50,-.5230,
1 1190,0.,1.,-1.,.0805)
CALL LINE(PT,PVDT,N,1,0,0)
CALL PLOT(0.,2.,3)
CALL PLOT(5.,2.,2)
CALL PLOT(-1.,-.8,3)
CALL PLOT(7.0,-.8,2)
CALL PLOT(7.0,4.8,2)
CALL PLOT(-1.,4.8,2)
CALL PLOT(-1.,-.8,2)

```

```

C
C***** DRAW DELF VS TIME PLOT
C

```

```

DM = 0.
DO = 4.
POF(N) = 0.

```

```

PDF(N+1) = 34
PDF(N+2) = 00
CALL PLOT(14.,0.,-3)
CALL SPAXIS(0.,0.,154 DELF (HZ) ,15,4.0,30.,34,00,-.60,1.20,
1 1190,30.,1.,-1.,.0905)
CALL SPAXIS(0.,0.,104TIME (SEC),-10,5.0,0.0,14,TD,2.50,-.5230,
1 1190,0.,1.,-1.,.0805)
CALL LINE(PT,PDF,N,1,0,0)
CALL PLOT(0.,2.,3)
CALL PLOT(5.,2.,2)
CALL PLOT(-1.,-.8,3)
CALL PLOT(7.0,-.8,2)
CALL PLOT(7.0,4.8,2)
CALL PLOT(-1.,4.8,2)
CALL PLOT(-1.,-.8,2)

```

```

C
C***** DRAW DY AND DZ VS RANGE PLOT
C

```

```

DM = -50.
DD = 25.
RM = 15000.
RD = -3000.
PDY(N3+1) = DM
PDY(N3+2) = DD
PDZ(N3+1) = DM
PDZ(N3+2) = DD
PR3(N3+1) = RM
PR3(N3+2) = RD
CALL PLOT(14.,0.,-3)
CALL SPAXIS(0.,0.,114DY, DZ (FT),11,4.0,30.,34,00,-.50,1.35,
1 1190,30.,1.,-1.,.0905)
CALL SPAXIS(0.,0.,104RANGE (FT),-10,5.0,0.0,14,20,2.50,-.5230,
1 1190,0.,1.,-1.,.0805)
CALL LINE(PR3,PDY,43,1,0,0)
CALL LINE(PR3,PDZ,43,1,0,0)
CALL PLOT(0.,2.,3)
CALL PLOT(5.,2.,2)
CALL PLOT(5.30,3.94,3)
CALL PLOT(5.55,3.94,2)
CALL SY430.(5.70,3.90, 0805,2HDY,0.,2)
CALL PLOT(5.30,3.91,3)
CALL PLOT(5.55,3.91,2)
CALL SY430.(5.70,3.77, 0805,2HDZ,0.,2)
CALL SY430.(5.47,3.817,.0700,1,0.,-1)
CALL PLOT(-1.,-.8,3)
CALL PLOT(7.0,-.8,2)
CALL PLOT(7.0,4.8,2)
CALL PLOT(-1.,4.8,2)
CALL PLOT(-1.,-.8,2)
CALL PLOT(10,0,0)

```

```

C
C
RETURN
END

```


RETRAM MISSILE SIMULATION

INITIAL FLIGHT CONDITIONS

YEA -20000.00 YEA 20000.00 XEAD -5000.00 XEAD 0.00 ZEAD 0.00
 T-4 3.33 PSA 0.00 P-4 0.00 XET 0.00 ZET 0.00
 W .001 GRAV 3.0 CMAS 0.0 TIME 10.0 PSIAS 0.0 CT 25.00 TR 20.00 ZI .50

OUTPUT LEGEND

TIME - ELAPSED FLIGHT TIME (SEC)
 VEL - MISSILE AIRSPEED (FT/SEC)
 DELF - RETRANSMITTED FREQUENCY ERROR (HZ)
 DVY - HORIZONTAL DISTANCE ERROR (FT)
 DVZ - VERTICAL DISTANCE ERROR (FT)
 1-3 - HOR. ACCELERATION COMMAND - GIMBAL FRAME (G'S)
 4-6 - HOR. ACCEL. COMMAND - GIMBAL FRAME (G'S)
 7-9 - VERT. ACCEL. COMMAND - GIMBAL FRAME (G'S)
 10-12 - EFFECTIVE PITCH CONTROL DEFLECTION (DEG)
 13-15 - MISSILE ACCELEROMETER OUTPUT (G'S)
 16-18 - MISSILE POSITION COORDINATES (FT)
 19-21 - MISSILE HEADING (DEG)
 22-24 - MISSILE PITCH ANGLE (DEG)
 25-27 - MISSILE ROLL ANGLE (DEG)
 28-30 - HEADING OF LINE OF SIGHT (DEG)
 31-33 - TIME REMAINING TO 1ST IMPACT (SEC)
 34-36 - MISSILE NAME NUMBER
 37-39 - HORIZONTAL VELOCITY ERROR (FT/SEC)
 40-42 - VERTICAL VELOCITY ERROR (FT/SEC)
 43-45 - HOR. ACCEL. COMMAND - MISSILE FRAME (G'S)
 46-48 - VERT. ACCEL. COMMAND - MISSILE FRAME (G'S)
 49-51 - ANGLE OF ATTACK (DEG)
 52-54 - EFFECTIVE PITCH CONTROL DEFLECTION (DEG)
 55-57 - MISSILE ACCELEROMETER OUTPUT (G'S)
 58-60 - AIRCRAFT POSITION COORDINATES (FT)
 61-63 - HORIZONTAL GIMBAL ANGLE (DEG)
 64-66 - VERTICAL GIMBAL ANGLE (DEG)
 67-69 - ROTATION RATE OF LINE OF SIGHT (RAD/SEC)
 70-72 - HORIZONTAL ALSCORITHM CODE
 73-75 - ISJID = 0 : COMMAND TO HEADING
 76-78 - ISJID = 1 : COMMAND TO TRACK

TIME	.03	ITS	31.35	DELF	0.00	ISJID	0	BETA	0.00	DC	0.00	ACV	0.00
VEL	800.00	YACM	.73	AMC	-.99	A4	-.93	ALPHA	0.00	DS	0.00	ACZ	0.00
DVY	0.0	DVZ	0.00	AVG	1.00	AV	.93	MCA	-.45.00				
DZ	0.0												
YE	-13875.01	PS	0.00	XEA	-19376.00	PS2A	-.45.00						
YF	27673.20	T4	0.00	YEA	20000.09	T43A	-10.02						
ZE	-5997.37	34	0.00	ZEA	-5000.00	WZ	-.02						

TIME	1.02	ITS	31.04	DELF	0.00	ISJID	0	BETA	0.98	DC	3.11	ACV	-11.42
VEL	1235.42	YACM	1.13	AMC	-5.43	A4	-7.53	ALPHA	-0.61	DS	-1.07	ACZ	5.62
DVY	165.9	DVZ	236.9	AVG	-.00	AV	-1.71	MCA	-.66.22				
DZ	-23.9		-40.11										
YE	-11093.52	PS	-11.40	XEA	-19106.20	PS2A	-.53.15						
YF	19993.25	T4	-6.31	YEA	20052.27	TW3A	-10.21						
ZE	-6597.76	34	.93	ZEA	-5000.00	WZ	-.02						

Appendix C

Program Optraaj Listing

PROGRAM OPTRAJ(INPJ,OUTPUT,PLOT)

```

C
C* .....
C*
C*          OPTIMIZATION OF RETRAN MISSILE TRAJECTORY
C* .....
C
C
C* .....
C*
C*          DEFINITION OF INPUT VARIABLES
C*
C*  X0,Y0,Z0 - INITIAL MISSILE POSITION IN EARTH-FIXED
C*             COORDINATES (FT)
C*
C*  VM0 - INITIAL MISSILE TRUE AIRSPEED (FT/SEC)
C*
C*  GAM0,PSI0 - INITIAL MISSILE FLIGHT PATH ANGLE AND HEADING
C*             (RADIAN)
C*
C*  AL0,SE0 - INITIAL MISSILE ANGLE OF ATTACK AND SIDESLIP
C*            ANGLE (RADIAN)
C*
C*  T0 - INITIAL TIME (SEC)
C*
C*  H0 - INTEGRATION TIME STEP SIZE (SEC)
C*
C*  TMAX - MAXIMUM FLIGHT TIME (SEC) (SUBROUTINE STATED
C*        TERMINATES WHEN TMAX IS EXCEEDED)
C*
C*  XA0,YA0,ZA0 - INITIAL AIRCRAFT POSITION IN EARTH-FIXED
C*               COORDINATES (FT)
C*
C*  VAO - AIRCRAFT TRUE AIRSPEED (FT/SEC)
C*
C*  MAXRUN - MAXIMUM NUMBER OF ITERATIONS OF MAIN PROGRAM
C*           (PROGRAM TERMINATES IF MIN PAYOFF NOT REACHED
C*           IN MAXRUN ITERATIONS)
C*
C*  TOL - PROGRAM TERMINATES IF J(N)-J(N-1) IS LESS THAN TOL
C*
C*  CO - INITIAL VALUE OF CONTROL VARIABLE ADJUSTMENT COEFFICIENT
C*
C*  DELCO - STEP SIZE USED IN SEARCH ROUTINE TO ADJUST C
C*
C*  K010,K020 - COEFFICIENTS OF 2ND ORDER CURVE FIT TO VELOCITY
C*             ON LOS FUNCTION
C*
C*  K10,K20,K30 - PENALTY FUNCTION COEFFICIENTS
C*
C*  TR - ACCELERATION COMMAND REFERENCE RANGE (FT)
C*
C*  GGBIAS - BIAS COMMAND IN VERTICAL PLANE IN G'S
C*
C*  CT - GAIN COEFFICIENT FOR COMMAND TO HEADING GUIDANCE ALGORITHM
C*

```

```

C* CZI - DAMPING RATIO IN COMMAND TO LOS GUIDANCE ALGORITHM
C*
C* IPT - INTEGER SWITCH CONTROLLING PLOTTING. PLOTTING TAKES
C* PLACE ONLY IF IPT = 1
C*
C*****
C
COMMON/AFIND/XLOSE,YLOSE,ZLOSE,PSLF,THLOS
COMMON/AIC/VA0,XA0,YA0,ZA0
COMMON/CTR/AH(410),AV(410),HO,IRJN,TMAX,DHAI(410),DAIV(410)
1,TR,GBIAS,CT,CZI
COMMON/AFIND/VMF,GMF,PSIF,XF,YF,ZF,ALF,BEF,TF,N,ISLN
COMMON/MIC/VMO,GA10,PS10,X0,Y0,Z0,ALO,BEO,T0
COMMON/PAYOFF/K01,K02,K1,K2,K3,RANGE=
COMMON/PENCOF/K010,K020,K10,K20,K30
COMMON/STATE/SX(410),SY(410),SZ(410),SVM(410),SPRI(410),SSAM(410)
COMMON/PLDATA/XI( 52),YI( 52),ZI( 52),XS( 52),YS( 52),ZS( 52),
1NPTSI,NPTSF
COMMON/PLDT2/PDHI( 52),PDZI( 52),PDHS( 52),PDZS( 52),AHGI( 52),
1AVGI( 52),AHGS( 52),AVGS( 52)
COMMON/PLDT3/PTI( 52),PTS( 52),RANGI( 52),RANGS( 52),ALPI( 52),
1BEPI( 52),ALPS( 52),BEPS( 52),VOTI( 52),VOTS( 52)
REAL J1,J2,JT1,JT2,K01,K02,K1,K2,K3
REAL K010,K020,K10,K20,K30
C
C***** READ INITIAL CONDITIONS AND TIME STEP
C
READ 10,X0,Y0,Z0,VMO,GAHO,PS10,ALO,BEO,T0,HO,TMAX,XA0,YA0,ZA0,VA0,
1MAXRUN,TOL,Z0,DELCO
10 FORMAT(8F10.0/7F10.0/I3/3F10.0)
READ 15,K010,K020,K10,K20,K30
15 FORMAT(5E10.0)
READ 15,TR,GBIAS,CT,CZI,IPT
15 FORMAT(4F10.0,I2)
PRINT 21
21 FORMAT(1X//3X,"OPTIMIZATION OF RETRAN MISSILE TRAJECTORY"//3X
1"PENALTY FUNCTIONS COEFFICIENTS")
PRINT 25,K010,K020,K10,K20,K30
25 FORMAT(1X/3X,4HK01 ,E10.4,3X,4HK02 ,E10.4,3X,3HK1 ,E10.4,3X,3HK2 ,
1E10.4,3X,3HK3 ,E10.4/1X)
C
C***** INITIALIZE PLOTTING ARRAYS AND RUN COUNTER
C
NPTSI = 1
NPTSF = 1
XI(1) = X0
YI(1) = Y0
ZI(1) = -Z0
XS(1) = X0
YS(1) = Y0
ZS(1) = -Z0
PDHI(1) = SQRT((X0-XA0)**2+(Y0-YA0)**2)
PDHS(1) = PDHI(1)
PDZI(1) = Z0-ZA0
PDZS(1) = Z0-ZA0
AHGI(1) = 0.
AHGS(1) = 0.
AVGI(1) = 0.

```



```

AVGS(1) = 0.
PTI(1) = T0
PTS(1) = T0
RANGI(1) = SQRT(X0*X0+Y0*Y0+Z0*Z0)
RANGS(1) = RANGI(1)
ALPI(1) = AL0*57.235
ALPS(1) = AL0*57.235
PEPI(1) = PE0*57.235
PEPS(1) = PE0*57.235
VDTI(1) = 0.
VDTs(1) = 0.
IRJN = 0
C1 = C0
DEL C1 = DEL C0
AH(1) = 0.
AV(1) = 0.

```

```

C
C***** INTEGRATE STATE EQUATIONS FORWARD
C

```

```

30 IRUN = IRJN+1
   PRINT 13,IRUN
33 FORMAT(1X//3X,"ITERATION NO. ",I3/1X)
   IF(IRUN.EQ.1) PRINT 13
19 FORMAT(3X,"INITIAL TRAJECTORY"/1X)
   IF(IRJN.EQ.1) PRINT 20,T0,VMO,X0,Y0,Z0,H0
20 FORMAT(1X/3X,34T0 ,F7.1,3X,34VM0,F3.2,3X,34X0 ,F7.0,3X,34Y0 ,F6.0,
13X,34Z0 ,F3.0,3X,34H0 ,F9.2).
   CALL STATVEC(0.)
   IF(ISLV.EQ.1) GO TO 30

```

```

C
C***** CALCULATE PAYOFF AND PENALTIES
C

```

```

   CALL PAYOFF(J1)
   VT = VMF-K01*RANGE**2-K02*RANGEF
   RERR = 15000.-RANGEF
   PSERR = PSIF-PSLF
   GAERR = GAMF-TALOS
   PRINT 34
34 FORMAT(1X//3X,"PAYOFF AND ERRORS")
   PRINT 35,J1,VT,RERR,PSERR,GAERR
35 FORMAT(1X/ 3X,34J1 315 7,3X,34VT ,F10.2,3X,54RERR ,F10.2,3X,
154PSERR ,F3.5,3X,54GAERR ,F8.6/1X)

```

```

C
C***** TEST FOR STOPPING CONDITIONS
C

```

```

   IF(IRUN.EQ.1) GO TO 40
   IF(IRUN.GE.MAXRUN) GO TO 80
   IF(ABS(J1-J2).LE.TOL) GO TO 80
40 J2 = J1

```

```

C
C***** CALCULATE DHAN AND DHAV
C

```

```

   CALL DHU

```

```

C
C***** PERFORM ONE DIMENSIONAL SEARCH TO MINIMIZE J
C

```

```

   PRINT 19
39 FORMAT(1X/3X,"ONE-DIMENSIONAL ALPHA SEARCH")

```

```

      C = C1
      DELC = DELC1
      ID = 0
      DO 50 I = 1,100
41    CALL STATVEC(C)
      IF(ISLN.EQ.0) GO TO 45
      PRINT 43,C
43    FORMAT(1X/3X,3HC ,E10.4,3X,"NO SOLUTION")
      IF(C.GT.C1) GO TO 50
42    C1 = C1/50.
      DELC1 = DELC1/50.
      C = C1
      DELC = DELC1
      ID = ID+1
      IF(ID.GT.10) GO TO 80
      GO TO 41
45    CALL PAYOFF(JT1)
      PRINT 75,C,JT1,C1,DELC1
      IF(I.EQ.1) GO TO 43
      IF(JT1.GE.JT2) GO TO 47
43    JT2 = JT1
      C = C+DELC
      GO TO 50
47    IF(I.NE.2) GO TO 53
      C1 = C1/50.
      DELC1 = DELC1/50.
      C = C1
      DELC = DELC1
53    CONTINUE
60    C = C-DELC
      PRINT 75,C,JT2,C1,DELC1
75    FORMAT(1X/ 3X,3HC ,E10.4,3X,2HJ ,F15.4,3X,3HJ1 ,E10.4,3X,5HDELC1
1,E10.4)
      DO 70 I = 1,N
      AH(I) = AH(I)-C*DH1H(I)
      AV(I) = AV(I)-C*DH1V(I)
70    CONTINUE
C
C***** RETURN FOR NEXT ITERATION
C
      GO TO 30
C
C***** PLOT INITIAL AND FINAL TRAJECTORIES
C
80    PRINT 95
83    FORMAT(1X/3X,"OPTIMIZED TRAJECTORY"/1X)
      PRINT 20,T0,V40,X0,Y0,Z0,H0
      CALL STATVEC(99.)
      PRINT 95,NPTS1,NPTS2
85    FORMAT(1X/3X,6HNPTS1 ,F3,3X,6HNPTS2 ,I3)
      VDTI(1) = VDTI(2)
      VOTS(1) = VOTS(2)
      IF(IPT.EQ.1) CALL PLTRAJ
      IF(IRUN.GE.MXRUN) GO TO 90
      IF(ID.GT.10.) GO TO 30
      STOP
C
C***** IF JMIN NOT REACHED, PRINT MESSAGE

```



```

C
90  LRUN = LRUN+1
    PRINT 100, LRUN, J1
100  FORMAT(1X/3X,"JMIN NOT REACHED IN",I4," ITERATIONS.  J = ",F12.5//
      1/1X)
    STOP
C
    END
    SUBROUTINE STATVEC(C)
C
C*****
C*
C*   THIS SUBROUTINE INTEGRATES THE STATE VECTOR EQUATIONS
C*
C*****
C
    COMMON/AFIND/XLOSF,YLOSF,ZLOSF,PSLF,THLOS
    COMMON/AID/VAO,XAO,YAO,ZAO
    COMMON/CNTRL/AH(410),AV(410),HO,IRJN,TMAX,DHAI(410),CHAV(410)
    1,TR,GGBIAS,CT,CZI
    COMMON/AFIND/VME,GME,PSIF,XF,YF,ZF,ALF,BEF,TF,N,ISLN
    COMMON/MIC/VMO,GAM,PSIO,XO,YO,ZO,AO,BO,TO
    COMMON/STATE/SX(410),SY(410),SZ(410),SVH(410),SPSI(410),SSAH(410)
    COMMON/PLDATA/XI( 52),YI( 52),ZI( 52),XS( 52),YS( 52),ZS( 52),
    1NPTSI,VPTSF
    COMMON/PLDT2/PDHI( 52),PDZI( 52),PDHS( 52),PDZS( 52),AHGI( 52),
    1AVGI( 52),AHSS( 52),AVSS( 52)
    COMMON/PLDT3/PTI( 52),PTS( 52),RANGI( 52),RANGS( 52),ALPI( 52),
    1AEPI( 52),ALPS( 52),BEPS( 52),VOTI( 52),VOTS( 52)
    REAL MACH,M,LIG1,LIG2,LIG3,LIG4,LIG5,LIG6,LIG7,LIG8,LIG9,
    1LVI1,LVI2,LVI3,LVI4,LVI5,LVI6,LVI7,LVI8,LVI9,
    1LVG4,LVG5,LVG6,LVG7,LVG8,LVG9
C
C***** INITIALIZE THE INTEGRATION STEP COUNTER
C
    I = 1
C
C***** INITIALIZE THE MISSILE PARAMETERS
C
    AL = AO
    BE = BO
    VM = VMO
    GAM = GAM
    PSI = PSIO
    X = XO
    Y = YO
    Z = ZO
    T = TO
    S = .925
    IGUID = 0
    H = HO
    ISLN = 0
    IPLOT = 0
    IF(C.NE.99) GO TO 13
    C = 0.
    IPLOT = 1
C
C***** FIND TIME VARIANT PARAMETERS

```

```

C
10  TAU = .003565*7+519.59
    PHO = 2.3905E-15*TAU**4.26
    MACH = .1204*V4/SQRT(TAU)
    Z = RH77/M*V4/2.
    M = 12.42
    IF(T.LT.4.5) M = 14.39-.4764*(T-.63)
    TH = 0.
    IF(T.LT.4.5) TH = 2000

```

```

C
C***** CALCULATE COMMANDED ALPHA AND BETA
C

```

```

    AVV = AV(I)-C*DHAV(I)
    IF(AVV.GT.20.) AVV = 20.
    IF(AVV.LT.-20.) AVV = -20.
    AVV = AVV*32.2
    AHM = AH(I)-C*DHAH(I)
    IF(AHM.GT.20.) AHM = 20.
    IF(AHM.LT.-20.) AHM = -20.
    AHM = AHM*32.2
    AL = (AVV +32.2*CCS(GAM))*M/(20.1*S*Q)
    IF(AL.GT..350) AL = .350
    IF(AL.LT.-.350) AL = -.350
    BE = -AHM * 1/(20.1*S*Q)
    IF(BE.GT..350) BE = .350
    IF(BE.LT.-.350) BE = -.350
    ALTOT = SQRT(AL**2+BE**2)

```

```

C
C***** CALCULATE AERODYNAMIC FORCES
C

```

```

    CDD = -51.553*MACH**7+390.974*MACH**5-1151.24*MACH**3+1844.332*
1MACH**4-1593.781*MACH**3+885.382*MACH**2-245.293*MACH+28.253
    DELCC = -2.951E-05*ALTOT**2-1.8286E-03*ALTOT+9.5714E-03
    DELCDF = -7.4060E-12*Z**2-1.0785E-07*(-Z)-8.3773E-05
    FX = -S*Q*(CDD+DELCC+DELCDF)
    FY = -S*Q*(20.1*BE)
    FZ = -S*Q*(20.1*AL)

```

```

C
C***** INTEGRATE MISSILE EQUATIONS OF MOTION
C

```

```

    CAL = CCS(AL)
    SAL = SIN(AL)
    CBE = CCS(BE)
    SBE = SIN(BE)
    VMDOOT = ((FX+TH)*CAL+CBE+FY*SBE+FZ*SAL*CBE)/M-32.2*SIN(GAM)
    AY = (- (FX+TH)*CAL+SBE+FY*CBE-FZ*SAL*SBE)/M
    AZ = (- (FX+TH)*SAL+FZ*CAL)/M+32.2*CCS(GAM)
    PSIDOT = AY/(V4*CCS(GAM))
    GAMDOOT = -AZ/V4
    VM = V4+H*VMDOOT
    GAM = GAM+H*GAMDOOT
    PSI = PSI+H*PSIDOT
    XDOT = V4*CCS(GAM)*CCS(PSI)
    YDOT = V4*CCS(GAM)*SIN(PSI)
    ZDOT = -V4*SIN(GAM)
    X = X+H*XDOT
    Y = Y+H*YDOT
    Z = Z+H*ZDOT

```



```

C
C***** STORE STATE VALUES
C
      IF(C.NE.0.) GO TO 12
      SV4(I) = VM
      SG4(I) = GAM
      SPSI(I) = PSI
      SX(I) = X
      SY(I) = Y
      SZ(I) = Z

C
C***** TEST FOR STOPPING CONDITION
C
12    T = T+H
      IF(T GT. TMAX) GO TO 51
      IF(Z GT. 0.) GO TO 50
      PSLOS = ATAN(YA0/XA0) - (T-T0)*VA0/SQRT(XA0**2+YA0**2)
      THLOS = ATAN(ZA0/SQRT(XA0**2+YA0**2))
      RANGE = SQRT(X**2+Y**2)
      XLOS = -RANGE*COS(PSLOS)
      YLOS = -RANGE*SIN(PSLOS)
      ZLOS = RANGE*TAN(THLOS)
      DZ = Z-ZLOS
      DH = SQRT((X-XLOS)**2+(Y-YLOS)**2)
      W = X-XLOS
      DH = SIGN(DH,W)
      DVZ = VM*SIN(THLOS-GAM)
      VMH = XROT*COS(PSLOS+3.1416/2.)+YROT*SIN(PSLOS+3.1416/2.)
      DERR2 = (X-XLOS)**2+(Y-YLOS)**2+(Z-ZLOS)**2
      IF(DERR2.LE.2500.) GO TO 15

C
C***** MAKE ACCELERATION COMMAND DECISION
C
      T = T+1
      IF(IPLDT.EQ.1) GO TO 21
      IF(IRUN.EQ.1.AND.C.EQ.0.) GO TO 20
      IF(IRUN.NE.1.AND.I.LE.N) GO TO 10
      IF(C.NE.0.AND.I.LE.N) GO TO 10
      DELAH = AH(N)-AH(N-1)
      DELAV = AV(N)-AV(N-1)
      DELOHH = JAH(N)-JAH(N-1)
      DELOHV = JAV(N)-JAV(N-1)
      AH(I) = AH(I-1)+DELAH
      AV(I) = AV(I-1)+DELAV
      JAH(I) = JAH(I-1)+DELOHH
      JAV(I) = JAV(I-1)+DELOHV
      GO TO 10

C
C***** RECORD FINAL CONDITIONS
C
15    TF = T
      XF = X
      YF = Y
      ZF = Z
      VMF = VM
      GAMF = GAM
      PSIF = PSI

```

```

      ALF = AL
      3EF = 3E
      IF(C.E).0.) N=I
      XLOSF = XLJS
      YLOSF = YLJS
      ZLOSF = ZLJS
      PSLF = PSLJS
      IF(C.E).0.) PRINT 17,T,VM,X,Y,Z,34.0Z,AM(I-1),AV(I-1)
17    FORMAT(1X/3X,2HTF ,F5.1,3X,3HVMF ,F5.2,3X,3HXF ,F7.0,3X,3HYF ,
      1F6.0,3X,3HZF ,F8.0,3X,3HDMF ,F8.2,3X,3HDMZF ,F9.2,3X,3AH ,F5.2,3X,
      13HAV ,F5.2)
C
      RETURN
C
C***** COMPUTE TRANSFORMATION FROM GIMBA. AXES TO EARTH AXES
C
20    CPL = COS(PSLOS)
      SPL = SIN(PSLOS)
      CTL = COS(THLOS)
      STL = SIN(THLOS)
      LIG1 = CPL*CTL
      LIG2 = -SPL
      LIG3 = CPL*STL
      LIG4 = SPL*CTL
      LIG5 = CPL
      LIG6 = SPL*STL
      LIG7 = -STL
      LIG8 = 0.
      LIG9 = CTL
C
C***** COMPUTE TRANSFORMATION FROM EARTH AXES TO VELOCITY AXES
C
      CPS = COS(PSI)
      SPS = SIN(PSI)
      CGA = COS(GAM)
      SGA = SIN(GAM)
      LVI1 = CPS*SGA
      LVI2 = SPS*CGA
      LVI3 = -SGA
      LVI4 = -SPS
      LVI5 = CPS
      LVI6 = 0.
      LVI7 = CPS*SGA
      LVI8 = SPS*SGA
      LVI9 = CGA
C
C***** COMPUTE TRANSFORMATION FROM GIMBA. AXES TO VELOCITY AXES
C
      LVG1 = LVI1*LIG1+LVI2*LIG4+LVI3*LIG7
      LVG2 = LVI1*LIG2+LVI2*LIG5+LVI3*LIG8
      LVG3 = LVI1*LIG3+LVI2*LIG6+LVI3*LIG9
      LVG4 = LVI4*LIG1+LVI5*LIG4+LVI6*LIG7
      LVG5 = LVI4*LIG2+LVI5*LIG5+LVI6*LIG8
      LVG6 = LVI4*LIG3+LVI5*LIG6+LVI6*LIG9
      LVG7 = LVI7*LIG1+LVI8*LIG4+LVI9*LIG7
      LVG8 = LVI7*LIG2+LVI8*LIG5+LVI9*LIG8
      LVG9 = LVI7*LIG3+LVI8*LIG6+LVI9*LIG9
      N = LVG1*LVG5*LVG9+LVG2*LVG6*LVG7+.LVG3*LVG4*.LVG9-.LVG3*LVG5*.LVG7-

```



```

1LVG2*LV34*LV39-LV31*LV5*LVG8
IF(IPLDT.E2.1) GO TO 31
C
C***** COMPUTE GUIDANCE COMMANDS FOR FIRST RUN
C
CH = CT*TR/RANGE
C1 = .0521*(TR/RANGE)**2
C2 = C7I*.249*(TR/RANGE)
C
C***** IF AHEAD OF LOS, COMMAND TURN TO PARALLEL LOS
C
IF(IGUID.E2.1) GO TO 25
IF(DH.LT.0.) GO TO 25
AH(I) = CH*(PSLOS-PSI)
AXG = -LV32/D*AH(I)
AHG = LV35/D*AH(I)
AVG = C1*DZ+C2*DVZ+33BIAS
AV(I) = -(LV37*AXG+LV38*AHG-LVG9*AVG)
AHTEST = -C1*D+(-C2*D)/4
IF(AHTEST.LT.0.) GO TO 31
IF(T.GT.2.) IGUID = 1
C
C***** COMMAND TO LOS
C
25 AHG = -C1*D+C2*DVZ
30 AVG = C1*DZ+C2*DVZ+33BIAS
AH(I) = LV35*AHG-LVG3*AVG
AV(I) = LV33*AVG-LVG3*AHG
C
C***** PRINT OUTPUT AND UPDATE PLOT ARRAYS FOR FIRST AND FINAL RUNS
C
31 L = 2.0/H0
K = 1/L-(I+1)/L
PRINT 35,T,V4,X,Y,Z,D4,DZ,AH(I-1),AV(I-1)
35 FORMAT(1X/3X,24T ,F5.1,3X,34VM ,F5.2,3X,34H ,F7.0,3X,34Y ,
1F6.0,3X,34Z ,F8.0,3X,4H0H ,F8.2,3X,4H0Z ,F3.2,3X,34AH ,F5.2,3X,
134AV ,F5.2)
IF(K.E2.0) GO TO 13
IF(IPLDT.E2.1) GO TO 45
NPTSI = NPTSI+1
XI(NPTSI) = X
YI(NPTSI) = Y
ZI(NPTSI) = -Z
IF(AHG.GT.20) AH3=20.
IF(AHG.LT.-20) AH3=-20.
AHGI(NPTSI) = AHG
IF(AVG.GT.20) AV3=20.
IF(AVG.LT.-20) AV3=-20.
AVGI(NPTSI) = AVG
PDHI(NPTSI) = DH
PDZI(NPTSI) = DZ
PTI(NPTSI) = T
RANGI(NPTSI) = SQRT(X*X+Y*Y+Z*Z)
ALPI(NPTSI) = AL*57.295
REPI(NPTSI) = RE*57.295
VDTI(NPTSI) = VMDT
IF(VDTI(NPTSI).GT.100.) VDTI(NPTSI) = 100.
IF(VDTI(NPTSI).LT.-100) VDTI(NPTSI) = -100.

```

```

40 GO TO 10
45 NPTSF = NPTSF+1
   XS(NPTSF) = X
   YS(NPTSF) = Y
   ZS(NPTSF) = -Z
   AHGS(NPTSF) = (LVG3*AV(I) + LVG6*AV(I))/
   IF(AHGS(NPTSF).GT.20.) AHGS(NPTSF)=20.
   IF(AHGS(NPTSF).LT.-20.) AHGS(NPTSF)=-20.
   AVGS(NPTSF) = (LVG3*AV(I) + LVG5*AV(I))/O
   IF(AVGS(NPTSF).GT.20.) AVGS(NPTSF)=20.
   IF(AVGS(NPTSF).LT.-20.) AVGS(NPTSF)=-20.
   POHS(NPTSF) = OH
   POZS(NPTSF) = OZ
   PTS(NPTSF) = T
   RANGS(NPTSF) = SQRT(X*Y + Y*Z + Z)
   ALPS(NPTSF) = AL*57.295
   BEPS(NPTSF) = BE*57.295
   VOTS(NPTSF) = VMODT
   IF(VOTS(NPTSF).GT.100.) VOTS(NPTSF) = 100.
   IF(VOTS(NPTSF).LT.-100.) VOTS(NPTSF) = -100.
   GO TO 10

C
50 IF(C EQ.0.) PRINT 55
55 FORMAT(IX/3X,"NO SOLUTION")
   ISLN = 1

C
   RETURN

C
   END
   SUBROUTINE DHU

C
C*****
C*
C*   THIS SUBROUTINE INTEGRATES THE LAMDA-DOT AND X-DOT EQUATIONS
C*   BACKWARDS AND STORES LAMDA(I) AND DHAV(I)
C*
C*****
C
COMMON/AFIND/XLOSF,YLOSF,ZLOSF,PSLF,THLOS
COMMON/CTRL/AH(410),AL(-20),HO,IRJN,THAX,DHAI(410),DHAV(410)
1,TR,GG3IAS,DT,ZI
COMMON/MIC/VMO,G410,PO,PC,XO,YO,ZO,ALO,BEO,T0
COMMON/MFIND/VMF,GAMF,PSIF,XF,YF,ZF,ALF,BEF,TF,N,ISLN
COMMON/PAYDFF/K01,K02,K1,K2,K3,RANGEF
COMMON/STATE/SX(410),SY(-20),SZ(410),SVM(410),SOSI(410),SSAI(410)
REAL MACH,M,LVMF,LPSF,LPSF,LXF,LYF,LZF,LVM,LPS,L3A,LX,LY,LZ,K01,
1K02,K1,K2,K3,LOTV,LOTP,LOTT,LOTX,LOTY,LOTZ

C
C***** CALCULATE LAMDA(TF)
C
RANGEF = SQRT(XF*XF + YF*YF + ZF*ZF)
IF(RANGEF.EQ.0.) RANGEF = 1.E-10
LVMF = -1.
LPSF = K1*(PSIF-PSLF)
LGAF = K2*(GAMF-T4.03)
LXF = 2.*K01*XF + K02*XF/2.1*BEF - K3*XF/RANGEF*(15000.-RANGEF)
LYF = 2.*K01*YF + K02*YF/2.1*BEF - K3*YF/RANGEF*(15000.-RANGEF)
LZF = 2.*K01*ZF + K02*ZF/2.1*BEF - K3*ZF/RANGEF*(15000.-RANGEF)

```



```

C
C***** INITIALIZE PARAMETERS
C
AL = ALF
BE = BEF
VM = VMF
GAM = GAMF
PSI = PSIF
X = XF
Y = YF
Z = ZF
T = TF
S = .795
H = -H0
LVH = LVHF
LPS = LPSF
LGA = LGAF
LX = LXF
LY = LYF
LZ = LZF
I = N+1
PRINT 24
24 FORMAT(1X/3X,"BACKWARD INTEGRATION"/1X)
C
C***** CALCULATE TIME VARIANT PARAMETERS AND DERIVATIVES
C
10 I = I-1
TAU = .003565*Z+519.59
RHO = 5.3305E-15*TAU**3.26
MACH = .0204*VM/SQRT(TAU)
Q = RHO*VM*VM/2.
M = 12.42
IF(T.LT.4.5) M = 14.99-.4764*(T-.60)
TH = 0.
IF(T.LT.4.5) TH = 2000.
DTAUZ = .003565
DRHOZ = 2.7131E-14*TAU**3.26*DTAUZ
DMACH = .0204/SQRT(TAU)
DMACHZ = -.0102*VM/TAU**1.5*DTAUZ
QV = RHO*VM
QZ = VM**2/2.*DRHOZ
C
C***** CALCULATE COMMANDS ALPHA AND BETA AND DERIVATIVES
C
AVV = AV(I)
IF(AVV.GT.20.) AVV = 20.
IF(AVV.LT.-20.) AVV = -20.
AVV = AVV*32.2
AHV = AH(I)
IF(AHV.GT.20.) AHV = 20.
IF(AHV.LT.-20.) AHV = -20.
AHV = AHV*32.2
AL = (AVV +32.2*CS(GAM))*M/(20.1*S*Q)
IF(AL.GT..350) AL = .350
IF(AL.LT.-.350) AL = -.350
BE = -AHV *4/(20.1*S*Q)
IF(BE.GT..350) BE = .350
IF(BE.LT.-.350) BE = -.350

```

```

ALTOT = SQRT(AL**2+BE**2)
IF(ALTOT.EQ.0.) ALTOT = 1.E-10
DALV = -AL/D*QDV
DALG = -32.2*M/(20.1*S*D)*SIN(GAM)
DAL7 = -AL/D*DQZ
DBEV = -BE/D*QDV
DBEZ = -BE/D*DQZ
DALTV = AL/ALTOT*DALV+BE/ALTOT*DBEV
DALTG = AL/ALTOT*DALG
DALTZ = AL/ALTOT*DALZ+BE/ALTOT*DBEZ
DAVVA = 32.2
DAHHA = 32.2
DALAV = M/(20.1*S*D)*DAVVA
DBEAM = -M/(20.1*S*D)*DAHHA
DALTAH = BE*57.295/ALTOT*DBEAM
DALTAV = AL*57.295/ALTOT*DALAV

```

C
C***** CALCULATE AERODYNAMIC FORCES AND DERIVATIVES
C

```

CDD = -51.553*MACH**7+380.974*MACH**5-1151.244*MACH**3+1844.332*
1*MACH**1-1589.781*MACH**3+895.882*MACH**2-246.239*MACH+28.250
DELCG = -2.851E-05*ALTOT**2-1.8286E-03*ALTOT+3.5714E-03
DELCDF = -7.4060E-12*Z**2-1.0785E-07*(-Z)-8.8779E-05
FX = -S*Q*(CDD+DELCG+DELCDF)
FY = -S*Q*(20.1*BE)
FZ = -S*Q*(20.1*AL)
DCDOV = (-351.506*MACH**6+2295.844*MACH**5-5755.220*MACH**4+
17377.329*MACH**3-5059.343*MACH**2+1771.754*MACH-245.238)*DDELGV
DCDOZ = (-351.506*MACH**6+2295.844*MACH**5-5755.220*MACH**4+
17377.329*MACH**3-5059.343*MACH**2+1771.754*MACH-245.238)*DDELGZ
DDELGV = (-5.702E-05*ALTOT-1.8286E-03)*DALTV
DDELGZ = (-5.702E-05*ALTOT-1.8286E-03)*DALTG
DDELGZ = (-5.702E-05*ALTOT-1.8286E-03)*DALTZ
DELFZ = -14.9120E-12*Z**2+1.0785E-07
DFXV = -FX/D*QDV-S*Q*(DCDOV+DDELGV)
DFXG = -S*Q*DDELGZ
DFXZ = -FX/D*DQZ-S*Q*(DCDOZ+DDELGZ+DELFZ)
DFYV = -S*Q*20.1*DBEV-S*Q*20.1*BE*DQV
DFZV = -S*Q*20.1*DALV-S*Q*20.1*AL*DQV
DFZG = -S*Q*20.1*DALG
DELAH = (-5.702E-05*ALTOT-1.8286E-03)*DALTAH
DELAH = (-5.702E-05*ALTOT-1.8286E-03)*DALTAH
DFXAH = -S*Q*DELAH
DFXAV = -S*Q*DELAH
DFYAH = -S*Q*20.1*DBEAM
DFZAV = -S*Q*20.1*DALAV

```

C
C***** CALCULATE VMDOT,PSIDOT AND GAMDOT AND DERIVATIVES
C

```

CAL = COS(AL)
SAL = SIN(AL)
CBE = COS(BE)
SBE = SIN(BE)
VMDOT = ((FX+TH)*CAL*CBE+FY*SBE+FZ*SAL*CBE)/4-32.2*SIN(GAM)
AY = (-FX+TH)*CAL*SBE+FY*CBE-FZ*SAL*SBE)/M
AZ = (-FX+TH)*SAL+FZ*CAL)/M+32.2*COS(GAM)
PSIDOT = AY/(VM*COS(GAM))
GAMDOT = -AZ/VM

```



```

DVDTV = (DFXV*CAL*DBE-FX*SAL*CRE*DAL/-FX*CAL*SBE*DBEV+DFYV*SBE+FY*
1CRE*DBEV+DFZV*SAL*DBE-FZ*CAL*CRE*DALV-FZ*SAL*SBE*DBEV-TH*SAL*DBE*
1DALV-TH*CAL*SBE*DBEV)/M
DVDTG = (DFXG*CAL*DBE-FX*SAL*CRE*DALG+DFZG*SAL*CRE*FZ*CAL*DBE*DALG
1-TH*SAL*CRE*DALG)/1-32 2*COS(GAM)
DVDTZ = (DFXZ*CAL*DBE-FX*SAL*CRE*DALZ-FX*CAL*SBE*DBEZ+FY*CRE*DBEZ+
1FZ*CAL*DBE*DALZ-FZ*SAL*SBE*DBEZ-TH*SAL*CRE*DALZ-TH*CAL*SBE*DBEZ)/M
DPDTV = (-DFXV 1*CAL*SBE-(FX+TH)*SAL*SBE*DALV-(FX+TH)*CAL*DBE*
1DBEV+DFYV*DBE-FX*SBE*DBEV-DFZV*SAL*SBE-FZ*CAL*SBE*DALV-FZ*SAL*DBE*
1DBEV)/(M*COS(GAM)*VM)-PSIDOT/VM
DPDTG = (-DFXG 1*CAL*SBE-(FX+TH)*SAL*SBE*DALG-DFZG*SAL*SBE-FZ
1*CAL*SBE*DALG)/(M*COS(GAM)*VM)+SIN(GAM)*PSIDOT/COS(GAM)
DPDTZ = (-DFXZ 1*CAL*SBE+(FX+TH)*SAL*SBE*DALZ-(FX+TH)*CAL*DBE*
1DBEZ-FY*SBE*DBEZ-FZ*CAL*SBE*DALZ-FZ*SAL*DBE*DBEZ)/(M*COS(GAM)*VM)
DGDTV = -(-DFXV 1*SAL-(FX+TH)*CAL*DALV+DFZV*CAL-FZ*SAL*DALV)/
1(M*VM)-GAMDOT/VM
DGDTG = -(-DFXG 1*SAL-(FX+TH)*CAL*DALG+DFZG*CAL-FZ*SAL*DALG)/
1(M*VM)+32.2*SIN(GAM)/VM
DGDTZ = -(-DFXZ 1*SAL-(FX+TH)*CAL*DALZ-FZ*SAL*DALZ)/(M*VM)
DVDTAH = ((DFXAH 1*CAL*DBE-(FX+TH)*CAL*SBE*DBEAH+DFYAH*SBE+FY*
1CRE*DBEAH-FZ*SAL*SBE*DBEAH)/M
DVDTAV = ((DFXAV 1*CAL*DBE-(FX+TH)*SAL*DBE*DALAV+DFZAV*SAL*DBE+
1FZ*CAL*DBE*DALAV)/1
DPDTAH = (-DFXAH 1*CAL*SBE-(FX+TH)*CAL*DBE*DBEAH+DFYAH*DBE-FY*
1SBE*DBEAH-FZ*SAL*DBE*DBEAH)/(M*VM*COS(GAM))
DPDTAV = (-DFXAV 1*CAL*SBE+(FX+TH)*SAL*SBE*DALAV-DFZAV*SAL*SBE-
1FZ*CAL*SBE*DALAV)/(M*VM*COS(GAM))
DGDTAH = (DFXAH 1*SAL)/(M*VM)
DGDTAV = -(-DFXAV 1*SAL-(FX+TH)*CAL*DALAV+DFZAV*CAL-FZ*SAL*
1DALAV)/(M*VM)

```

C
C***** UPDATE VM, PSI AND GAM AND CALCULATE DERIVATIVES
C

```

VM = SVM(I-1)
PSI = SPSI(I-1)
GAM = SGAM(I-1)
CGA = COS(GAM)
SGA = SIN(GAM)
CPS = COS(PSI)
SPS = SIN(PSI)
XDOT = VM*CGA*CPS
YDOT = VM*SGA*SPS
ZDOT = -VM*SGA
DXDTV = CGA*CPS
DXDTP = -VM*SGA*SPS
DXDTG = -VM*SGA*CPS
DYDTV = CGA*SPS
DYDTP = VM*CGA*CPS
DYDTG = -VM*SGA*SPS
DZDTV = -SGA
DZDTG = -VM*CGA

```

C
C***** UPDATE X, Y AND Z
C

```

X = SX(I-1)
Y = SY(I-1)
Z = SZ(I-1)

```

C

C***** CALCULATE LAMDA-DOT

C

LDTV = -(LV4*DVDTV+LPS*DPDTV+LGA*DGDTV+LX*DXDTV+LY*DYDTV+LZ*DZDTV)
 LDTP = -(LX*DXDTP+LY*DYDTP)
 LD TG = -(LV4*DVDTG+LPS*DPDTG+LGA*DGDTG+LX*DXDTG+LY*DYDTG+LZ*
 1DZDTG)
 LDTX = 0.
 LDY = 0.
 LDZ = -(LV4*DVDTZ+LPS*DPDTZ+LGA*DGDTZ)

C

C***** INTEGRATE LAMDA-DOT TO GET LAMDA.

C

LV4 = LV4+1*LDTV
 LPS = LPS+1*LDTP
 LGA = LGA+1*LD TG
 LX = LX+H*LDTX
 LY = LY+H*LDY
 LZ = LZ+H*LDZ

C

C***** CALCULATE AND STORE DH4H AND DH4V

C

DH4H(I) = LV4*DVDT4H+LPS*DPDT4H+LGA*DGDT4H
 DH4V(I) = LV4*DVDT4V+LPS*DPDT4V+LGA*DGDT4V

T = T+1

L = 2./40

K = I/L-(I+1)/L

IF(K EQ. 0) GO TO 3)

PRINT 25,T,V4,DH4H(I),DH4V(I),X,Y,Z,4H(I),4V(I)

25 FORMAT(1X/3X,24T ,F 5.1,3X,3HVM ,F8.2,3X,5HD4H ,E15.7,3X,54DH4V,
 1E15.7,3X,24K ,F7.0,3X,24Y ,F7.0,3X,24Z ,F7.0,3X,344H ,F6.2,3X,
 13H4V ,F5.2)

C

C***** CHECK FOR STOPPING CONDITION

C

30 IF(I GT. 1) GO TO 1)

RETURN

END

SUBROUTINE PAYOFF(J)

C

C*****

C*

THIS SUBROUTINE COMPUTES THE VALUE OF THE PAYOFF FUNCTION J

C*

C*****

C

COMMON/AFINC/XLOSE,YLOSE,ZLOSE,PSLF,THLOS
 COMMON/4FINC/VMF,34MF,PSIF,XF,YF,ZF,4LF,9EF,TF,N,ISLN
 COMMON/PAYDEF/K01,K02,<1,K2,K3,RANGE
 COMMON/PENCOF/K010,<021,K10,K20,K30
 REAL J,K01,K02,K1,<2,K3
 REAL K010,<020,K10,<20,K30

C

C***** ESTABLISH PENALTY FUNCTION COEFFICIENTS

C

K01 = K010
 K02 = <020
 K1 = K10
 K2 = K20


```

      K3 = K30
C
C***** MODIFY PENALTY FUNCTION COEFFICIENTS IF FINAL VALUES ARE
C      WITHIN TOLERANCES
C
      RANGEF = SQRT(XF*XF+YF*YF+ZF*ZF)
      IF(PSIF-PSLF.LE..230.AND.PSIF-PSLF.GE.0.) K1 = 0.
      IF(ABS(GAMF-THLOS).LE..175) K2 = 0.
      IF(RANGEF.GE.16000.) K3 = 0.
C
C***** CALCULATE PAYOFF FUNCTION
C
      J = -VMF+K01 *RANGEF**2+K02 *RANGEF+K1 /2.*(PSIF-PSLF)**2+K2 /2.*
      1 (GAMF-THLOS)**2+K3 /2.*(16000.-RANGEF)**2
C
      RETURN
      END
      SUBROUTINE PLTRAJ
C
C*****
C*
C*      THIS SUBROUTINE PLOTS COMPARISONS BETWEEN THE INITIAL
C*      PERFORMANCE PARAMETERS AND THE OPTIMIZED PERFORMANCE
C*      PARAMETERS
C*
C*****
C
      COMMON/AFIND/XLOSE,YLOSE,ZLOSE,PSLF,THLOS
      COMMON/AIG/VA0,XA0,YA0,ZA0
      COMMON/PLDATA/XI( 52),YI( 52),ZI( 52),XS( 52),YS( 52),ZS( 52),
      1NI,NF
      COMMON/PLDT2/PDHI( 52),PDZI( 52),PDHS( 52),PDZS( 52),AHGI( 52),
      1AVGI( 52),AHGS( 52),AVGS( 52)
      COMMON/PLDT3/PTI( 52),PTS( 52),RANGI( 52),RANGS( 52),ALPI( 52),
      1BEPI( 52),ALPS( 52),BEPS( 52),VDTI( 52),VDTS( 52)
      DIMENSION ZO(4),ZO(4)
C
C***** DRAW HORIZONTAL TRAJECTORY PLOT
C
      IF(ZA0.NE.-35000.) GO TO 5
      XM = -50000.
      XD = 15000.
      YM = 60000.
      YD = -15000.
      GO TO 15
5      IF(ZA0.NE.-20000.) GO TO 10
      XM = -50000.
      XD = 10000.
      YM = 50000.
      YD = -10000.
      GO TO 15
10     CONTINUE
15     XI(NI+1) = XM
      XI(NI+2) = XD
      XS(NF+1) = XM
      XS(NF+2) = XD
      YI(NI+1) = YM
      YI(NI+2) = YD

```

```

YS(NF+1) = YM
YS(NF+2) = YO
CALL PLOTS(30)
CALL PLOT(5.,-5.,-3)
CALL PLOT(1.5,2.0,-3)
CALL SPAXIS(0.,0.,15,4,CROSSRANGE (FT),15,4.0,90.,YM,YO,-.65,1.20,
1 1190,90.,1.,-1.,.0305)
CALL SPAXIS(0.,4.0,1.4,CJHNRANGE (FT),14,7.0,0.0,XM,XO,2.80,1.50,
1.1190,0.,1.,-1.,.0935)
CALL LINE(XI,YI,NI,1,0,0)
CALL LINE(XS,YS,NF,1,3,1)
CALL SYMBOL(4.00,4.00, 126,2,0.,-1)
CALL PLOT(5.30,3.44,3)
CALL PLOT(5.55,3.44,2)
CALL SYMBOL(5.70,3.40, 0805,4,HINTL,0.,4)
CALL PLOT(5.30,3.31,3)
CALL PLOT(5.55,3.31,2)
CALL SYMBOL(5.70,3.27, 0805,3,HOPT,0.,3)
CALL SYMBOL(5.47,3.307,.0700,1,0.,-1)
CALL PLOT(-1.,-.8,3)
CALL PLOT(3.0,-.8,2)
CALL PLOT(3.0,4.8,2)
CALL PLOT(-1.,4.8,2)
CALL PLOT(-1.,-.8,2)

```

```

C
C***** DRAW VERTICAL TRAJECTORY PLOT
C

```

```

IF(ZA0.NE.-35000.) GO TO 95
RM = 120000.
RD = -20000.
ZM = 0.
ZO = 10000.
GO TO 105
95 IF(ZA0.NE.-20000.) GO TO 100
RM = 60000.
RD = -10000.
ZM = 0.
ZO = 5000.
GO TO 105
100 CONTINUE
105 ZI(NI+1) = ZM
ZI(NI+2) = ZO
ZS(NF+1) = ZM
ZS(NF+2) = ZO
RANGI(NI+1) = RM
RANGI(NI+2) = RD
RANGS(NF+1) = RM
RANGS(NF+2) = RD
R0(1) = RANGI(1)
Z0(1) = -ZM
R0(2) = 0.
Z0(2) = 0.
R0(3) = ZM
R0(4) = ZO
Z0(3) = ZM
Z0(4) = ZO
CALL PLOT(14.,0.,-3)
CALL SPAXIS(0.,0.,13,4,ALTITUDE (FT),13,4.0,90.,ZM,ZO,-.65,1.30,

```



```

1 1190,90.,1.,-1.,0305)
  CALL SPAXIS(0.,0.,104RNGE (FT),-10,5.0,0.0,R1,20,2.50,-.5230,
1 1190,1.,1.,-1.,0305)
  CALL LINE(RANGI,7I,NI,1,0,0)
  CALL LINE(RANGS,ZS,NF,1,3,1)
  CALL DASHLN(20,20,2,1)
  CALL SYM30(.5.,0.,125,2,0.,-1)
  CALL PLOT(0.50,3.94,3)
  CALL PLOT(0.55,3.94,2)
  CALL SYM30(.0.90,3.30, 0805,4HINTL,0.,4)
  CALL PLOT(0.50,3.91,3)
  CALL PLOT(0.55,3.81,2)
  CALL SYM30(.0.90,3.77, 0305,3HOPT,0.,3)
  CALL SYM30(.0.57,3.837,.0700,1,0.,-1)
  CALL PLOT(-1.,-.8,3)
  CALL PLOT(7.0,-.8,2)
  CALL PLOT(7.0,4.8,2)
  CALL PLOT(-1.,4.8,2)
  CALL PLOT(-1.,-.8,2)

```

```

C
C***** DRAW VMDOOT VS. TIME PLOT
C

```

```

  VM = -100.
  VD = 50.
  IF(ZA0.NE.-35000.) GO TO 25
  TM = 0.
  TD = 15.
  GO TO 35
25 IF(ZA0.NE.-20000.) GO TO 30
  TM = 0.
  TD = 10.
  GO TO 35
30 CONTINUE
35 PTI(NI+1) = TM
  PTI(NI+2) = TD
  PTS(NF+1) = TM
  PTS(NF+2) = TD
  VDTI(NI+1) = VM
  VDTI(NI+2) = VD
  VOTS(NF+1) = VM
  VOTS(NF+2) = VD
  VDTI(1) = VDTI(3)
  VDTI(2) = VDTI(3)
  VOTS(1) = VOTS(3)
  VOTS(2) = VOTS(3)
  CALL PLOT(14.,0.,-3)
  CALL SPAXIS(0.,0.,154VMDOOT (FT/SEC2),15,4.0,30.,VM,VD,-.50,1.20,
1 1190,90.,1.,-1.,0305)
  CALL SPAXIS(0.,0.,104TIME (SEC),-10,5.0,0.0,TM,TD,2.5),-.5230,
1 1190,0.,1.,-1.,0305)
  CALL LINE(PTI,VDTI,NI,1,0,0)
  CALL LINE(PTS,VOTS,NF,1,3,1)
  CALL PLOT(0.,2.,3)
  CALL PLOT(5.,2.,2)
  CALL PLOT(0.50,3.94,3)
  CALL PLOT(0.55,3.94,2)
  CALL SYM30(.0.90,3.90, 0805,4HINTL,0.,4)
  CALL PLOT(0.50,3.91,3)

```

```

CALL PLOT(3.35,3.91,2)
CALL SYMBO(7.30,3.77, 0805,3HOPT,0.,3)
CALL SYMBO(0.67,3.817,.0700,1,0.,-1)
CALL PLOT(-1.,-.8,3)
CALL PLOT(7.0,-.8,2)
CALL PLOT(7.0,4.8,2)
CALL PLOT(-1.,4.8,2)
CALL PLOT(-1.,-.8,2)

```

C
C***** DRAW AVG VS. TIME PLOT
C

```

AM = -20.
AD = 10.
AHGI(NI+1) = AM
AHGI(NI+2) = AD
AHGS(NF+1) = AM
AHGS(NF+2) = AD
CALL PLOT(14.,0.,-3)
CALL SPAXIS(0.,0.,3HAGS (G'S),9,4.0,30.,AM,AD,-.50,1.40,
1.1190,30.,1.,-1.,0905)
CALL SPAXIS(0.,0.,10TIME (SEC),-10,5.0,0.0,T4,T0,2.50,-.5230,
1.1190,0.,1.,-1.,0905)
CALL LINE(PTI,AHGI,NI,1,0,0)
CALL LINE(PTS,AHGS,NF,1,3,1)
CALL PLOT(0.,2.,3)
CALL PLOT(5.,2.,2)
CALL PLOT(5.30,3.94,3)
CALL PLOT(5.55,3.94,2)
CALL SYMBO(5.70,3.91, 0805,4HINTL,0.,4)
CALL PLOT(5.30,3.81,3)
CALL PLOT(5.55,3.81,2)
CALL SYMBO(5.70,3.77, 0805,3HOPT,0.,3)
CALL SYMBO(5.7,3.817,.0700,1,0.,-1)
CALL PLOT(-1.,-.8,3)
CALL PLOT(7.0,-.8,2)
CALL PLOT(7.0,4.8,2)
CALL PLOT(-1.,4.8,2)
CALL PLOT(-1.,-.8,2)

```

C
C***** DRAW AVG VS. TIME PLOT
C

```

AVGI(NI+1) = AM
AVGI(NI+2) = AD
AVGS(NF+1) = AM
AVGS(NF+2) = AD
CALL PLOT(14.,0.,-3)
CALL SPAXIS(0.,0.,3HAGS (G'S),9,4.0,30.,AM,AD,-.50,1.40,
1.1190,30.,1.,-1.,0905)
CALL SPAXIS(0.,0.,10TIME (SEC),-10,5.0,0.0,T4,T0,2.50,-.5230,
1.1190,0.,1.,-1.,0905)
CALL LINE(PTI,AVGI,NI,1,0,0)
CALL LINE(PTS,AVGS,NF,1,3,1)
CALL PLOT(0.,2.,3)
CALL PLOT(5.,2.,2)
CALL PLOT(5.30,3.94,3)
CALL PLOT(5.55,3.94,2)
CALL SYMBO(5.70,3.91, 0805,4HINTL,0.,4)
CALL PLOT(5.30,3.91,3)

```



```

CALL PLOT(5.65,3.81,2)
CALL SYM3D(5.70,3.77, 0805,3HOPT,3,,3)
CALL SYM3D(5.47,3.807,.0700,1,0,-1)
CALL PLOT(-1,-.8,3)
CALL PLOT(7.0,-.8,2)
CALL PLOT(7.0,4.8,2)
CALL PLOT(-1,4.8,2)
CALL PLOT(-1,-.8,2)

```

```

C
C***** DRAW ALPHA VS. TIME PLOT
C

```

```

ALPI(NI+1) = AM
ALPI(NI+2) = AD
ALPS(NF+1) = AM
ALPS(NF+2) = AD
CALL PLOT(14,0,-3)
CALL SPAXIS(0,0,114,PHA (DEG),11,4,0,90.,44,AD,-.60,1.30,
1 1190,90.,1,-1,.0305)
CALL SPAXIS(0,0,104,TIME (SEC),-10,5.0,0.0,T4,TD,2.50,-.5230,
1 1190,0.,1,-1,.0805)
CALL LINE(PTI,ALPI,NI,1,0,0)
CALL LINE(PTS,ALPS,NF,1,3,1)
CALL PLOT(0,2,3)
CALL PLOT(5,2,2)
CALL PLOT(5.30,3.94,3)
CALL PLOT(5.65,3.94,2)
CALL SYM3D(5.70,3.90, 0805,4HINTL,0.,4)
CALL PLOT(5.30,3.91,3)
CALL PLOT(5.65,3.81,2)
CALL SYM3D(5.70,3.77, 0805,3HOPT,0.,3)
CALL SYM3D(5.47,3.807,.0700,1,0,-1)
CALL PLOT(-1,-.8,3)
CALL PLOT(7.0,-.8,2)
CALL PLOT(7.0,4.8,2)
CALL PLOT(-1,4.8,2)
CALL PLOT(-1,-.8,2)

```

```

C
C***** DRAW BETA VS. TIME PLOT
C

```

```

BEPI(NI+1) = AM
BEPI(NI+2) = AD
BEPS(NF+1) = AM
BEPS(NF+2) = AD
CALL PLOT(14,0,-3)
CALL SPAXIS(0,0,114,BETA (DEG),11,4,0,90.,44,AD,-.60,1.30,
1 1190,90.,1,-1,.0305)
CALL SPAXIS(0,0,104,TIME (SEC),-10,5.0,0.0,T4,TD,2.50,-.5230,
1 1190,0.,1,-1,.0805)
CALL LINE(PTI,BEPI,NI,1,0,0)
CALL LINE(PTS,BEPS,NF,1,3,1)
CALL PLOT(0,2,3)
CALL PLOT(5,2,2)
CALL PLOT(5.30,3.94,3)
CALL PLOT(5.65,3.94,2)
CALL SYM3D(5.70,3.90, 0805,4HINTL,0.,4)
CALL PLOT(5.30,3.91,3)
CALL PLOT(5.65,3.81,2)
CALL SYM3D(5.70,3.77,.0805,3HOPT,0.,3)

```

```

CALL SYM30L(5.47,3.817,.0700,1,0.,-1)
CALL PLOT(-1.,-.8,3)
CALL PLOT(7.0,-.8,2)
CALL PLOT(7.0,4.8,2)
CALL PLOT(-1.,4.8,2)
CALL PLOT(-1.,-.8,2)

```

C

C***** DRAW OH VS. RANGE PLOT

C

```

IF(ZA0.NE.-35000.) GO TO 75
OH = -1000.
OD = 1000.
GO TO 35
75 IF(ZA0.NE.-20000.) GO TO 80
OH = -1000.
OD = 1000.
GO TO 35
80 CONTINUE
95 POHI(NI+1) = OH
POHI(NI+2) = OD
PDHS(NF+1) = OH
PDHS(NF+2) = OD
CALL PLOT(14.,0.,-3)
CALL SPAXIS(0.,0.,7HCH (FT),7,4.0,90.,OH,OD,-.50,1.50,
1 1190,90.,1.,-1.,0305)
CALL SPAXIS(0.,0.,10HANGE (FT),-10,5.0,0.0,R4,R0,2.50,-.5290,
1 1190,0.,1.,-1.,0815)
CALL LINE(RANGI,PDHI,NI,1,0,0)
CALL LINE(RANGS,PDHS,NF,1,3,1)
CALL PLOT(0.,1.,3)
CALL PLOT(5.,1.,2)
CALL PLOT(5.30,3.34,3)
CALL PLOT(5.55,3.94,2)
CALL SYM30L(5.70,3.90,0805,4HINTL,0.,4)
CALL PLOT(5.30,3.91,3)
CALL PLOT(5.55,3.61,2)
CALL SYM30L(5.47,3.817,.0700,1,0.,-1)
CALL SYM30L(5.70,3.77,0805,3HOPT,0.,3)
CALL PLOT(-1.,-.8,3)
CALL PLOT(7.0,-.8,2)
CALL PLOT(7.0,4.8,2)
CALL PLOT(-1.,4.8,2)
CALL PLOT(-1.,-.8,2)

```

C

C***** DRAW OZ VS. RANGE PLOT

C

```

IF(ZA0.NE.-35000.) GO TO 110
OH = 1000.
OD = -500.
GO TO 120
110 IF(ZA0.NE.-20000.) GO TO 115
OH = 500.
OD = -250.
GO TO 120
115 CONTINUE
120 POZI(NI+1) = OH
POZI(NI+2) = OD
POZS(NF+1) = OH

```



```

PDZS(NF+2) = 00
CALL PLOT(14.,0.,-3)
CALL SPAXIS(0.,0.,740Z (FT),7,4.0,30.,DM,00,-.50,1.50,
1:1190,00.,1.,-1.,.0805)
CALL SPAXIS(0.,0.,104RANGE (FT),-10,5.0,0.0,24,R0,2.50,-.5230,
1:1190,0.,1.,-1.,.0805)
CALL LINE(RANG1,PDZ1,N1,1,0,0)
CALL LINE(RANGS,PDZS,NF,1,3,1)
CALL PLOT(0.,2.,3)
CALL PLOT(5.,2.,2)
CALL PLOT(5.30,3.94,3)
CALL PLOT(5.55,3.94,2)
CALL SYMBOL(5.70,3.90, 0805,4HINTL,0.,4)
CALL PLOT(5.30,3.91,3)
CALL PLOT(5.55,3.81,2)
CALL SYMBOL(5.70,3.77, 0805,3HOPT,0.,3)
CALL SYMBOL(5.47,3.837,.0700,1,0.,-1)
CALL PLOT(-1,-.8,3)
CALL PLOT(7.0,-.8,2)
CALL PLOT(7.0,4.8,2)
CALL PLOT(-1,4.8,2)
CALL PLOT(-1,-.8,2)
C
CALL PLOTE(IDUMHY)
RETURN
END

```

Appendix D

Retran Simulation Parameter Plots

Figs. 58-64 are parameter plots for a 15° , 35,000 ft altitude launch. Figs. 65-71 are plots for a 90° , 35,000 ft altitude launch. Figs. 72-78 are plots for a 15° , 5,000 ft altitude launch. Figs. 79-85 are plots for a 45° , 5,000 ft altitude launch. Figs. 86-92 are plots for a 90° , 5,000 ft altitude launch.

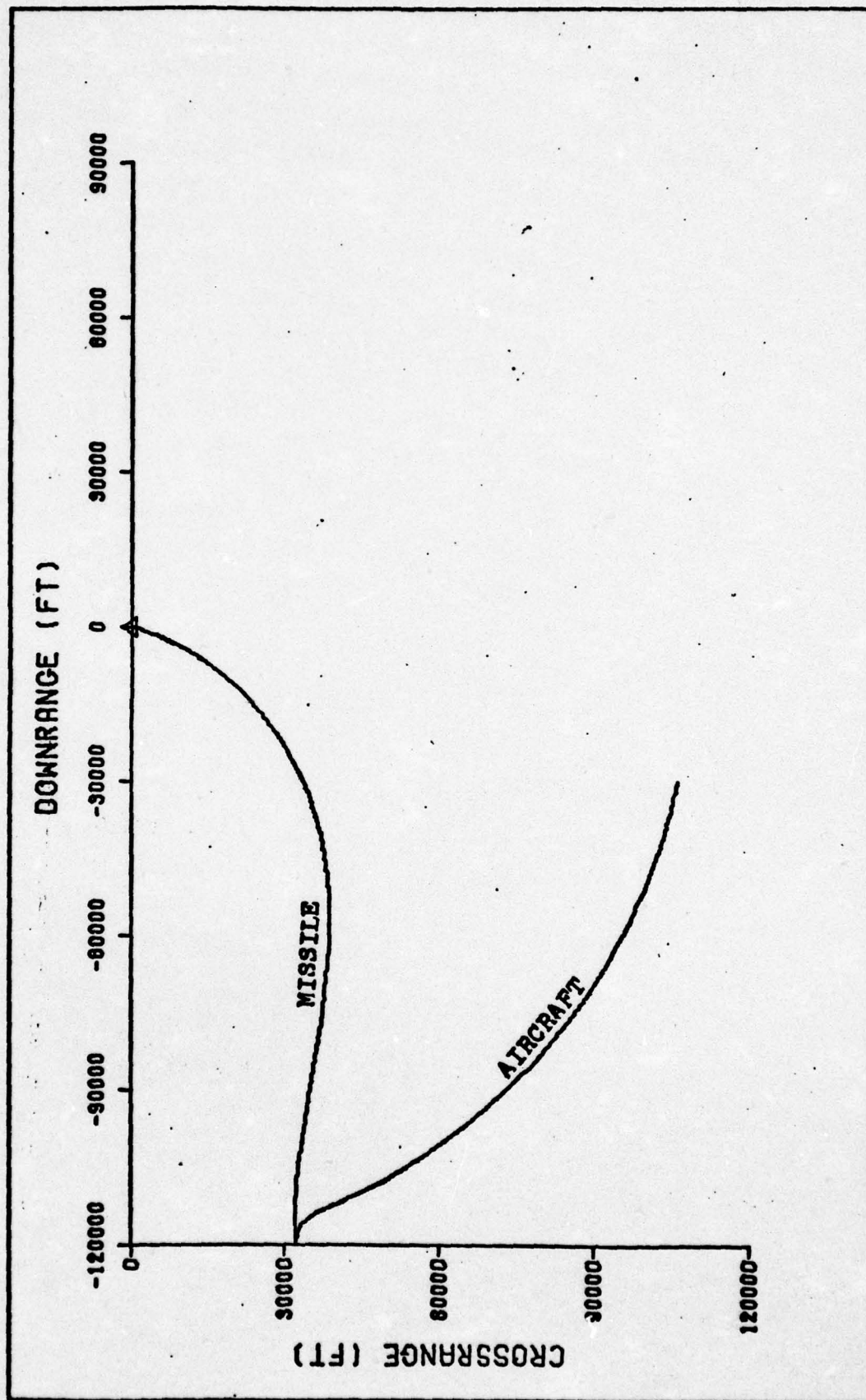


Fig. 58 Trajectory Planview - 15°, 35,000 ft Launch

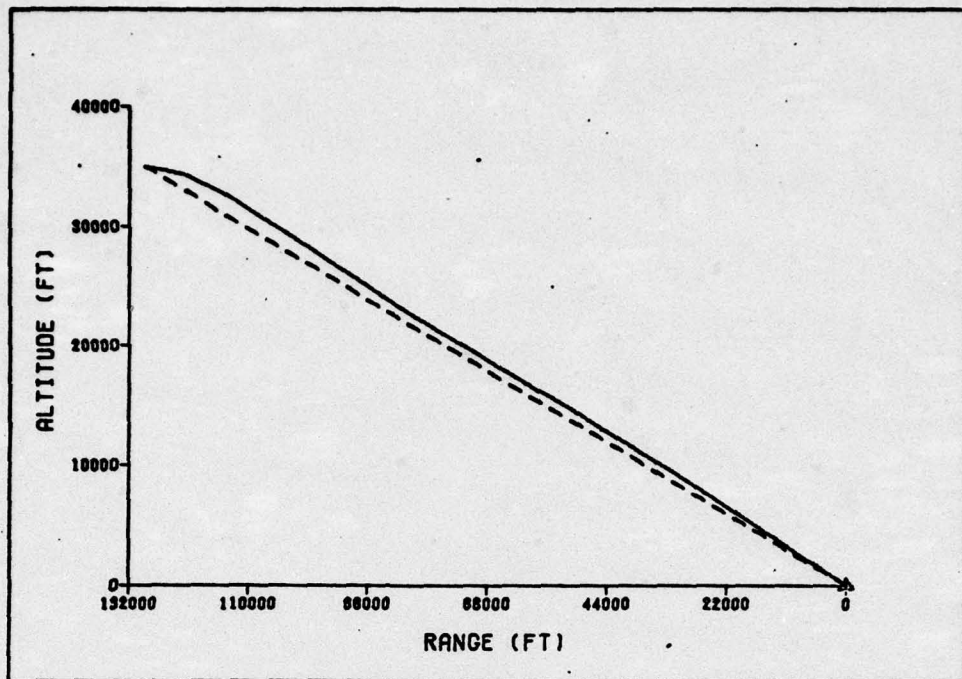


Fig. 59 Trajectory Vertical Profile - 15°, 35,000 ft Launch

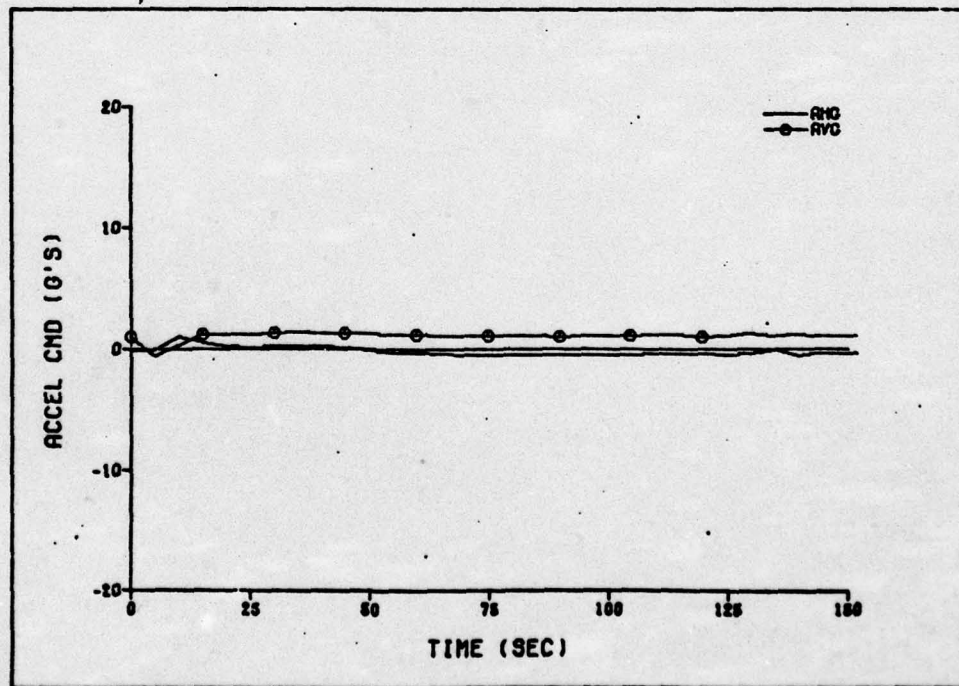


Fig. 60 Acceleration Commands - 15°, 35,000 ft Launch

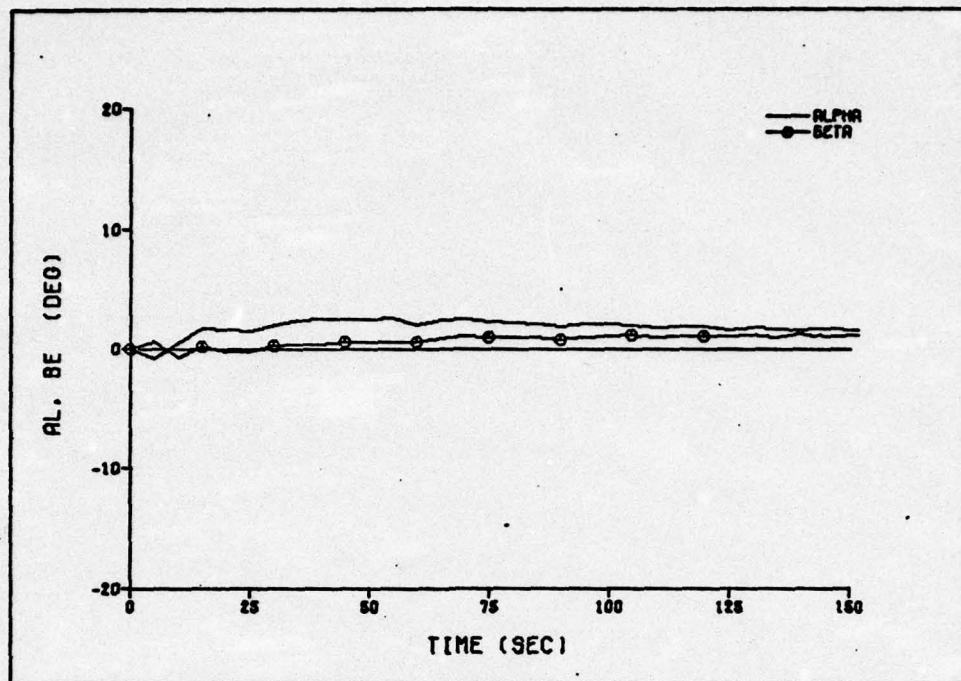


Fig. 61 Alpha and Beta - 15°, 35,000 ft Launch

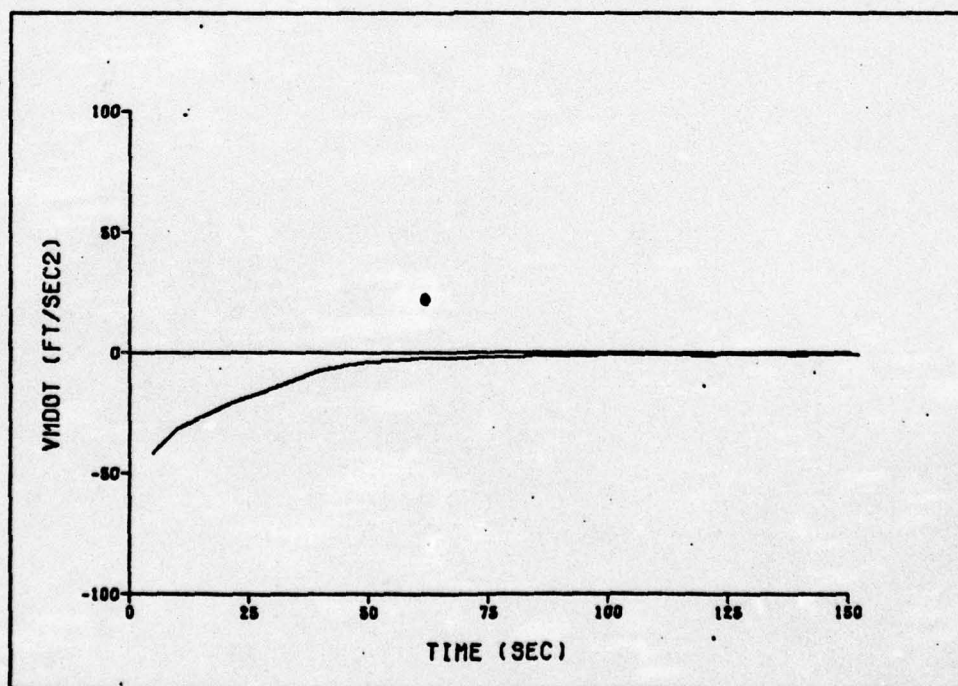


Fig. 62 Deceleration Due to Aerodynamic Drag - 15°, 35,000 ft Launch

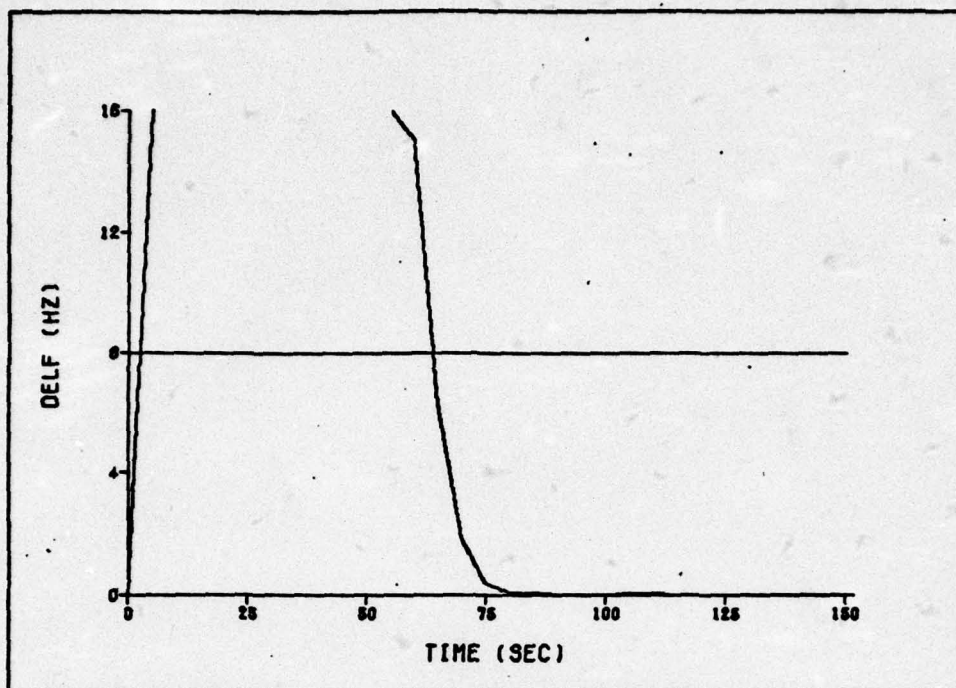


Fig. 63 Retrmitted Frequency Error - 15°, 35,000 ft Launch

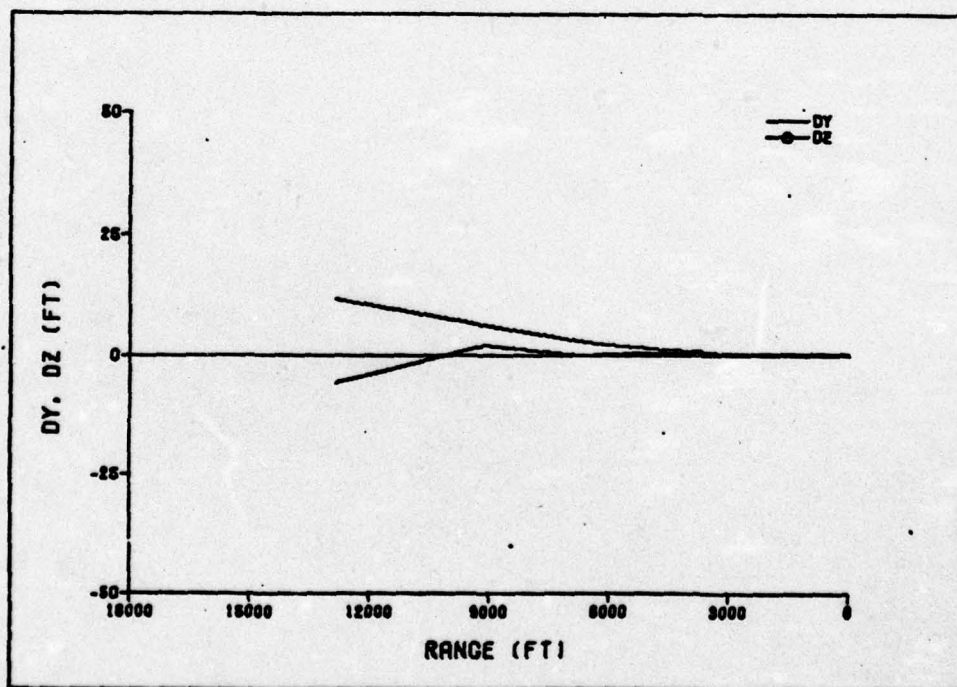


Fig. 64 Missile Distance Errors, Terminal Phase - 15°, 35,000 ft Launch

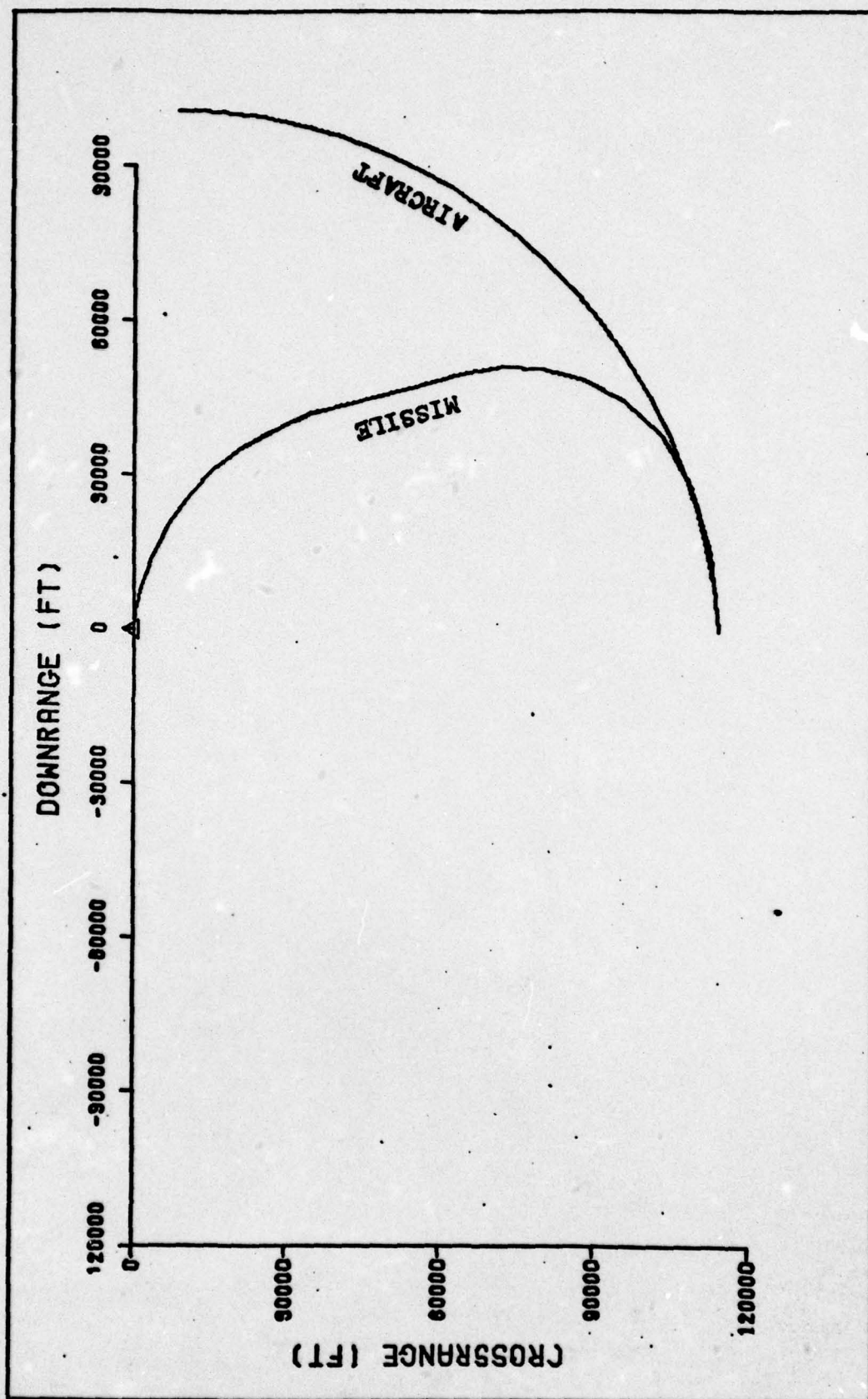


Fig. 65 Trajectory Plan View - 90°, 35,000 ft Launch

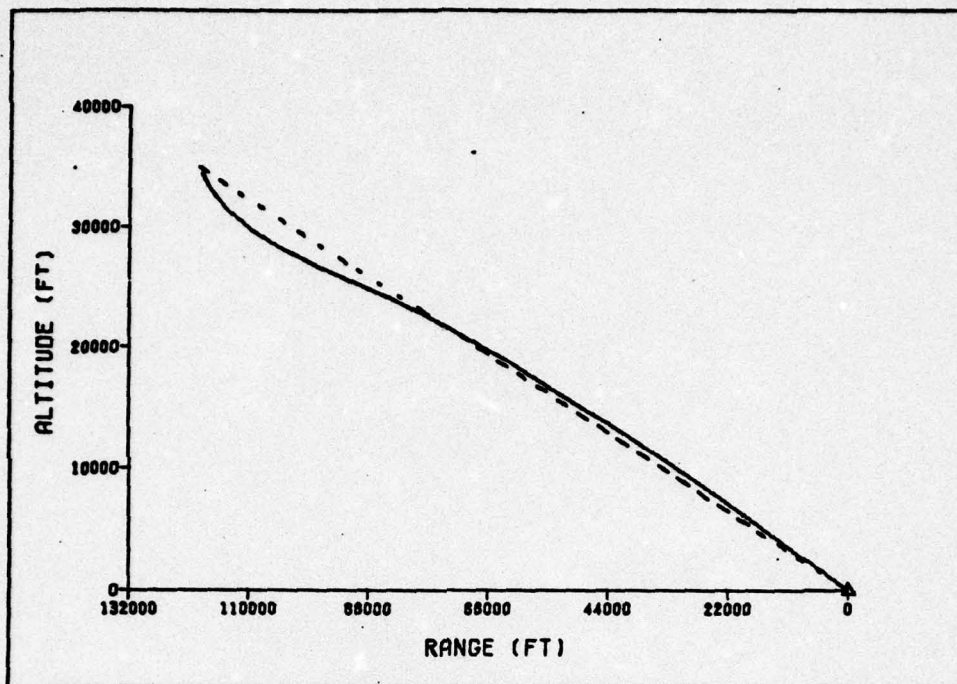


Fig. 66 Trajectory Vertical Profile - 90°, 35,000 ft Launch

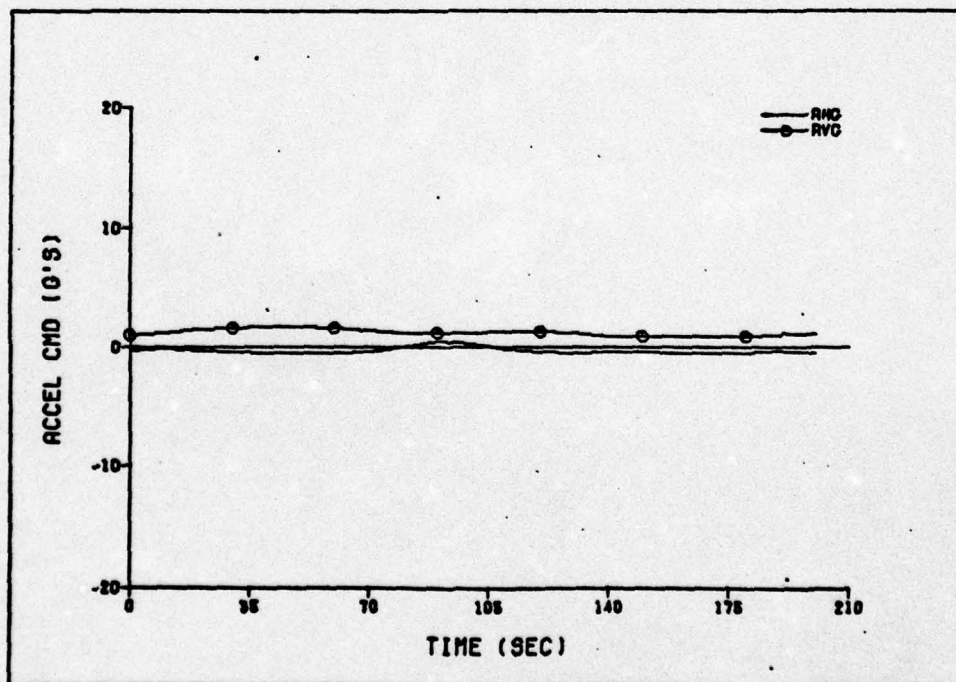


Fig. 67 Acceleration Commands - 90°, 35,000 ft Launch

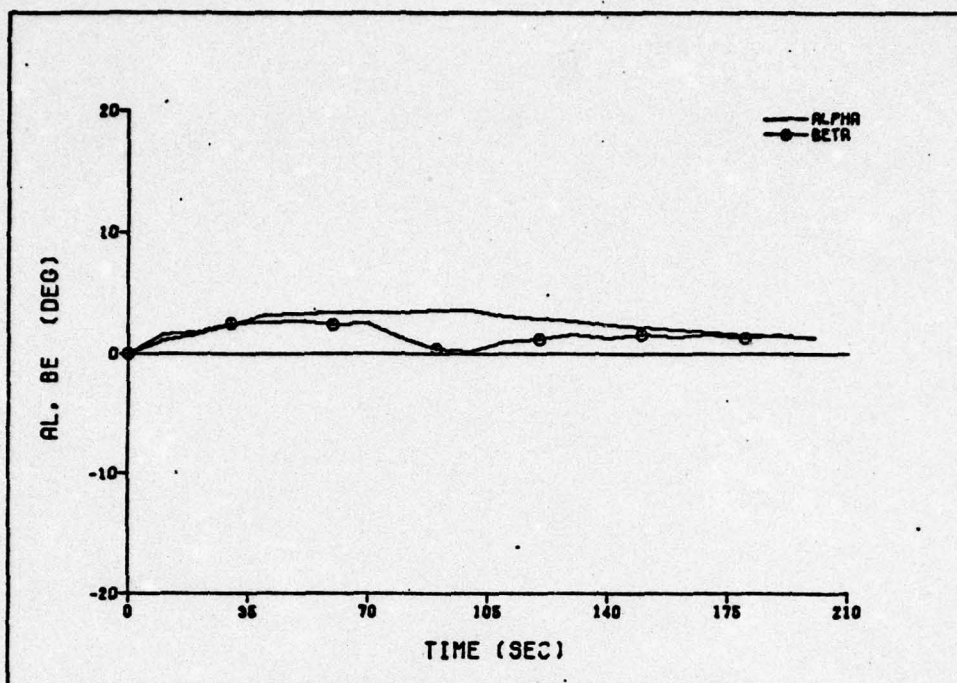


Fig. 68 Alpha and Beta - 90°, 35,000 ft Launch

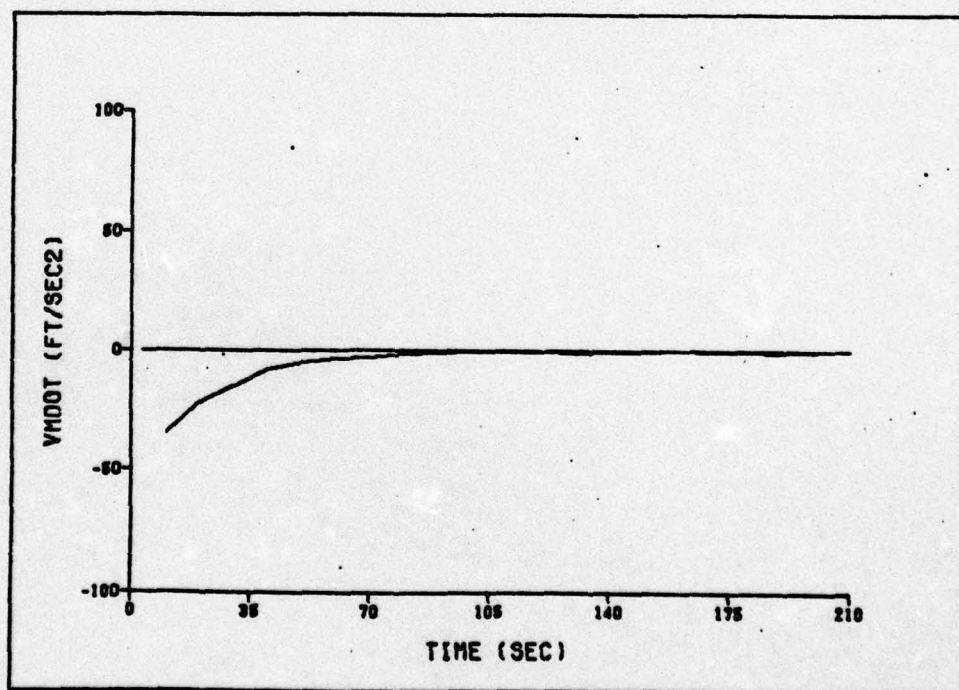


Fig. 69 Deceleration Due to Aerodynamic Drag - 90°, 35,000 ft Launch

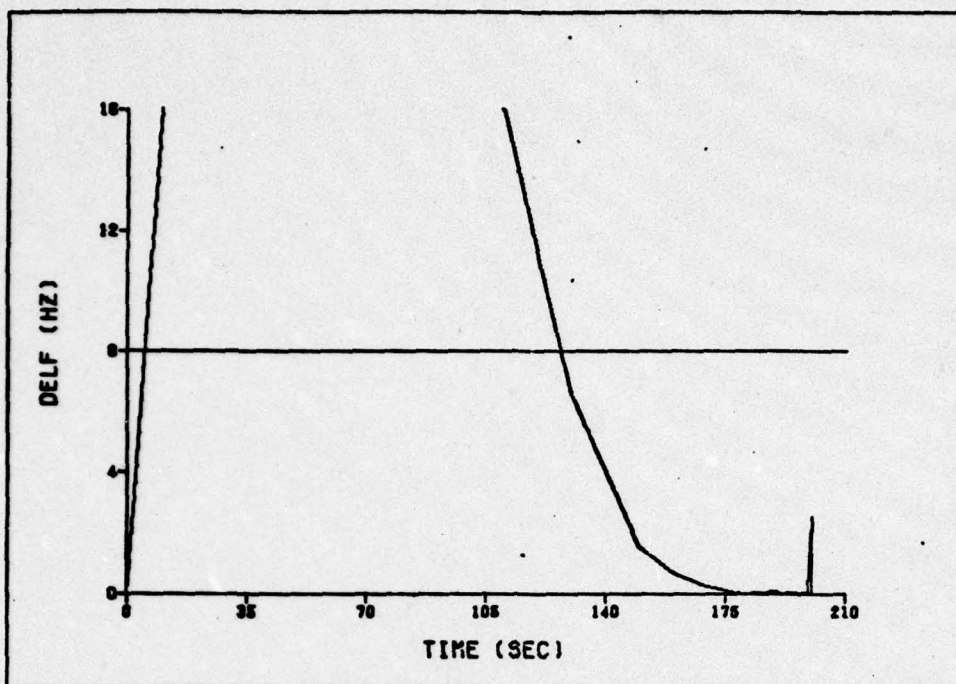


Fig. 70 Retrmitted Frequency Error - 90°, 35,000 ft Launch

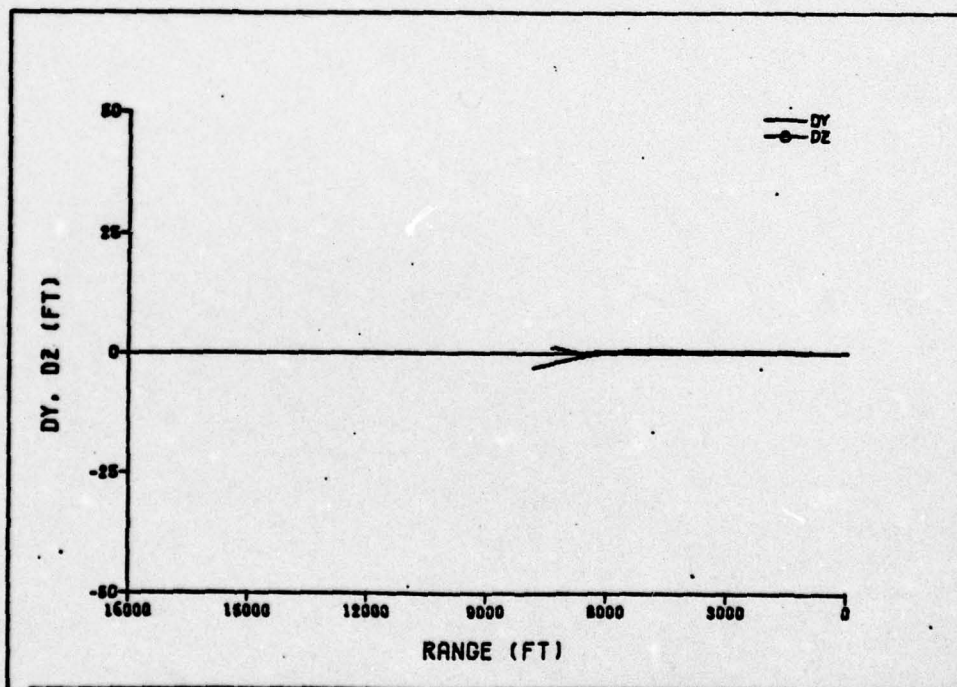


Fig. 71 Missile Distance Errors, Terminal Phase - 90°, 35,000 ft Launch

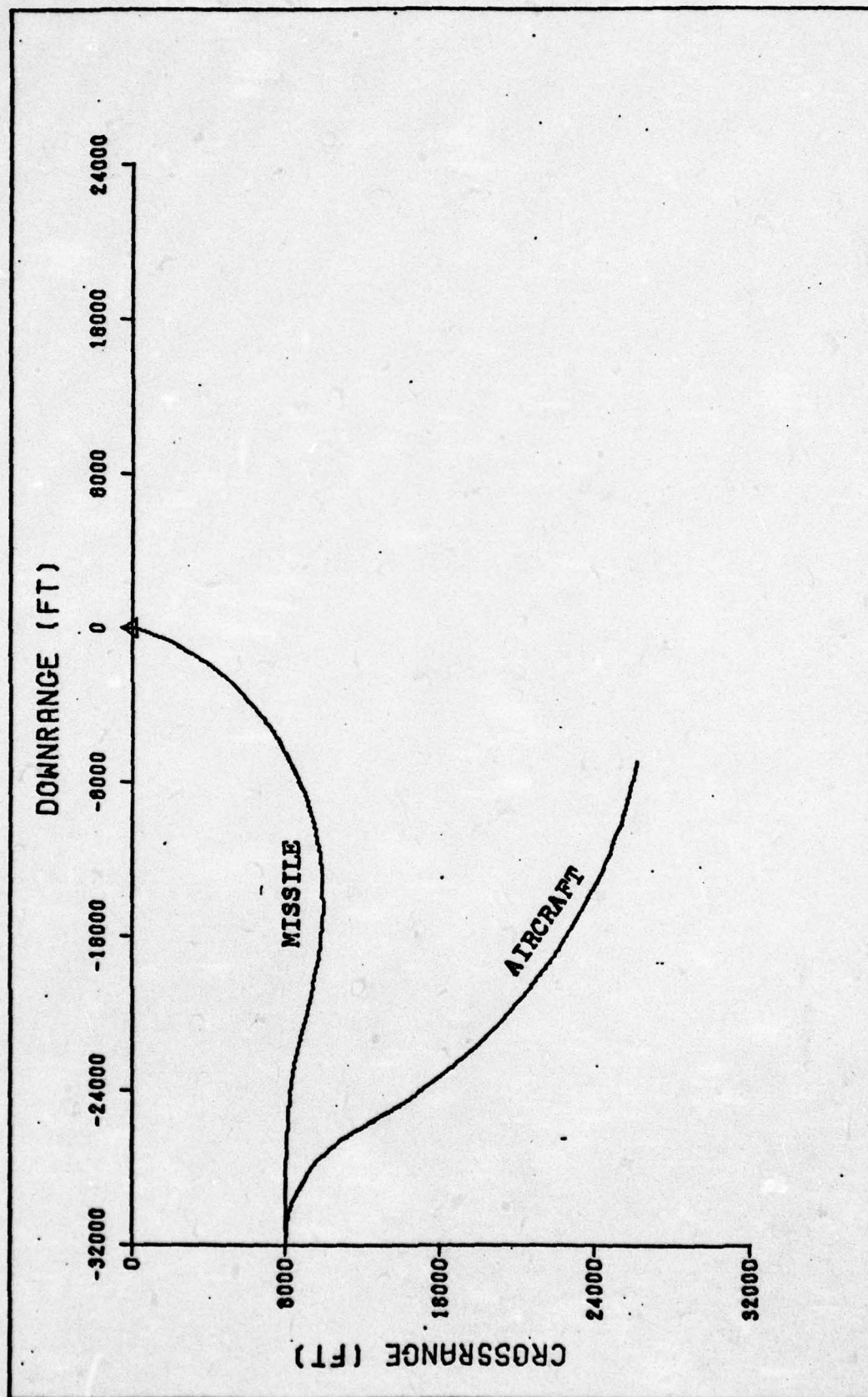


Fig. 72 Trajectory Plan View - 15°, 5,000 ft Launch

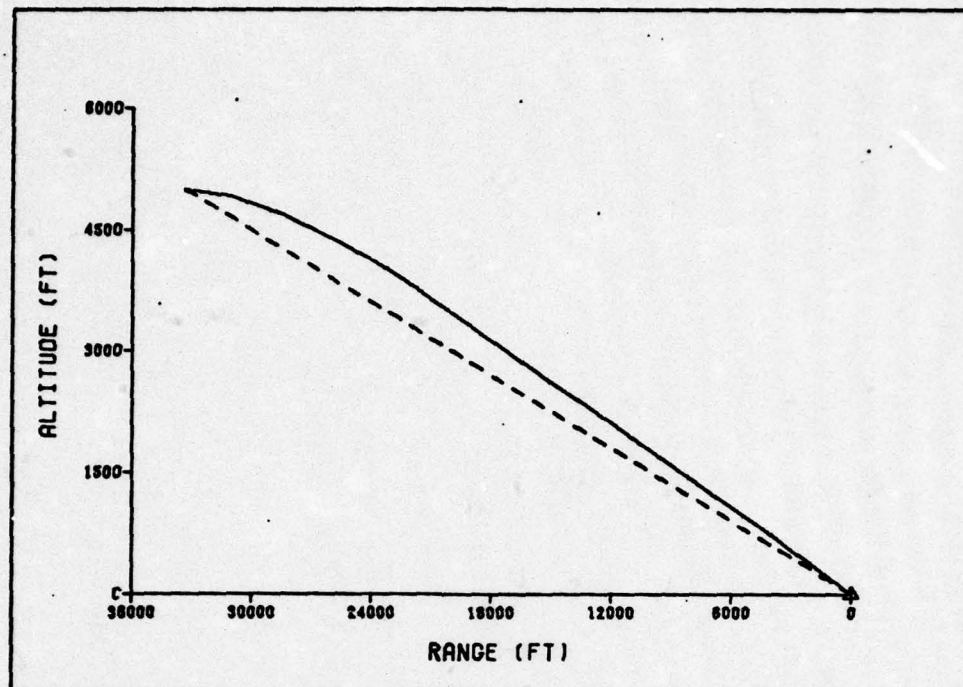


Fig. 73 Trajectory Vertical Profile - 15°, 5,000 ft Launch

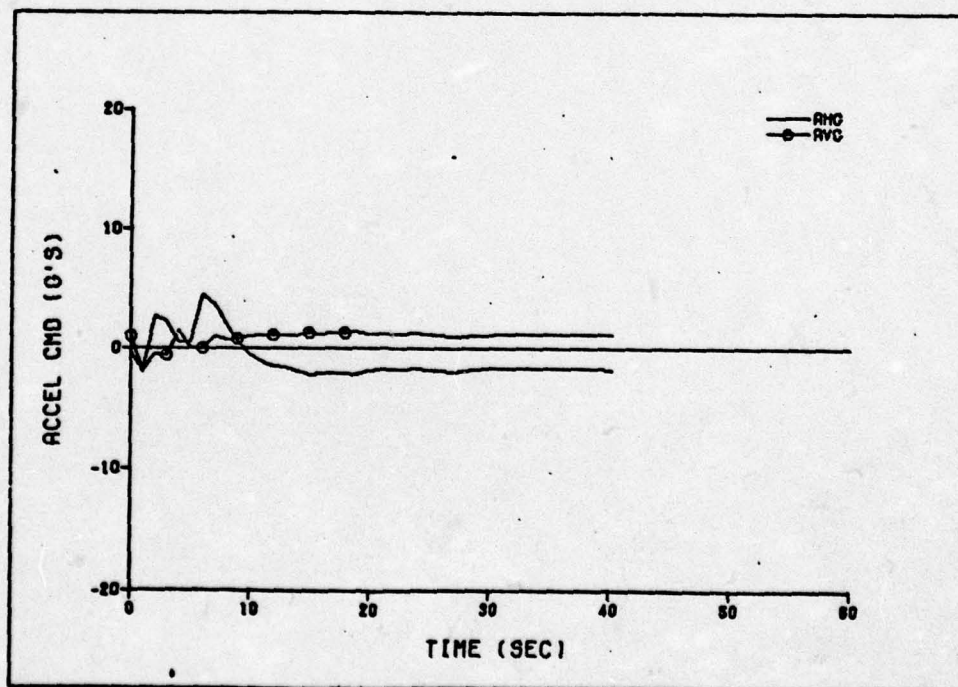


Fig. 74 Acceleration Commands - 15°, 5,000 ft Launch

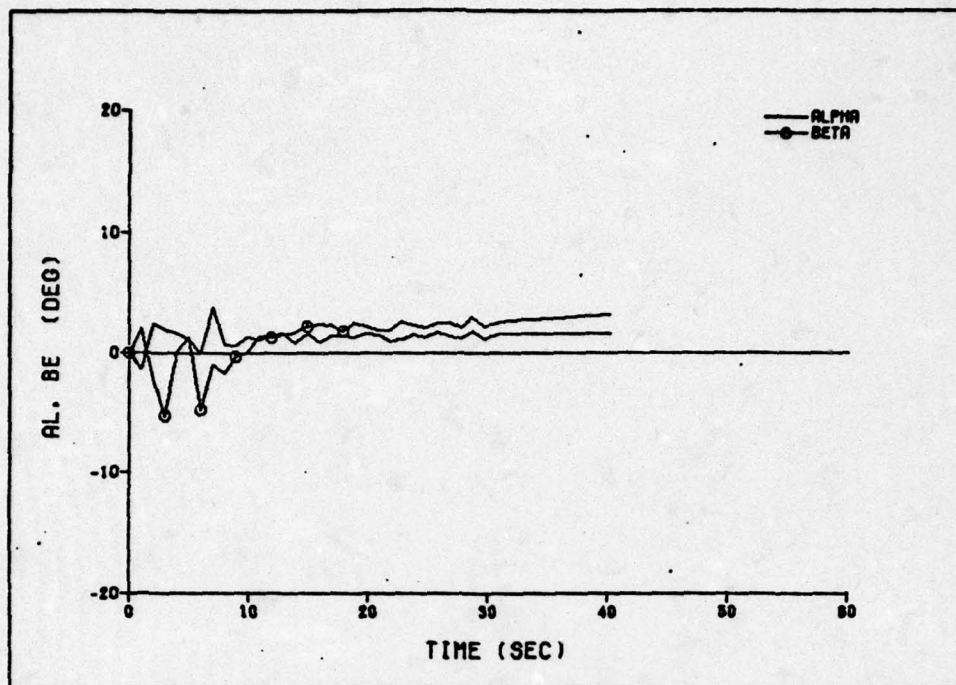


Fig. 75 Alpha and Beta - 15°, 5,000 ft Launch

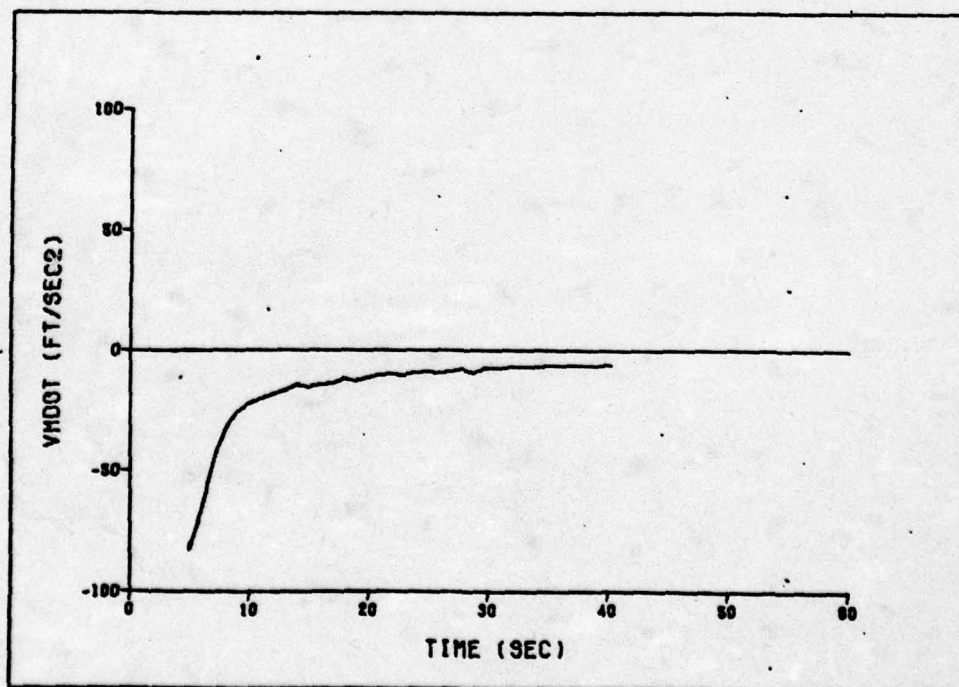


Fig. 76 Deceleration Due to Aerodynamic Drag - 15°, 5,000 ft Launch

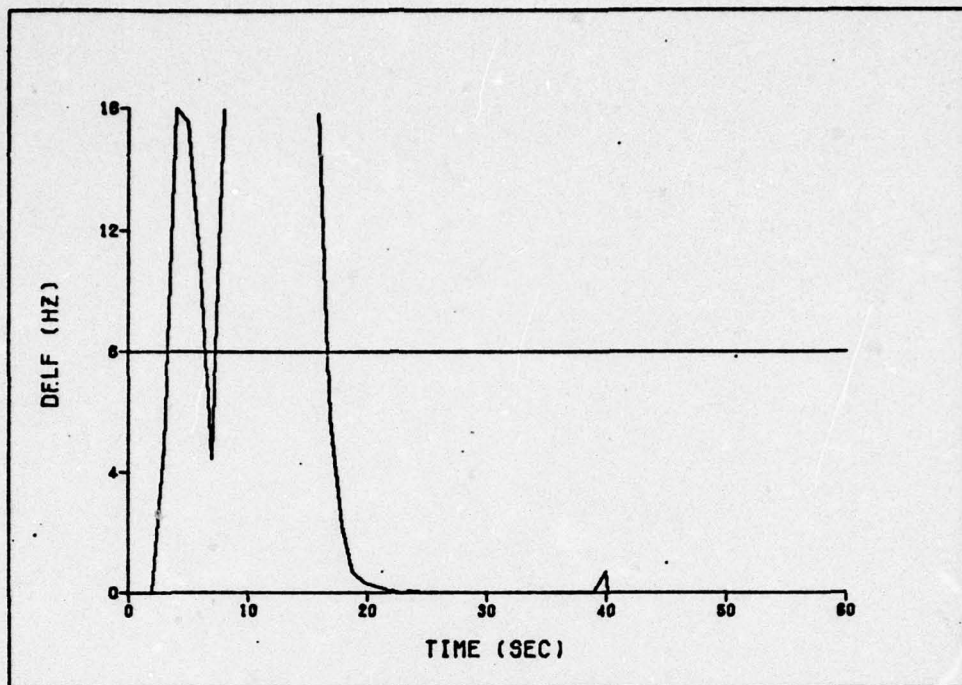


Fig. 77 Retrmitted Frequency Error - 15°, 5,000 ft Launch

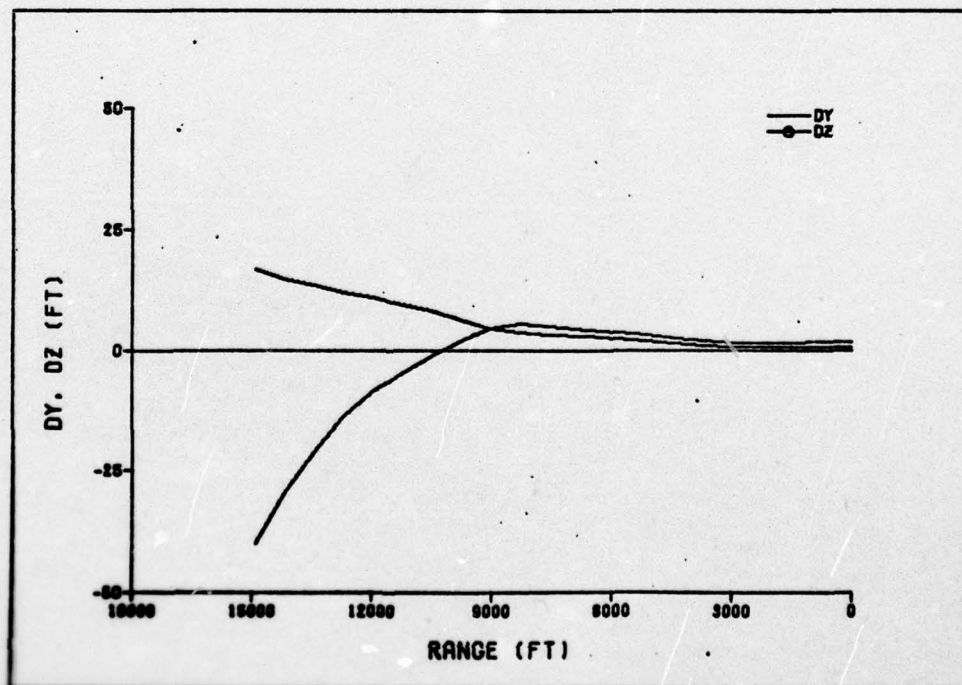


Fig. 78 Missile Distance Errors, Terminal Phase - 15°, 5,000 ft Launch

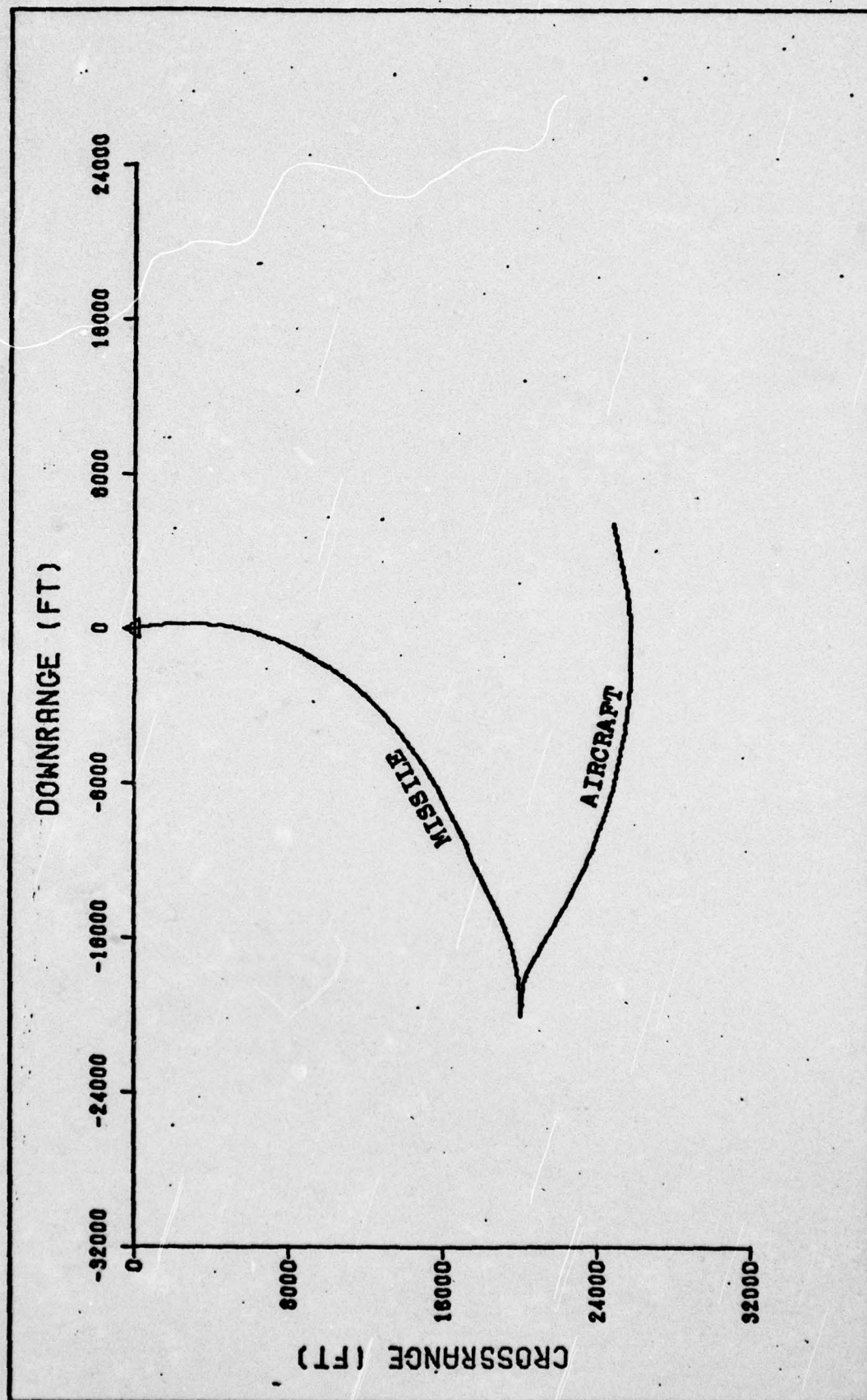


Fig. 79 Trajectory Plan View - 45°, 5,000 ft Launch

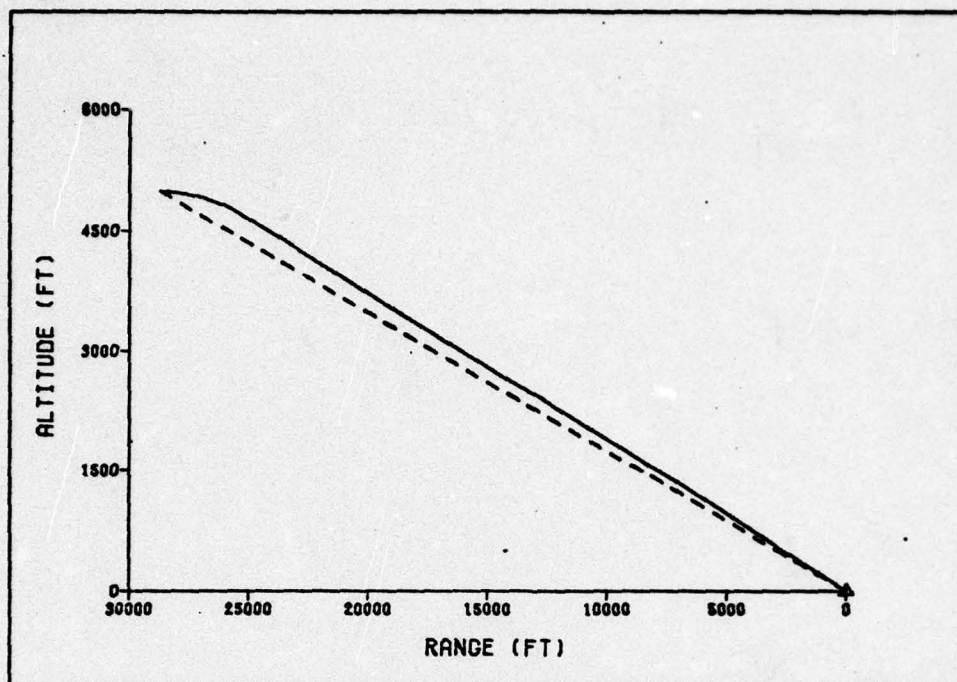


Fig. 80 Trajectory Vertical Profile - 45°, 5,000 ft Launch

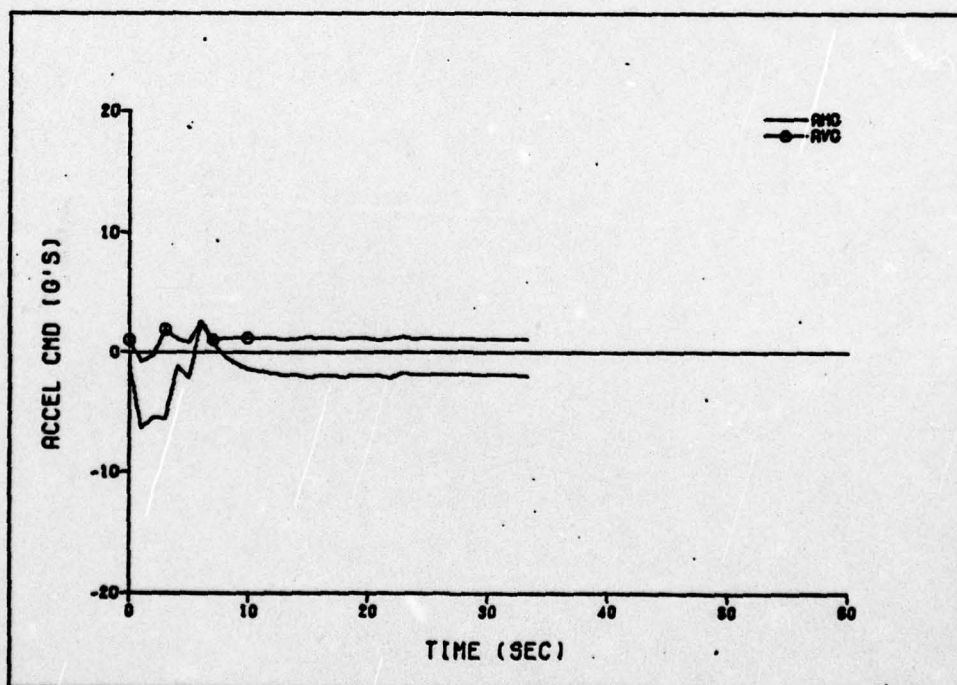


Fig. 81 Acceleration Commands - 45°, 5,000 ft Launch

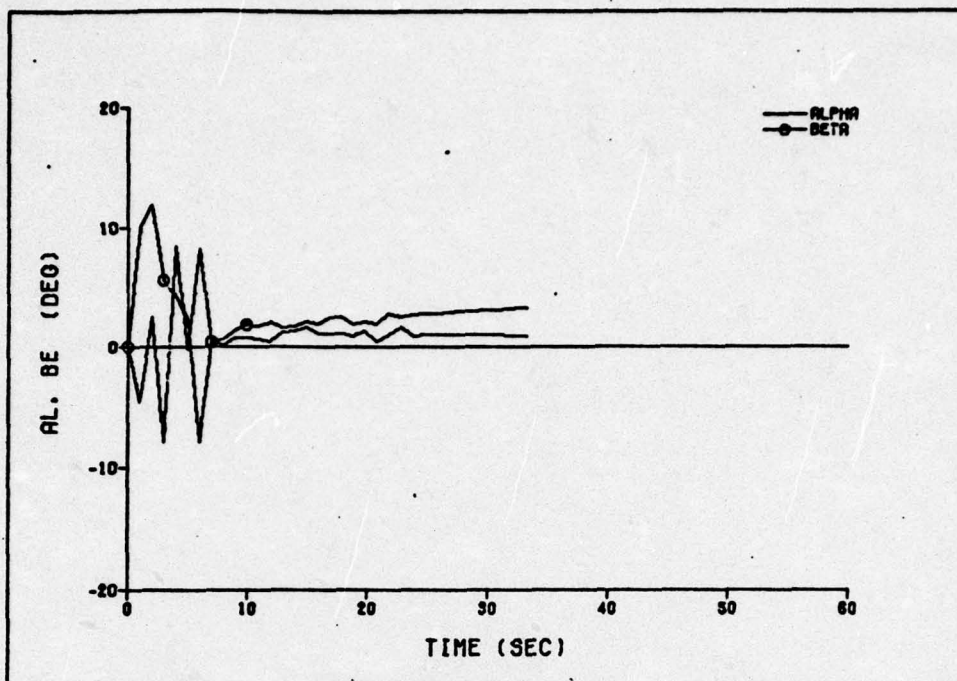


Fig. 82 Alpha and Beta - 45°, 5,000 ft Launch

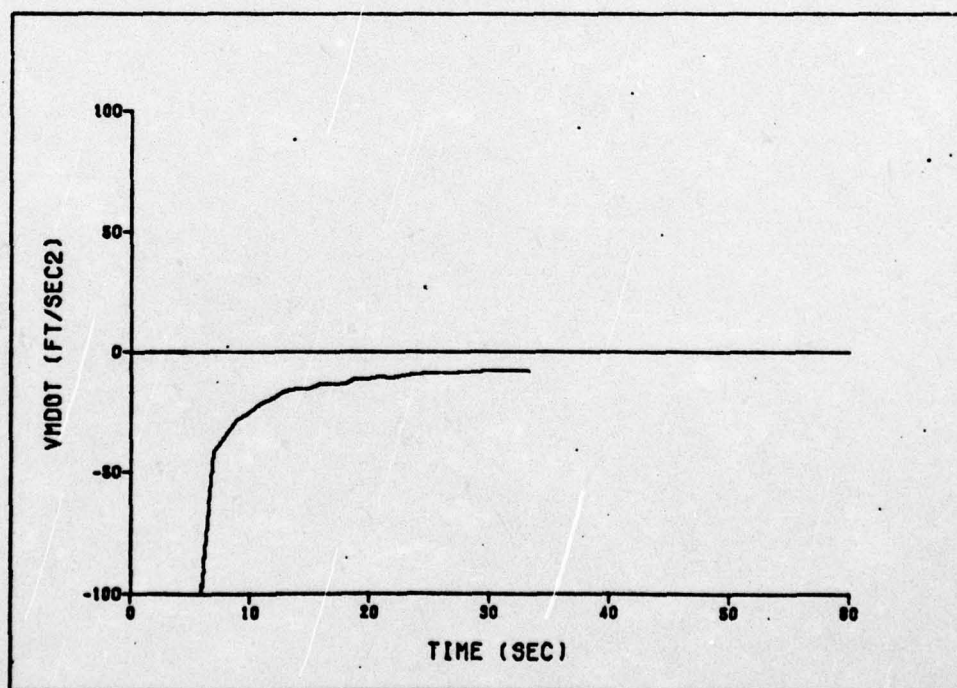


Fig. 83 Deceleration Due to Aerodynamic Drag - 45°, 5,000 ft Launch

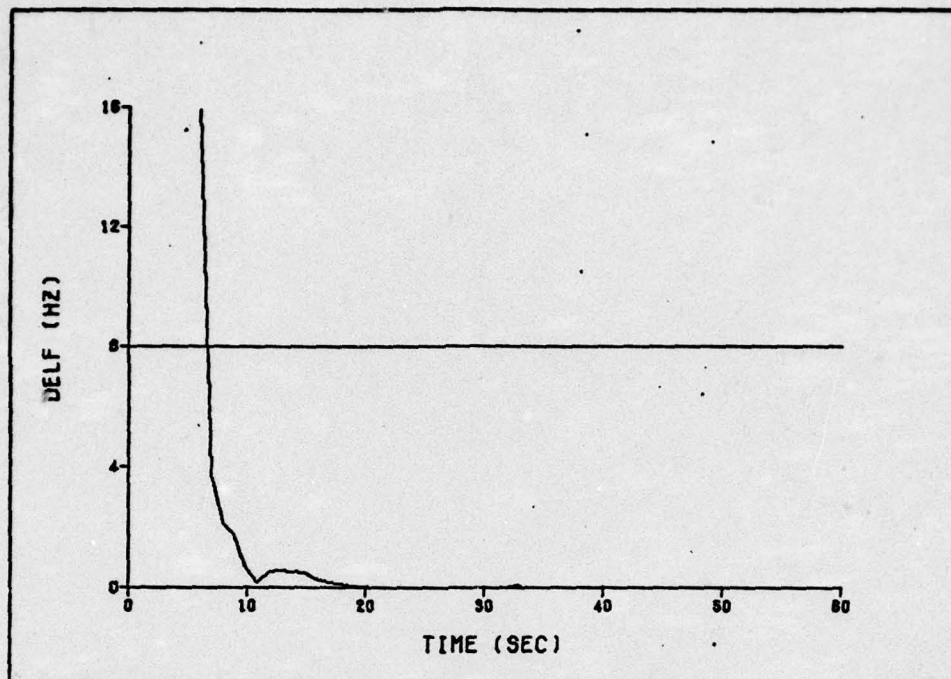


Fig. 84 Retrmitted Frequency Error - 45°, 5,000 ft Launch

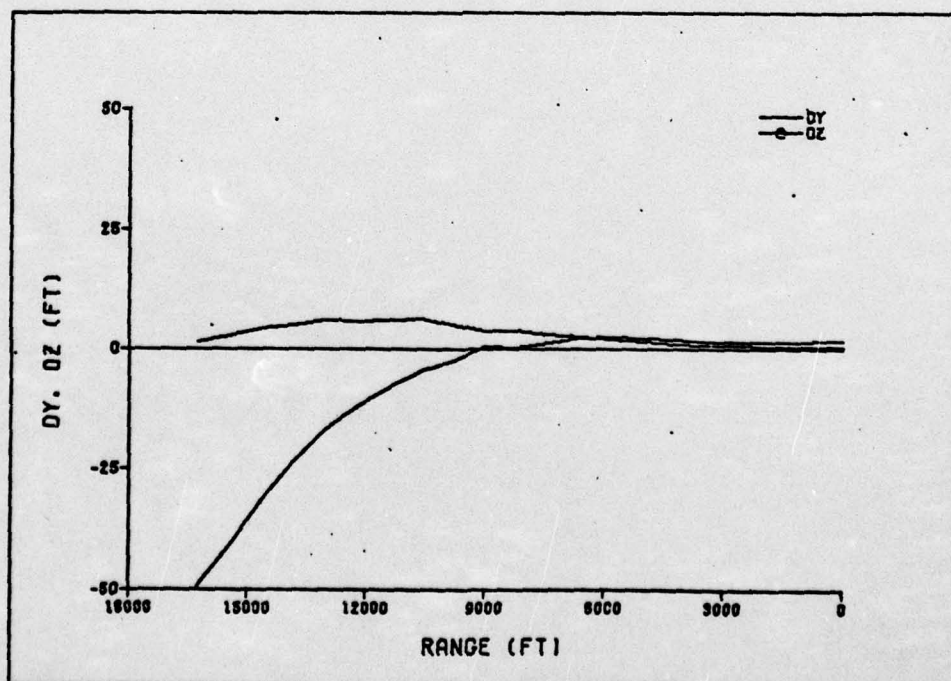


Fig. 85 Missile Distance Errors, Terminal Phase - 45°, 5,000 ft Launch

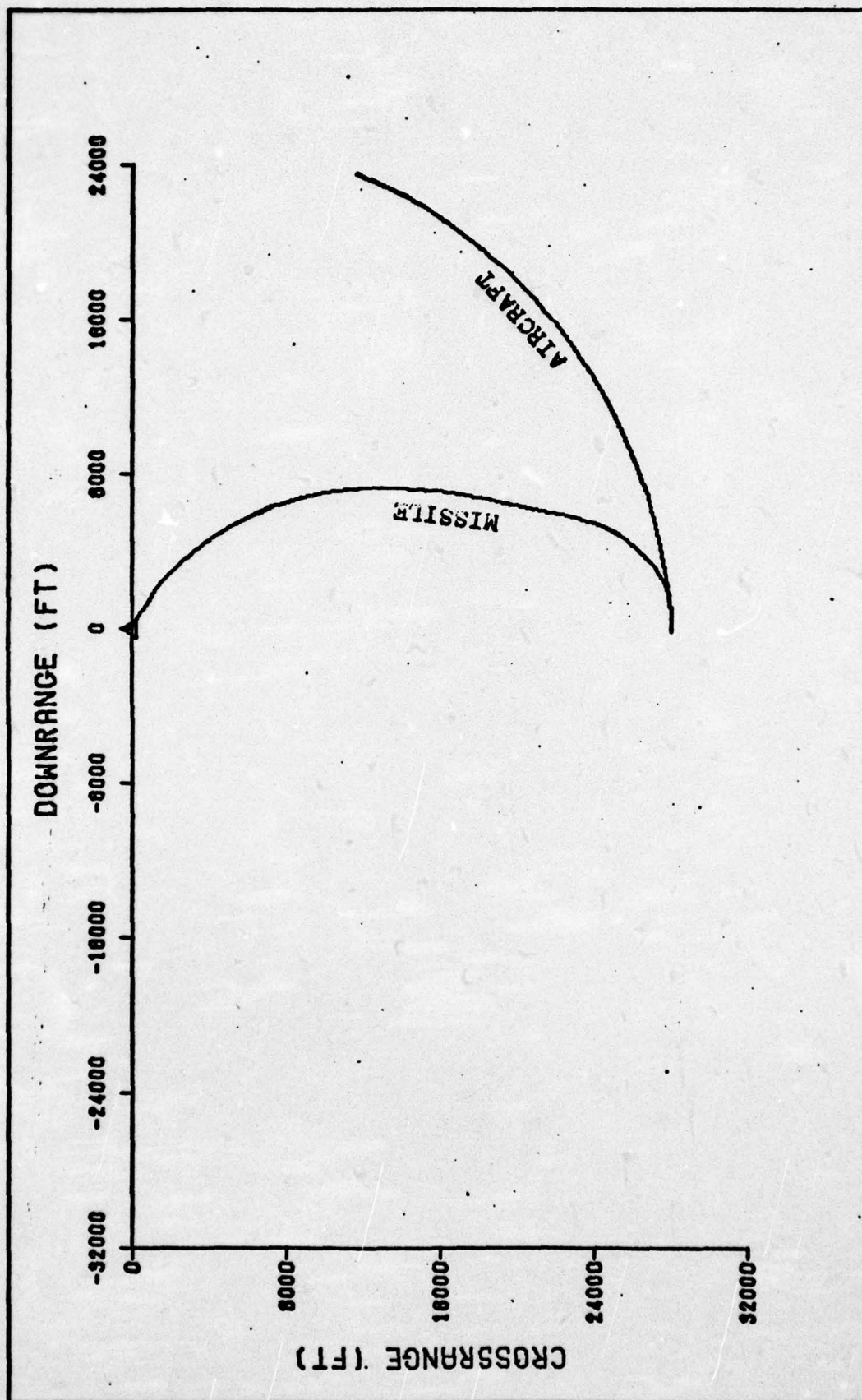


Fig. 86 Trajectory Plan View - 90°, 5,000 ft Launch

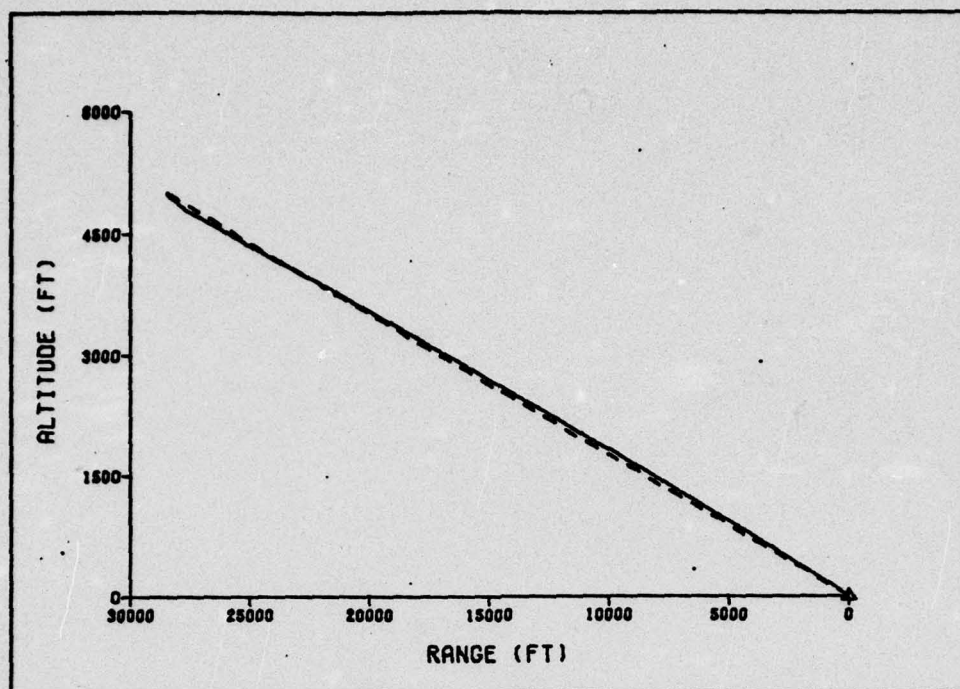


Fig. 87 Trajectory Vertical Profile - 90°, 5,000 ft Launch

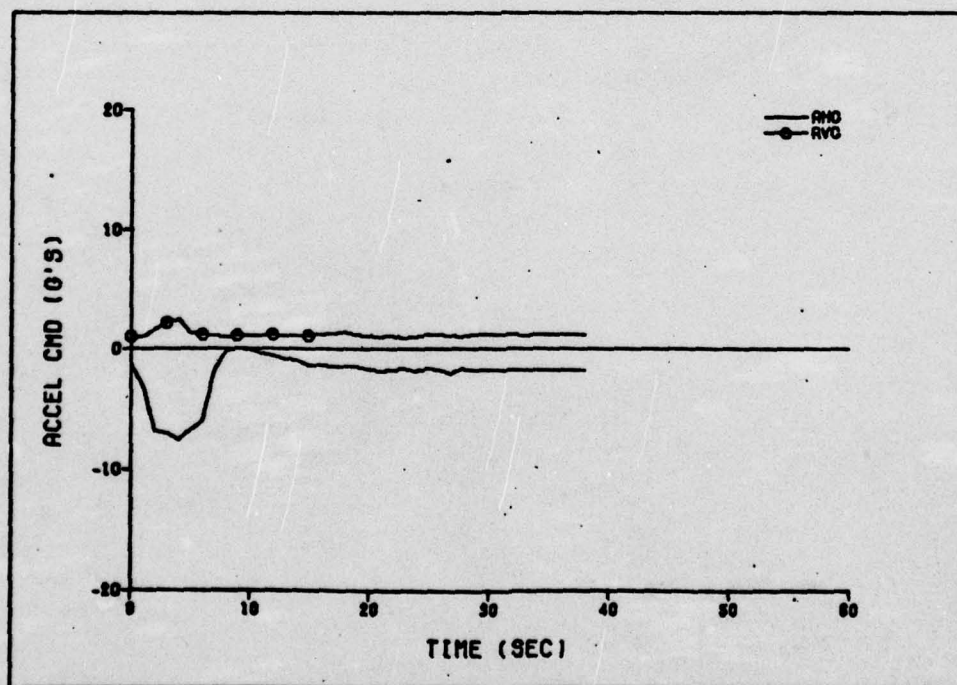


Fig. 88 Acceleration Commands - 90°, 5,000 ft Launch

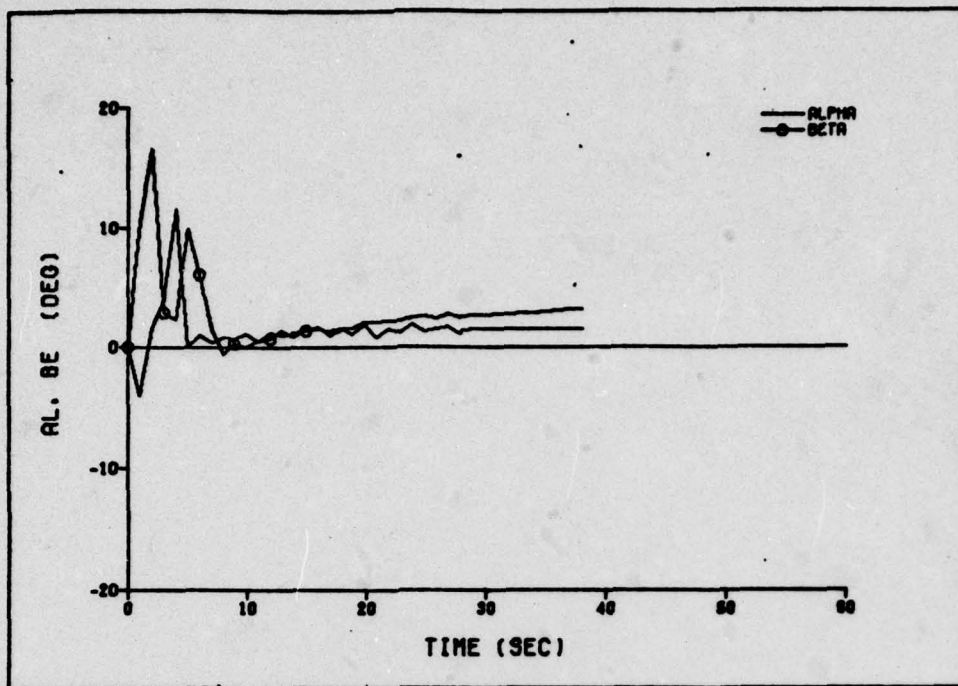


Fig. 89 Alpha and Beta - 90°, 5,000 ft Launch

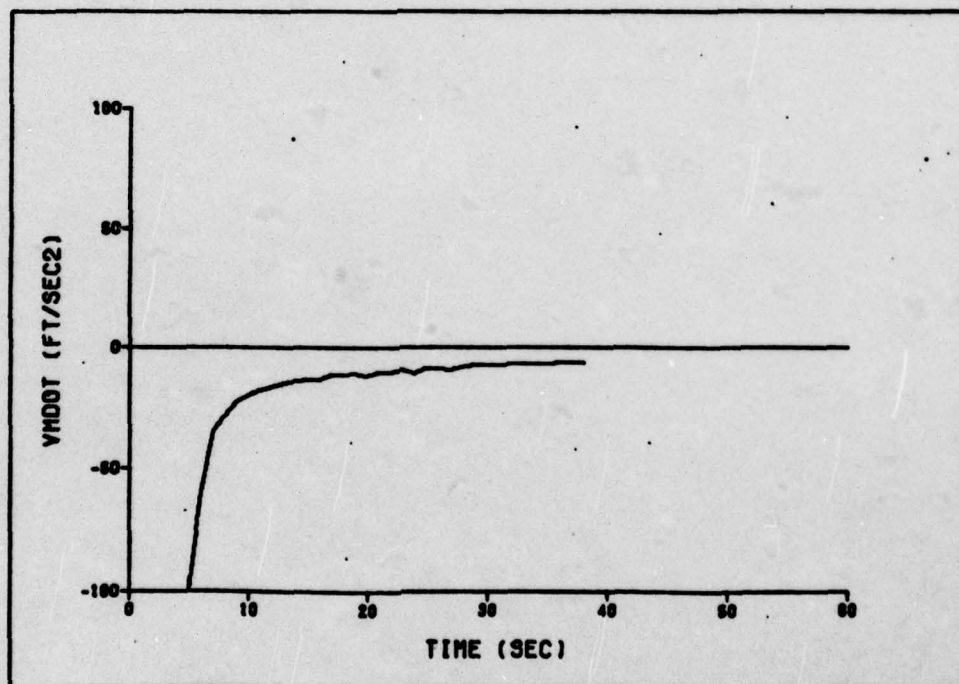


Fig. 90 Deceleration Due to Aerodynamic Drag - 90°, 5,000 ft Launch

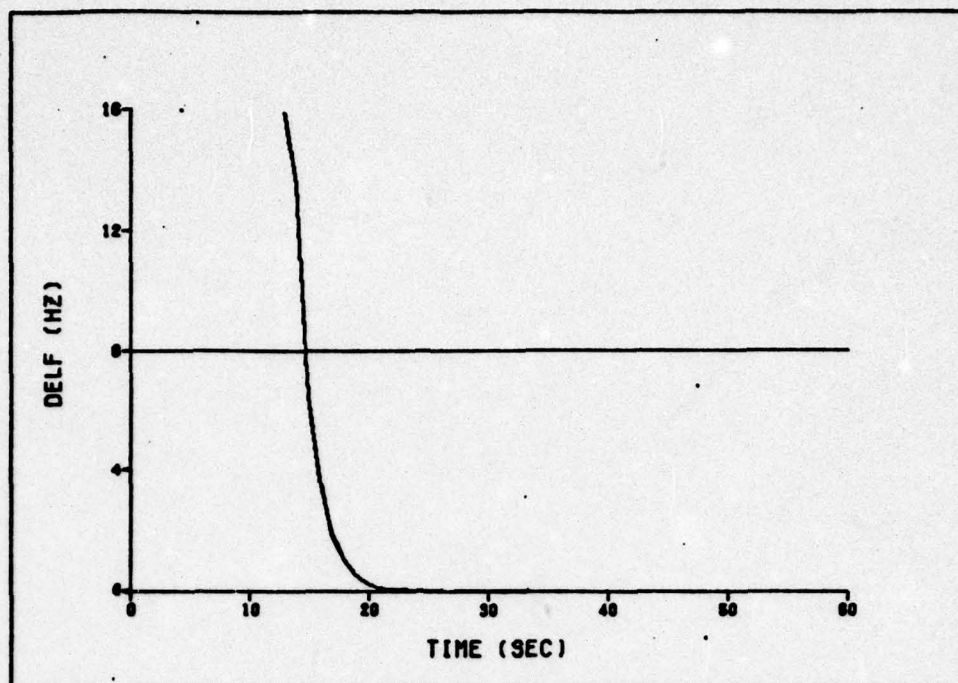


Fig. 91 Retrmitted Frequency Error - 90°, 5,000 ft Launch

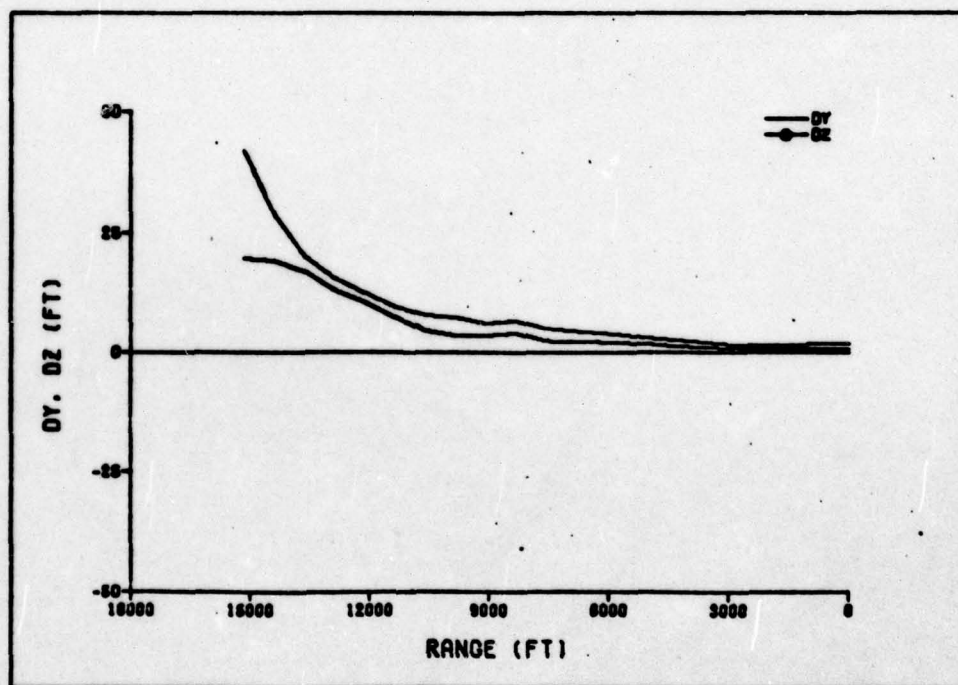


Fig. 92 Missile Distance Errors, Terminal Phase - 90°, 5,000 ft Launch

Appendix E

Guidance Algorithms Which Were Rejected

Several horizontal guidance algorithms were tested in the Retran simulation. Initially, the study concentrated on launches from low initial squint angles of 15° to 30° (squint angle is the angular displacement of the line of sight from the aircraft velocity vector). Later, emphasis was shifted to medium to high initial squint angles of 30° to 90° . The algorithms discussed in section II were found to yield the largest usable launch envelope and the longest maximum launch ranges. The algorithms presented here generally resulted in poorer missile performance.

Straight Ahead Intercept

For launches at low initial squint angles, the missile tends to fall behind the line of sight in the early portion of the flight. Therefore, the first algorithm tested commanded no horizontal acceleration until line of sight intercept, then commanded a turn to place the missile on the line of sight. A typical trajectory is illustrated in Fig. 93.

This algorithm required determination of the point at which to start the intercept turn. Determination of this point is complicated by the deceleration of the missile during the turn; also, for a randomly maneuvering aircraft, the rotation rate of the line of sight during the time of the turn cannot be accurately predicted at the start of the turn. To make a precise intercept turn would require varying the acceleration commands throughout the turn, and the necessary algorithm

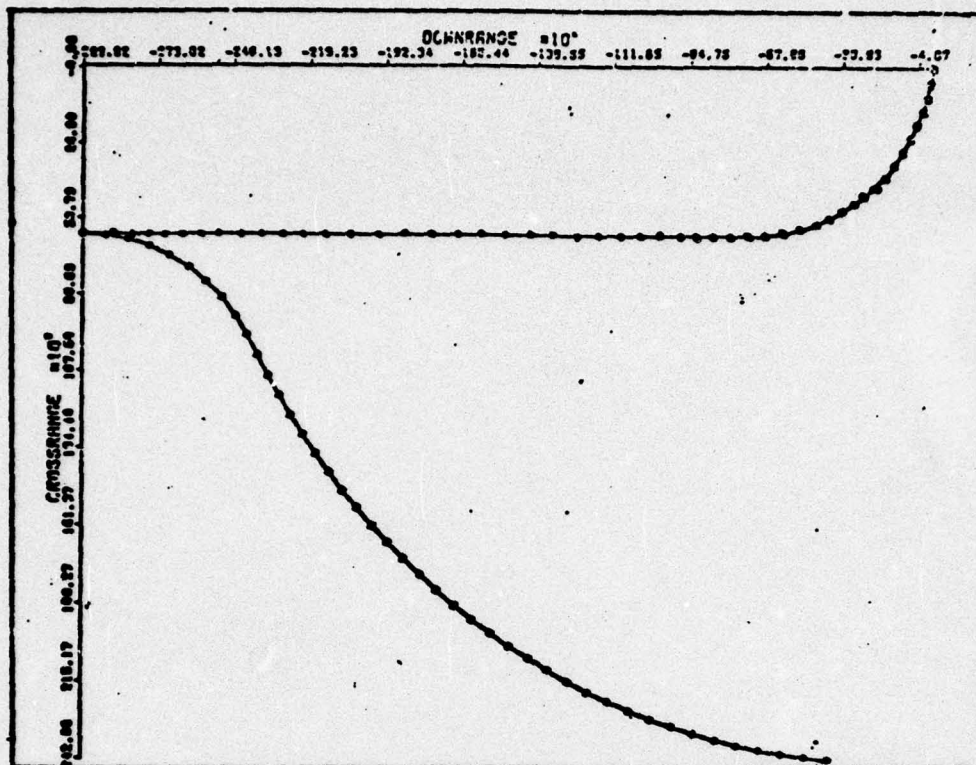


Fig. 93 Trajectory Plan View - Straight Ahead Intercept Algorithm

would be very complex. In order to keep the algorithm relatively simple, a constant-g intercept turn was commanded. A conservative estimation of the start turn point was incorporated which would allow completion of the turn with the missile slightly ahead of the line of sight. The rotation of the line of sight toward the missile would then result in a successful intercept.

The required turning angle for intercept is

$$\Delta\psi = \psi_{LOS_{ST}} + \omega_z \cdot \Delta t_T - \psi_{ST} - \psi_B \quad (103)$$

$$= \dot{\psi} \cdot \Delta t_T \quad (104)$$

where $\psi_{LOS_{ST}}$ - heading of the line of sight at start turn
 ω_Z - average rotation rate of the line of sight
 Δt_T - time required for turn
 ψ_{ST} - missile heading at start turn
 ψ_B - arbitrary heading bias at completion of turn
 (missile heading must be offset slightly from
 line of sight in order for missile to track
 the rotating line of sight)
 $\dot{\psi}$ - average missile turn rate

The missile turning rate for a constant g turn is

$$\dot{\psi} = \frac{g}{V_M} a_h \quad (105)$$

where V_M is missile airspeed in the turn and a_h is the commanded acceleration. Assuming constant rotation of the line of sight and assuming that the average turn rate will be approximately equal to the initial turn rate (this is conservative, since the turn rate will increase as airspeed decreases in the turn), the time required for the turn is

$$\Delta t_T = \frac{\psi_{LOS_{ST}} - \psi_{ST} - \psi_B}{\dot{\psi} - \omega_Z} \quad (106)$$

In order to start the turn so that the missile will complete the turn on or beyond the line of sight, the missile must have sufficient overtake speed on the line of sight to close the distance to the line of sight during the turn. Here it was estimated that the average overtake speed would equal half of the initial missile velocity

normal to the line of sight. The approximate arc distance normal to the line of sight which must be covered during the turn is

$$L = \Delta Y_{ST} + \omega_Z \cdot R_{MT_{ST}} \quad (107)$$

where ΔY_{ST} is the missile distance normal to the line of sight at start turn and $R_{MT_{ST}}$ is the missile-to-target range at start turn (again, this is conservative because R_{MT} will decrease during the turn). Therefore, the required overtake velocity at the start turn point is

$$\Delta \dot{Y} = \frac{2}{\Delta t_T} (\Delta Y_{ST} + \omega_Z \cdot R_{MT_{ST}}) \quad (108)$$

In this algorithm, the interception turn was initiated when $\Delta \dot{Y}$ was sufficient to insure turn completion on or beyond the line of sight. A constant 4g turn was commanded; however, if during the turn the current $\Delta \dot{Y}$ was insufficient to cover the distance remaining to turn completion, no acceleration was commanded and the missile continued on present heading until overtake was again sufficient to continue the turn. A command to track algorithm similar to the one discussed in section II was employed for line of sight tracking once tracking heading was reached.

This algorithm proved to have only limited interception capability. Successful intercepts were made from an initial squint angle of 20°; however, attempted intercepts from larger squint angles resulted in the missile completing the turn behind the line of sight, with subsequent high-g maneuvering required to catch the line of sight. Even when interception was successful, tracking time on the line of

sight was insufficient and terminal airspeed was low due to the drag encountered during the interception turn.

Turn to Initial Intercept Heading

To correct the insufficient tracking time of the straight ahead intercept, the algorithm was modified to initially turn the missile to a predetermined intercept heading. This heading was computed as an empirical function of initial squint angle and range from the target, and was chosen to insure interception of the line of sight at ranges greater than 5000 ft slant range from the target. (Note, at this phase of the study, lower terminal airspeeds and shorter tracking times were being considered than were finally chosen as the minimums required). The initial acceleration command was computed so as to produce a turning rate equal in magnitude to the angular error between the computed heading ψ_I and the missile heading ψ . This turning rate is

$$\dot{\psi} = \frac{a_h (32.2)}{V_M} = (\psi_I - \psi) \quad (109)$$

The required acceleration command is therefore

$$a_h = \frac{V_M}{32.2} (\psi_I - \psi) \quad (110)$$

A typical trajectory resulting from this algorithm is shown in Fig. 94. Basically, this algorithm had the same deficiencies encountered with the straight ahead intercept, except that tracking time was increased.

AD-A034 941

AIR FORCE INST OF TECH WRIGHT-PATTERSON AFB OHIO SCH--ETC F/G 17/9
PERFORMANCE OF AN AIR-TO-GROUND MISSILE EMPLOYING SAR-RETRAN GU--ETC(U)
DEC 76 E H JESSUP
6AE/MC/76D-6

UNCLASSIFIED

NL

3 OF 3

AD
A034941



END

DATE
FILMED
3-77

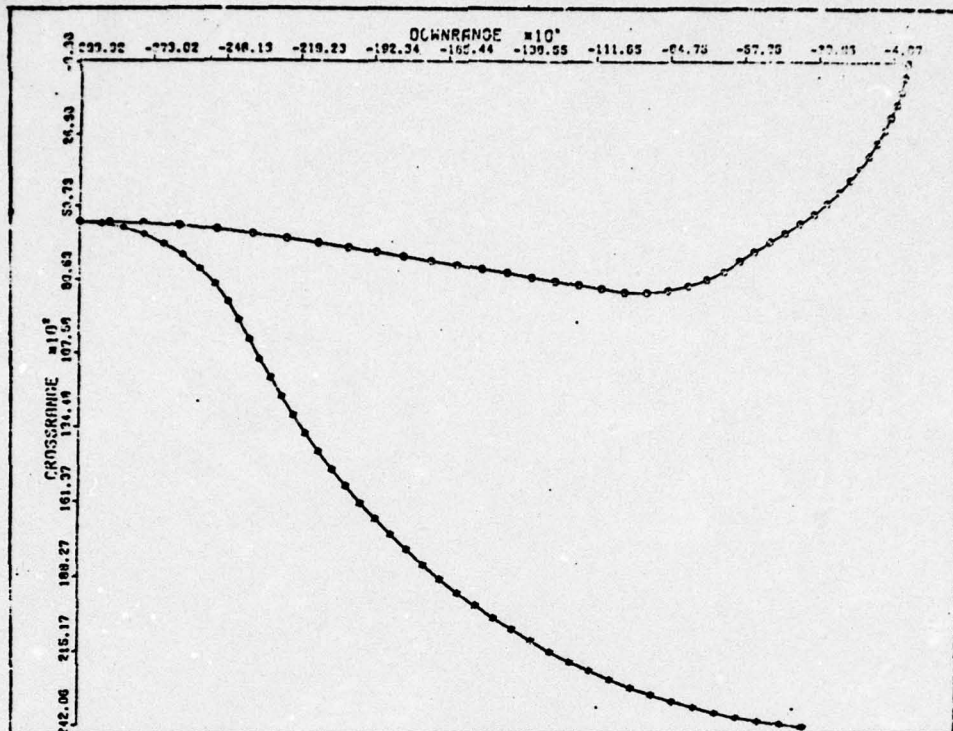


Fig. 94 Trajectory Plan View - Trun to Initial Intercept Heading Algorithm

Command to Fixed Intercept Angle

In an attempt to avoid the high turning accelerations required by both of the previous algorithms, the missile was commanded to maintain a constant 30° intercept angle to the line of sight. The commanded acceleration was calculated proportional to the square root of the angular difference between the heading of the line of sight and the missile heading. A variable gain was employed, which increased gain as the square root of missile to target range decreased. The algorithm was

$$a_h = \frac{9000.}{\text{Range}} (\psi_{\text{LOS}} - \psi) \quad (111)$$

when the angular difference was less than or equal to 30° , no acceleration was commanded.

At $t_{tg} \leq 10$ seconds, the algorithm reverted to command-to-track. This algorithm proved inferior to the initial heading algorithm for low squint angle launches, as the reversion to command to track produced a sharply turning trajectory as illustrated in Fig. 95. However, the algorithm gave superior results at medium initial squint angles, with lower terminal airspeed and increased tracking time. A typical trajectory for a medium squint angle launch is shown in Fig. 96. It was observed that the trajectories produced by this algorithm were similar to those which could be obtained by utilizing the command-to-track algorithm throughout the flight.

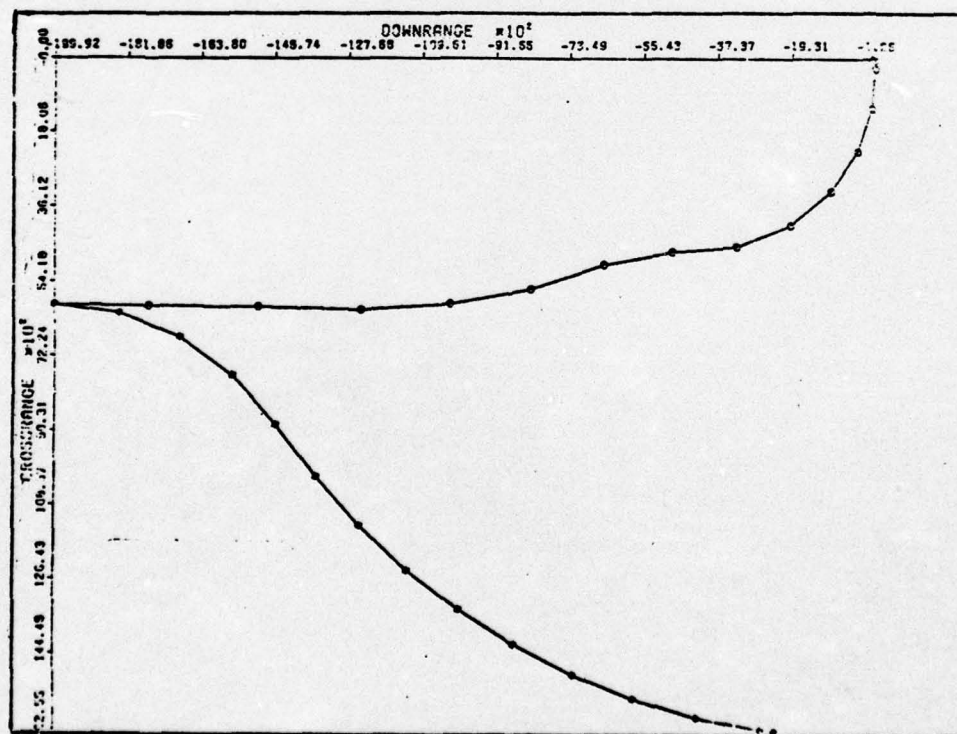


Fig. 95 Trajectory Plan View - Command to Fixed Intercept Angle Algorithm, Low Squint Angle Launch

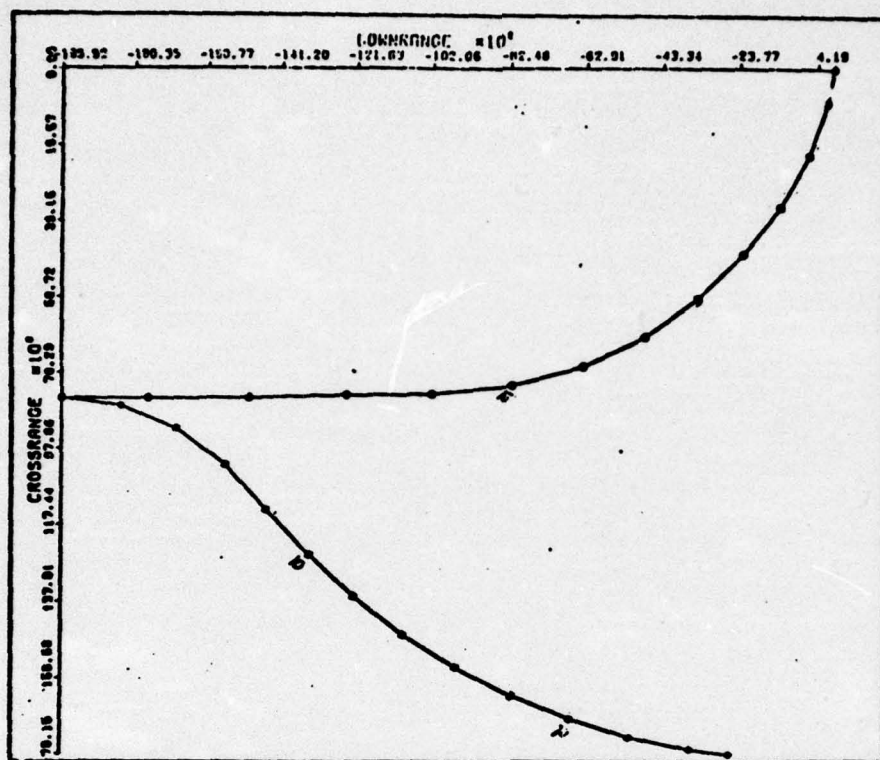


Fig. 96 Trajectory Plan View - Command to Fixed Intercept Angle Algorithm, Medium Squint Angle Launch

Command to Track Throughout Flight

The trend in missile performance during the development of the previous algorithms indicated that gradual turning maneuvers were requisite for maximum range, even at the expense of increased flight distance. Preliminary studies by the Air Force Avionics Laboratory indicated that such gradual turning trajectories could be obtained by employing the command to track algorithm throughout the flight. This algorithm was essentially the same as the horizontal command to track algorithm discussed in section II.

Satisfactory trajectories were obtained for low to medium initial squint angles, with fairly low g (<4) maneuvering throughout. Two resulting trajectories are presented in Figs. 97 and 98. Terminal

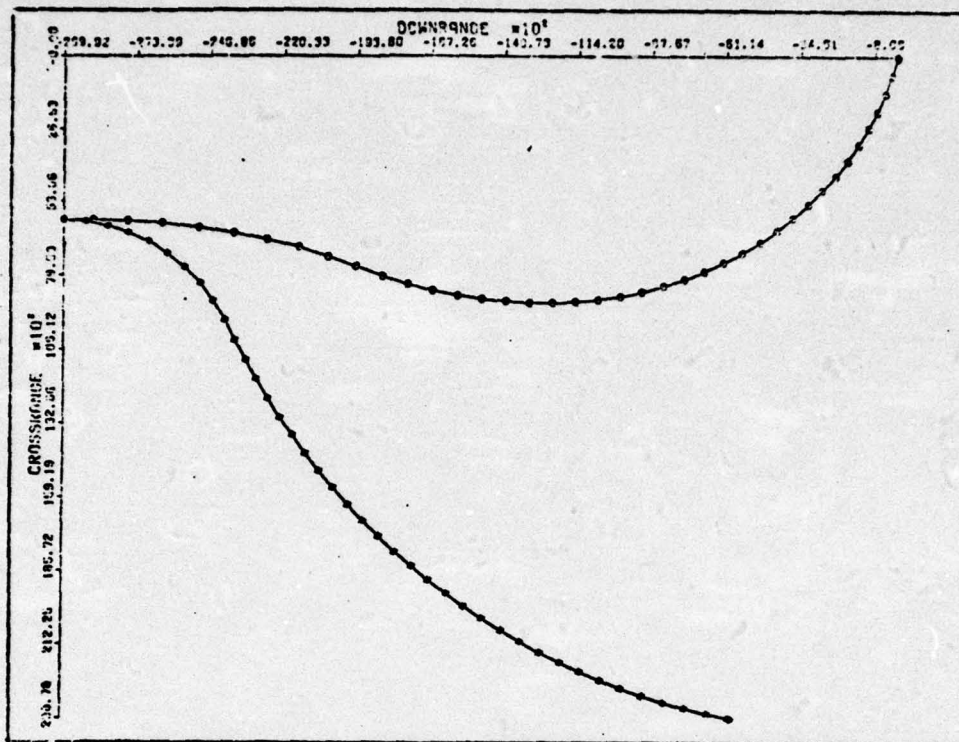


Fig. 97 Trajectory Plan View - Command to Track Algorithm,
Low Squint Angle Launch

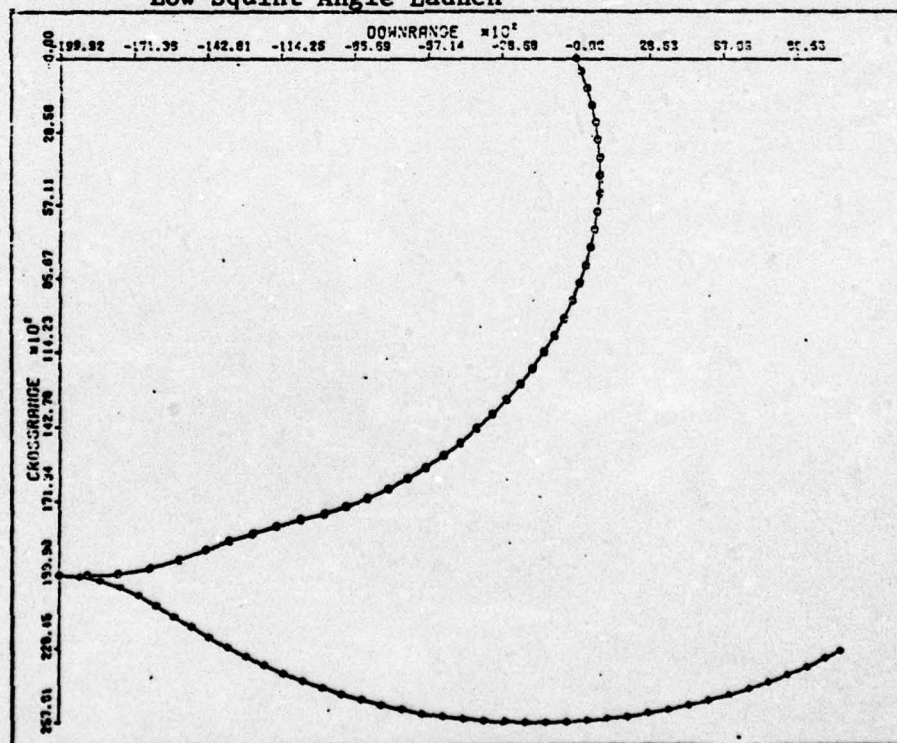


Fig. 98 Trajectory Plan View - Command to Track Algorithms,
Medium Squint Angle Launch

airspeed was higher than obtained with the previous algorithms and tracking time was sufficient. However, at initial squint angles greater than 45° the missile was initially heading away from the line of sight, resulting in large g turns (6-8 g's) to bring the missile back toward the line of sight. Even with the large accelerations commanded, sizable distance errors developed during the initial turn; consequently, large intercept angles coming back to the line of sight were commanded. This resulted in high g maneuvering (10-15 g's) to complete the interception turn onto the line of sight. The trajectory for a 60° angle launch is shown in Fig. 99. For initial squint angles greater than 60° , the required maneuvering sometimes exceeded missile capability and intercepts were not accomplished.

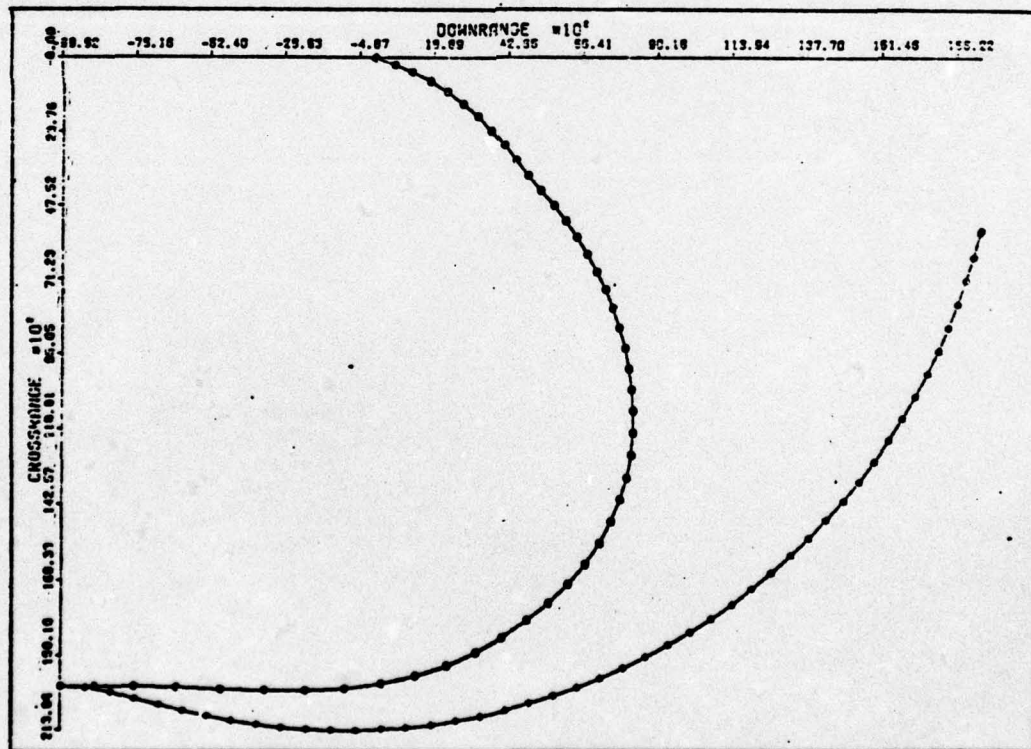


Fig. 99 Trajectory Plan View - Command to Track Algorithm, High Squint Angle Launch

In order to achieve satisfactory performance from high initial squint angles, the command to heading algorithm discussed in section II was added.

Appendix F

Program Optraj Output Listings

T 9.5	V4	131.25	K	-58074.	Y	59325.	Z	-32044.	JH	1300.99	OZ	103.77	AH	-.50	AV	.19
T 9.0	V4	133.33	K	-57307.	Y	59255.	Z	-31041.	JH	2005.11	OZ	130.93	AH	-.50	AV	.10
T 7.5	V4	1327.92	K	-56706.	Y	59180.	Z	-31540.	JH	2106.92	OZ	156.64	AH	-.50	AV	.17
T 12.9	V4	1316.84	K	-56031.	Y	59101.	Z	-31142.	JH	2206.48	OZ	180.97	AH	-.50	AV	.17
T 12.5	V4	1335.98	K	-55360.	Y	59013.	Z	-31247.	JH	2303.02	OZ	203.95	AH	-.50	AV	.15
T 11.0	V4	1395.25	K	-54593.	Y	58933.	Z	-31034.	JH	2398.94	OZ	225.65	AH	-.51	AV	.15
T 11.5	V4	1344.57	K	-54036.	Y	58844.	Z	-30854.	JH	2491.01	OZ	245.07	AH	-.51	AV	.15
T 12.0	V4	1373.09	K	-53302.	Y	58752.	Z	-30675.	JH	2582.41	OZ	265.25	AH	-.51	AV	.15
T 12.3	V4	1353.14	K	-52733.	Y	58657.	Z	-30430.	JH	2670.66	OZ	283.22	AH	-.51	AV	.14
T 12.0	V4	1352.31	K	-52090.	Y	58558.	Z	-30305.	JH	2756.51	OZ	300.00	AH	-.51	AV	.14
T 12.5	V4	1341.37	K	-51452.	Y	58455.	Z	-30125.	JH	2839.99	OZ	315.61	AH	-.51	AV	.14
T 14.0	V4	1339.30	K	-50820.	Y	58351.	Z	-29346.	JH	2920.71	OZ	330.07	AH	-.51	AV	.14
T 12.5	V4	1313.10	K	-50194.	Y	58243.	Z	-29770.	JH	2998.91	OZ	343.39	AH	-.52	AV	.13
T 15.0	V4	1307.76	K	-49573.	Y	58132.	Z	-29535.	JH	3074.40	OZ	355.60	AH	-.52	AV	.13
T 15.5	V4	1295.30	K	-48959.	Y	58019.	Z	-29423.	JH	3147.13	OZ	355.71	AH	-.52	AV	.13
T 14.0	V4	1234.74	K	-48350.	Y	57901.	Z	-29254.	JH	3217.01	OZ	375.73	AH	-.52	AV	.13
T 14.5	V4	1273.09	K	-47748.	Y	57781.	Z	-29085.	JH	3284.00	OZ	395.59	AH	-.52	AV	.13
T 17.0	V4	1231.39	K	-47152.	Y	57599.	Z	-28921.	JH	3348.04	OZ	393.61	AH	-.52	AV	.12
T 17.5	V4	1249.67	K	-46562.	Y	57533.	Z	-28758.	JH	3409.09	OZ	400.50	AH	-.52	AV	.12
T 14.0	V4	1237.97	K	-45978.	Y	57404.	Z	-28537.	JH	3457.13	OZ	405.37	AH	-.52	AV	.12
T 14.5	V4	1225.32	K	-45401.	Y	57273.	Z	-28439.	JH	3522.14	OZ	411.25	AH	-.52	AV	.12
T 12.0	V4	1214.76	K	-44829.	Y	57133.	Z	-28232.	JH	3574.13	OZ	415.19	AH	-.53	AV	.11
T 17.5	V4	1233.34	K	-44264.	Y	57002.	Z	-28127.	JH	3623.10	OZ	414.15	AH	-.53	AV	.11
T 22.0	V4	1132.08	K	-43705.	Y	56863.	Z	-27374.	JH	3669.08	OZ	420.21	AH	-.53	AV	.11
T 21.5	V4	1141.02	K	-43152.	Y	56721.	Z	-27424.	JH	3712.09	OZ	421.36	AH	-.53	AV	.10
T 21.0	V4	1179.18	K	-42605.	Y	56575.	Z	-27675.	JH	3752.18	OZ	421.63	AH	-.53	AV	.10

T 21.5	V4	1199.60	K	-42064.	Y	55429.	Z	-27920.	JH	3789.41	OZ	421.05	AM	-.53	AV	.10
T 22.0	V4	1199.29	K	-41529.	Y	55279.	Z	-27333.	J4	3823.83	OZ	419.64	AM	-.53	AV	.09
T 22.5	V4	1199.27	K	-40999.	Y	56126.	Z	-27239.	J4	3855.49	OZ	417.41	AM	-.53	AV	.09
T 23.0	V4	1129.55	K	-40475.	Y	55970.	Z	-27038.	JH	3884.48	OZ	414.39	AM	-.53	AV	.09
T 23.5	V4	1120.14	K	-39956.	Y	55812.	Z	-26937.	J4	3310.86	OZ	410.59	AM	-.53	AV	.09
T 24.0	V4	1111.04	K	-39443.	Y	55652.	Z	-26819.	JH	1934.71	OZ	405.00	AM	-.53	AV	.09
T 24.5	V4	1102.25	K	-38935.	Y	55483.	Z	-26582.	J4	3956.10	OZ	400.63	AM	-.53	AV	.09
T 25.0	V4	1093.76	K	-38431.	Y	55323.	Z	-26546.	J4	3975.10	OZ	394.52	AM	-.53	AV	.09
T 25.5	V4	1095.57	K	-37933.	Y	55154.	Z	-26412.	JH	3991.00	OZ	387.59	AM	-.53	AV	.09
T 26.0	V4	1077.67	K	-37440.	Y	54983.	Z	-26279.	JH	4006.28	OZ	379.82	AM	-.53	AV	.09
T 26.5	V4	1070.05	K	-36951.	Y	54805.	Z	-26148.	JH	4018.60	OZ	371.13	AM	-.53	AV	.10
T 27.0	V4	1052.69	K	-36467.	Y	54532.	Z	-26018.	J4	4028.86	OZ	361.42	AM	-.53	AV	.11
T 27.5	V4	1055.55	K	-35988.	Y	54452.	Z	-25930.	J4	4037.13	OZ	350.45	AM	-.53	AV	.14
T 28.0	V4	1048.59	K	-35513.	Y	54270.	Z	-25754.	JH	4043.51	OZ	337.90	AM	-.53	AV	.18
T 28.5	V4	1041.70	K	-35042.	Y	54085.	Z	-25540.	J4	4048.12	OZ	322.93	AM	-.53	AV	.29
T 29.0	V4	1034.55	K	-34575.	Y	53897.	Z	-25322.	JH	4051.13	OZ	303.64	AM	-.53	AV	.53
T 29.5	V4	1023.40	K	-34111.	Y	53705.	Z	-25110.	J4	4052.72	OZ	259.24	AM	-.53	AV	1.90
T 30.0	V4	1005.92	K	-33666.	Y	53513.	Z	-25278.	J4	4043.74	OZ	275.64	AM	-.53	AV	-5.12
T 30.5	V4	974.48	K	-33228.	Y	53330.	Z	-25130.	JH	4031.30	OZ	241.99	AM	-.52	AV	5.27
T 31.0	V4	954.01	K	-32902.	Y	53143.	Z	-25053.	JH	4011.68	OZ	240.31	AM	-.52	AV	-3.97
T 31.5	V4	940.06	K	-32396.	Y	52960.	Z	-24830.	JH	3980.05	OZ	279.14	AM	-.52	AV	-5.16
T 32.0	V4	910.05	K	-31997.	Y	52776.	Z	-24773.	J4	3945.49	OZ	272.71	AM	-.52	AV	59.71
T 32.5	V4	909.20	K	-31602.	Y	52590.	Z	-24547.	J4	3308.53	OZ	275.92	AM	-.52	AV	-1.34
T 33.0	V4	908.51	K	-31210.	Y	52400.	Z	-24517.	JH	3870.41	OZ	283.54	AM	-.52	AV	-3.34
T 33.5	V4	906.86	K	-30920.	Y	52207.	Z	-24330.	JH	3931.69	OZ	287.25	AM	-.52	AV	.31
T 34.0	V4	904.85	K	-30431.	Y	52010.	Z	-24237.	J4	3792.45	OZ	236.97	AM	-.52	AV	.44
T 34.5	V4	903.03	K	-30045.	Y	51810.	Z	-24146.	JH	3752.62	OZ	283.65	AM	-.51	AV	.33

T 35.0	J4	331.66	K	-29861.	Y	51807.	Z	-24027.	J4	3715.00	OZ	270.39	AM	-0.51	AV	-0.19
T 35.5	J4	999.99	K	-29280.	Y	51800.	Z	-23908.	J4	3570.79	OZ	271.85	AM	-0.51	AV	-0.11
T 36.0	J4	999.64	K	-28900.	Y	51190.	Z	-23790.	J4	3526.74	OZ	254.50	AM	-0.51	AV	-0.05
T 36.5	J4	937.34	K	-28523.	Y	50976.	Z	-23573.	J4	3585.91	OZ	256.52	AM	-0.51	AV	-0.03
T 37.0	J4	935.09	K	-28149.	Y	50760.	Z	-23335.	J4	3542.30	OZ	249.10	AM	-0.50	AV	-0.01
T 37.5	J4	935.88	K	-27777.	Y	50540.	Z	-23418.	O4	3497.93	OZ	239.33	AM	-0.50	AV	-0.00
T 38.0	J4	933.72	K	-27408.	Y	50319.	Z	-23320.	J4	3452.81	OZ	230.30	AM	-0.50	AV	-0.01
T 38.5	J4	932.59	K	-27042.	Y	50092.	Z	-23203.	J4	3406.94	OZ	221.08	AM	-0.50	AV	-0.02
T 39.0	J4	931.49	K	-26679.	Y	49867.	Z	-23035.	J4	3350.34	OZ	211.71	AM	-0.50	AV	-0.02
T 39.5	J4	930.43	K	-26316.	Y	49632.	Z	-22957.	J4	3313.03	OZ	202.25	AM	-0.49	AV	-0.03
T 40.0	J4	929.41	K	-25957.	Y	49397.	Z	-22849.	J4	3265.01	OZ	192.72	AM	-0.49	AV	-0.03
T 40.5	J4	928.41	K	-25601.	Y	49159.	Z	-22731.	J4	3216.31	OZ	183.13	AM	-0.49	AV	-0.03
T 41.0	J4	897.45	K	-25249.	Y	48919.	Z	-22612.	J4	3166.94	OZ	173.58	AM	-0.49	AV	-0.04
T 41.5	J4	935.52	K	-24897.	Y	48675.	Z	-22433.	J4	3116.91	OZ	164.03	AM	-0.49	AV	-0.04
T 42.0	J4	935.62	K	-24546.	Y	48430.	Z	-22374.	J4	3066.25	OZ	154.52	AM	-0.49	AV	-0.04
T 42.5	J4	934.74	K	-24203.	Y	48181.	Z	-22234.	J4	3014.96	OZ	145.05	AM	-0.49	AV	-0.04
T 43.0	J4	933.90	K	-23860.	Y	47929.	Z	-22134.	J4	2963.07	OZ	135.67	AM	-0.49	AV	-0.04
T 43.5	J4	933.08	K	-23519.	Y	47675.	Z	-22014.	J4	2910.59	OZ	125.37	AM	-0.49	AV	-0.05
T 44.0	J4	932.30	K	-23182.	Y	47418.	Z	-21934.	J4	2857.54	OZ	117.17	AM	-0.49	AV	-0.05
T 44.5	J4	931.53	K	-22847.	Y	47159.	Z	-21773.	J4	2803.93	OZ	109.07	AM	-0.47	AV	-0.05
T 45.0	J4	893.80	K	-22515.	Y	46895.	Z	-21651.	J4	2749.78	OZ	99.09	AM	-0.47	AV	-0.05
T 45.5	J4	950.09	K	-22195.	Y	46531.	Z	-21530.	J4	2595.10	OZ	30.24	AM	-0.47	AV	-0.05
T 46.0	J4	979.40	K	-21858.	Y	46363.	Z	-21407.	J4	2539.92	OZ	81.53	AM	-0.47	AV	-0.05
T 46.5	J4	978.74	K	-21534.	Y	46093.	Z	-21235.	J4	2584.25	OZ	72.95	AM	-0.47	AV	-0.05
T 47.0	J4	976.10	K	-21213.	Y	45820.	Z	-21152.	J4	2529.11	OZ	54.53	AM	-0.47	AV	-0.05
T 47.5	J4	977.48	K	-20894.	Y	45543.	Z	-21039.	J4	2471.51	OZ	55.23	AM	-0.45	AV	-0.05
T 48.0	J4	876.89	K	-20579.	Y	45267.	Z	-20915.	J4	2414.46	OZ	48.14	AM	-0.45	AV	-0.05

T 43.5	V4	976.31	K	-20265.	Y	54987.	Z	-20731.	JM	2356.99	OZ	60.19	AM	-0.43	AV	-0.05
T 43.0	V4	975.75	K	-19954.	Y	54705.	Z	-20655.	JM	2299.11	OZ	32.41	AM	-0.43	AV	-0.05
T 42.5	V4	975.22	K	-19647.	Y	54420.	Z	-20542.	JM	2240.04	OZ	24.73	AM	-0.45	AV	-0.05
T 53.0	V4	974.71	K	-19342.	Y	54132.	Z	-20416.	JM	2182.18	OZ	17.35	AM	-0.45	AV	-0.05
T 52.5	V4	974.21	K	-19039.	Y	53843.	Z	-20231.	JM	2123.17	OZ	10.09	AM	-0.43	AV	-0.05
T 51.0	V4	973.73	K	-18740.	Y	53551.	Z	-20134.	JM	2063.81	OZ	3.00	AM	-0.43	AV	-0.05
T 51.5	V4	973.27	K	-18443.	Y	53257.	Z	-20038.	JM	2004.11	OZ	-3.91	AM	-0.43	AV	-0.05
T 52.0	V4	972.83	K	-18149.	Y	52960.	Z	-19941.	JM	1944.10	OZ	-10.53	AM	-0.45	AV	-0.05
T 52.5	V4	972.40	K	-17856.	Y	52661.	Z	-19734.	JM	1883.79	OZ	-17.19	AM	-0.45	AV	-0.05
T 53.0	V4	971.99	K	-17569.	Y	52360.	Z	-19536.	JM	1823.19	OZ	-23.54	AM	-0.44	AV	-0.05
T 53.5	V4	971.59	K	-17284.	Y	52057.	Z	-19339.	JM	1752.33	OZ	-23.72	AM	-0.44	AV	-0.05
T 54.0	V4	971.20	K	-17001.	Y	51752.	Z	-19141.	JM	1701.20	OZ	-35.72	AM	-0.44	AV	-0.05
T 54.5	V4	970.84	K	-16721.	Y	51445.	Z	-18941.	JM	1639.84	OZ	-41.53	AM	-0.44	AV	-0.05
T 55.0	V4	970.48	K	-16443.	Y	51135.	Z	-18730.	JM	1578.25	OZ	-47.15	AM	-0.44	AV	-0.05
T 55.5	V4	970.14	K	-16169.	Y	50824.	Z	-18519.	JM	1516.45	OZ	-52.61	AM	-0.44	AV	-0.04
T 56.0	V4	969.81	K	-15897.	Y	50510.	Z	-18311.	JM	1454.45	OZ	-57.87	AM	-0.43	AV	-0.04
T 56.5	V4	969.49	K	-15528.	Y	50195.	Z	-18100.	JM	1392.27	OZ	-52.93	AM	-0.43	AV	-0.04
T 57.0	V4	969.16	K	-15262.	Y	49877.	Z	-17889.	JM	1329.92	OZ	-57.83	AM	-0.43	AV	-0.04
T 57.5	V4	968.88	K	-15098.	Y	49557.	Z	-17678.	JM	1267.42	OZ	-72.58	AM	-0.43	AV	-0.04
T 58.0	V4	968.59	K	-14838.	Y	49236.	Z	-17467.	JM	1204.72	OZ	-77.12	AM	-0.43	AV	-0.04
T 58.5	V4	968.31	K	-14580.	Y	48913.	Z	-17256.	JM	1142.00	OZ	-81.49	AM	-0.43	AV	-0.04
T 59.0	V4	968.04	K	-14323.	Y	48587.	Z	-17045.	JM	1079.12	OZ	-85.59	AM	-0.42	AV	-0.04
T 59.5	V4	967.76	K	-14072.	Y	48260.	Z	-16834.	JM	1016.14	OZ	-89.59	AM	-0.42	AV	-0.04
T 60.0	V4	967.53	K	-13823.	Y	47931.	Z	-16623.	JM	953.07	OZ	-93.54	AM	-0.42	AV	-0.04
T 60.5	V4	967.22	K	-13572.	Y	47604.	Z	-16412.	JM	890.30	OZ	-97.23	AM	-0.29	AV	-0.05
T 61.0	V4	966.91	K	-13321.	Y	47276.	Z	-16201.	JM	827.47	OZ	-99.88	AM	-0.01	AV	-0.10
T 61.5	V4	966.62	K	-13070.	Y	46949.	Z	-15990.	JM	764.67	OZ	-102.12	AM	-0.01	AV	-0.01
T 62.0	V4	966.31	K	-12819.	Y	46622.	Z	-15779.	JM	701.74	OZ	-103.80	AM	-0.02	AV	-0.04
T 62.5	V4	966.00	K	-12569.	Y	46295.	Z	-15568.	JM	638.84	OZ	-105.05	AM	-0.04	AV	-0.02

T 67.0	V4	956.64	C	-12319.	Y	43967.	Z	-17022.	DM	549.94	OZ	-105.87	AM	-.05	AV	-.02
T 67.5	V4	955.50	C	-12070.	Y	45640.	Z	-16837.	DM	508.81	OZ	-105.33	AM	-.03	AV	-.02
T 68.0	V4	956.35	C	-11922.	Y	45311.	Z	-16732.	DM	570.03	OZ	-105.45	AM	-.09	AV	-.02
T 68.5	V4	956.19	C	-11574.	Y	44983.	Z	-16617.	DM	533.47	OZ	-105.29	AM	-.11	AV	-.01
T 69.0	V4	955.02	C	-11327.	Y	44554.	Z	-16492.	DM	499.03	OZ	-105.86	AM	-.13	AV	-.01
T 69.5	V4	955.84	C	-11081.	Y	44324.	Z	-16346.	DM	466.60	OZ	-105.21	AM	-.14	AV	-.01
T 70.0	V4	955.66	C	-10936.	Y	43994.	Z	-16210.	DM	436.08	OZ	-104.35	AM	-.15	AV	-.01
T 70.5	V4	955.46	C	-10593.	Y	43563.	Z	-16074.	DM	407.35	OZ	-103.34	AM	-.17	AV	-.01
T 71.0	V4	955.25	C	-10350.	Y	43332.	Z	-15939.	DM	380.35	OZ	-102.18	AM	-.19	AV	-.00
T 71.5	V4	955.03	C	-10109.	Y	43001.	Z	-15803.	DM	354.97	OZ	-100.89	AM	-.19	AV	-.00
T 72.0	V4	954.81	C	-9869.	Y	42666.	Z	-15536.	DM	331.11	OZ	-99.50	AM	-.20	AV	-.00
T 72.5	V4	954.57	C	-9531.	Y	42332.	Z	-15330.	DM	308.71	OZ	-98.03	AM	-.21	AV	-.00
T 73.0	V4	954.32	C	-9395.	Y	41997.	Z	-15334.	DM	287.69	OZ	-95.53	AM	-.22	AV	-.00
T 73.5	V4	954.06	C	-9159.	Y	41662.	Z	-15255.	DM	267.96	OZ	-94.92	AM	-.23	AV	-.00
T 74.0	V4	953.79	C	-8926.	Y	41325.	Z	-15122.	DM	249.45	OZ	-93.30	AM	-.24	AV	-.00
T 74.5	V4	953.51	C	-8694.	Y	40987.	Z	-14999.	DM	232.11	OZ	-91.65	AM	-.25	AV	-.00
T 75.0	V4	953.22	C	-8465.	Y	40649.	Z	-14849.	DM	215.86	OZ	-90.01	AM	-.25	AV	-.00
T 75.5	V4	952.93	C	-8237.	Y	40309.	Z	-14713.	DM	200.64	OZ	-88.35	AM	-.27	AV	-.00
T 76.0	V4	952.62	C	-8010.	Y	39967.	Z	-14576.	DM	186.39	OZ	-86.71	AM	-.29	AV	-.00
T 76.5	V4	952.30	C	-7786.	Y	39625.	Z	-14440.	DM	173.06	OZ	-85.09	AM	-.29	AV	-.00
T 77.0	V4	951.98	C	-7564.	Y	39281.	Z	-14303.	DM	160.60	OZ	-83.47	AM	-.29	AV	-.00
T 77.5	V4	951.64	C	-7344.	Y	38937.	Z	-14157.	DM	148.94	OZ	-81.89	AM	-.30	AV	-.00
T 78.0	V4	951.30	C	-7127.	Y	38592.	Z	-14030.	DM	138.06	OZ	-80.34	AM	-.31	AV	-.00
T 78.5	V4	950.95	C	-6911.	Y	38245.	Z	-13894.	DM	127.89	OZ	-78.82	AM	-.31	AV	-.00
T 79.0	V4	950.59	C	-6698.	Y	37897.	Z	-13757.	DM	118.40	OZ	-77.34	AM	-.32	AV	-.00
T 79.5	V4	950.22	C	-6487.	Y	37544.	Z	-13521.	DM	109.54	OZ	-75.91	AM	-.32	AV	-.00
T 80.0	V4	950.05	C	-6278.	Y	37199.	Z	-13434.	DM	101.29	OZ	-74.51	AM	-.33	AV	-.00

74.5	74	959.47	€	-5072.	Y	35847.	Z	-13347.	34	93.59	OZ	-73.13	AM	-0.33	AV	.00
77.2	74	959.08	€	-5959.	Y	35494.	Z	-13211.	34	86.42	OZ	-71.04	AM	-0.34	AV	.00
77.3	74	958.69	€	-5566.	Y	35140.	Z	-13074.	34	79.74	OZ	-70.57	AM	-0.34	AV	.00
79.0	74	958.29	€	-5467.	Y	35795.	Z	-12938.	34	73.53	OZ	-59.35	AM	-0.34	AV	.00
79.5	74	957.88	€	-5271.	Y	35430.	Z	-12931.	34	57.74	OZ	-59.15	AM	-0.35	AV	.00
79.0	74	957.47	€	-5077.	Y	35073.	Z	-12634.	34	62.37	OZ	-57.02	AM	-0.35	AV	.00
79.3	74	957.05	€	-4885.	Y	34714.	Z	-12527.	34	57.37	OZ	-65.92	AM	-0.35	AV	.00
79.0	74	956.62	€	-4595.	Y	34355.	Z	-12331.	34	52.72	OZ	-64.65	AM	-0.35	AV	.00
79.5	74	956.20	€	-4510.	Y	33995.	Z	-12254.	34	48.41	OZ	-63.83	AM	-0.35	AV	.00
81.0	74	955.76	€	-4327.	Y	33633.	Z	-12117.	34	44.41	OZ	-52.84	AM	-0.35	AV	.00
81.5	74	955.32	€	-4146.	Y	33271.	Z	-11930.	34	40.69	OZ	-51.89	AM	-0.37	AV	.00
82.0	74	954.98	€	-3969.	Y	32907.	Z	-11843.	34	37.25	OZ	-60.95	AM	-0.37	AV	.00
82.5	74	954.43	€	-3793.	Y	32542.	Z	-11706.	34	34.05	OZ	-50.05	AM	-0.37	AV	.00
83.0	74	953.97	€	-3620.	Y	32176.	Z	-11559.	34	31.09	OZ	-59.19	AM	-0.37	AV	.00
83.5	74	953.52	€	-3451.	Y	31810.	Z	-11432.	34	29.35	OZ	-58.34	AM	-0.37	AV	.00
84.0	74	953.05	€	-3284.	Y	31442.	Z	-11235.	34	25.61	OZ	-57.52	AM	-0.38	AV	.00
84.5	74	952.59	€	-3120.	Y	31073.	Z	-11159.	34	23.46	OZ	-55.72	AM	-0.38	AV	.00
85.0	74	952.11	€	-2959.	Y	30703.	Z	-11020.	34	21.29	OZ	-55.93	AM	-0.38	AV	.00
85.3	74	951.64	€	-2800.	Y	30333.	Z	-10933.	34	19.27	OZ	-55.16	AM	-0.38	AV	.00
85.0	74	951.16	€	-2645.	Y	29961.	Z	-10746.	34	17.41	OZ	-54.41	AM	-0.38	AV	.00
85.5	74	950.68	€	-2492.	Y	29589.	Z	-10509.	34	15.69	OZ	-53.65	AM	-0.39	AV	.00
85.0	74	950.19	€	-2347.	Y	29215.	Z	-10471.	34	14.10	OZ	-52.93	AM	-0.39	AV	.00
85.5	74	949.69	€	-2196.	Y	28841.	Z	-10334.	34	12.63	OZ	-52.20	AM	-0.39	AV	.00
85.0	74	949.20	€	-2053.	Y	28465.	Z	-10136.	34	11.27	OZ	-51.49	AM	-0.39	AV	.00
85.5	74	948.70	€	-1912.	Y	28089.	Z	-10039.	34	10.02	OZ	-50.75	AM	-0.39	AV	.00
85.0	74	948.19	€	-1774.	Y	27713.	Z	-9921.	34	8.85	OZ	-50.05	AM	-0.39	AV	.00
85.5	74	947.69	€	-1640.	Y	27335.	Z	-9793.	34	7.79	OZ	-49.34	AM	-0.39	AV	.00

PAYOFF AND ERRORS

J1 -731.922

AT

771.79

ERR -13073.37

PERR .232431

GERR .010019

BACKWARD INTERPOLATION

T 01.0	V4	949.20	J414	.1023538E+02	D41V	.0204332E+01	X -2093.	Y 29463.	Z -10195.	AM	-39	AV	-39
T 05.0	V4	951.16	J414	.1021432E+02	D41V	.5339411E+01	X -2545.	Y 29961.	Z -10745.	AM	-38	AV	-38
T 09.0	V4	953.05	J414	.1020317E+02	D41V	.9358381E+01	X -3286.	Y 31442.	Z -11295.	AM	-38	AV	-38
T 13.0	V4	954.38	J414	.1020134E+02	D41V	.1235943E+02	X -3969.	Y 32907.	Z -11943.	AM	-37	AV	-37
T 17.0	V4	955.62	J414	.1021233E+02	D41V	.1524064E+02	X -4695.	Y 34353.	Z -12391.	AM	-35	AV	-35
T 21.0	V4	958.29	J414	.1023834E+02	D41V	.1819993E+02	X -5467.	Y 35785.	Z -12339.	AM	-35	AV	-35
T 25.0	V4	959.05	J414	.1028091E+02	D41V	.2123545E+02	X -6278.	Y 37199.	Z -13466.	AM	-33	AV	-33
T 29.0	V4	961.30	J414	.1034349E+02	D41V	.2434433E+02	X -7127.	Y 38592.	Z -14030.	AM	-31	AV	-31
T 33.0	V4	962.62	J414	.1043005E+02	D41V	.2752623E+02	X -8010.	Y 39967.	Z -14575.	AM	-29	AV	-29
T 37.0	V4	963.79	J414	.1054475E+02	D41V	.3077695E+02	X -8925.	Y 41323.	Z -15122.	AM	-25	AV	-25
T 41.0	V4	964.81	J414	.1063232E+02	D41V	.3409433E+02	X -9869.	Y 42666.	Z -15565.	AM	-21	AV	-21
T 45.0	V4	965.65	J414	.1077730E+02	D41V	.3747475E+02	X -10836.	Y 43994.	Z -16210.	AM	-17	AV	-17
T 49.0	V4	965.35	J414	.1110672E+02	D41V	.4091361E+02	X -11922.	Y 45311.	Z -16792.	AM	-11	AV	-11
T 53.0	V4	966.91	J414	.1135158E+02	D41V	.4441125E+02	X -12819.	Y 46522.	Z -17291.	AM	-04	AV	-02
T 57.0	V4	967.53	J414	.1267698E+02	D41V	.4827064E+02	X -13923.	Y 47931.	Z -17925.	AM	29	AV	05
T 61.0	V4	968.59	J414	.9981033E+01	D41V	.5170100E+02	X -14838.	Y 49236.	Z -18355.	AM	-43	AV	-04
T 65.0	V4	969.61	J414	.9963937E+01	D41V	.5545287E+02	X -15997.	Y 50310.	Z -19361.	AM	-43	AV	-04
T 69.0	V4	971.20	J414	.9943373E+01	D41V	.5322877E+02	X -17001.	Y 51752.	Z -19393.	AM	-44	AV	-05
T 73.0	V4	972.63	J414	.9935159E+01	D41V	.6301813E+02	X -18149.	Y 52963.	Z -19311.	AM	-45	AV	-05
T 77.0	V4	974.71	J414	.9925736E+01	D41V	.6581094E+02	X -19342.	Y 54132.	Z -20415.	AM	-45	AV	-05
T 81.0	V4	975.88	J414	.9917809E+01	D41V	.7059533E+02	X -20378.	Y 55267.	Z -20315.	AM	-45	AV	-05
T 85.0	V4	979.40	J414	.9912447E+01	D41V	.7435973E+02	X -21858.	Y 56363.	Z -21407.	AM	-47	AV	-05
T 89.0	V4	982.30	J414	.9903577E+01	D41V	.7909316E+02	X -23182.	Y 57419.	Z -21394.	AM	-47	AV	-35

T 42.0	V4	895.62	J444	.9908056E+01	044V	.8176591E+02	X -24540.	Y 58430.	Z -22374.	AM	-48	AV	-34
T 42.0	V4	939.41	J444	.9903437E+01	044V	.8543293E+02	X -23397.	Y 59397.	Z -22843.	AM	-49	AV	-33
T 31.0	V4	893.72	J444	.9908020E+01	044V	.8304265E+02	X -27408.	Y 60318.	Z -23720.	AM	-50	AV	-32
T 34.0	V4	839.64	J444	.9893300E+01	044V	.9266603E+02	X -26900.	Y 61190.	Z -23790.	AM	-51	AV	-31
T 34.0	V4	904.85	J444	.9812631E+01	044V	.9711585E+02	X -30431.	Y 52010.	Z -24267.	AM	-51	AV	-33
T 32.0	V4	910.05	J444	.1010011E+02	044V	.9453490E+02	X -31997.	Y 52775.	Z -24773.	AM	-52	AV	-134
T 32.0	V4	1005.92	J444	.8019135E+01	044V	.1019055E+03	X -33666.	Y 63519.	Z -25279.	AM	-52	AV	5.27
T 24.0	V4	1040.59	J444	.8837793E+01	044V	.9357753E+02	X -35513.	Y 64270.	Z -25754.	AM	-53	AV	-29
T 24.0	V4	1077.67	J444	.8740122E+01	044V	.9432023E+02	X -37440.	Y 64993.	Z -26279.	AM	-53	AV	-10
T 24.0	V4	1111.04	J444	.8589002E+01	044V	.9323833E+02	X -39443.	Y 55552.	Z -26119.	AM	-53	AV	-39
T 22.0	V4	1149.29	J444	.8383514E+01	044V	.9398671E+02	X -41529.	Y 65279.	Z -27393.	AM	-53	AV	-39
T 22.0	V4	1192.08	J444	.8140053E+01	044V	.9570073E+02	X -43705.	Y 65363.	Z -27374.	AM	-53	AV	-12
T 18.0	V4	1237.97	J444	.7842702E+01	044V	.9754015E+02	X -45979.	Y 57404.	Z -29597.	AM	-52	AV	-12
T 16.0	V4	1294.74	J444	.7501395E+01	044V	.9910963E+02	X -48350.	Y 57901.	Z -29254.	AM	-52	AV	-13
T 14.0	V4	1330.39	J444	.7135040E+01	044V	.1013333E+03	X -50820.	Y 68351.	Z -29945.	AM	-52	AV	-13
T 12.0	V4	1373.89	J444	.6770492E+01	044V	.1043253E+03	X -53382.	Y 68752.	Z -30575.	AM	-51	AV	-14
T 17.0	V4	1415.84	J444	.6480108E+01	044V	.1377705E+03	X -56031.	Y 59101.	Z -31442.	AM	-50	AV	-15
T 9.0	V4	1453.99	J444	.6374932E+01	044V	.1106603E+03	X -58766.	Y 59397.	Z -32253.	AM	-50	AV	-19
T 6.0	V4	1530.04	J444	.6547504E+01	044V	.1117143E+03	X -61502.	Y 59540.	Z -33105.	AM	-49	AV	-26
T 4.0	V4	1503.33	J444	.6627134E+01	044V	.1084331E+03	X -64514.	Y 59835.	Z -34039.	AM	-48	AV	-17
T 2.0	V4	1332.56	J444	.9720454E+01	044V	.1350933E+03	X -67515.	Y 59864.	Z -34984.	AM	-48	AV	-3.98

ONE-TWENTY-ALPHA SEARCH

2	.1000E-07	J	-731.8932	C1	.1000E-07	DE.C1	.5000E-09
2	.1500E-07	J	-731.8936	C1	.1000E-07	DE.C1	.5000E-09
2	.2000E-07	J	-731.8941	C1	.1000E-07	DE.C1	.5000E-09
2	.2500E-07	J	-731.8946	C1	.1000E-07	DE.C1	.5000E-09
2	.3000E-07	J	-731.8951	C1	.1000E-07	DE.C1	.5000E-09

C	.3530E-07	J	-731.8955	31	.1000E-07	DE.C1	.5000E-03
C	.4070E-07	J	-731.8960	31	.1000E-07	DE.C1	.5000E-03
C	.4530E-07	J	-731.8965	31	.1000E-07	DE.C1	.5000E-03
C	.5070E-07	J	-731.8970	31	.1000E-07	DE.C1	.5000E-03
C	.5500E-07	J	-731.8974	31	.1000E-07	DE.C1	.5000E-03
C	.6070E-07	J	-731.8979	31	.1000E-07	DE.C1	.5000E-03
C	.6530E-07	J	-731.8984	31	.1000E-07	DE.C1	.5000E-03
C	.7070E-07	J	-731.8989	31	.1000E-07	DE.C1	.5000E-03
C	.7530E-07	J	-731.8993	31	.1000E-07	DE.C1	.5000E-03
C	.8070E-07	J	-731.8998	31	.1000E-07	DE.C1	.5000E-03

C	.8530E-07	J	-731.9003	31	.1000E-07	DE.C1	.5000E-03
C	.9070E-07	J	-731.9007	31	.1000E-07	DE.C1	.5000E-03
C	.9530E-07	J	-731.9012	31	.1000E-07	DE.C1	.5000E-03
C	.1000E-05	J	-731.9017	31	.1000E-07	DE.C1	.5000E-03
C	.1050E-05	J	-730.6301	31	.1000E-07	DE.C1	.5000E-03
C	.1090E-05	J	-731.9017	31	.1000E-07	DE.C1	.5000E-03

ITERATION NO. 2

T	89.3	V	367.89	C	-1640.	Y	27335.	Z	-9733.	J	7.79	D	-48.52	A	-0.39	V	-0.00
---	------	---	--------	---	--------	---	--------	---	--------	---	------	---	--------	---	-------	---	-------

PAVCE AND FORCES

J1	-731.9017	WT	771.80	REAR	-13079.94	PSERR	.282490	GAERR	.010902
----	-----------	----	--------	------	-----------	-------	---------	-------	---------

OPTIMIZED TRAJECTORY

T	1.0	V	1324.00	C	-68390.	Y	70000.	Z	-34935.	W	.50
T	1.5	V	1324.95	C	-68206.	Y	59984.	Z	-34979.	W	.34
T	2.0	V	1322.56	C	-67516.	Y	59964.	Z	-34834.	W	.34
T	2.5	V	1322.56	C	-67516.	Y	59964.	Z	-34834.	W	.34
T	3.0	V	1322.56	C	-67516.	Y	59964.	Z	-34834.	W	.34

T 2.5	V4	1417.64	K	-66930.	Y	65940.	Z	-34709.	JH	426.01	OZ	-322.59	AH	-49	AV	-0.98
T 3.0	V4	1432.72	K	-66119.	Y	65911.	Z	-34500.	JH	526.64	OZ	-295.60	AH	-49	AV	-2.69
T 3.5	V4	1547.43	K	-65380.	Y	65876.	Z	-34275.	JH	644.27	OZ	-299.51	AH	-49	AV	-0.93
T 4.0	V4	1503.33	K	-64614.	Y	65836.	Z	-34039.	JH	749.16	OZ	-219.41	AH	-49	AV	-0.37
T 4.5	V4	1344.87	K	-63830.	Y	65790.	Z	-33735.	JH	945.36	OZ	-177.12	AH	-48	AV	-0.17
T 5.0	V4	1330.81	K	-63072.	Y	65743.	Z	-33550.	JH	1004.70	OZ	-134.87	AH	-49	AV	-0.07
T 5.5	V4	1555.44	K	-62331.	Y	65693.	Z	-33331.	JH	1214.99	OZ	-94.59	AH	-49	AV	.22
T 6.0	V4	1330.04	K	-61602.	Y	65640.	Z	-33106.	JH	1336.90	OZ	-55.61	AH	-49	AV	.27
T 6.5	V4	1509.73	K	-60882.	Y	65584.	Z	-32937.	JH	1458.02	OZ	-20.83	AH	-49	AV	.26
T 7.0	V4	1432.58	K	-60170.	Y	65525.	Z	-32571.	JH	1573.29	OZ	12.94	AH	-49	AV	.24
T 7.5	V4	1477.51	K	-59465.	Y	65462.	Z	-32439.	JH	1685.30	OZ	44.89	AH	-49	AV	.22
T 8.0	V4	1453.89	K	-58766.	Y	65397.	Z	-32250.	JH	1794.45	OZ	75.13	AH	-50	AV	.20
T 8.5	V4	1451.25	K	-58074.	Y	65329.	Z	-32044.	JH	1900.99	OZ	103.79	AH	-50	AV	.19
T 9.0	V4	1439.33	K	-57387.	Y	65255.	Z	-31844.	JH	2005.11	OZ	130.94	AH	-50	AV	.18
T 9.5	V4	1427.92	K	-56706.	Y	65180.	Z	-31648.	JH	2106.92	OZ	155.65	AH	-50	AV	.17
T 10.0	V4	1416.84	K	-56031.	Y	65101.	Z	-31442.	JH	2206.48	OZ	180.99	AH	-50	AV	.17
T 10.5	V4	1403.98	K	-55360.	Y	65019.	Z	-31247.	JH	2303.02	OZ	203.98	AH	-50	AV	.16
T 11.0	V4	1395.25	K	-54695.	Y	64933.	Z	-31054.	JH	2398.94	OZ	225.67	AH	-51	AV	.15
T 11.5	V4	1386.57	K	-54035.	Y	64844.	Z	-30934.	OH	2491.81	OZ	246.03	AH	-51	AV	.15
T 12.0	V4	1373.89	K	-53382.	Y	64752.	Z	-30875.	JH	2582.40	OZ	265.29	AH	-51	AV	.15
T 12.5	V4	1353.14	K	-52733.	Y	64657.	Z	-30430.	OH	2570.65	OZ	283.25	AH	-51	AV	.14
T 13.0	V4	1352.32	K	-52090.	Y	64554.	Z	-30336.	JH	2756.50	OZ	300.03	AH	-51	AV	.14
T 13.5	V4	1341.37	K	-51452.	Y	64455.	Z	-30125.	JH	2839.87	OZ	315.64	AH	-51	AV	.14
T 14.0	V4	1330.30	K	-50820.	Y	64351.	Z	-29946.	JH	2920.70	OZ	330.10	AH	-51	AV	.14
T 14.5	V4	1319.10	K	-50194.	Y	64243.	Z	-29770.	JH	2988.90	OZ	343.42	AH	-52	AV	.13
T 15.0	V4	1307.76	K	-49573.	Y	64132.	Z	-29535.	JH	3074.40	OZ	355.63	AH	-52	AV	.13
T 15.5	V4	1296.30	K	-48959.	Y	64019.	Z	-29423.	JH	3147.12	OZ	355.74	AH	-52	AV	.13

T 15.0	V4	1254.74	K	-40350.	Y	67901.	Z	-29234.	JM	3217.00	OZ	376.77	AM	-.52	AV	.13
T 15.5	V4	1273.09	K	-47749.	Y	57781.	Z	-29096.	JM	3283.99	OZ	399.74	AM	-.52	AV	.13
T 17.0	V4	1251.39	K	-47152.	Y	57554.	Z	-20321.	J4	3340.03	OZ	393.65	AM	-.52	AV	.12
T 17.5	V4	1249.67	K	-46562.	Y	57533.	Z	-20739.	JM	3409.00	OZ	400.54	AM	-.52	AV	.12
T 19.0	V4	1237.97	K	-45970.	Y	57404.	Z	-20537.	JM	3467.12	OZ	405.42	AM	-.52	AV	.12
T 19.5	V4	1226.32	K	-45401.	Y	57273.	Z	-20430.	JM	3522.13	OZ	411.32	AM	-.52	AV	.12
T 19.0	V4	1214.76	K	-44929.	Y	57139.	Z	-20292.	J4	3574.12	OZ	413.24	AM	-.53	AV	.11
T 19.5	V4	1203.34	K	-44264.	Y	57002.	Z	-20127.	J4	3523.09	OZ	410.22	AM	-.53	AV	.11
T 20.0	V4	1192.08	K	-43705.	Y	56863.	Z	-27374.	JM	3569.07	OZ	420.27	AM	-.53	AV	.11
T 20.5	V4	1181.02	K	-43152.	Y	56721.	Z	-27024.	JM	3712.08	OZ	421.42	AM	-.53	AV	.10
T 21.0	V4	1170.19	K	-42605.	Y	56576.	Z	-27675.	JM	3752.17	OZ	421.70	AM	-.53	AV	.10
T 21.5	V4	1159.63	K	-42064.	Y	56429.	Z	-27328.	JM	3799.40	OZ	421.12	AM	-.53	AV	.10
T 22.0	V4	1149.30	K	-41529.	Y	56279.	Z	-27393.	J4	3823.01	OZ	419.71	AM	-.53	AV	.09
T 22.5	V4	1139.28	K	-40999.	Y	56126.	Z	-27239.	JM	3855.40	OZ	417.49	AM	-.53	AV	.09
T 23.0	V4	1129.56	K	-40475.	Y	55970.	Z	-27030.	JM	3884.47	OZ	414.47	AM	-.53	AV	.09
T 23.5	V4	1120.14	K	-39956.	Y	55812.	Z	-26337.	JM	3910.03	OZ	410.65	AM	-.53	AV	.09
T 24.0	V4	1111.04	K	-39443.	Y	55652.	Z	-26019.	J4	3934.69	OZ	406.09	AM	-.53	AV	.08
T 24.5	V4	1102.25	K	-38935.	Y	55409.	Z	-25832.	D4	3956.08	OZ	400.74	AM	-.53	AV	.08
T 25.0	V4	1093.76	K	-38431.	Y	55323.	Z	-26546.	JM	3975.09	OZ	394.61	AM	-.53	AV	.08
T 25.5	V4	1085.57	K	-37933.	Y	55154.	Z	-26412.	JM	3991.79	OZ	387.60	AM	-.53	AV	.09
T 25.0	V4	1077.68	K	-37440.	Y	54903.	Z	-26279.	JM	4006.25	OZ	379.92	AM	-.53	AV	.09
T 25.5	V4	1070.05	K	-36951.	Y	54809.	Z	-26147.	D4	4010.59	OZ	371.24	AM	-.53	AV	.10
T 27.0	V4	1052.69	K	-36467.	Y	54632.	Z	-26010.	J4	4020.84	OZ	361.52	AM	-.53	AV	.11
T 27.5	V4	1045.55	K	-35980.	Y	54452.	Z	-25830.	JM	4037.11	OZ	350.57	AM	-.53	AV	.14
T 28.0	V4	1034.59	K	-35513.	Y	54270.	Z	-25733.	JM	4043.49	OZ	338.01	AM	-.53	AV	.18
T 28.5	V4	1021.71	K	-35042.	Y	54005.	Z	-25640.	JM	4040.10	OZ	323.09	AM	-.53	AV	.29
T 29.0	V4	1014.55	K	-34575.	Y	53897.	Z	-25521.	J4	4051.11	OZ	303.75	AM	-.53	AV	.53

T 29.5	V4	1023.40	K	-34111.	V	63706.	Z	-29410.	J4	4052.71	OZ	269.35	AM	-0.53	AV	1.90
T 29.5	V4	1093.92	K	-33666.	V	63513.	Z	-29270.	J4	4043.72	OZ	275.77	AM	-0.53	AV	-5.12
T 30.5	V4	374.40	K	-33220.	V	53330.	Z	-29190.	J4	4031.20	OZ	242.12	AM	-0.52	AV	5.27
T 31.0	V4	354.01	K	-32802.	V	53143.	Z	-29033.	J4	4011.46	OZ	240.45	AM	-0.52	AV	-3.97
T 31.5	V4	345.07	K	-32396.	V	52960.	Z	-24030.	J4	3990.03	OZ	279.20	AM	-0.52	AV	-5.16
T 32.0	V4	310.06	K	-31997.	V	62775.	Z	-24773.	J4	3945.47	OZ	272.05	AM	-0.52	AV	56.71
T 32.5	V4	309.20	K	-31602.	V	62590.	Z	-24647.	J4	3900.51	OZ	277.06	AM	-0.52	AV	-1.34
T 33.0	V4	308.51	K	-31210.	V	52800.	Z	-24517.	J4	3870.39	OZ	293.68	AM	-0.52	AV	-0.34
T 33.5	V4	306.06	K	-30920.	V	52207.	Z	-24330.	J4	3831.67	OZ	267.40	AM	-0.52	AV	.31
T 34.0	V4	304.55	K	-30431.	V	52010.	Z	-24237.	J4	3792.44	OZ	297.13	AM	-0.52	AV	.44
T 34.5	V4	303.03	K	-30045.	V	51810.	Z	-24146.	J4	3752.60	OZ	293.01	AM	-0.51	AV	.33
T 35.0	V4	301.44	K	-29661.	V	51607.	Z	-24027.	J4	3712.06	OZ	279.55	AM	-0.51	AV	.19
T 35.5	V4	300.00	K	-29280.	V	61400.	Z	-23908.	J4	3570.77	OZ	272.03	AM	-0.51	AV	.11
T 36.0	V4	299.64	K	-28900.	V	61190.	Z	-23730.	J4	3528.72	OZ	254.55	AM	-0.51	AV	.06
T 36.5	V4	297.34	K	-28523.	V	60976.	Z	-23673.	J4	3505.89	OZ	256.63	AM	-0.51	AV	.03
T 37.0	V4	295.09	K	-28149.	V	60780.	Z	-23535.	J4	3442.20	OZ	248.27	AM	-0.50	AV	.01
T 37.5	V4	294.09	K	-27777.	V	60540.	Z	-23438.	J4	3497.91	OZ	239.51	AM	-0.50	AV	.00
T 38.0	V4	293.72	K	-27403.	V	60310.	Z	-23320.	J4	3452.79	OZ	230.40	AM	-0.50	AV	-0.01
T 38.5	V4	292.59	K	-27042.	V	60092.	Z	-23203.	J4	3406.92	OZ	221.25	AM	-0.50	AV	-0.02
T 39.0	V4	291.50	K	-26670.	V	59863.	Z	-23035.	J4	3360.32	OZ	211.90	AM	-0.50	AV	-0.02
T 39.5	V4	290.44	K	-26316.	V	59631.	Z	-22937.	J4	3313.01	OZ	202.44	AM	-0.49	AV	-0.03
T 40.0	V4	289.41	K	-25957.	V	59397.	Z	-22849.	J4	3264.99	OZ	132.91	AM	-0.49	AV	-0.03
T 40.5	V4	288.42	K	-25601.	V	59159.	Z	-22730.	J4	3216.23	OZ	193.35	AM	-0.49	AV	-0.03
T 41.0	V4	287.45	K	-25246.	V	58913.	Z	-22512.	J4	3166.92	OZ	173.73	AM	-0.49	AV	-0.04
T 41.5	V4	286.52	K	-24997.	V	58676.	Z	-22433.	J4	3116.09	OZ	154.24	AM	-0.49	AV	-0.04
T 42.0	V4	285.62	K	-24646.	V	58430.	Z	-22374.	J4	3066.22	OZ	154.73	AM	-0.49	AV	-0.04
T 42.5	V4	284.75	K	-24283.	V	58181.	Z	-22234.	J4	3014.94	OZ	143.23	AM	-0.49	AV	-0.04

T 47.0	J4	933.90	K	-23860.	Y	57929.	Z	-22134..	JH	2963.05	OZ	135.90	AM	-4.49	AV	-0.05
T 47.5	J4	933.09	K	-23819.	Y	57875.	Z	-22014.	JH	2910.57	OZ	125.60	AM	-4.49	AV	-0.05
T 48.0	J4	932.30	K	-23102.	Y	57419.	Z	-21933.	DM	2957.51	OZ	117.40	AM	-4.49	AV	-0.05
T 48.5	J4	931.54	K	-22847.	Y	57159.	Z	-21772.	J4	2803.90	OZ	109.31	AM	-4.47	AV	-0.05
T 49.0	J4	930.80	K	-22515.	Y	56895.	Z	-21651.	JH	2749.75	OZ	99.33	AM	-4.47	AV	-0.05
T 49.5	J4	930.09	K	-22195.	Y	56531.	Z	-21529.	DM	2695.08	OZ	90.49	AM	-4.47	AV	-0.05
T 50.0	J4	929.40	K	-21859.	Y	56361.	Z	-21407.	JH	2539.90	OZ	81.79	AM	-4.47	AV	-0.05
T 50.5	J4	928.74	K	-21534.	Y	55993.	Z	-21295.	J4	2584.23	OZ	73.21	AM	-4.47	AV	-0.05
T 51.0	J4	928.10	K	-21213.	Y	55820.	Z	-21152.	DM	2528.09	OZ	64.79	AM	-4.47	AV	-0.05
T 51.5	J4	927.48	K	-20894.	Y	55545.	Z	-21039.	JH	2471.48	OZ	56.52	AM	-4.45	AV	-0.05
T 52.0	J4	926.89	K	-20579.	Y	55267.	Z	-20915.	J4	2416.44	OZ	48.41	AM	-4.43	AV	-0.05
T 52.5	J4	926.31	K	-20265.	Y	54987.	Z	-20791.	J4	2356.97	OZ	40.47	AM	-4.45	AV	-0.05
T 53.0	J4	925.76	K	-19954.	Y	54705.	Z	-20656.	DM	2299.09	OZ	32.63	AM	-4.46	AV	-0.05
T 53.5	J4	925.22	K	-19647.	Y	54420.	Z	-20531.	J4	2240.81	OZ	25.09	AM	-4.45	AV	-0.05
T 54.0	J4	924.71	K	-19342.	Y	54132.	Z	-20416.	DM	2182.16	OZ	17.65	AM	-4.45	AV	-0.05
T 54.5	J4	924.21	K	-19039.	Y	53843.	Z	-20290.	J4	2123.15	OZ	10.39	AM	-4.45	AV	-0.05
T 55.0	J4	923.74	K	-18740.	Y	53551.	Z	-20154.	JH	2063.78	OZ	3.31	AM	-4.43	AV	-0.05
T 55.5	J4	923.27	K	-18443.	Y	53257.	Z	-20030.	J4	2004.09	OZ	-3.60	AM	-4.45	AV	-0.05
T 56.0	J4	922.83	K	-18149.	Y	52960.	Z	-19911.	J4	1944.03	OZ	-10.32	AM	-4.45	AV	-0.05
T 56.5	J4	922.40	K	-17950.	Y	52661.	Z	-19793.	DM	1883.77	OZ	-16.86	AM	-4.43	AV	-0.05
T 57.0	J4	921.99	K	-17659.	Y	52360.	Z	-19655.	JH	1823.17	OZ	-23.22	AM	-4.44	AV	-0.05
T 57.5	J4	921.59	K	-17284.	Y	52057.	Z	-19527.	JH	1762.30	OZ	-29.39	AM	-4.44	AV	-0.05
T 58.0	J4	921.21	K	-17001.	Y	51752.	Z	-19399.	J4	1701.18	OZ	-35.39	AM	-4.44	AV	-0.05
T 58.5	J4	920.84	K	-16721.	Y	51445.	Z	-19270.	J4	1639.82	OZ	-41.13	AM	-4.44	AV	-0.05
T 59.0	J4	920.48	K	-16443.	Y	51135.	Z	-19140.	JH	1576.23	OZ	-46.81	AM	-4.44	AV	-0.05
T 59.5	J4	920.14	K	-16169.	Y	50824.	Z	-19011.	JH	1516.43	OZ	-52.25	AM	-4.44	AV	-0.04
T 60.0	J4	919.81	K	-15897.	Y	50510.	Z	-18890.	JH	1456.43	OZ	-57.51	AM	-4.43	AV	-0.04
T 60.5	J4	919.49	K	-15620.	Y	50195.	Z	-18750.	JH	1392.25	OZ	-62.59	AM	-4.43	AV	-0.04

T 37.0	J4	959.18	K	-19362.	Y	49877.	Z	-18319.	J4	1329.90	OZ	-57.49	AM	-0.43	AV	-0.04
T 37.5	J4	958.89	K	-19098.	Y	49557.	Z	-18498.	J4	1257.39	OZ	-72.20	AM	-0.43	AV	-0.04
T 38.0	J4	958.60	K	-14839.	Y	49236.	Z	-18356.	J4	1204.75	OZ	-76.74	AM	-0.43	AV	-0.04
T 38.5	J4	959.32	K	-14589.	Y	49917.	Z	-19224.	J4	1141.99	OZ	-91.19	AM	-0.43	AV	-0.04
T 39.0	J4	959.05	K	-14325.	Y	48587.	Z	-18031.	J4	1079.10	OZ	-95.29	AM	-0.42	AV	-0.04
T 39.5	J4	957.79	K	-14072.	Y	48260.	Z	-17959.	J4	1016.12	OZ	-89.29	AM	-0.42	AV	-0.04
T 40.0	J4	957.54	K	-13923.	Y	47931.	Z	-17825.	J4	953.05	OZ	-93.13	AM	-0.42	AV	-0.04
T 40.5	J4	957.22	K	-13572.	Y	47604.	Z	-17533.	J4	895.29	OZ	-95.84	AM	.29	AV	.05
T 41.0	J4	957.18	K	-13321.	Y	47275.	Z	-17559.	J4	940.45	OZ	-99.45	AM	-0.01	AV	-0.10
T 41.5	J4	957.03	K	-13070.	Y	45949.	Z	-17425.	J4	788.64	OZ	-101.69	AM	-0.01	AV	-0.01
T 42.0	J4	955.91	K	-12919.	Y	45622.	Z	-17231.	J4	739.72	OZ	-103.37	AM	-0.02	AV	-0.04
T 42.5	J4	955.78	K	-12569.	Y	46295.	Z	-17137.	J4	593.52	OZ	-104.61	AM	-0.04	AV	-0.02
T 43.0	J4	955.64	K	-12319.	Y	45967.	Z	-17022.	J4	549.92	OZ	-105.43	AM	-0.05	AV	-0.02
T 43.5	J4	955.50	K	-12070.	Y	45639.	Z	-16837.	J4	608.79	OZ	-105.89	AM	-0.05	AV	-0.02
T 44.0	J4	955.35	K	-11822.	Y	45311.	Z	-16752.	J4	570.00	OZ	-106.00	AM	-0.09	AV	-0.02
T 44.5	J4	955.19	K	-11574.	Y	44983.	Z	-16617.	J4	533.45	OZ	-105.82	AM	-0.11	AV	-0.01
T 45.0	J4	955.03	K	-11327.	Y	44654.	Z	-16481.	J4	499.01	OZ	-105.39	AM	-0.13	AV	-0.01
T 45.5	J4	953.85	K	-11081.	Y	44324.	Z	-16345.	J4	456.58	OZ	-104.73	AM	-0.14	AV	-0.01
T 46.0	J4	955.66	K	-10934.	Y	43994.	Z	-16210.	J4	436.06	OZ	-103.88	AM	-0.15	AV	-0.01
T 46.5	J4	955.47	K	-10593.	Y	43663.	Z	-16074.	J4	407.34	OZ	-102.85	AM	-0.17	AV	-0.01
T 47.0	J4	955.26	K	-10350.	Y	43332.	Z	-15938.	J4	380.33	OZ	-101.69	AM	-0.19	AV	-0.00
T 47.5	J4	955.04	K	-10109.	Y	43000.	Z	-15802.	J4	354.95	OZ	-100.39	AM	-0.19	AV	-0.00
T 48.0	J4	954.81	K	-9869.	Y	42665.	Z	-15556.	J4	331.10	OZ	-98.99	AM	-0.20	AV	-0.00
T 48.5	J4	954.59	K	-9631.	Y	42332.	Z	-15310.	J4	308.69	OZ	-97.52	AM	-0.21	AV	-0.00
T 49.0	J4	954.33	K	-9395.	Y	41997.	Z	-15334.	J4	287.67	OZ	-95.98	AM	-0.22	AV	.00
T 49.5	J4	954.07	K	-9159.	Y	41661.	Z	-15237.	J4	267.94	OZ	-94.39	AM	-0.23	AV	.00
T 50.0	J4	953.80	K	-8925.	Y	41325.	Z	-15121.	J4	249.44	OZ	-92.75	AM	-0.24	AV	.00

T 70.5	V4	953.52	K	-8694.	Y	40987.	Z	-14935.	JH	232.09	OZ	-91.12	AH	-25	AV	.00
T 71.0	V4	953.23	K	-8465.	Y	40640.	Z	-14848.	JH	215.04	OZ	-89.45	AH	-25	AV	.00
T 71.5	V4	952.93	K	-8237.	Y	40300.	Z	-14712.	JH	200.62	OZ	-87.80	AH	-27	AV	.00
T 72.0	V4	952.63	K	-8010.	Y	39967.	Z	-14576.	JH	186.37	OZ	-86.15	AH	-28	AV	.00
T 72.5	V4	952.31	K	-7786.	Y	39625.	Z	-14439.	JH	173.04	OZ	-84.51	AH	-23	AV	.00
T 73.0	V4	951.98	K	-7564.	Y	39281.	Z	-14303.	JH	160.58	OZ	-82.89	AH	-29	AV	.00
T 73.5	V4	951.65	K	-7344.	Y	38937.	Z	-14156.	JH	148.93	OZ	-81.30	AH	-31	AV	.00
T 74.0	V4	951.31	K	-7127.	Y	38591.	Z	-14030.	JH	138.04	OZ	-79.75	AH	-31	AV	.00
T 74.5	V4	950.96	K	-6911.	Y	38245.	Z	-13833.	JH	127.87	OZ	-78.22	AH	-31	AV	.00
T 75.0	V4	950.60	K	-6598.	Y	37897.	Z	-13737.	JH	118.38	OZ	-75.74	AH	-32	AV	.00
T 75.5	V4	950.23	K	-6487.	Y	37543.	Z	-13520.	JH	109.53	OZ	-75.23	AH	-32	AV	.00
T 76.0	V4	959.86	K	-6278.	Y	37195.	Z	-13493.	JH	101.27	OZ	-73.89	AH	-33	AV	.00
T 76.5	V4	959.48	K	-6072.	Y	36845.	Z	-13347.	JH	93.57	OZ	-72.52	AH	-33	AV	.00
T 77.0	V4	959.09	K	-5860.	Y	35494.	Z	-13210.	JH	86.40	OZ	-71.21	AH	-34	AV	.00
T 77.5	V4	958.69	K	-5666.	Y	36140.	Z	-13074.	JH	79.73	OZ	-59.93	AH	-34	AV	.00
T 78.0	V4	958.29	K	-5467.	Y	35785.	Z	-12937.	JH	73.51	OZ	-58.70	AH	-34	AV	.00
T 78.5	V4	957.89	K	-5271.	Y	35430.	Z	-12800.	JH	67.73	OZ	-57.51	AH	-35	AV	.00
T 79.0	V4	957.48	K	-5077.	Y	35073.	Z	-12553.	JH	62.35	OZ	-55.35	AH	-35	AV	.00
T 79.5	V4	957.06	K	-4885.	Y	34714.	Z	-12527.	JH	57.36	OZ	-55.25	AH	-35	AV	.00
T 80.0	V4	956.63	K	-4696.	Y	34355.	Z	-12330.	JH	52.71	OZ	-54.19	AH	-35	AV	.00
T 80.5	V4	956.20	K	-4510.	Y	33995.	Z	-12253.	JH	48.40	OZ	-53.15	AH	-35	AV	.00
T 81.0	V4	955.77	K	-4327.	Y	33633.	Z	-12116.	JH	44.40	OZ	-52.15	AH	-35	AV	.00
T 81.5	V4	955.33	K	-4146.	Y	33270.	Z	-11979.	JH	40.60	OZ	-51.16	AH	-37	AV	.00
T 82.0	V4	954.89	K	-3968.	Y	32907.	Z	-11842.	JH	37.24	OZ	-50.25	AH	-37	AV	.00
T 82.5	V4	954.44	K	-3793.	Y	32542.	Z	-11705.	JH	34.04	OZ	-59.35	AH	-37	AV	.00
T 83.0	V4	953.99	K	-3620.	Y	32176.	Z	-11558.	JH	31.09	OZ	-58.47	AH	-37	AV	.00
T 83.5	V4	953.52	K	-3451.	Y	31803.	Z	-11431.	JH	28.34	OZ	-57.62	AH	-37	AV	.00

T 84.0	V4	953.06	K	-3204.	V	31442.	Z	-11294.	DM	25.00	OZ	-55.79	AM	-39	AV	-0.00
T 84.3	V4	952.59	K	-3120.	V	31073.	Z	-11137.	DM	23.45	OZ	-55.97	AM	-39	AV	-0.00
T 85.0	V4	952.12	K	-2959.	V	30703.	Z	-11020.	DM	21.28	OZ	-55.19	AM	-39	AV	-0.00
T 85.5	V4	951.65	K	-2800.	V	30332.	Z	-10892.	DM	19.27	OZ	-54.40	AM	-39	AV	-0.00
T 86.0	V4	951.17	K	-2645.	V	29961.	Z	-10745.	DM	17.41	OZ	-53.64	AM	-39	AV	-0.00
T 86.5	V4	950.60	K	-2492.	V	29589.	Z	-10508.	DM	15.69	OZ	-52.89	AM	-39	AV	-0.00
T 87.0	V4	950.20	K	-2343.	V	29215.	Z	-10470.	DM	14.10	OZ	-52.15	AM	-39	AV	-0.00
T 87.5	V4	949.70	K	-2196.	V	28840.	Z	-10333.	DM	12.63	OZ	-51.41	AM	-39	AV	-0.00
T 88.0	V4	949.21	K	-2053.	V	28465.	Z	-10195.	DM	11.27	OZ	-50.69	AM	-39	AV	-0.00
T 88.5	V4	948.71	K	-1912.	V	28089.	Z	-10058.	DM	10.02	OZ	-49.95	AM	-39	AV	-0.00
T 89.0	V4	948.20	K	-1774.	V	27712.	Z	-9920.	DM	8.65	OZ	-49.24	AM	-39	AV	-0.00
TF 91.5	V4F	947.69	CF	-1640.	VF	27335.	ZF	-9733.	DM	7.79	OZF	-48.52	AM	-39	AV	-0.00

196

T	3.0	V4	1355.99	C	-27994.	Y	39872.	Z	-16732.	J4	1915.51	OZ	324.55	AH	-.91	AV	.31
T	3.5	J4	1444.47	C	-27260.	Y	39751.	Z	-16536.	J4	1904.53	OZ	343.74	AH	-.92	AV	.30
T	17.0	J4	1321.91	C	-26537.	Y	39625.	Z	-15335.	J4	1998.15	OZ	350.29	AH	-.92	AV	.29
T	17.5	V4	1233.48	C	-25025.	Y	39493.	Z	-15210.	J4	2066.31	OZ	374.23	AH	-.93	AV	.29
T	11.0	J4	1277.35	C	-25425.	Y	39357.	Z	-16038.	J4	2138.94	OZ	355.65	AH	-.93	AV	.25
T	11.5	V4	1255.73	C	-24836.	Y	39217.	Z	-15672.	J4	2206.12	OZ	395.09	AH	-.93	AV	.25
T	12.0	J4	1234.78	C	-24258.	Y	39071.	Z	-15710.	J4	2257.92	OZ	402.09	AH	-.94	AV	.24
T	12.5	J4	1214.65	C	-23692.	Y	37921.	Z	-15532.	O4	2324.50	OZ	407.00	AH	-.94	AV	.22
T	17.0	J4	1135.44	C	-23135.	Y	37765.	Z	-15337.	J4	2376.04	OZ	409.92	AH	-.94	AV	.21
T	17.5	V4	1177.21	C	-22599.	Y	37607.	Z	-15246.	J4	2422.75	OZ	410.93	AH	-.94	AV	.20
T	14.0	V4	1150.00	C	-22033.	Y	37443.	Z	-15039.	J4	2454.85	OZ	410.12	AH	-.94	AV	.19
T	14.5	J4	1133.79	C	-21525.	Y	37274.	Z	-14935.	J4	2502.57	OZ	407.55	AH	-.95	AV	.18
T	15.0	J4	1123.55	C	-21009.	Y	37100.	Z	-14813.	O4	2536.15	OZ	403.24	AH	-.95	AV	.17
T	17.5	J4	1114.24	C	-20499.	Y	35921.	Z	-14575.	J4	2565.81	OZ	397.11	AH	-.95	AV	.15
T	15.0	J4	1100.79	C	-19999.	Y	35739.	Z	-14540.	J4	2591.79	OZ	396.95	AH	-.95	AV	.21
T	15.5	V4	1038.05	C	-19595.	Y	35550.	Z	-14408.	J4	2514.35	OZ	378.15	AH	-.95	AV	.28
T	17.0	J4	1075.92	C	-19019.	Y	35356.	Z	-14291.	J4	2533.83	OZ	353.03	AH	-.95	AV	.50
T	17.5	V4	1052.13	C	-18540.	Y	35153.	Z	-14158.	O4	2550.95	OZ	334.42	AH	-.94	AV	1.64
T	13.0	V4	1014.19	C	-18104.	Y	35970.	Z	-13939.	J4	2541.95	OZ	393.64	AH	-.94	AV	-10.21
T	19.5	V4	945.91	C	-17581.	Y	35782.	Z	-13830.	J4	2526.38	OZ	354.58	AH	-.94	AV	18.44
T	19.0	V4	933.80	C	-17276.	Y	35593.	Z	-13735.	J4	2500.75	OZ	355.35	AH	-.94	AV	-4.97
T	17.5	J4	930.83	C	-16876.	Y	35393.	Z	-13517.	J4	2572.77	OZ	378.93	AH	-.94	AV	-4.45
T	21.0	J4	922.38	C	-16479.	Y	35197.	Z	-13438.	J4	2544.37	OZ	373.13	AH	-.93	AV	2.29
T	27.5	V4	919.52	C	-16086.	Y	34930.	Z	-13331.	J4	2514.47	OZ	353.17	AH	-.92	AV	.41
T	21.0	V4	915.20	C	-15597.	Y	34777.	Z	-13236.	J4	2482.79	OZ	352.29	AH	-.92	AV	.02
T	21.5	V4	911.95	C	-15314.	Y	34553.	Z	-13151.	J4	2449.40	OZ	340.33	AH	-.91	AV	.04
T	22.0	V4	908.66	C	-14936.	Y	34335.	Z	-13036.	J4	2414.29	OZ	327.94	AH	-.91	AV	-.93
T	22.5	V4	905.87	C	-14562.	Y	34105.	Z	-12921.	J4	2377.51	OZ	315.15	AH	-.90	AV	-.04
T	21.0	J4	903.00	C	-14194.	Y	33872.	Z	-12905.	J4	2339.10	OZ	302.21	AH	-.93	AV	-.05

T	27.3	V4	908.22	K	-13031.	Y	33632.	Z	2334.16	J4	2299.09	OZ	259.16	AM	-0.59	AV	-0.07
T	27.0	V4	937.54	K	-13472.	Y	33689.	Z	2299.09	J4	2299.09	OZ	275.12	AM	-0.59	AV	-0.03
T	27.3	V4	934.96	K	-13119.	Y	33139.	Z	2214.51	J4	2214.51	OZ	263.13	AM	-0.63	AV	-0.03
T	27.0	V4	932.45	K	-12772.	Y	32885.	Z	2170.03	J4	2170.03	OZ	230.27	AM	-0.67	AV	-0.09
T	27.5	V4	930.06	K	-12429.	Y	32625.	Z	2124.15	J4	2124.15	OZ	237.55	AM	-0.63	AV	-0.09
T	27.0	V4	937.73	K	-12092.	Y	32363.	Z	2076.93	J4	2076.93	OZ	223.04	AM	-0.65	AV	-0.10
T	27.3	V4	893.49	K	-11759.	Y	32095.	Z	2026.42	J4	2026.42	OZ	212.75	AM	-0.65	AV	-0.10
T	27.0	V4	833.33	K	-11433.	Y	31823.	Z	1978.66	J4	1978.66	OZ	200.71	AM	-0.65	AV	-0.10
T	27.5	V4	931.24	K	-11111.	Y	31547.	Z	1927.72	J4	1927.72	OZ	193.94	AM	-0.64	AV	-0.10
T	27.0	V4	973.22	K	-10794.	Y	31267.	Z	1875.64	J4	1875.64	OZ	177.47	AM	-0.63	AV	-0.10
T	27.3	V4	977.27	K	-10483.	Y	30982.	Z	1822.45	J4	1822.45	OZ	156.23	AM	-0.63	AV	-0.10
T	27.0	V4	975.39	K	-10177.	Y	30693.	Z	1756.25	J4	1756.25	OZ	135.43	AM	-0.62	AV	-0.10
T	27.3	V4	973.57	K	-9977.	Y	30401.	Z	1713.05	J4	1713.05	OZ	144.83	AM	-0.62	AV	-0.10
T	27.0	V4	971.61	K	-9551.	Y	30105.	Z	1656.91	J4	1656.91	OZ	134.69	AM	-0.61	AV	-0.10
T	27.5	V4	970.11	K	-9291.	Y	29805.	Z	1599.89	J4	1599.89	OZ	124.83	AM	-0.59	AV	-0.10
T	27.0	V4	959.47	K	-9007.	Y	29501.	Z	1542.03	J4	1542.03	OZ	115.31	AM	-0.60	AV	-0.10
T	27.3	V4	955.36	K	-8727.	Y	29194.	Z	1483.39	J4	1483.39	OZ	106.13	AM	-0.73	AV	-0.10
T	27.0	V4	955.35	K	-8453.	Y	28884.	Z	1423.93	J4	1423.93	OZ	97.31	AM	-0.73	AV	-0.10
T	27.5	V4	953.85	K	-8184.	Y	28570.	Z	1363.92	J4	1363.92	OZ	96.62	AM	-0.73	AV	-0.09
T	27.0	V4	952.43	K	-7921.	Y	28253.	Z	1303.21	J4	1303.21	OZ	90.59	AM	-0.77	AV	-0.09
T	27.3	V4	951.04	K	-7663.	Y	27933.	Z	1241.91	J4	1241.91	OZ	72.90	AM	-0.77	AV	-0.09
T	27.0	V4	953.69	K	-7410.	Y	27609.	Z	1190.07	J4	1190.07	OZ	55.45	AM	-0.75	AV	-0.09
T	27.3	V4	953.39	K	-7162.	Y	27283.	Z	1117.73	J4	1117.73	OZ	56.35	AM	-0.75	AV	-0.09
T	27.0	V4	957.13	K	-6920.	Y	26954.	Z	1054.95	J4	1054.95	OZ	51.59	AM	-0.73	AV	-0.09
T	27.5	V4	955.90	K	-6562.	Y	26622.	Z	991.79	J4	991.79	OZ	45.14	AM	-0.75	AV	-0.08
T	27.0	V4	934.71	K	-6451.	Y	26287.	Z	928.25	J4	928.25	OZ	33.04	AM	-0.74	AV	-0.08
T	27.3	V4	933.56	K	-6224.	Y	25950.	Z	864.43	J4	864.43	OZ	33.24	AM	-0.73	AV	-0.08
T	27.0	V4	952.44	K	-6003.	Y	25610.	Z	800.35	J4	800.35	OZ	27.79	AM	-0.73	AV	-0.09

T 37.3	04	951.35	C	-5705.	Y	25255.	Z	-9229.	04	736.05	OZ	22.39	AM	-0.72	AV	-0.07
T 39.0	04	950.30	C	-5575.	Y	24923.	Z	-9037.	04	571.60	OZ	17.79	AM	-0.72	AV	-0.09
T 39.3	04	949.26	C	-5369.	Y	24576.	Z	-8955.	04	507.04	OZ	13.12	AM	-0.71	AV	-0.05
T 37.0	04	949.29	C	-5169.	Y	24227.	Z	-8832.	04	542.38	OZ	9.02	AM	-0.71	AV	-0.10
T 39.5	04	947.23	C	-4973.	Y	23076.	Z	-8639.	04	477.73	OZ	4.71	AM	-0.70	AV	-0.01
T 42.0	04	946.54	C	-4775.	Y	23525.	Z	-8556.	04	420.54	OZ	1.57	AM	.29	AV	-0.07
T 40.5	04	943.00	C	-4500.	Y	23175.	Z	-8432.	04	350.39.	OZ	-0.09	AM	-0.04	AV	-0.06
T 41.0	04	945.12	C	-4391.	Y	22927.	Z	-8239.	04	323.61	OZ	-2.53	AM	.27	AV	.09
T 41.5	04	944.44	C	-4196.	Y	22473.	Z	-8133.	04	280.83	OZ	-3.09	AM	-0.42	AV	-0.13
T 42.0	04	943.13	C	-3987.	Y	22130.	Z	-8031.	04	247.73	OZ	-5.57	AM	.55	AV	.39
T 42.5	04	942.00	C	-3790.	Y	21781.	Z	-7932.	04	209.86	OZ	-0.54	AM	-1.22	AV	-1.02
T 43.0	04	933.61	C	-3597.	Y	21437.	Z	-7771.	04	190.49	OZ	-13.79	AM	1.69	AV	2.45
T 43.5	04	914.02	C	-3426.	Y	21103.	Z	-7513.	04	147.35	OZ	17.79	AM	-3.01	AV	-5.75
T 44.0	04	744.55	C	-3230.	Y	20793.	Z	-7310.	04	139.43	OZ	-5.23	AM	5.51	AV	13.54
T 44.5	04	533.15	C	-3079.	Y	20520.	Z	-7374.	04	95.94	OZ	31.55	AM	-3.92	AV	-10.29
T 45.0	04	526.06	C	-2902.	Y	20275.	Z	-7279.	04	80.13	OZ	32.05	AM	7.92	AV	17.37
T 47.5	04	522.59	C	-2743.	Y	20027.	Z	-7195.	04	64.37	OZ	29.21	AM	-2.53	AV	.05
T 45.0	04	502.03	C	-2563.	Y	19001.	Z	-7110.	04	50.80	OZ	25.67	AM	4.24	AV	.00
T 46.5	04	372.14	C	-2426.	Y	19573.	Z	-6937.	04	35.39	OZ	42.15	AM	-5.41	AV	-3.19
T 47.0	04	327.69	C	-2269.	Y	19372.	Z	-6823.	04	24.83	OZ	35.73	AM	-5.41	AV	-3.19

PSYOPF 340 22335

31 -307 1353 452.00 RERR -4637.44 PSERR .539237 GAERR .064921

31-44807 14733010N

T 44.0	04	502.03	0444	.7395055E+01	044V	-.1494547E+02	X	-2563.	Y	19901.	Z	-7100.	AM	-5.41	AV	-3.19
T 44.0	04	749.95	0444	-.1504744E+01	044V	-.3778415E+02	X	-3230.	Y	20793.	Z	-7319.	AM	-3.92	AV	-10.29
T 42.0	04	943.13	0444	.1495133E+02	044V	.3321155E+01	X	-3907.	Y	22139.	Z	-8031.	AM	-1.22	AV	-1.02
T 43.0	04	946.54	0444	.2144934E+02	044V	.2100353E+02	X	-4775.	Y	23525.	Z	-8565.	AM	-0.04	AV	-0.06

T	34.0	04	950.30	0414	.1732622E+02	0414	.2322235E+02	X	-5875.	Y	24923.	Z	-9097.	AM	-.71	AV	-.33
T	34.0	04	956.71	0414	.1703031E+02	0414	.3537610E+02	X	-6451.	Y	25237.	Z	-9521.	AM	-.73	AV	-.33
T	34.0	04	939.69	0414	.1673762E+02	0414	.6612350E+02	X	-7410.	Y	27503.	Z	-10137.	AM	-.75	AV	-.39
T	32.0	04	955.35	0414	.1645+30E+02	0414	.3170033E+02	X	-8453.	Y	29804.	Z	-10544.	AM	-.79	AV	-.33
T	32.0	04	971.01	0414	.1618392E+02	0414	.5369116E+02	X	-9581.	Y	30103.	Z	-11141.	AM	-.80	AV	-.10
T	24.0	04	973.22	0414	.1594973E+02	0414	.5720545E+02	X	-10734.	Y	31257.	Z	-11529.	AM	-.83	AV	-.10
T	24.0	04	977.73	0414	.1573610E+02	0414	.7407395E+02	X	-12092.	Y	32363.	Z	-12103.	AM	-.93	AV	-.10
T	24.0	04	937.54	0414	.1555301E+02	0414	.9246303E+02	X	-13472.	Y	33393.	Z	-12574.	AM	-.88	AV	-.09
T	22.0	04	909.86	0414	.1540703E+02	0414	.9304301E+02	X	-14335.	Y	34333.	Z	-13035.	AM	-.90	AV	-.04
T	22.0	04	922.38	0414	.1513572E+02	0414	.9390450E+02	X	-15479.	Y	35197.	Z	-13693.	AM	-.92	AV	-.01
T	13.0	04	1014.19	0414	.1151291E+02	0414	.1449315E+03	X	-18104.	Y	35970.	Z	-13939.	AM	-.94	AV	18.44
T	14.0	04	1100.78	0414	.1315303E+02	0414	.9318333E+02	X	-19398.	Y	36739.	Z	-14580.	AM	-.95	AV	.24
T	14.0	04	1150.80	0414	.1239175E+02	0414	.1011191E+03	X	-22053.	Y	37443.	Z	-15093.	AM	-.93	AV	.19
T	12.0	04	1234.78	0414	.1247733E+02	0414	.1741943E+03	X	-24259.	Y	38071.	Z	-15719.	AM	-.94	AV	.32
T	10.0	04	1321.91	0414	.1199112E+02	0414	.1076793E+03	X	-25537.	Y	39523.	Z	-16193.	AM	-.93	AV	.24
T	4.0	04	1411.47	0414	.1035236E+02	0414	.1132703E+03	X	-29198.	Y	39093.	Z	-17139.	AM	-.91	AV	.32
T	6.0	04	1439.92	0414	.9277336E+01	0414	.1212293E+03	X	-31334.	Y	39489.	Z	-17977.	AM	-.99	AV	.39
T	4.0	04	1423.69	0414	.9785937E+01	0414	.1243943E+03	X	-34050.	Y	39787.	Z	-19314.	AM	-.95	AV	.11
T	2.0	04	1331.62	0414	.9773496E+01	0414	.7294519E+02	X	-37567.	Y	39953.	Z	-19930.	AM	-.85	AV	-18.78

THE-DIAGNOSTIC ALPHA 32324

C	.1000E-04	J	-297.0317	C1	.1000E-04	DE-C1	.5000E-03
C	.1500E-04	J	-13.3407	C1	.1000E-04	DE-C1	.5000E-03
C	.2000E-04	J	-307.4905	C1	.2000E-03	DE-C1	.1000E-03
C	.3000E-04	J	-307.4929	C1	.2000E-03	DE-C1	.1000E-06
C	.4000E-04	J	-317.4953	C1	.2000E-03	DE-C1	.1000E-03
C	.5000E-04	J	-317.4977	C1	.2000E-03	DE-C1	.1000E-03
C	.6000E-04	J	-307.5003	C1	.2000E-03	DE-C1	.1000E-03
C	.7000E-04	J	-317.5024	C1	.2000E-03	DE-C1	.1000E-06

2	.0099E-06	J	-307.5040	C1	.2000E-05	DE.C1	.1000E-05
2	.0099E-06	J	-307.5071	C1	.2000E-05	DE.C1	.1000E-05
2	.0099E-06	J	-307.5095	C1	.2000E-05	DE.C1	.1000E-05
2	.0099E-06	J	-307.5119	C1	.2000E-05	DE.C1	.1000E-05
2	.0099E-06	J	-307.5142	C1	.2000E-05	DE.C1	.1000E-05
2	.0099E-06	J	-307.5165	C1	.2000E-05	DE.C1	.1000E-05
2	.0099E-06	J	-307.5190	C1	.2000E-05	DE.C1	.1000E-05
2	.0099E-06	J	-307.5213	C1	.2000E-05	DE.C1	.1000E-05
2	.0099E-06	J	-307.5237	C1	.2000E-05	DE.C1	.1000E-05
2	.0099E-06	J	-307.5261	C1	.2000E-05	DE.C1	.1000E-05
2	.0099E-06	J	-307.5284	C1	.2000E-05	DE.C1	.1000E-05
2	.0099E-06	J	-307.5308	C1	.2000E-05	DE.C1	.1000E-05
2	.0099E-06	J	-307.5332	C1	.2000E-05	DE.C1	.1000E-05
2	.0099E-06	J	-307.5355	C1	.2000E-05	DE.C1	.1000E-05
2	.0099E-06	J	-307.5379	C1	.2000E-05	DE.C1	.1000E-05
2	.0099E-06	J	-307.5403	C1	.2000E-05	DE.C1	.1000E-05
2	.0099E-06	J	-307.5425	C1	.2000E-05	DE.C1	.1000E-05
2	.0099E-06	J	-307.5450	C1	.2000E-05	DE.C1	.1000E-05
2	.0099E-06	J	-307.5474	C1	.2000E-05	DE.C1	.1000E-05
2	.0099E-06	J	-307.5497	C1	.2000E-05	DE.C1	.1000E-05
2	.0099E-06	J	-307.5521	C1	.2000E-05	DE.C1	.1000E-05
2	.0099E-06	J	-307.5544	C1	.2000E-05	DE.C1	.1000E-05
2	.0099E-06	J	-307.5568	C1	.2000E-05	DE.C1	.1000E-05
2	.0099E-06	J	-307.5592	C1	.2000E-05	DE.C1	.1000E-05
2	.0099E-06	J	-307.5615	C1	.2000E-05	DE.C1	.1000E-05
2	.0099E-06	J	-295.9531	C1	.2000E-05	DE.C1	.1000E-05
2	.0099E-06	J	-307.5615	C1	.2000E-05	DE.C1	.1000E-05

2

2V -3.19

APR 23 1955

.339241 GAEER .054773

66T141ZEN T3J3C733Y

[illegible]

10.3	14	1273.69	€	-26025.	Y	39433.	Z	-18239.	34	2066.17	OZ	374.90	AM	-.93	AV	.20
11.0	14	1277.36	€	-25425.	Y	39337.	Z	-18030.	34	2138.79	OZ	396.51	AM	-.93	AV	.26
11.5	14	1285.74	€	-24936.	Y	39217.	Z	-18971.	34	2205.93	OZ	395.89	AM	-.93	AV	.25
12.0	14	1294.79	€	-24293.	Y	39071.	Z	-18739.	34	2267.74	OZ	402.85	AM	-.93	AV	.24
12.5	14	1214.66	€	-23592.	Y	37921.	Z	-18531.	34	2324.31	OZ	407.95	AM	-.94	AV	.22
13.0	14	1145.45	€	-23136.	Y	37765.	Z	-18336.	34	2375.64	OZ	410.82	AM	-.94	AV	.21
13.5	14	1177.27	€	-22539.	Y	37607.	Z	-18245.	34	2422.54	OZ	411.90	AM	-.94	AV	.20
14.0	14	1150.01	€	-22033.	Y	37443.	Z	-18039.	34	2464.63	OZ	411.15	AM	-.94	AV	.18
14.5	14	1143.90	€	-21528.	Y	37274.	Z	-18334.	34	2502.34	OZ	408.65	AM	-.93	AV	.18
15.0	14	1129.57	€	-21009.	Y	37109.	Z	-18412.	34	2535.90	OZ	404.41	AM	-.93	AV	.17
15.5	14	1114.25	€	-20499.	Y	35921.	Z	-18574.	34	2565.55	OZ	399.35	AM	-.93	AV	.19
16.0	14	1100.79	€	-19998.	Y	35739.	Z	-18539.	34	2591.52	OZ	390.25	AM	-.93	AV	.21
16.5	14	1098.07	€	-19505.	Y	36589.	Z	-18435.	34	2514.05	OZ	379.54	AM	-.93	AV	.29
17.0	14	1075.84	€	-19019.	Y	36356.	Z	-18230.	34	2533.52	OZ	354.43	AM	-.93	AV	.50
17.5	14	1052.20	€	-18540.	Y	35159.	Z	-18156.	34	2550.64	OZ	335.35	AM	-.94	AV	1.64
18.0	14	1014.21	€	-18104.	Y	35970.	Z	-18937.	34	2541.62	OZ	395.24	AM	-.94	AV	-10.21
18.5	14	945.92	€	-17691.	Y	35781.	Z	-18619.	34	2526.03	OZ	355.35	AM	-.94	AV	18.44
19.0	14	933.62	€	-17276.	Y	35593.	Z	-18734.	34	2500.40	OZ	357.89	AM	-.94	AV	-4.97
19.5	14	930.95	€	-16976.	Y	35399.	Z	-18515.	34	2572.33	OZ	390.72	AM	-.94	AV	-.45
20.0	14	922.41	€	-16479.	Y	35197.	Z	-18436.	34	2543.93	OZ	374.98	AM	-.93	AV	2.23
20.5	14	913.55	€	-16085.	Y	34930.	Z	-18390.	34	2514.07	OZ	365.03	AM	-.92	AV	.41
21.0	14	913.23	€	-15598.	Y	34777.	Z	-18254.	34	2482.38	OZ	354.23	AM	-.92	AV	.02
21.5	14	911.99	€	-15314.	Y	34599.	Z	-18149.	34	2448.99	OZ	342.33	AM	-.91	AV	.04
22.0	14	909.99	€	-14935.	Y	34335.	Z	-18034.	34	2413.85	OZ	330.07	AM	-.91	AV	-.03
22.5	14	905.90	€	-14563.	Y	34105.	Z	-18218.	34	2377.05	OZ	317.35	AM	-.90	AV	-.04
23.0	14	903.03	€	-14194.	Y	33872.	Z	-18030.	34	2338.61	OZ	304.50	AM	-.89	AV	-.06
23.5	14	900.25	€	-13931.	Y	33632.	Z	-18097.	34	2298.61	OZ	291.53	AM	-.89	AV	-.07
24.0	14	937.59	€	-13473.	Y	33304.	Z	-18571.	34	2257.05	OZ	279.57	AM	-.89	AV	-.08
24.5	14	935.00	€	-13120.	Y	33133.	Z	-18435.	34	2214.00	OZ	265.57	AM	-.89	AV	-.09

Y 27.6	J4	932.58	E	-12772.	Y	32005.	Z	-12330.	J4	2169.50	OZ	232.03	AM	-07	AV	-09
Y 27.5	J4	930.18	E	-12430.	Y	32625.	Z	-12221.	J4	2123.61	OZ	240.25	AM	-05	AV	-09
Y 27.0	J4	937.70	E	-12092.	Y	32363.	Z	-12103.	J4	2076.30	OZ	227.84	AM	-03	AV	-10
Y 26.5	J4	945.94	E	-11768.	Y	32095.	Z	-11334.	J4	2027.95	OZ	215.64	AM	-03	AV	-10
Y 27.0	J4	943.30	E	-11473.	Y	31024.	Z	-11353.	J4	1978.00	OZ	203.59	AM	-03	AV	-10
Y 27.5	J4	931.29	E	-11111.	Y	31547.	Z	-11745.	J4	1927.12	OZ	192.02	AM	-04	AV	-10
Y 27.0	J4	979.27	E	-10795.	Y	31265.	Z	-11625.	J4	1975.02	OZ	190.64	AM	-03	AV	-10
Y 27.5	J4	977.32	E	-10494.	Y	30902.	Z	-11334.	J4	1821.83	OZ	159.55	AM	-03	AV	-10
Y 27.0	J4	975.44	E	-10179.	Y	30693.	Z	-11332.	J4	1757.60	OZ	158.79	AM	-02	AV	-10
Y 27.5	J4	973.63	E	-9977.	Y	30401.	Z	-11250.	J4	1712.39	OZ	146.35	AM	-02	AV	-10
Y 27.0	J4	971.07	E	-9502.	Y	30104.	Z	-11137.	J4	1556.23	OZ	139.26	AM	-01	AV	-10
Y 27.5	J4	970.17	E	-9292.	Y	29806.	Z	-11014.	J4	1599.19	OZ	126.50	AM	-00	AV	-10
Y 31.0	J4	953.54	E	-9007.	Y	29501.	Z	-10930.	J4	1541.31	OZ	119.09	AM	-00	AV	-10
Y 31.5	J4	955.95	E	-8728.	Y	29194.	Z	-10755.	J4	1482.55	OZ	110.01	AM	-79	AV	-10
Y 32.0	J4	955.42	E	-8454.	Y	29083.	Z	-10540.	J4	1423.25	OZ	101.29	AM	-79	AV	-10
Y 32.5	J4	953.94	E	-8105.	Y	28570.	Z	-10514.	J4	1363.16	OZ	92.91	AM	-78	AV	-10
Y 33.0	J4	952.50	E	-7922.	Y	28255.	Z	-10337.	J4	1302.43	OZ	94.69	AM	-77	AV	-09
Y 33.5	J4	951.11	E	-7653.	Y	27932.	Z	-10250.	J4	1241.11	OZ	77.21	AM	-77	AV	-09
Y 34.0	J4	953.77	E	-7410.	Y	27609.	Z	-10133.	J4	1179.23	OZ	59.08	AM	-75	AV	-09
Y 34.5	J4	953.47	E	-7163.	Y	27293.	Z	-10034.	J4	1116.90	OZ	52.83	AM	-75	AV	-09
Y 35.0	J4	957.21	E	-6920.	Y	25953.	Z	-9975.	J4	1054.11	OZ	35.23	AM	-73	AV	-09
Y 35.5	J4	955.99	E	-6603.	Y	25621.	Z	-9745.	J4	990.92	OZ	49.90	AM	-73	AV	-09
Y 36.0	J4	954.80	E	-6451.	Y	25287.	Z	-9516.	J4	927.38	OZ	43.91	AM	-74	AV	-09
Y 36.5	J4	953.63	E	-6225.	Y	25949.	Z	-9456.	J4	863.53	OZ	38.22	AM	-73	AV	-08
Y 37.0	J4	952.54	E	-6003.	Y	25603.	Z	-9335.	J4	799.43	OZ	32.89	AM	-73	AV	-08
Y 37.5	J4	951.44	E	-5707.	Y	25267.	Z	-9224.	J4	735.13	OZ	27.90	AM	-72	AV	-07
Y 38.0	J4	950.40	E	-5576.	Y	24922.	Z	-9032.	J4	670.65	OZ	23.12	AM	-72	AV	-09
Y 38.5	J4	949.35	E	-5370.	Y	24573.	Z	-8939.	J4	506.07	OZ	19.57	AM	-71	AV	-05

T 39.0	44	9-3.39	€	-5170.	V	24225.	Z	-8025.	34	541.40	OZ	14.53	44	-71	4V	-1.10
T 39.5	44	9-7.36	€	-4974.	V	23074.	Z	-8533.	34	476.73	OZ	10.40	44	-70	4V	-0.01
T 40.0	44	9-6.65	€	-4777.	V	23224.	Z	-8550.	34	419.52	OZ	7.33	44	.23	4V	-0.07
T 40.5	44	9-3.99	€	-4580.	V	23175.	Z	-8425.	34	367.35	OZ	5.13	44	-0.01	4V	-0.05
T 41.0	44	9-3.23	€	-4382.	V	22025.	Z	-8232.	34	322.55	OZ	3.42	44	.27	4V	.00
T 41.5	44	9-0.59	€	-4187.	V	22477.	Z	-8137.	34	279.70	OZ	3.17	44	-42	4V	-1.18
T 42.0	44	9-3.24	€	-3959.	V	22129.	Z	-8025.	34	246.67	OZ	.52	44	.53	4V	.33
T 42.5	44	9-2.12	€	-3799.	V	21790.	Z	-7335.	34	208.75	OZ	3.87	44	-1.22	4V	-1.02
T 43.0	44	9-1.73	€	-3599.	V	21435.	Z	-7755.	34	199.37	OZ	-7.17	44	1.63	4V	2.46
T 43.5	44	9-1.15	€	-3427.	V	21102.	Z	-7505.	34	146.22	OZ	24.43	44	-3.01	4V	-5.76
T 44.0	44	7-8.67	€	-3231.	V	20797.	Z	-7511.	34	138.29	OZ	.45	44	5.50	4V	13.54
T 44.5	44	5-5.25	€	-3080.	V	20513.	Z	-7357.	34	94.79	OZ	38.45	44	-3.92	4V	-10.28
T 45.0	44	5-1.92	€	-2903.	V	20277.	Z	-7272.	34	96.99	OZ	38.92	44	7.92	4V	17.37
T 45.5	44	5-2.66	€	-2744.	V	20025.	Z	-7178.	34	53.25	OZ	35.13	44	-2.63	4V	.05
T 46.0	44	5-2.92	€	-2564.	V	19800.	Z	-7033.	34	67.69	OZ	32.67	44	4.24	4V	.80
T 46.5	44	5-2.22	€	-2425.	V	19572.	Z	-6930.	34	34.27	OZ	49.20	44	-5.41	4V	-3.13
T 47.0	44	5-7.73	€	-2270.	V	19371.	Z	-6917.	34	23.79	OZ	43.82	44	-5.41	4V	-3.19

VITA

Edwin H. Jessup was born on 5 March 1947 in New Haven, Connecticut. He graduated from Bordentown Military Institute, New Jersey, in 1964, and from Brown University, Rhode Island in 1968. He completed pilot training at Craig Air Force Base, Alabama in 1969. After serving a one year tour at Bien Hoa Air Base, Vietnam, as an A-37B pilot, he returned to Westover Air Force Base, Massachusetts, to pilot the B-52D. This led to five temporary duty tours flying the B-52D in Southeast Asia under Operation Bullet Shot. He transferred to Mather Air Force Base, California, in 1973, following deactivation of the B-52 wing at Westover. In June 1975, he entered the Air Force Institute of Technology as a graduate student in Aeronautical Engineering.

Permanent Address: Smoke Rise
Kinnelon, New Jersey

This thesis was typed by Neila Carey.

Unclassified

SECURITY CLASSIFICATION OF THIS PAGE (When Data Entered)

REPORT DOCUMENTATION PAGE		READ INSTRUCTIONS BEFORE COMPLETING FORM
1. REPORT NUMBER GAE/MC/76D-6	2. GOVT ACCESSION NO.	3. RECIPIENT'S CATALOG NUMBER
4. TITLE (and Subtitle) PERFORMANCE OF AN AIR-TO-GROUND MISSILE EMPLOYING SAR-RETRAN GUIDANCE		5. TYPE OF REPORT & PERIOD COVERED MS Thesis
		6. PERFORMING ORG. REPORT NUMBER
7. AUTHOR(s) Edwin H. Jessup Capt., USAF		8. CONTRACT OR GRANT NUMBER(s)
9. PERFORMING ORGANIZATION NAME AND ADDRESS Air Force Institute of Technology (AFIT/EN) Wright-Patterson AFB, Ohio 45433		10. PROGRAM ELEMENT, PROJECT, TASK AREA & WORK UNIT NUMBERS
11. CONTROLLING OFFICE NAME AND ADDRESS		12. REPORT DATE December, 1976
		13. NUMBER OF PAGES 206
14. MONITORING AGENCY NAME & ADDRESS (if different from Controlling Office) Fire Control Branch (RWT) Air Force Avionics Laboratory Wright-Patterson AFB, Ohio 45433		15. SECURITY CLASS. (of this report) Unclassified
		15a. DECLASSIFICATION/DOWNGRADING SCHEDULE
16. DISTRIBUTION STATEMENT (of this Report) Approved for public release; distribution unlimited.		
17. DISTRIBUTION STATEMENT (of the abstract entered in Block 20, if different from Report)		
18. SUPPLEMENTARY NOTES Approved for public release IAW AFR 190-17 JERRAL F. GUESS, Captain, USAF Director of Information		
19. KEY WORDS (Continue on reverse side if necessary and identify by block number) Synthetic Aperture Radar Synthetic Aperture Radar-Retransmission Air-to-Ground Missile		
20. ABSTRACT (Continue on reverse side if necessary and identify by block number) The compatibility of a representative 500 pound weight boost-glide air-to-ground missile with the trajectory constraints imposed by a Synthetic Aperture Radar - Retransmission guidance system was investigated using a digital flight simulation. A demonstration flight profile was assumed, with a minimum of 20 seconds of tracking on the aircraft-to-target line of sight required. A guidance algorithm was developed which produced satisfactory trajectories. A first order gradient technique was employed in an unsuccessful attempt to optimize the trajectories for maximum range. A useable launch envelope		

DD FORM 1 JAN 73 1473

EDITION OF 1 NOV 65 IS OBSOLETE

Unclassified

SECURITY CLASSIFICATION OF THIS PAGE (When Data Entered)

UNCLASSIFIED

SECURITY CLASSIFICATION OF THIS PAGE(When Data Entered)

for this missile was determined. The azimuthal extent of the envelope was limited by radar system constraints to 15° - 90° from the aircraft velocity vector. A maximum slant range of 21 nautical miles was obtained from a launch altitude of 35,000 ft. Range deteriorated rapidly with decreasing launch altitude, with 5,000 ft being the lowest altitude at which a useable launch envelope was obtained. Maximum slant range at 5,000 ft launch altitude was 5.5 nautical miles.

UNCLASSIFIED

SECURITY CLASSIFICATION OF THIS PAGE(When Data Entered)